Nicotinic Acetylcholine Receptor Subtypes in Primary Cultures of Hippocampal Neurons

Barrantes, Georgina Elida

Award date:
1994

Awarding institution:
University of Bath

NICOTINIC ACETYLCHOLINE RECEPTOR SUBTYPES IN PRIMARY CULTURES OF HIPPOCAMPAL NEURONS

Submitted by Georgina Elida Barrantes

for the degree of Doctor of Philosophy

of the University of Bath

1994

ProQuest LLC
789 East Eisenhower Parkway
P.O. Box 1346
Ann Arbor, MI 48106-1346

Abstract

Nicotinic Acetylcholine Receptor Subtypes in Primary Cultures of Hippocampal Neurons

Primary cultures of hippocampal neurons were established and used as a model system to characterize neuronal α-Bungarotoxin-sensitive (α-Bgt) nicotinic acetylcholine receptor (nAChR), whose functional significance is unknown.

Long term (7 weeks) neuronal hippocampal (<5% glia) and cortical (<20% glia) cultures were generated by plating cell suspensions on polyethylenimine substrate with serum-supplemented, chemically defined medium. Cultures were changed to serum-free chemically defined medium 2h after plating. In hippocampal glial cultures, grown on poly-L-lysine substrate with serum supplemented medium, the presence of nAChR was ruled out.

Hippocampal neurons displayed high affinity [^{125}I]-α-Bgt binding (B_{max}=128 ± 7 fmol/mg protein; K_d=0.62 ± 0.01 nM) inhibited by nicotine (K_i=1.3 μM) and methyllycaconitine (MLA) [K_i=6.1 nM]. Cortical neurons displayed 29 ± 7 fmol [^{125}I]-α-Bgt sites/mg protein. Surface rhodamine-α-Bgt (Rd-α-Bgt) labelling was observed in 60 ± 3% and 19 ± 2% of hippocampal and cortical neurons, respectively, yielding 51,000 [^{125}I]-α-Bgt binding sites/hippocampal and 18,000 sites/cortical neuron. Binding with [^{3}H]nicotine, which displays high affinity to a distinct population of nAChR, was not detected.

Subtypes of nAChR subunit expressed by cultured neurons were investigated by immunocytochemistry. Binding of a monoclonal antibody (mAb) to the α7 subunit colocalised with Rd-α-Bgt sites in both types of neuronal cultures. Fewer hippocampal neurons were positive for a mAb against the α4 subunit; those labelled did not display surface Rd-α-Bgt labelling. All cortical neurons reacted to the mAb against the α4 subunit, but few colocalised surface Rd-α-Bgt sites.

Functional assays with Fura-2 showed that nicotine and cytisine increased the intracellular free Ca^{2+} ($[Ca^{2+}]_i$). This effect was prevented by MLA, in contrast to K^+-evoked increases in $[Ca^{2+}]_i$. The nicotinic increase in $[Ca^{2+}]_i$ was dependent on extracellular Ca^{2+} and blocked by Ni^{2+} and Cd^{2+}, suggesting that activation of α7 nAChR causes the opening of voltage-gated Ca^{2+} channels.

It is concluded that hippocampal neurons have high affinity α-Bgt binding sites that respond to nicotine and colocalise with α7 nAChR.

Acknowledgements

I would like to express my gratitude to my supervisor Dr. Susan Wonnacott for her advice, encouragement and inspiration throughout this project. I will always remember with much happiness the resources Sue used to make me feel at home.

Sincere thanks to Professor John Westwick for his interest in my project and allowing the use of the spectrophotofluorimeter.

I would also like to take this opportunity to thank Professor George Lunt to whom I will always be indebted.

Everyone in the Biochemistry Department has been very helpful and friendly, making my stay at Bath an enjoyable experience. Some deserve special mention, Dr. Robert Eisenthal, Dr. Pnina Osguthorpe, Mrs. Glenys Lunt and the "nicotine research group". Thanks to Dr A. Rogers, for his invaluable help in the laboratory and for generously reading the manuscript. My thanks are extended to all members of the animal house for their kind attention.

To Professor Francisco Barrantes who helped me to embark upon a PhD course, and who has followed my progress with much enthusiasm and encouragement, I offer my deepest gratitude.

The fact I was able to realise a thesis in a foreign country without speaking in my native language it is owed to my parents, Elida and Enrique, which made every possible effort to guarantee me a bilingual education. I thank them for teaching me to choose with total freedom the way to survive with honesty in this intricate world.

To my husband, colleague and friend for being so patient and helpful and for copeing with my eccentric time tables. Thank you dear Marcelo for your love and eight wonderful years togehter.

To my sisters Irene, Analía and Verónica which in one way or another support my audacious decisions throughout my carrier. Special thanks to Verónica who attenuated in my parents' home, the "effects" of my long absence.

I am grateful to my aunt Rosa Forastieri de Celhabe for being so generous and following with much affection my achievements.

I would also like to acknowledge Silvina and Mariano Tarruella who manage to be close to my husband and me during our stay in England. A big thanks to you two for your friendship.

Alejandra, Cecilia, Daniela, Marcia, Mirtha, Paula and Tati in "alphabetical order", my Argentinian friends for either visiting or keeping me busy reading their letters.

I am grateful to the British Council and CONICET Argentina for financial support.

for Marcelo,

Elida and Enrique

The work presented in this thesis has been presented or is being submitted elsewhere:

Barrantes, G.E. and Wonnacott, S. Preliminary characterization of nicotinic receptors in primary cultures of hippocampal neurons. *Fidia Research Foundation.* Synapses and Receptors. A Molecular Perspective, Cambridge, England, September 1992:44.

Rogers, A.T., Barrantes, G.E., Rogers, S.W. and Wonnacott, S. Nicotinic acetylcholine receptors in primary cultures of hippocampal neurons. *14th International Society for Neuroscience*, Montpelier, France, August 22-27, 1993:20.

Barrantes, G.E, Rogers, A.T. and Wonnacott, S. Nicotinic acetylcholine receptors in primary cultures of hippocampal neurons. *23rd Annual Meeting of the Society for Neuroscience*, Washington, D.C., USA, November 7-12, 1993: 464.

Barrantes, G.E., Westwick, J. and Wonnacott, S. Pharmacology of nicotinic acetylcholine receptors in primary cultures of hippocampus. Wales and West Biochemistry society group, *Cardiff Postgraduate meeting*, Cardiff, April 10-11, 1994.

Barrantes, G.E., Westwick, J. and Wonnacott, S. (1994) Nicotinic acetylcholine receptors in primary cultures of hippocampal neurons: pharmacology and Ca^{2+} permeability. *Biochemical Society transactions*. 22:294.

Barrantes, G.E, Rogers, A.T., Lindstrom, J. and Wonnacott, S. α-Bungarotoxin binding sites in rat hippocampal and cortical cultures: initial characterization and upregultaion by chronic nicotine treatment. *Document in preparation.*

Abbreviations

α-Bgt	α-Bungarotoxin
ACh	Acetylcholine
B_{max}	Total concentration of receptors
BSA	Bovine serum albumin
$[Ca^{2+}]_i$	Intracellular free calcium
CNS	Central nervous system
[^{3}H]cytisine	[3,5-^{3}H(N)]-Cytisine hydrochloride
DMEM	Dulbecco's Modification of Eagle's Medium
EC_{50}	Concentration of drug which produces 50% of the maximum response
E(18)	Embryonic day 18
FCS	Fetal calf serum
5'FDU	5'Fluorodeoxyuridine-uridine
FITC	Fluorescein isothiocyanate
FITC-α-Bgt	Fluorescein isothiocyanate conjugate α-Bgt
Fura-2	1-[2-(5-carboxyoxazol-2-yl)-6-aminobenzofuran-5-oxy]-2-(2'-amino-5'-methylphenoxy)ethane N,N,N',N'-tetraacetic acid
GFAP	Glial fibrillary acidic protein
HEPES	N-[2-hydroxyethyl]piperazine-N'-[2-ethanesulphonic acid]
IC_{50}	Concentration of inhibitor that blocks 50% of binding
IgG	Immunoglobulin G
IgM	Immunoglobulin M
K_D	Equilibrium dissociation constant
Kda	Kilo Dalton
K_i	Affinity constant
LGICs	Ligand-gated ion channels
mAb-GFAP	Glial fibrillary acidic protein monoclonal antibody

mAb-NF	Neurofilament monoclonal antibody
mAb 299	Monoclonal antibody to purified rat brain α4 nAChR subunit
mAb 307	Monoclonal antibody against chick α7 nAChR
MLA	Methyllycaconitine
Mr	Molecular weight
nAChR	Nicotinic acetylcholine receptor
n-Bgt	Neuronal bungarotoxin
n_H	Hill number
(-)[^{3}H]nicotine	L-(-)-[N-methyl-^{3}H]-nicotine
NMDA	N-methyl-D-aspartate
PBS	Phosphate-buffered saline
PEI	Polyethylenimine
PLL	Poly-L-lysine
[^{3}H]-QNB	L-[Benzilate-4,4'-^{3}H]-quinuclidinyl benzilate
Rd	Rhodamine
Rd-α-Bgt	Rhodamine conjugate α-Bungarotoxin
SDS	Sodium dodecyl sulphate
TTX	Tetrodotoxin

Contents

List of Figures

List of Plates

List of Tables

Chapter 1
Introduction

1.1. The hippocampus

It was the anatomist Arantius (Arantius, 1587) *who, inspired by a sea-horse, termed the bilateral structure situated in the subcortex of the brain the "hippocampus". Today it is still an enigma which end of the structure represents the animal's head.*

Fields of the hippocampus

The hippocampus occupies most of the ventroposterior and ventral walls of the mammalian cerebral cortex. Internally are rows of densely packed cells which, when viewed in cross section, are arranged in two prominent C-shaped bands; these are the *dentate gyrus* of granule neurons and the *hippocampus proper* (*Cornu ammonis* (*CA*) or Ammon's horn) which consists of pyramidal neurons (Fig. 1A and B). In attempts to provide a useful nomenclature for the areas of the *hippocampus proper* it has been subdivided into several regions. The most common nomenclature (Lorente de Nó, 1934) designated 4 regions (Fig. 1B), *CA1* through *CA4*. As represented in Fig. 1B, granule neurons extend two or more primary dendrites from one pole of the cell body. Their axons present a dense, mossy appearance (mossy fibers). Pyramidal neurons, in contrast, exhibit a large primary apical dendrite with numerous higher order branches and many radially orientated basal dendrites. Their axons arise either from the perikaryon or from a proximal segment of a basal dendrite. In addition, both pyramidal and granule cell dendrites are richly endowed with spines that perform asymmetrical synaptic contact. Other morphological cell types (i.e., bipolar, multipolar and aspiny cells), correspond to local circuit neurons or interneurons (Shepherd, 1988; Milner and Bacon, 1989; Banker and Goslin, 1991).

Figure 1. Diagrammatic representation of the orientation, neuroarchitecture and circuitry of the rat hippocampus.

A: side-view of rat head to illustrate the location of the hippocampus (**dashes**) beneath the cortex. A transverse section of the hippocampus (**arrow**) shows the *dentate gyrus* (**red**) and the *hippocampus proper* (**blue**).

B: neuroarchitecture of a transverse section of the hippocampus corresponding to the standard Plate 60 (Paxinos and Watson, 1986).

Abbreviations: **a**, *alveus*; **e**, entorhinal cortex, **f**, *fimbria* and *fornix*; **G**, granule cell layer; **l**, *stratum lacunosum*; **m**, *stratum moleculare*; **M**, molecular layer of the *dentate gyrus*; **o**, *stratum oriens*; **p**, *stratum pyramidale*; **r**, *stratum radiatum*; **sb**, *subiculum*. **1** to **4**, *CA1* to *CA4* pyramidal cell fields.

Highlighted with **red** is the *dentate gyrus*. One granule cell has been completely drawn to show its mossy fiber projecting to *CA3* and *CA2* fields (both fields indicated with **3** and **2**, respectively). In **blue** is the stratum pyramidale. Two pyramidal neurons have been traced completely to show their axonic projections. In *CA3*, there is a pyramidal neuron (**thin arrow**) that projects one collateral to the *fornix* and the other to *CA1* field (this last indicated with **1**). A typical pyramidal *CA1* neuron (**thick black arrow**) sends its collateral to the *subiculum* while the other collateral heads towards the *fimbria*. A cortical input is indicated with a thick empty arrow.

C: Schematic sagital drawing of the rat brain showing the cholinergic input to the hippocampus.

Abbreviations: **d**, nuclei of the diagonal band of Broca; **H**, hippocampus showing the *dentate gyrus* (**red**) and the *hippocampus proper* (**blue**); **s**, medial septal nucleus.

Traced in **green** is the septo-hippocampal cholinergic projection into the hippocampus.

A

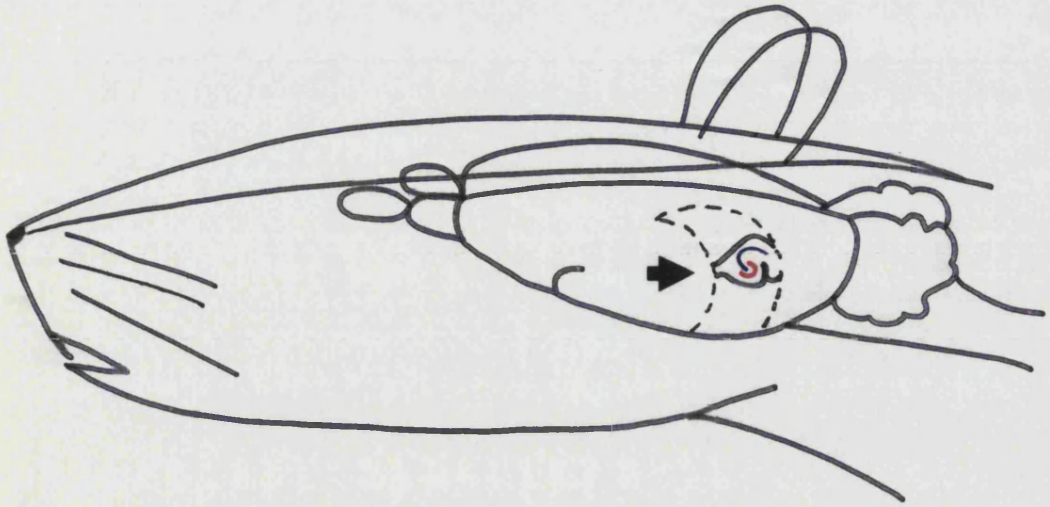

B

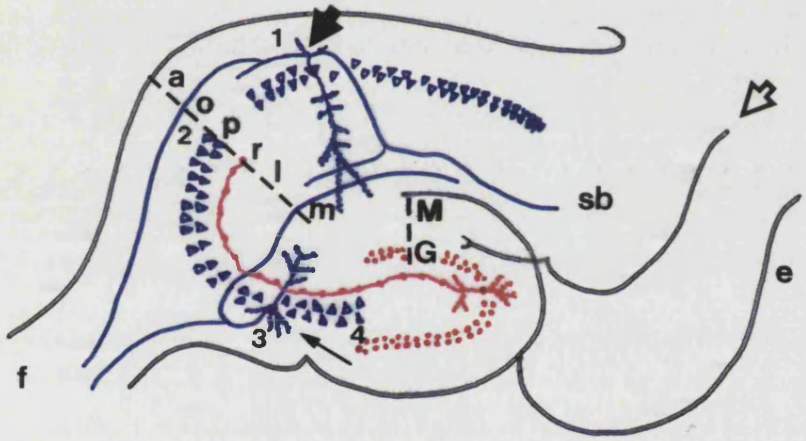

C

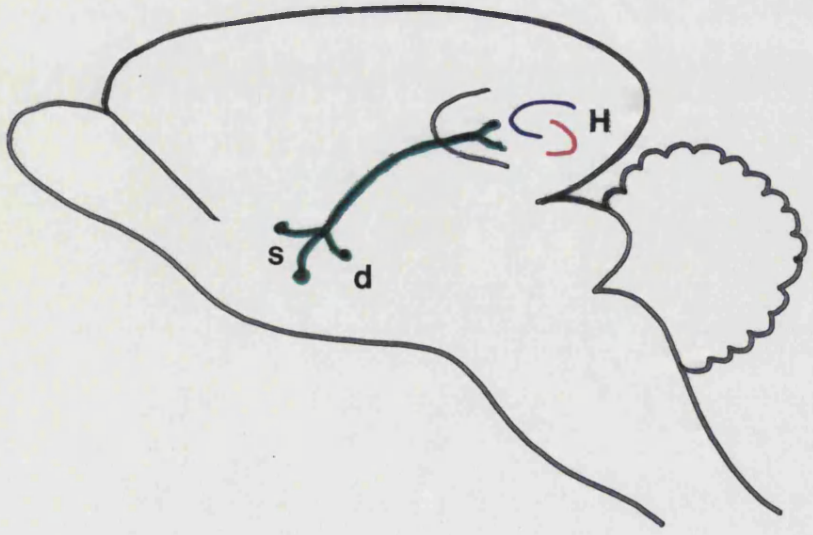

Neuroarchitecture of the hippocampus

The characteristic lamellar neuroarchitecture of the hippocampus has been described in detail by Ramón y Cajal a century ago (Isaacson, 1974).

The areas corresponding to each of these layers are indicated in Fig. 1B. The zone of the *hippocampus proper* designated *stratum moleculare* contains dendritic processes from pyramidal cells projecting from other layers. Also, a few cells bearing short fibers are present. Next to this layer is, the *stratum lacunosum* with many irregularly spaced cells and a rather large number of fibers projected from other layers. Some fibers end in this layer, while others project into the *stratum moleculare.* Then follows the *stratum radiatum*, populated with few non-pyramidal neurons. It contains many fiber systems coursing through it from various points of origin. Also presents a dense network of dendritic arborizations characteristic of the pyramidal neurons from the *stratum pyramidale* situated next to it. The *stratum oriens*, with its densely packed polymorphic cells that project to other zones of the hippocampus, lies adjacent to the *stratum pyramidale* from which receives fibers. Then follows the *alveus* which, for the most part, it is composed of white matter, i.e., axons arising from the *stratum pyramidale.* Separating the hippocampus from the lateral ventricle there are epithelial cells from the epithelial zone.

The *dentate gyrus* has also been assigned a molecular layer (*stratum moleculare*) with many nerve fibers but few neurons bearing short processes. Next to it is the granule cell layer with densely packed cells followed by the polymorphic zone composed of pyramidal, stellate and bipolar cells.

Neuronal circuitry in the mammalian hippocampus

The major system of information flow originates from the entorhinal cortex (refer to Fig. 1B) which receives converging cortical inputs from all sensory modalities as well as inputs from the limbic system and, in turn, sends afferents to dentate granule cells. Granule cell axons (mossy fibers) impinge upon pyramidal neuron dendrites in region *CA3*. Axons of *CA3* pyramidal neurons give off recurrent

branches (the Schaffer collaterals). One branch of the collaterals travel to *strata lacunosum* and *moleculare* to reach and provide input to *CA1* neurons. The other branch of collateral exit at the *alveus* to the fornix and then distribute to the brain. Schaffer collaterals are thought to provide the main route by which pyramidal neurons of the *CA3* and *CA4* influence activities of neurons in the areas *CA1* and *CA2*. Finally, one branch of *CA1* collaterals travels towards the subiculum while other branch heads towards the fimbria to terminate sparsely outside the hippocampus (Lauterborn *et al.*, 1993; Bayer, 1985; Mattson, 1988).

Afferent fibers to the hippocampus contain the transmitter candidates acetylcholine (ACh), histamine, noradrenaline, serotonin, glutamate and aspartate (Haas, 1983; Shepherd, 1988). Studies combining histochemistry and immunocytochemistry have provided direct evidence that cholinergic neurons in the medial septal nucleus and in the nuclei of the diagonal band of Broca (Fig. 1C.), project to the rat hippocampal formation (Amaral and Kurz, 1985) in agreement with earlier lesion studies (Lewis *et al.*, 1967). However, a combined light- and electron-microscopic immunocytochemical study (Frotscher *et al.*, 1986) provided evidence for an intrinsic source of cholinergic hippocampal innervation from a small number of non-pyramidal neurons in addition to the well-established septo-hippocampal cholinergic projection.

In addition to this well-defined spatial ordering of neurotransmitter inputs, there also exists correlation between developmental patterns and anatomical connection, i.e., a temporally ordered sequence of innervation (Bayer, 1985; Isaacson, 1974). Throughout the hippocampus, there is an interstructural neurogenetic and morphogenetic gradient such that those structures closest to the rhinal fissure (Fig. 1) are older, while progressively younger structures are located near the dentate gyrus. This spatiotemporally ordered development of hippocampal neuronal cytoarchitecture has provided a model for experiments designed to examine roles for neurotransmitters

in the regulation of neuroarchitecture. The hippocampus has also been a model for studies of plasticity of neuronal circuitry. Deafferentation experiments have provided insights into the capacity of the brain for compensatory neuronal outgrowth, while studies of long term potentiation (LTP, a sustained enhancement of synaptic transmission following stimuli of the presynaptic neurons) have improved the knowledge of the cellular mechanisms underlying learning and memory processes. A further feature which makes the hippocampus attractive for studies of neurotransmitter regulation of cytoarchitecture, as well as for examination of structure-function relationships is that specific neurons in this region are vulnerable in several neurodegenerative disorders. For example, pyramidal neurons are destroyed in Alzheimer's disease, epilepsy, and stroke.

The relatively simple, ordered structure of hippocampal circuitry and the temporally defined formation of the circuitry have allowed investigators to approach its neurobiology at several levels of complexity. These levels include individual isolated neurons of identified phenotype (e.g. pyramidal neurons), combinations of intrinsic and input neurons, *in vitro* slices consisting of complete intrinsic circuits, and intact brain.

1.2. Synaptic transmission

The principal means of neuronal organization to form functional systems is through the synapse. The term synapse is derived from the Greek, meaning to connect or join. The origin of the idea of the synapse is particularly associated with Charles Sherrington, an English physiologist who early in this century proposed a synapse to be the transverse membranes that separate two neurons in regions of close juxtaposition (Shepherd, 1988).

The process of synaptic transmission is well known (Bradley, 1989). Transmission at synapses is usually mediated chemically, i.e. by the release of a neurotransmitter. Thus, while the transfer of information from one part of a nerve cell

to another is electrical (e.g. by propagated action potentials), the transfer of information between neurons is via a neurotransmitter which is released from one neuron and acts on the other.

In the brain, a single nerve fibre may synapse with many other neurons, and may itself have presynaptic terminals from a number of other neurons impinging on it. In the central nervous system (CNS), impulses in presynaptic terminals may result in either excitation or inhibition of the postsynaptic neuron. During the synaptic transmission, the transmitter is released from the presynaptic nerve terminals as the result of the arrival of an action potential. The released transmitter diffuses across the synaptic cleft to stimulate "receptor molecules" on the postsynaptic neuron and this action results in a local response in the postsynaptic cell. Receptors for neurotransmitters are molecules which protrude from cell membranes and mediate the conversion of chemical signals into electrical activity (Changeux, 1993).

The action of an excitatory transmitter is an increase in the permeability of the postsynaptic membrane to Na^+, K^+ and Ca^{2+} which results in a decrease in the membrane potential, i.e. there is a local depolarization of brief duration. The neurotransmitter is removed and the postsynaptic membrane is repolarized. An inhibitory transmitter has the opposite action as it causes local hyperpolarization by inducing K^+ and Cl^- influx.

1.3. Ligand-gated ion channels with reference to the nAChR

Fast ion channel receptor molecules have been found to constitute a superfamily of neurotransmitter receptors that are known as ligand-gated ion channels (LGICs). Ionotrophic receptors for acetylcholine (nicotinic), 5-hydroxy-tryptamine ($5HT_3$), gamma amino-butyric acid ($GABA_A$) and glycine are highly homologous in structural terms in spite of diverse physiological roles (Unwin, 1993a). The first two excite/depolarise postsynaptic membranes by increasing cation conductance, whereas GABA and glycine inhibit neurons bearing these receptors by increasing chloride

conductance (which usually hyperpolarises the cell away from threshold for action potential propagation). Ion-selective pathways are formed by packing proteinaceous subunits, perpendicular to the membrane, rather like staves in a barrel around a central, relatively hydrophilic core (Fig. 2).

1.3.1. Structure of LGICs with reference to the nAChR

All four classes of receptor in this superfamily appear to comprise subunits of approximately 48-60 Kilo Daltons (Kd) (Lees *et al.*, 1994). Solubilised/purified receptor oligomers range more widely in molecular mass (220-355 Kd), possibly reflecting glycosylation of the peptides or co-purification of intimately associated proteins thought to form a link with the sub-membranous cytoskeleton [e.g. nicotinic receptors with 43 Kd protein (Unwin, 1993a)]. Each subunit has four domains which are sufficiently long and hydrophobic to completely span the lipid bilayer. Both the N and C-terminals are thought to lie on the extracellular side of the membrane (Fig. 2).

The four putative membrane spanning domains, particularly M1-M3, are highly conserved but cytoplasmic loops on the inner membrane face vary in length and bear potential sites for phosphorylation (Poulter *et al.*, 1989). The hydrophobic segments are thought to stack in the membrane with the amphiphilic M2 helix orientated towards the channel lumen to form the permeant pathway (Karlin, 1993). At least in the nicotinic receptor, a kink in this helix projects a hydrophobic leucine residue into the pore in the closed conformation (Unwin, 1993b). Ultrastructural data also suggests that the density of the surrounding rim in this receptor is low suggesting that the M1, M3 and M4 may be beta-sheets rather than the helical structures previously proposed. This view is reinforced by other types of studies (Görne-Tschelnokow *et al.*, 1994). M2 itself forms a rather non-selective channel, largely by virtue of hydroxylated serine and threonine residues which line the inner face and is identical or highly homologous in excitatory (cation channel) and inhibitory (anion channel) receptors (Imoto *et al.*, 1991; Villarroel *et al.*, 1991; Konno *et al.*, 1991; Villarroel

and Sakmann, 1992; Bertrand *et al.*, 1993). Ionic selectivity appears to be conferred by rings of fully charged amino acids just outside the bilayer plane which may attract permeant counterions to each end of the pore (Imoto *et al.*, 1988).

A molecular model of the nAChR is shown in Figure 3. Agonist recognition is thought to be largely due to one particular subunit, the alpha subunit (α), in the nicotinic receptors. The presence of two copies of this subunit in the receptor produces steep-dose response relationships by a co-operative mechanism following binding of two agonist molecules. A broadly conserved pair of adjacent cysteine residues may be intimately associated with this hypothetical transmitter binding pocket (Karlin, 1993).

The receptor macromolecules are normally hetero-oligomers, composed most likely of five subunits (Unwin, 1993a). With the presence of numerous gene products there is much scope for isomerism. In the muscle, the receptor is composed by four different subunits, two alphas, one beta, one delta and one gamma (epsilon in the adult of mammals). In the brain, at least seven different types of alpha subunits (α2-α8) and three betas (β2-β4) exist. Potentially, this gives an enormous variability of receptors. Expression of brain nAChR subunits in *Xenopus* oocytes have shown that only one or two different subunits are needed to form functional channels (α or ACh binding subunit and β or structural subunit) (Deneris *et al.*, 1991).

One of the key questions in the field is whether all these combinations actually exist in the brain and where. Based on *in situ* hybridization and immunohistochemical studies, evidence for discrete anatomical and cellular expression of subunits is beginning to emerge (see below). The potential pharmacological significance of these receptor isoforms/hybrids cannot be overstated as deletion or replacement of a single amino acid can confer insensitivity to drugs or drastically alter ionic selectivity.

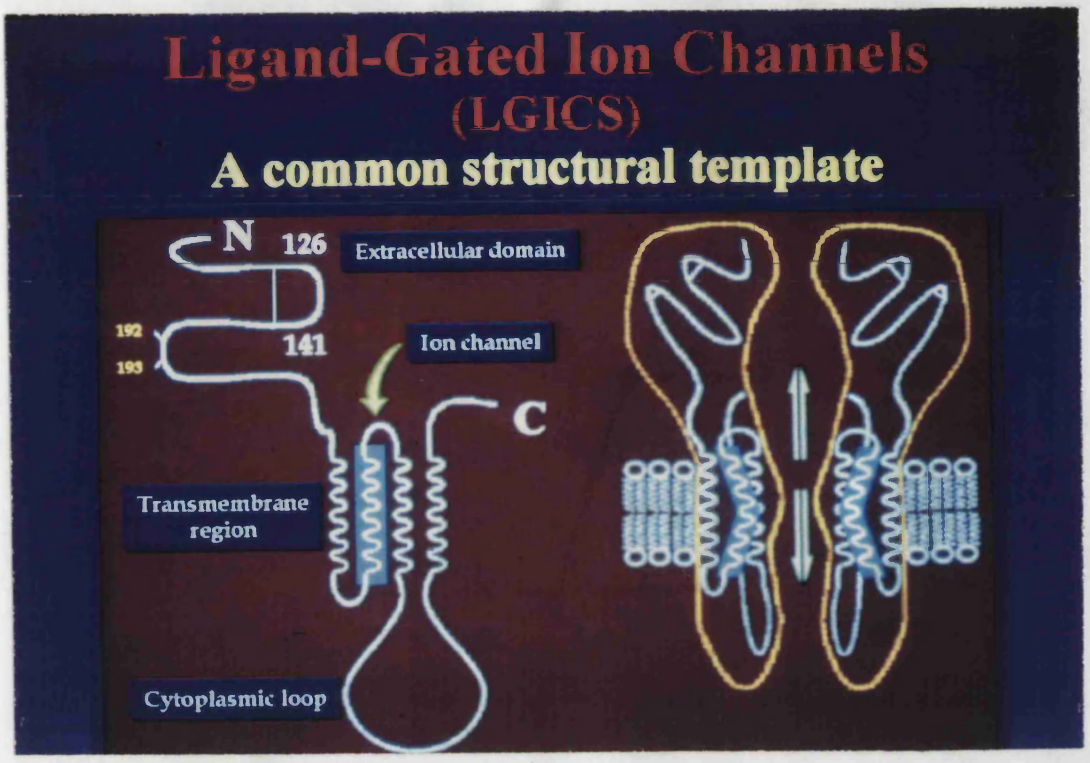

Figure 2. Structure of ligand gated ion channels.

On the left, the transmembrane orientation of an α subunit of the nicotinic acetylcholine receptor is depicted. Cysteine residues delineating domains implicated in transmitter recognition are numbered on the large extracellular N-terminal domain (126, 141, 192, 193). Hydrophobic, putative membrane-spanning segments M1-M4 are depicted in helical form with M2, thought to form the lining of the permeation pathway, with a light-blue frame. **On the right,** the tertiary subunit structure showed is based on ultrastructural evidence which suggests a kink in the M2 helix (light-blue frame) which projects hydrophobic leucine residues into the centre of the closed channel. M1, M3 and M4, at least in the nicotinic receptor, probably adopt a more condensed secondary structure than the alpha-helixes proposed in models like this.

Pictures were kindly donated by Dr. M. Ortells

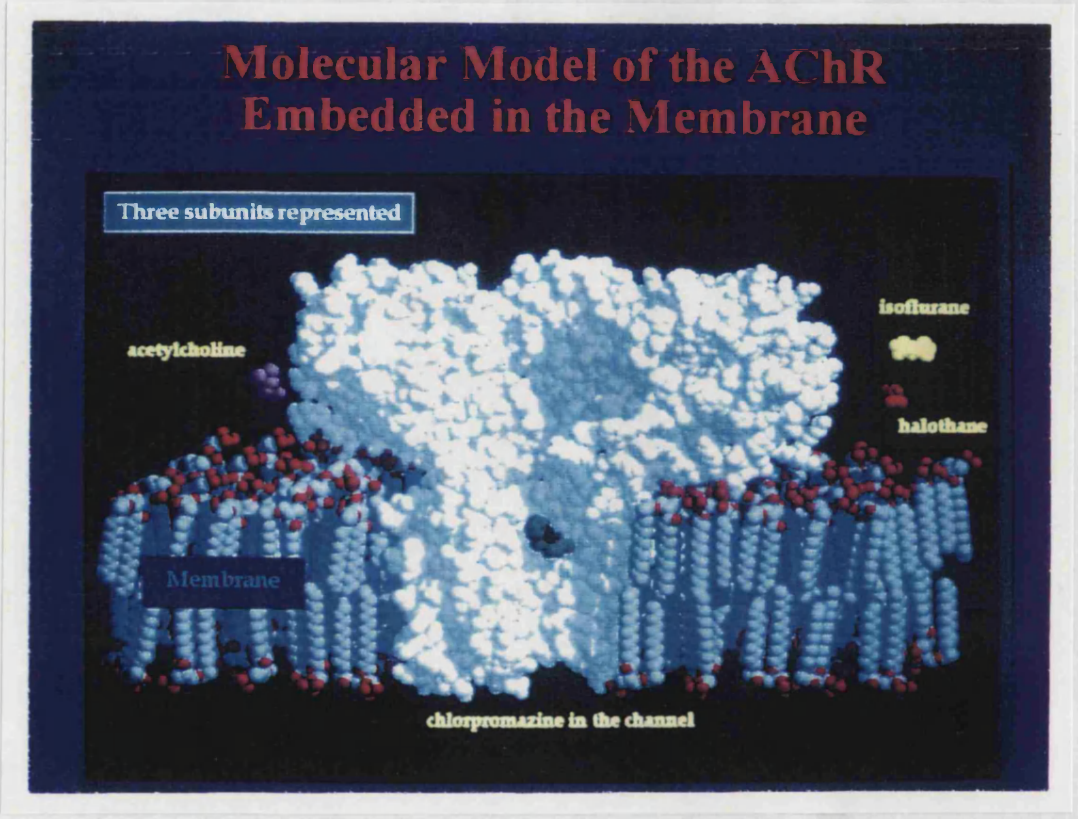

Figure 3. Molecular model of the nAChR.

Molecular graphic of the quaternary structure of the cut-away nicotinic receptor (three subunits shown). Drawn to scale at the side of the picture are acetylcholine (left), two local anaesthetics, isoflurane and halothane, and in the ion channel, the open channel blocker chlorpromazine.

Pictures were kindly donated by Dr. M. Ortells

1.3.2. The contribution of drugs and toxins to characterize nAChR diversity

The use of drugs and toxins for the analysis of nervous system function is over 100 years old. It predates the general acceptance of the theory of chemical transmission at synapses, and indeed provided much of the evidence that led to the formulation of the theory. Studies with drugs and toxins have since helped to elucidate the detailed mechanisms of neurotransmission, and to classify cholinergic receptor types and subtypes (Table 1).

Ligand	[^{125}I]-α-Bgt	MLA [^{125}I]-α-Bgt	[^{125}I]-n-Bgt	[^{3}H]cytisine [^{3}H]nicotine
Subunit	$(\alpha 1)^2\beta 1\gamma\delta$	α7	α3β2/β4	α4β2
Tissue	muscle	brain & ganglia	brain & ganglia	brain

Table 1. nAChR subtypes distinguished by high affinity (nanomolar) binding to ligands.

[^{125}I]-n-Bgt: [^{125}I]-neuronal-Bungarotoxin

The alkaloid nicotine isolated from the plant *Nicotiana tabacum* is responsible for much of the response to smoking (Whittaker, 1990). It was instrumental in the subclassification of acetylcholine receptors into muscarinic (sensitive to muscarine) and nicotinic types (Dale, 1914). However, the earliest indications that, aside from the clear distinctions between muscarinic and nicotinic cholinergic receptors, there might be diversity in nAChR came from seminal studies of the neuromuscular junction and autonomic ganglia (Paton and Zaimis, 1949). Whereas actions of nicotine at either site lead to rapid depolarization of the postsynaptic cell, some drugs, such as decamethonium (C10) and hexamethonium (C6) of the bisonium series of linked quaternary ammonium ions, were found to selectively affect nicotinic responses on muscle cells and postganglionic neurons, respectively. Central nAChR labelled by [^{3}H]nicotine and [^{3}H]ACh are pharmacologically similar to ganglionic (C6) nAChR

(reviewed by Clark, 1990). In the CNS, [^{3}H]nicotine binds with high affinity (nanomolar concentration) to the α4β2 nAChR subtype (Whiting and Lindstrom, 1987a). Similarly, cytisine, an alkaloid found in the seeds of *Laburnum anagyroides*, binds with high affinity (nanomolar concentrations) to [^{3}H]nicotine binding sites (Pabreza *et al.*, 1991), i.e. the α4β2 nAChR subtype (Flores *et al.*, 1992). What distinguishes [^{3}H]cytisine from [^{3}H]nicotine as a ligand for the same nAChR is its low rate of dissociation from its binding site, low nonspecific binding and high stability (Pabreza *et al.*, 1991).

Snakebites, such as that of the banded krait (*Bungarus multicinctus*), can be fatal because their venom contains toxin molecules that block transmission by motor nerves. Among these molecules, α-Bungarotoxin, a basic polypeptide of 74 amino acid residues with a molecular weight of 8000, irreversibly blocks the effects of acetylcholine on the muscles of vertebrates. Thus the characterization of peripheral nAChR was facilitated by the availability of this potent probe [reviewed by (Changeux, 1993)]. Therefore, α-Bgt was the former ligand used to explore nAChR in the vertebrate nervous system (Doucette-Stamm *et al.*, 1993). The toxin can be iodinated ([^{125}I]-α-Bgt) at very high specific activity, c.a. 700 Ci/mmol (Wonnacott *et al.*, 1982). α-Bgt binds to **distinct** nAChR sites in brain preparations, which do not display high affinity binding to [^{3}H]nicotine (Wonnacott, 1986). However, the identity of α-Bgt binding sites with neuronal nAChR has been controversial since the toxin was unable to antagonise nicotinic responses in neuronal preparations [reviewed by (Clarke, 1992)]. During the past few years a functional status for this nAChR subtype is beginning to emerge (see below).

Another toxin present in the venom of *Bungarus multicinctus*, κ-Bungarotoxin or neuronal Bungarotoxin (n-Bgt) has been found to block ganglionic nAChR at nanomolar concentrations (reviewed by Wonnacott, 1990). For all ganglionic preparations, n-Bgt is more potent that α-Bgt. Muscle nAChR, by contrast, have greater affinity for α-Bgt than for n-Bgt (refer to Table 1).

Methyllycaconitine is an alkaloid isolated from the seeds of *Delphinium brownii*, that displays high affinity and selectivity for the neuronal α-Bgt-sensitive nAChR (Ward *et al.*, 1990).

Therefore, [^{3}H]nicotine (or [^{3}H]cytisine) and [^{125}I]-α-Bgt discriminate two distinct populations of neuronal nicotinic binding sites (Wonnacott, 1986).

Studies aimed at the autoradiographic localization of high affinity rat brain nicotinic binding sites have used [^{3}H]nicotine, [^{3}H]ACh, [^{125}I]-α-Bgt (Clarke *et al.*, 1985) and [^{3}H]n-methyl-carbamylcholine (Boksa and Quirion, 1987). In the case of [^{3}H]ACh, acetylcholinesterase inhibitors need to be used. In addition, the nicotinic component of the binding pattern had to be discriminated from the muscarinic one by incubation of the brain slices in the presence of an excess of the muscarinic antagonist atropine.

High-affinity agonist binding sites are localized throughout the rat brain in discrete regions as shown in Table 2.

Brain region	[^{3}H]nicotine	[^{3}H]ACh	[^{125}I]-α-Bgt
Cerebellum	++	++	-
Dentate gyrus (molecular layer)	+++	+	-
Dorsal tegmental nucleus	++	++	-
Hippocampus proper	-	-	+++
Hypothalamus	-	-	+++
Inferior colliculus	-	-	+++
Interpeduncular nucleus	+++	+++	-
Layers I of cerebral cortex	+++	+	+++
Layers III,IV of cerebral cortex	+++	+++	-
Layer VI of cerebral cortex	-	-	+++
Medial habenula	+++	+++	+
Motor and sensory nuclei (thalamus)	+++	+++	-
Neostriatum	++	++	-
Presubiculum	+++	+++	-
Substantia nigra pars compacta	+++	+++	-
Superficial layers of superior colliculus	+++	+++	-
Superior colliculus	+++	+++	+++
Ventral striatum	++	++	-
Ventral tegmental area	+++	+++	-

Table 2. Distribution of high affinity [^{3}H]nicotine, [^{3}H]ACh and [^{125}I]-α-Bgt binding sites in rat brain.

+++: strong binding, ++: moderate binding, +: low binding, -: no detectable binding (Clarke *et al.*, 1985).

The maps of high affinity agonist labelling ([^{3}H]nicotine or [^{3}H]ACh) are concordant, with highest densities in the interpeduncular nucleus, most thalamic nuclei, superior colliculus, medial habenula, presubiculum, some layers of cerebral cortex, substantia nigra and tegmental area. The pattern of [^{125}I]-α-Bgt binding is strikingly different, the only notable overlap with agonist binding is in the cerebral cortex (layer I) and superior colliculus. The anatomical divergence between [^{3}H]nicotine or [^{3}H]ACh and [^{125}I]-α-Bgt distinguishes two classes of nicotine binding sites of different affinities. Displacement experiments confirmed that nicotine and ACh displace [^{125}I]-α-Bgt binding only at micromolar concentrations, this explained why the tritiated agonists (nicotine and ACh) failed to label α-Bgt sites at the nanomolar concentrations used (Clarke *et al.*, 1985).

A transitory expression of α-Bgt binding sites in thalamic input zones of primary sensory areas in neonatal rat brain (Fuchs, 1989) suggests a specific role of these nAChR in development of cortical connectivity. The distribution of high-affinity nicotine binding sites is compatible with the presence of cholinergic innervation in regions such as the cerebral cortex, dentate gyrus, thalamus, interpeduncular nucleus and medial habenula (Bayer, 1985; Shepherd, 1988).

These same radioligand regional correlations have been observed in dissected rat brain preparations (Wonnacott, 1990a). However, ligand binding assays in dissected brain preparations are more rudimentary with respect to the slice autoradiography technique which individualizes brain cell layers. For example, [^{3}H]nicotine binding sites are found in cortical layers III and IV whereas [^{125}I]-α-Bgt binding is negligible (Table 2). Conversely, [^{3}H]nicotine binding sites are not detected in layer VI of the cortex where [^{125}I]-α-Bgt binding sites are very abundant. In cortical brain preparations, in contrast, it is impossible to distinguish between layers. Thus, it is expected that brain cortical preparations will display high affinity binding for both radioligands. This is the case (Marks *et al.*, 1986). The same deduction can be made for the hippocampus where autoradiographic studies

demonstrated that only [^{125}I]-α-Bgt was able to bind with high affinity (nanomolar concentrations). However, in preparations of dissected hippocampus which included hippocampus proper and dentate gyrus, both [^{3}H]nicotine and [^{125}I]-α-Bgt binding sites are detected (Marks *et al.*, 1986).

1.3.3. Heterogeneity of neuronal nAChR subunit subtypes disclosed by molecular biology

The accessibility of the neuromuscular junction in muscle and the large abundance of analogous receptors in the electric organs of *Torpedo* initiated biochemical, molecular biological, ultrastructural and physiological approaches designed to understand the structure and function of the protein. Based on cDNA probes for muscle nAChR under conditions of low stringency, the neuronal nAChR variability began to emerge. At present, recombinant DNA technology has resulted in the identification of several genes coding for α and β nAChR subunits. Table 3 shows the nAChR subunit subtypes identified so far in chicken, rat and human (*Drosophila* and goldfish also present nAChR subunit subtype variability) as reviewed by Sargent (1993).

As presented in Table 3, in rat brain at least six different types of alpha subunits (α2-α7) and three betas (β2-β4) have been identified so far. *In situ* hybridization methods have allowed the identification of brain regions expressing these genes. In the rat hippocampus, α2, α3, α4 (Wada *et al.*, 1989), α5 (Wada *et al.*, 1990), α7 (Séguéla *et al.*, 1993) and β2 (Deneris *et al.*, 1988) nAChR subunits are moderately to highly expressed. Thus, most putative nAChR subunits are expressed in the hippocampus which is characterized by strong α7 mRNA expression.

Several lines of evidence demonstrated that the genes identified, cloned and sequenced from rat and chicken nervous tissues encode nAChR subunits (Sargent, 1993). First, non-neuronal cells express functional nAChR when injected with some combinations of these genes. Second, these genes are expressed in autonomic neurons

and in many brain nuclei from which nicotinic responses have been obtained. And third, nAChR immunopurified from brain correspond to nAChR gene products.

Species	Subunit	Probe	Mr (Kda)	Reference
Chicken	α2	chicken α1, τ	58.1	(Nef *et al.*, 1988)
	α3	chicken α2	54.8	(Nef *et al.*, 1988)
				(Couturier *et al.*, 1990)
	α4	chicken α2	68.4	(Nef *et al.*, 1988)
	α5	linkage to α3	49.0	(Couturier *et al.*, 1990)
	α6	chicken ß4	54.1	* (Sargent, 1993)
	α7	chicken α3	54.6	(Couturier *et al.*, 1990)
		α-Bgt-binding protein 1		(Schoepfer *et al.*, 1990)
	α8	chicken α7	55.2	(Schoepfer *et al.*, 1990)
	ß2	chicken α7	54.0	(Schoepfer *et al.*, 1988)
	ß3	chicken α5	50.1	* (Sargent, 1993)
	ß4	linkage to α3	53.5	(Couturier *et al.*, 1990)
Rat	α2	chicken α2	55.5	(Wada *et al.*, 1988)
	α3	mouse α1	54.8	(Boulter *et al.*, 1986)
	α4	rat α3,	67.1	(Boulter *et al.*, 1987)
		mouse α1		(Goldman *et al.*, 1987)
	α5	rat ß3	48.8	(Boulter *et al.*, 1990)
	α6	Polymerase chain reaction	53.3	(Lamar *et al.*, 1990)
	α7	" (primers: α7)	54.2	(Séguéla *et al.*, 1993)
	ß2	rat α3	54.3	(Deneris *et al.*, 1988)
	ß3	rat α3	50.2	(Deneris *et al.*, 1989)
	ß4	rat ß2	53.3	(Duvoisin *et al.*, 1989)
	non-α2#	universal oligonucleotide	56.1	(Isenberg and Meyer, 1989)
Human	α3	rat α3	54.1	(Fornasari *et al.*, 1990)
	α5	rat α5	51.0	(Chini *et al.*, 1992)
	α7	rat α7	n.a.	(Doucette-Stamm *et al.*, 1993)
				(Peng *et al.*, 1994)
	ß2	chicken ß2	54.7	(Anand and Lindstrom, 1990)
	ß4	rat ß2	51.4	* (Sargent, 1993)

Table 3. Neuronal nAChR genes.

* Sequence not published; # probably an alternatively spliced ß4; n.a.: not available

1.3.4. Purification of neuronal nAChR: from Torpedo electric organ to mammalian brain

Neuronal nAChR were immunopurified by virtue of the cross-reactivity that antibodies raised against electric tissue nAChR displayed with vertebrate muscle and

neuronal nAChR which in turn were used as antigens for the production of other antibodies. This protocol allowed the immunopurification of several putative ganglionic and central neuronal nAChR (reviewed by Sargent, 1993). Table 4A and B shows the characteristics of purified nAChR from rat brain as well as the nAChR subunits identified by matching the purified peptides with the predicted products of rat brain nAChR genes.

Rat brain nAChR were immunopurified with anti-chicken mAb 270 (refer to Table 4A and B) and were found to contain two bands on denaturing gels, 52 and 80 Kda (Whiting and Lindstrom, 1987a). The 80 Kda subunit displayed reactivity with ACh affinity alkylating agents, suggesting that it contains the ACh binding site (Whiting and Lindstrom, 1987b) and its sequence corresponds to the sequence encoded by the α4 transcript (Whiting *et al.*, 1987a). The 52 Kda subunit corresponds to the sequence encoded by the β2 transcript (Schoepfer *et al.*, 1988; Wada *et al.*, 1988). Immunoprecipitation of detergent-solubilized rat brain extracts with either mAb 270 (specific for 52 Kda band in blot) or mAb 299 (specific for 80 Kda band in blot) removed > 90% of the high-affinity [^{3}H]nicotine binding sites from solution. This suggests that an nAChR containing α4 and β2 subunits accounts for a majority of the high affinity [^{3}H]nicotine binding sites in rat brain. Similar results were obtained with antisera to α4 and β2 fusion proteins (Flores *et al.*, 1992), which removed more than 90% of the high-affinity [^{3}H]cytisine binding sites from rat brain extracts. Depletion experiments (Flores *et al.*, 1992) also proved that α4 and β2 subunits in rat must associate principally (but not necessarily exclusively) with one another.

As stated in section 1.3.2, vertebrate brain nicotinic receptors that recognize α-Bgt (α-Bgt nAChR) with high affinity are distinct from those that do not. These receptors do not display high-affinity binding for [^{3}H]nicotine (Wonnacott, 1986). α-Bgt affinity purification of α-Bgt nAChR from brain yields fractions containing 1 to 5 bands on denaturing gels in the Mr range of 45-70 Kda (Conti-Tronconi *et al.*, 1985;

Kemp *et al.*, 1985; Whiting and Lindstrom, 1987a). A component of about 55 Kda displays reactivity with ACh affinity alkylating agents, suggesting that it contains the ACh binding site of the α-Bgt nAChR (Kemp *et al.*, 1985). The other components that copurify with this subunit may represent other subunits that help form an α-Bgt nAChR heteroligomer, or they may be associated peptides or proteolytic breakdown products that are not an integral part of the native α-Bgt nAChR.

Clones encoding chicken α7 and α8 α-Bgt-binding proteins components were isolated by Couturier *et al.* (1990) and Schoepfer *et al.* (1990). The majority of α-Bgt nAChR in chicken brain contain α7 and/or α8 subunits, because mAb to α7 and α8 fusion proteins immunoprecipitate a large fraction of the high-affinity [^{125}I]-α-Bgt binding sites (Schoepfer *et al.*, 1990). An α7-specific mAb alone immunoprecipitates more than 90% of α-Bgt nAChR (Schoepfer *et al.*, 1990). Moreover, immunoadsorption of α-Bgt nAChR with an mAb to α7 does not precipitate material recognizable with mAb to α4 or β2, suggesting that α7 does not associate with α4 or β2 subunits. Although peptides unique to α5 bind α-Bgt (McLane *et al.*, 1990), it is uncertain whether α5-specific antibodies can immunoprecipitate [^{125}I]-α-Bgt binding sites from brain extracts. In chick, but not yet in mammals, α7 and α8 subunits have been immunohistochemically localized and α7 has been found to predominate in the brain, whereas α8 predominates in retina (Hamassaki-Britto *et al.*, 1993; Keyser *et al.*, 1993).

The anatomical distribution of rat brain regions expressing nAChR genes correlates with the distribution of high-affinity radioligand binding sites and with the distribution of anti-nAChR antibody binding. Thus, brain regions with high affinity [^{3}H]nicotine binding (Clarke *et al.*, 1985) have been shown to express α4 and β2 nAChR genes (Wada *et al.*, 1989) and are immunostained with anti-β2 mAb (Swanson *et al.*, 1987). A correspondence has also been found between the distribution of the α7 gene and that of high-affinity α-Bgt binding sites (Clarke *et al.*,

1985; Séguéla *et al.*, 1993). The immunohistochemical localization with mAb to α-Bgt nAChR in rat has not been performed.

Characteristics of the purified nAChR			
Purification procedure	**Mr (Kda)**	**nM binding**	**Reference**
Immunopurification with	52	[^{3}H]nicotine	Whiting and Lindstrom, 1987a
mAb 270 to chick brain	80 *		Whiting and Lindstrom, 1987b
α-Bgt affinity	1 to 5 bands	[^{125}I]-α-Bgt	Conti-Tronconi *et al.*, 1985
	(45 to 70)		Kemp *et al.*, 1985
	55 *		Whiting and Lindstrom, 1987a

Table 4A. Characteristics of nAChR purified from rat brain.

The ACh-binding sites were identified by affinity labelling with [^{3}H]MBTA (Whiting and Lindstrom, 1987b) and are indicated by *.

Purification procedure	**Correlation**	**Putative nAChR**	**Reference**
Immunopurification with mAb 270 to chick brain	N-terminal 52 Kda = β2 transcript	α4β2	Schoepfer *et al.*, 1988 Wada *et al.*, 1988
Immunopurification with mAb 299 to chick brain	N-terminal 80 Kda = α4 transcript		Whiting *et al.*, 1987a

Table 4B. Correlation of purified nAChR with nAChR genes from rat brain.

1.3.5. Functional expression of rat neuronal nAChR genes

Heterologous expression in *Xenopus* oocytes of either cDNA or mRNA coding for the rat α2, α3 or α4 gene in combination with either the β2 or β4 cDNA or mRNA results in functional nAChR (Boulter *et al.*, 1987; Wada *et al.*, 1988; Deneris *et al.*, 1989). However, injection of any one mRNA alone did not elicit any functional response, except α4, which inconsistently produced small depolarizations. The rat α5, α6 or β3 gene products likewise do not participate in the formation of functional nAChR in oocytes when injected in combination of several other α or β genes as mRNA (Deneris *et al.*, 1989; Boulter *et al.*, 1990).

Although α-Bgt is a potent antagonist at muscle nAChR, the nAChR status of α-Bgt binding sites in the central and autonomic nervous system has been controversial because a-Bgt failed to block neuronal nicotinic responses (Clarke, 1992). The cloning and expression of the α7 subunit has resolved this controversy (Couturier *et al.*, 1990; Séguéla *et al.*, 1993). Rat α7, was shown to form an α-Bgt-sensitive homooligomeric ACh-gated ion channel when expressed in *Xenopus* oocytes. The α7 nAChR is very sensitive to nicotine, **desensitises very fast** and has high relative permeability to Ca^{2+} (Couturier *et al.*, 1990; Séguéla *et al.*, 1993; Amar *et al.*, 1993; Peng *et al.*, 1994), but the α-Bgt-binding protein does not display high affinity [^{3}H]nicotine binding (Wonnacott, 1986). Therefore, the rapid desensitization may explain why brain α-Bgt nAChR have rarely been shown to function as nAChR in neurons [reviewed by (Clarke, 1992)]. The rapid desensitization (<2 sec) means that under most experimental conditions activation of α-Bgt nAChR would not be detected. Recently, using rapid drug perfusion systems, α-Bgt-sensitive currents have been demonstrated in cultured hippocampal neurons (Alkondon and Albuquerque, 1991; Alkondon *et al.*, 1992; Alkondon and Albuquerque, 1993) and ciliary ganglion neurons (Vijayaraghavan *et al.*, 1992).

1.3.6. Correlations between native and expressed neuronal nAChR with reference to the hippocampus

The ultimate goal of *in vitro* characterization of functional subunit combinations is to elucidate the composition and properties of nAChR subtypes in neurons (i.e. native nAChR).

A few early studies indicated that there are nicotinic responses in rat hippocampus (reviewed by Clark, 1990). At this time, the heterogeneity of nAChR subunits was largely unknown. It is unlikely that these nicotinic responses correlated with the α7 nAChR because of the slowness of the drug application technique. This problem was overcome with a rapid perfusion (Alkondon and Albuquerque, 1991) system. Thereafter, some clues regarding the identity of the subunits comprising the hippocampal nAChR were obtained by comparing the properties of the nicotinic currents (whole-cell current recordings) in hippocampal neurons with those elicited by nAChR expressed in *Xenoups* oocytes (Alkondon and Albuquerque, 1993). The fast desensitization displayed by the majority of the neurons (93%) in culture resembles those from the reconstituted α7 homooligomer in *Xenopus*. In addition, native and reconstituted channels are blocked by α-Bgt (10 nM) and MLA (1 nM). Therefore, the similarities between the characteristics of α-Bgt-sensitive currents in neurons and those reported for currents evoked from nAChR reconstituted from α7 subunits, could arise from activation of nAChR assembled from α7 nAChR subunits. In hippocampal cultures, n-Bgt-sensitive currents were also observed in 15% of the neurons (10% of these cells also expressed α-Bgt-sensitive currents) probably reflecting the α3β4 nAChR. Only 2% of the neurons had nicotinic currents blocked by mecamylamine but unaffected by either snake toxin probably elicited by the high affinity [^{3}H]nicotine site, i.e. α4β2 nAChR..

However, attempts to match native nAChR with heterologously expressed nAChR of defined composition have failed in some other rat brain regions (reviewed by Sargent, 1993). The inference regarding the subunit composition of the receptors

generating different types of currents are made with the assumption that the oocyte expression system reflects the properties of the native receptor. Do oocytes faithfully translate mRNA and modify and assemble their translation products?. Results from experiments on muscle nAChR suggest that oocyte can translate and assemble subunits for muscle nAChR accurately (reviewed by Lingle *et al.*, 1992). If the oocytes are not at fault, then the failure to match native and expressed nAChR may mean that additional nAChR genes are yet to be identified or that native nAChR consist of subunit combinations that have not been tested in oocytes.

1.4. Putative role of Ca^{2+} in neuronal regulation

To perform their communication function, neurons have evolved complex, specialized arrays of signalling and regulatory mechanisms, many of which include a central role for Ca^{2+}. Two main pathways promote Ca^{2+} entry through the neuronal membrane, namely voltage-gated Ca^{2+} channels and channels associated with the N-methyl-D-aspartate (NMDA)-sensitive glutamate receptor (reviewed by Bliss and Collingridge, 1993). Experimental evidence is attributing this role to nAChR as well (see below).

Voltage-gated calcium channels

Voltage-gated Ca^{2+} channels generate Ca^{2+}-dependent action potentials in dendrites, allow Ca^{2+} entry that initiates neurotransmitter release and other intracellular regulatory processes. In addition, voltage-gated Ca^{2+} channels play a pivotal role in the control of neuronal firing patterns and excitability. Four physiologically distinct classes of voltage-sensitive calcium channels have been identified (reviewed by Lees G. *et al.*, 1994); these are designated as T, L, N and P (Table 5). All these channels activate from their resting states in response to cellular depolarisation then turn off, by an independent mechanism; if the stimulus is sustained: both processes can occur at very different rates and differ in their voltage-dependence. The selectivity of electrically-operated Ca^{2+} channels is based on the

presence in the channel of a binding site. The binding of the penetrating ion to this site is necessary for its permeation through the channel; however, if the binding is too strong, the permeant ion becomes a channel blocker. The blockade of Ca^{2+} channels by Co^{2+}, Cd^{2+}, Ni^{2+} and related ions is based on this principle (reviewed by Kostyuk, 1989 and Lees *et al.*, 1994).

Nomenclature	Symbol	Activation	Inactivation	Blockers	Modulators
T (low voltage activated)	T	Rapid	Yes	Ni^{2+} ω-conotoxin?	Neurotransmitters
L (high voltage activated)	L	Slow	Slow/none	Ca antagonists	G-proteins
N (neuronal)	N	Intermediate	Intermediate	ω-conotoxin	Kinases
P (Purkinje)	P	High voltage	Slow	Funnel web toxin	Phosphatases

Table 5. Diversity of voltage-gated Ca^{2+} Channels

In the rat hippocampus all four (T-, L-, N- and P-type) Ca^{2+} channels have been identified (Luebke *et al.*, 1993). Evidence for the involvement of multiple Ca^{2+} channels types in the control of synaptic transmission in the nerve terminal have been reported (Miller, 1987; Luebke *et al.*, 1993). Ca^{2+} imaging techniques have revealed a postsynaptic, voltage-dependent Ca^{2+} entry pathway in the dendrites of *CA1* and *CA3* pyramidal neurons (Jaffe *et al.*, 1992; Regehr and Tank, 1992). What role these postsynaptic Ca^{2+} channels play is unknown.

During the development in culture of embryonic hippocampal cells only low-threshold, metabolically-independent Ca^{2+} channels can be detected in their membrane; later on when dendrite-like neurite outgrowth starts, the high threshold metabolically-dependent channels also appear. In the soma and dendrites of hippocampal neurons, repetitive activation of high-threshold Ca^{2+} channels induces a large increase of $[Ca^{2+}]_i$ (reviewed by Kostyuk, 1989).

nAChR Ca^{2+} permeability

The use of fluorescent Ca^{2+} indicators together with electrophysiological studies have revealed variations in $[Ca^{2+}]_i$ in response to nicotinic agonists. nAChR from muscle (reviewed by Muelle *et al.*, 1992) and chromaffin cells (Zhou and Neher, 1993) are known to permeate not only monovalent but also divalent cations. In rat medial habenula (Mulle *et al.*, 1992) and cortical neurons (Fluhler *et al.*, 1992; Deadwyler *et al.*, 1992), nicotine-evoked Ca^{2+} changes lead to Ca^{2+} influx into the cell. Such increases in $[Ca^{2+}]_i$ have been attributed either to Ca^{2+} entering through the nAChR or closely coupled Ca^{2+}-permeable channels. In ganglia, extrasynaptic α-Bgt binding sites have recently been shown to elevate intracellular Ca^{2+} levels in response to agonists (Vijayaraghavan *et al.*, 1992) and to function as ligand-gated ion channels (Zhang *et al.*, 1994). α7 Homooligomeric channels expressed in *Xenopus* have been found with relative Ca^{2+} permeability larger than that of non-α7 nAChR and NMDA channels (1.3.5.). Therefore, Ca^{2+} permeability through nAChR or coupled voltage-gated Ca^{2+} channels on neurons suggests involvement in longer term regulatory processes.

These observations imply that nAChR may influence a variety of cellular events using Ca^{2+} as a second messenger, as for example neurite extension and synaptic remodelling and, in the case of Ca^{2+} load, cell death (Lipton and Kater, 1989). Recent studies have demonstrated that nicotine inhibits neurite outgrowth of PC12 cells in culture by interacting with α-Bgt nAChR since this effect is prevented in the presence of α-Bgt (Chan and Quik, 1993).

Some excitatory neurotransmiters can stimulate sprouting or pruning of dendrites. While such diverse effects potentially allow a fine control of neuronal plasticity, they also raise the risk of neurotoxicity. There is evidence that neurotransmitters exert this effect largely by modulating levels of specific second messengers such as intracellular free Ca^{2+} (Lipton and Kater, 1989; Lauder, 1993). The fact that neurotransmitter receptors develop before synaptogenesis (Ben-Barak

and Dudai, 1979), lends additional evidence to the premise that modulation via these receptors may influence synaptogenesis.

1.5. Summary to chapter 1

The embryonic hippocampus provides a rather homogeneous population of neurons. Most putative nAChR subunits are expressed in the adult hippocampus and electrophysiological together with biochemical studies have demonstrated functional nAChR in this brain region.

The adult rat hippocampus displays dense [^{125}I]-α-bungarotoxin ([^{125}I]-α-Bgt) labelling and strong expression of α7 mRNA. The α7 gene product is an α-Bgt binding protein which forms homooligomeric channels responsive to ACh and nicotine in *Xenopus* oocytes. The α7 nAChR desensitize rapidly, and have high permeability to Ca^{2+}. Electrophysiological studies have disclosed similar α-Bgt-sensitive channels in hippocampal neurons. Thus, this preparation offers the prospect of biochemical studies of functional α-Bgt-sensitive nAChR whose physiological role is unknown.

1.6. The aim of this thesis

The goals of the present work were:

(a) To define a system for culturing hippocampal neurons from rat fetuses suitable for functional and biochemical analyses of their nAChRs. This requires a predominantly neuronal population of cells with a survival of several weeks to permit long term studies.

(b) To characterize nAChR subtypes in hippocampal neuronal cultures, establishing the amount, subtype distribution among cell types and their functional status.

(c) To compare nAChR from hippocampal and cortical neuronal cultures.

(d) To assess nAChR expression in hippocampal glial cultures.

Chapter 2
Establishment of rat hippocampal dispersed cell cultures

2.1. Introduction

Tissue culture as a reductionist tool

The science and application of tissue culture in neurobiology began together in the laboratory of Ross G. Harrison (Harrison, 1907) when fragments of frog neural tube were cultured for the first time. The demonstration that tissue could survive outside the body created widespread interest. Thereafter technical advances have continued and tissue culture is now an integral part of modern neurobiology.

The vast heterogeneity of both the neuronal and glial elements which constitute the nervous system has proved to be a major barrier to studies intended to elucidate the precise physiological function underlying the biochemistry of individual subclasses of neurons and glia. As in many other systems, tissue culture has been widely used in attempts to simplify such studies.

Cultures prepared from tissue taken directly from the animal are referred to as primary cultures. The way the tissue is dissected and prepared depends on experimental demands. According to this, several types of primary cultures have been developed. Organ, slice and explant (fragment) cultures have been favourite preparations for investigations requiring the greatest degree of original histotypic organization. Dissociated cell (attached) and reaggregated (in suspension) cultures have been preferred for those studies demanding cell accessibility and cell subset purification. Regardless, of the type of culture, all methods share several requirements. Preparations must be plated on a suitable substrate and maintained in an appropriate medium, temperature and atmosphere. In primary cultures, cells divide or not depending on their nature and the culture conditions, acquire differentiated

characteristics and ultimately die. For the next experiment, it is necessary to prepare new cultures.

As with all *in vitro* studies, tissue culture presents limitations. Whether the specific culture conditions allow physiologically relevant phenotype expression is uncertain. Dissociated cell cultures constrain neurons to grow in two dimensions. Neurons are unable to interact with many of their neuronal afferents and targets cells; and they are grown in a foreign medium and substrate. Nothing of the intricate architecture of the brain, with its organized layers of cells and fibers, is retained. However, the morphological and physiological properties of the cell populations present in culture correspond closely to the characteristics of their counterparts *in situ* (Banker and Cowan, 1977; Banker and Cowan, 1979; Kriegstein and Dichter, 1983; Banker and Waxman, 1988). Some few examples include, astroglial cell production of glial fibrillary acidic protein (GFAP), neuronal postmitosis, neuronal expression of action potentials, neurofilaments and process formation. It is generally agreed (reviewed by Banker and Goslin, 1991) that most phenotypes expressed *in vitro* by neuronal cells are responses to the extrinsic regulation imposed by the specific culture environment and that, as such, they may represent phenotypes expressed *in vivo* .

Although widely used, primary cultures are not ideal for all purposes. The amount of material that can be obtained limits biochemical analyses, and because most primary cultures contain an heterogeneous population of cell types, interpretation of such experiments can be ambiguous. Moreover, most genetic engineering techniques are simply not applicable to primary neuronal cultures. Because postmitotic neurons in primary cultures do not divide, mutant cells cannot be propagated and, with few exceptions (Geller and Freese, 1990), foreign genes cannot be stably integrated into the genome.

An alternative approach to primary culture is the use of cell lines derived from neuronal tumours. Unlike primary cells, cell lines can be grown indefinitely in cell culture. Cell lines can be stored frozen and thawed upon requirement. Their

maintenance often involves plating into untreated standard tissue culture dishes, feeding and subculture until the desired number of cells is reached. Then, they can be induced to differentiate, ceasing division and acquiring mature phenotype. Clonal cell lines are also electrically active, synthesize and expresses transmitter receptors [reviewed by (Lendahl and McKay, 1990)]. Moreover, since all cells in a cell line are clonal, they represent an almost uniform cell type, which has important implication for their use as experimental tools. Recent technical progress allowed the immortalization of cell populations by somatic cell fusion with a tumour cell line. Such cell lines retain features of the cells from which they originated [reviewed by (Geller *et al.*, 1991)]. The advantages of using cell lines must be weighed against the fact that many important aspects of neuronal differentiation are not expressed by tumoral cell lines.

The model system

Hippocampal cultures have offered a useful model system for cell biological studies of CNS neurons such as, the establishment of neuronal polarity (Bartlett and Banker, 1984a; Caceres *et al.*, 1984; Caceres *et al.*, 1986; Davis *et al.*, 1987; Davis *et al.*, 1990), the properties of dendrites (Dotti and Banker, 1987; Dotti *et al.*, 1988; Goslin *et al.*, 1988; Goslin *et al.*, 1990; Kleiman *et al.*, 1990), axonal outgrowth (Harel and Futerman, 1993) and synaptogenesis (Bartlett and Banker, 1984b). The effects of neurotransmitter, electrical activity, cellular regulation by calcium and the classical messenger systems on the outgrowth, architectural remodelling, and degeneration of cultured embryonic hippocampal pyramidal neurons have been intensively studied [reviewed by (Mattson, 1988)]. Hippocampal embryonic cultures have also been used for studying the role of growth factors (Walicke *et al.*, 1986; Mattson *et al.*, 1989; Ip *et al.*, 1991), platelet-activating factors (Haruhiko *et al.*, 1992) and neurotoxicity of peptides (Forloni *et al.*, 1993). This *in vitro* system has also been employed as a model for studies of LTP (Zilberter *et al.*, 1990; Malgaroli

and Tsien, 1992; Bliss and Collingridge, 1993) and Alzheimer's disease (Mattson *et al.*, 1993).

With regard to the neurotransmitter receptors, NMDA receptors (Segal, 1992), $GABA_B$ receptors (Pfrieger *et al.*, 1994), NMDA-associated glycine binding sites (Lester *et al.*, 1989), kainate receptors (Werner *et al.*, 1991) and muscarinic AChR (Kudo *et al.*, 1988; Iijima *et al.*, 1990; Fiszman *et al.*, 1991) have been described in hippocampal neurons cultured from fetal rats.

In particular, characterization of various nAChR channels has been performed in this system using electrophysiological techniques (Alkondon and Albuquerque, 1991; Alkondon *et al.*, 1992; Alkondon and Albuquerque, 1993). This has motivated the application of several other approaches that were carried out in this study.

Cell lines used for studying nAChR are of muscle [BC3H1 (Ashizawa *et al.*, 1982); TE671 (Lukas, 1991)] or autonomic [PC12 (Robinson and McGee, 1985)] origin, and therefore unrepresentative of CNS neurons. M10 cells, a mouse fibroblast cell line, has been stably transfected with the α4 and β2 nAChR subunit subtypes (Whiting *et al.*, 1991). Although providing a central receptor, the subunits are of avian origin. At the time the present study was begun, no brain cell line had been characterized with respect to nAChR, therefore primary cultures of brain neurons were the chosen system; these needed to be established and characterized. However, it has been possible to immortalize mouse hippocampal neurons (Lee *et al.*, 1990). Very recent results showed that this hippocampal cell line [HN33] expresses low levels of mRNA for the nicotinic subunits α3, α4 , α5, β3 and β4 and low levels (14 fmol/mg of protein) of [^{3}H]cytisine binding (Monteggia *et al.*, 1993). One of the reasons for the lack of expression of these mRNA nAChR might be the probe used since mouse neuronal nAChR sequences have not been cloned (refer to section 1.3.3.). It has also been observed that HN33 cells exhibit weak or no functional responses to nicotine (Briggs *et al.*, 1993). Moreover, the α7 mRNA is not expressed in this particular cell line making it unsuitable for the objectives of this thesis.

Unlike other brain regions such as cortex, the hippocampus has a relatively homogeneous population of pyramidal neurons (Banker and Waxman, 1988), and by manipulating the culture conditions it is possible to enrich further for a particular cell type, thus enhancing the certainty of cell assignment of a functional response. Moreover, rat hippocampal cultures are typically prepared from fetuses at embryonic day 18 [E(18)] because at this stage the generation of pyramidal neurons (which begins in the rat at about embryonic day 15) is essentially complete, but the generation of dentate granule cells (which largely occurs postnatally) has scarcely begun (Banker and Cowan, 1977; Schlessinger *et al.*, 1978; Bayer, 1980). Moreover, the number of glial cells is still modest since most of the gliogenesis occurs postnatally (Goslin and Banker, 1991). However, several groups have succeeded in culturing postnatal rat hippocampal neurons [1-2 day old] (Zorumski *et al.*, 1992). This preparation necessitates the use of antimitotic drugs and yields a much more heterogeneous cell population. Therefore, dissociated cell primary cultures from E(18) rats provide a good model for performing biochemical, immunocytochemical and functional studies in hippocampal neurons.

The present chapter focuses on the establishment of enriched primary hippocampal neuronal cultures. The establishment of glial cultures was carried out to assess their influence on neuronal cultures and for use as controls for further investigations. Finally, cortical cultures were established based upon the optimised conditions developed for culturing hippocampal cultures. Cortical cultures were produced in order to compare the results obtained from the nAChR characterization in hippocampal neuronal cultures as presented throughout this thesis. Culture protocols were based on different reports.

2.2. Experimental Procedures

Tissue culture manipulations were performed under sterile conditions.

2.2.1. Materials

Wistar rats at eighteen days of gestation were provided from Bath University Animal House breeding colony.

Media recipes are presented in the appendix A to this thesis.

For the purpose of coating dishes, a 5% (w/v) aqueous stock solution of polyethylenimine (PEI, Sigma Chemical Co. Ltd, Poole, Dorset, U.K.) was filter sterilized and stored at $4^{o}C$. On the day of the dissection it was diluted 1:100 in sterile borate buffer (150 mM, pH 8.3) and 0.5 ml was added to each 16 mm multiwell dish (Gibco BRL, Paisley PA3 4EF, Renfrewshire, Scotland). Two hours later, the dishes were washed in double distiled sterile water by first adding 1 ml of water, removing this immediately and then adding a further 1 ml of water. This was left for at least half an hour. Finally, wells were pre-incubated with plating media (see Appendix A).

To coat with poly-L-lysine (PLL), the same procedure as described above was used but a 0.4% (w/v) aqueous stock filter sterilized solution of PLL was stored at $4^{o}C$ and used diluted 1:20.

Monoclonal antibodies against GFAP (mAb-GFAP/IgM) and neurofilament (mAb-ANF/IgG) plus control cloning medium were produced and kindly provided by Dr. A. Rogers (Rogers, 1988).

Fluorescein isothiocyanate anti-mouse conjugate immunoglobulin G and M (IgG-FITC; IgM-FITC, respectively) were purchased from Sigma.

Vectashield, mounting medium for fluorescence, was purchased from Vector Laboratories, Peterborough, UK.

Cultures were photographed (400 ASA Kodak film) with a Nikon Diaphot inverted phase contrast microscope equipped for epifluorescence.

2.2.2. Methods

2.2.2.1. Tissue culture

Dissection of the cortices and hippocampi

Rats were sacrificed by cervical dislocation and the entire uterus containing the fetuses was removed. Starting from one end of the uterus and working along, each fetus was separated one at a time by cutting the umbilical cord. The fetuses were decapitated and the heads were placed in Dulbecco's Modification of Eagle's Medium (DMEM). The brains were removed and immersed immediately into fresh DMEM.

As shown in Plate 1, hippocampi were microdissected under 20x magnification using very fine spring scissors (Castro-Viejo style with angled blades) and Dumont-style forceps (N°5) by separating the cerebral hemispheres from the diencephalon and brainstem (Plate 1A). Once the thalamus was removed, the hippocampus ("C" shaped) could be seen on the posterior half of the hemisphere, beginning near the dorsal surface rostraly, then curving ventrally and caudally (Plate 1B). At this stage the meninges were removed in one piece. The hippocampi were dissected by cutting the boundary between the hippocampus and the adjoining cortex (Plate 1C). Hippocampi were placed into a 35 mm Petri dish containing DMEM for further cell dissociation. In order to prepare cortical cultures, the remainder cortices (without the hippocampi) were placed into a 35 mm Petri dish containing DMEM for further cell dissociation.

Plate 1: Dissection of the embryonic rat hippocampus.

A: ventral aspect of the brain of an 18 day old fetus, with olfactory bulbs (o.b.) at the top. Arrowheads demarcate the junction between the diencephalon and the left cerebral hemisphere. The dotted line indicates the approximate position of the right hippocampus projected onto the ventral surface of the hemisphere. **B**: the left hemisphere is viewed from the midline, with anterior to the right after the removal of the meninges. Arrowheads indicate the boundary between the hippocampus and the adjoining cortex. Small arrows mark the free edge of the hippocampus. **C**: the left hippocampus after it has been removed.

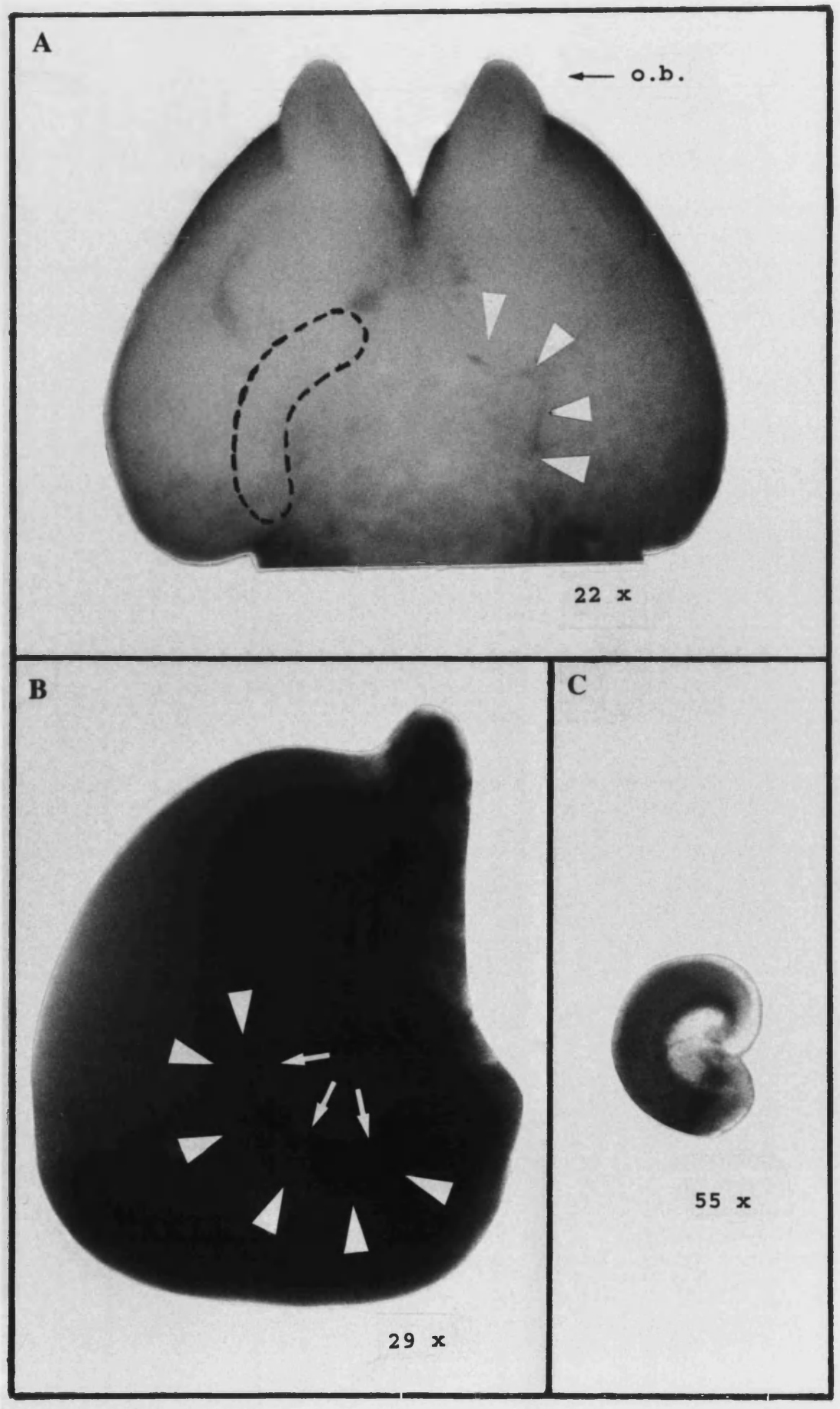
A
o.b.
22 x
B
29 x
C
55 x

Cell dissociation

The hippocampi were cut into pieces and transferred into a 12 ml test tube, the volume was made up to 10 ml with sterile phosphate-buffered saline pH 7.4 (PBS, refer to the appendix E) and the pieces were allowed to settle to the bottom of the tube. The PBS was removed without disturbing the pieces and the volume was made up to 2 ml with more PBS. Tissue was incubated in the 37°C water bath for 20 min with 50 µl of D-glucose 20% (w/v) and 200 µl trypsin 1% (v/v) (ICN Flow, Thame Oxon OX9 3XA, U.K.). Trypsinization was finished by adding 8 ml of serum supplemented defined medium. Cell suspensions were obtained by triturating the tissue with a fire-polished Pasteur pipette. Once a cloudy suspension was obtained, 8 ml of serum supplemented defined medium was added and the preparation was centrifuged for 8 min at 1500 rpm. Cells were resuspended in 1 ml of serum supplemented defined medium. At this stage the cells were ready to be plated.

When cortical cultures were prepared, the procedure to dissociate the cells was followed exactly as described above for hippocampal cells.

Plating, feeding and maintenance of hippocampal neuronal cultures

The fraction of viable, trypan-blue (1.5% (w/v)) excluding cells, was determined by counting with an hemacytometer. To achieve the maximum cell survival, the plating density, coating surface treatment, plating and feeding media conditions were empirically determined. The effects of these conditions with respect to culture viability was followed by visual inspection in parallel cultures.

Hippocampal cell suspensions were plated in either PEI or PLL coated 16 mm dishes at a density of 25×10^3; 12.5×10^4 and 25×10^5 cells/cm^2.

Three alternative media that differed on the supplementation of 10% FCS and/or hormones were tested (for media composition, refer to the appendix A). Cell suspensions were either plated in serum supplemented medium or serum supplemented defined medium. Under the latter condition, cells were allowed to

attach to the culture well before the medium was replaced by serum-free chemically defined medium. The time required for proper cell attachment was empirically determined. It ranged from 1 to 4 h.

Cultures were incubated at 36°C in an atmosphere containing 95% O_2 - 5% CO_2 and fed every four days by replacing half the volume of medium with fresh medium.

Additionally, to stop glial cell proliferation, anti-mitotic agents [5'fluorodeoxyuridine 0.02% (w/v), uridine 0.04% (w/v) (5'FDU)] were added to cultures grown in serum supplemented medium after three days in culture.

Plating, feeding and maintenance of cortical neuronal cultures

Cortical cell suspensions were plated at an initial density of 2 x 10^5 cells/cm^2 in serum supplemented chemically defined medium. After 2 h, cultures were switched to serum-free chemically defined medium.

Cultures were incubated at 36°C in an atmosphere containing 95% O_2 - 5% CO_2 and fed every four days by replacing half the volume of old medium with fresh medium.

Glial cells, glial conditioned medium and hippocampal neuron-glia cell co-cultures

Astrocyte-enriched cultures were prepared in order to follow the effect of glial conditioned medium on hippocampal neurons and to use as controls for further studies. As an alternative approach, hippocampal neuron-glial cell co-cultures were prepared to test the influence of glial cells on hippocampal neuronal cultures.

To select for glia, hippocampal cell suspensions were plated in PLL coated dishes with serum supplemented medium (refer to the appendix A). Cultures were incubated at 36°C in an atmosphere containing 95% O_2 - 5% CO_2 and fed every three days with serum supplemented medium. On reaching confluence (9 days approximately) and for a further ten days, medium was collected and stored at 4°C every time old medium was changed. This "conditioned" medium was warmed up and

used in some hippocampal neuronal cultures, either neat or diluted (1:1 or 1:2) with feeding medium, i.e. serum supplemented medium or serum-free chemically defined medium.

To prepare glial cultures for co-culture with hippocampal neurons, hippocampal cell suspensions were plated on PLL coated 13 mm round glass coverslips (Propper Ltd, Warley, UK) with paraffin sits (dots) to fit 16 mm dishes (Goslin and Banker, 1991). Three dots of paraffin (about 0.5 cm high) were placed near the outer edge of each coverslip at about an equal distance from each other to support the coverslips during co-culture. To apply dots, paraffin was heated to about 80^{o}C, a Pasteur pipette was dipped into the hot paraffin until it filled. Dots were generated by touching the coverslip with the paraffin-filled pipette tip. A few seconds were allowed for the paraffin to dry. At this stage, coverslips were ready to be transferred to the dishes. Subsequently, serum supplemented medium was added to the culture well. Dishes were left in the incubator (36^{o}C; 95% O_2 - 5% CO_2) until the moment of plating the cells. Glial cells were fed with serum supplemented medium every three days. On reaching confluence (9 days approximately) they were ready to be used in co-culture. As described in Figure 4, glass coverslips with glial monolayer growing on top of them were added to hippocampal neuronal cultures with the glial monolayer facing the neurons (Goslin and Banker, 1991). The transference of glia to hippocampal cultures was done immediately after hippocampal cultures were switched to serum-free chemically defined media.

Confluent glial cell monolayers were renewed every two weeks to avoid macrophage proliferation as these have been reported to produce compounds that are metabolized to highly toxic peroxides (Giulian and Baker, 1986; Giulian, 1987).

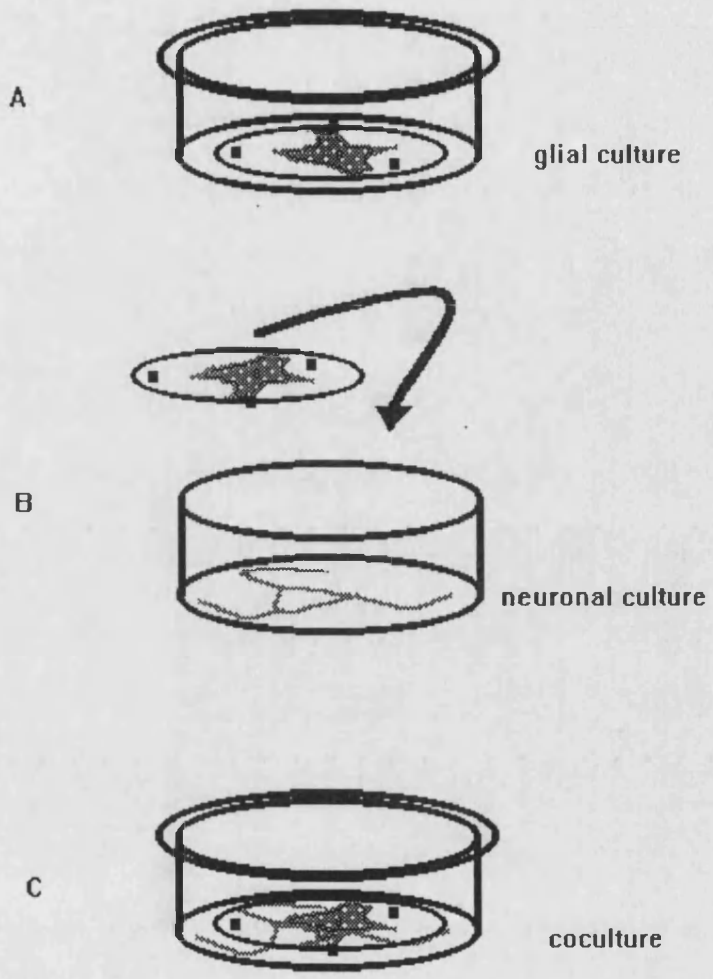

Figure 4: Representation of hippocampal-glial co-cultures.

A: three dots of paraffin of about 0.5 mm high were placed near the outer edge of each coverslip at about an equal distance from each other. Coverslips were placed in 16 mm multiwell dishes with the dots facing up and coated with PLL. Glial cells were plated and maintained in SSM until 100% confluence was achieved.

B: Coversilps of confluent glial culture are inverted over hippocampal cultures grown in serum free medium.

C: Hippocampal-glial co-cultures. Confluent glial culture facing plated hippocampal cells.

2.2.2.2. Characterization of the cultures

Morphological characterization of hippocampal neuronal cultures

The morphological appearance of hippocampal neurons was compared following a previous study (Banker and Cowan, 1979). According to it, neurons were grouped into three broad classes and the relative frequency of each class of cells was obtained. Four different cultures grown under optimised conditions were studied. Two different fields from each of those cultures were photomicrographed at 400x. The mean relative frequency and standard error for each morphological neuronal type was obtained by direct count.

Morphological characterization of cortical cultures

The morphological classification of cortical cultures was performed according to a previous study (Kriegstein and Dichter, 1983). The relative frequency of each neuronal cell type was determined as described for hippocampal neurons.

Total protein assays

The method used to determine was based on a modified Lowry (Lowry *et al.*, 1951) protein assay to allow protein quantification in membrane and lipoprotein samples (Markwell *et al.*, 1978). Standard curves were performed over the range 0-200 μg of protein, using bovine serum albumin (BSA) as the standard. Cells were first dissolved in 200 μl SDS solution (refer to the appendix E). After adding Folin and Ciocalteau's phenol reagent (Sigma) and incubating for 45 min at 20°C, the optical densities were read in a Multiskan MCC machine (Labsystems, UK) at 680 nm. A standard curve was constructed by linear regression analysis and protein values derived from this.

Neuronal cell counting

To correlate the amount of total protein with the number of neurons in culture a 0.5 cm graticule with 1:10 divisions to count the neurons without disturbing the cultures was used. In order to evaluate the minimum quadrant size to be measured, the mean-squares method (Greig-Smith, 1952) was used. In this method, a basic unit of

measurement is defined (0.25 mm^2 in this case, the minimum measurable unit size). Ten locations in the culture dish were chosen at random and the number of cells within the surface of a basic unit was measured. Starting from each of these 10 basic units, oblong pairs of two adjacent basic subunits (one of which was the originally randomly chosen) were formed (0.5 mm^2) and the number of cells within it counted. In turn, two of these pairs were combined into blocks of four (1 mm^2) and so on until an oblong block of 32 mm^2 was formed. The variance/mean ratio is then plotted against quadrant size. The minimum quadrant size to be measured is considered that where no further variation in the variance/mean ratio is observed. The variance/mean ratio was also used to determine the type of distribution. Regular distributions have a variance/mean ration equal to 1, whilst random and aggregated distributions have ratios below and above the unity respectively. This procedure was used in three different dishes.

Neuronal and glial markers

The presence of glial and neuronal cells in a culture dish was tested using immunocytochemical techniques as previously described (Rogers, 1988). Glial cells were detected with mAb-GFAP, whereas neurons were identified using mAb-NF.

The following procedures were carried out at room temperature. Cultures were washed three times in PBS and were fixed and permeabilized with the 5% acetic acid-70% ethanol solution method as described in the appendix C to this thesis. Subsequently, cells were gently washed three times in PBS and 0.5 ml of blocking mixture (1% normal goat serum in PBS) was added (1 h). Monoclonal antibody supernatant to the intracellular neurofilament or glial fibrillary acidic protein was applied to cultures neat (1 h). Cloning control medium was used to determine non-specific staining. Samples were washed three times in blocking mixture and 250 µl of second antibody (anti-mouse IgG/M Fit C, diluted in PBS 1:100) was added. After one hour, cells were washed three times in PBS, mounted with Vectashield (Vector Laboratories) and photomicrographed.

2.3. Results

2.3.1. Tissue culture

Establishment of hippocampal neuronal cultures

In order to optimise the conditions for growing primary hippocampal cultures, different conditions and media were tested and compared by visual inspection under a phase contrast microscope.

Obtaining successful neuronal cultures strongly depended on finding the appropriate substrate. Comparative pictures of cultures maintained under the same conditions but plated in PEI coated or non-coated dishes are shown in Plate 2. Coated dishes allowed neuron attachment in a monolayer arrangement and extension of processes. When dishes were not coated, the cells failed to adhere to the culture dish surface and formed aggregates in suspension that eventually adhered very loosely to the surface. Under the latter conditions, neurons did not survive for more than 5 days, whereas PEI or PLL coated plates extended neuronal survival from one to seven weeks depending on the plating density and the medium employed. Moreover, non-treated surfaces proved also to be suboptimal for culturing glia.

PEI and PLL coated dishes were also compared. When cells were plated in PEI coated dishes, neurons settled and attached in 5 min to the bottom of the dish, while with PLL up to 3 hours had to be allowed. Also, when cultures were grown in PEI coated dishes, the contribution of glial cells to cultures was smaller than when culturing on PLL coated dishes. Although treating dishes with PEI proved to be more effective in selecting for neurons, culture viability still depended on other factors as described below.

Plate 2: Neuronal distribution with and without coating surfaces.

A: 2 day old hippocampal neuronal cultures growing in polyethylenimine (PEI) coated dishes in a monolayer arrangement and extending processes. **B**: 2 day old hippocampal neuronal cultures growing in uncoated dishes formed clumps and did not survive for more than 5 days. **Bar: 50 μm.**

Almost 95% of the cells in the hippocampal suspension excluded trypan-blue. This maximum proportion of viable cells was obtained when the steps between sacrificing the pregnant rat and placing the cells in culture was completed in less than two hours. Even so, each pregnant rat yielded at most 8 x 10^6 viable hippocampal cells (approximately 5 x 10^5 cells per fetus). Thus, the lowest plating density was sought in order to achieve the maximum number of independent viable cultures. Plating densities ranging from 2.5 x 10^4 to 2.5 x 10^5 cells per cm^2 were compared. Low density cultures obtained at plating densities below 5 x 10^4 cells/cm^2 showed an increase in the mortality rate in comparison with high density cultures as judged by cell counting. However, cultures plated above 1.5 x 10^5 cells/cm^2 showed considerable neuronal aggregation. As further immunological characterization of cultures required the ability to discriminate between individual cell bodies, aggregated cultures were unacceptable. The optimum plating density was found to be between 1.25 x 10^5 to 1.5 x 10^5 cells per cm^2. At these densities, neurons displayed an almost random distribution and neuronal aggregation was minimal.

In addition, long-term enriched neuronal cultures were strongly dependent on the media employed as summarized in Table 6.

When hippocampal cell suspensions were plated in PLL treated dishes and grown in serum supplemented medium, glial cell division was triggered by mitogenic agents in serum. This resulted in enriched glial cultures and neuronal death as shown in Plate 3. The application of anti-mitotic drugs to cultures inhibited glial proliferation. However, this last condition yielded poor quality neuronal cultures (Plate 3A). After process readsorption and vacuolization of cell bodies, neurons died in about one week. Increasing either the ionic potassium levels in the culture medium to 50 mM or glucose to 6 g/l (Bottenstein, 1983) did not enhance neuronal survival. In contrast, when cells were plated in PEI-dishes, there was no need for antimitotic agents since few or any glial cells attached to the substrate. However these conditions were unsuitable for sustaining neuronal cultures for more than a week.

substrate	SSM -FDU	SSM +FDU	10% FCS-CDM switched to CDM
PLL	**glia**	neurons (1 week)	neurons (3-4 weeks) 10-20% glia
PEI	neurons (1 week)	neurons (1 week)	**neurons (7 weeks)** 5% glia
-	aggregated neurons (1 week)	aggregated neurons (1 week)	-

Table 6. Growing conditions used in parallel cultures: Selection for neurons or glia

CDM: serum-free chemically defined medium; 10% FCS-CDM: 10%: serum supplemented defined medium; ±FDU: with or without anti mitotics; SSM: serum supplemented medium. Dispersed hippocampal cell suspensions were plated at an initial density of 1.25 x 10^5 cells/cm^2. Times in brackets indicate the viability under the stated conditions.

The addition of supplements to the medium together with the implementation of the two step method (Bottenstein, 1983), i.e. plating in serum supplemented defined medium and switching to serum-free chemically defined medium, proved to increase substantially the neuronal survival. However, results showed that in cultures left for more than 3 h in serum supplemented defined medium before switching to serum-free chemically defined medium, about 20% of non-proliferative glial cells were present after one week in culture as judged by mAb-GFAP immunostaining. When serum was removed within 2 h of plating the cells, about 40% of cells were lost during the washes and the remainder did not develop properly. Thus, 2 h in serum supplemented defined medium proved to be the optimum time to allow cells to attach to the substrate and recover from the trauma of dissociation. Under these conditions, cultures were composed of robust neurons. When this two step method was used, not only did the neurons grow healthily but there was no need to use anti-mitotic drugs, because 2 h in the presence of serum was not enough time to induce glial cell proliferation.

Plate 3: Glial cell selection of hippocampal cultures grown in PLL-treated surfaces and maintained with serum supplemented medium

A: 6 day old hippocampal cells treated with anti-mitotics on day 3 in culture. Glial cells were present but did not proliferate. Astrocytes are indicated by small **arrows**. An oligodendrocyte-like cell is labelled with the **short thick arrow**. Culturing conditions were suboptimal for neuronal survival. The vacuolization of neuronal cell bodies and readsorbtion of processes is apparent (**long big arrow**). **B:** 10 day old confluent monolayer of glial cells has been selected from hippocampal preparations plated in PLL and maintained in serum supplemented medium. **Bar: 100 μm.**

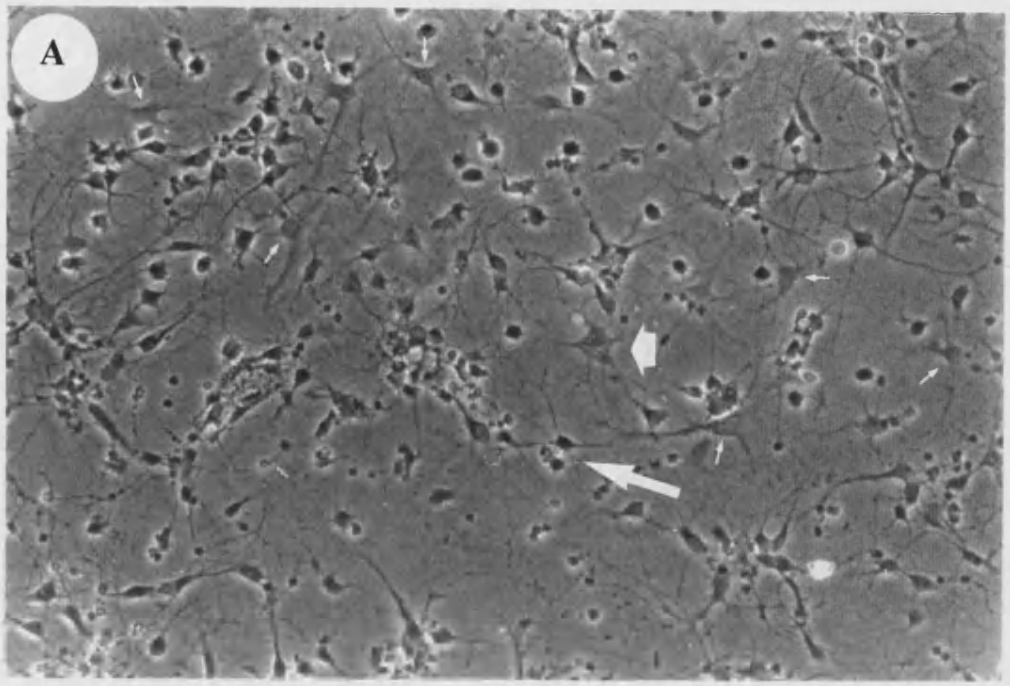
A

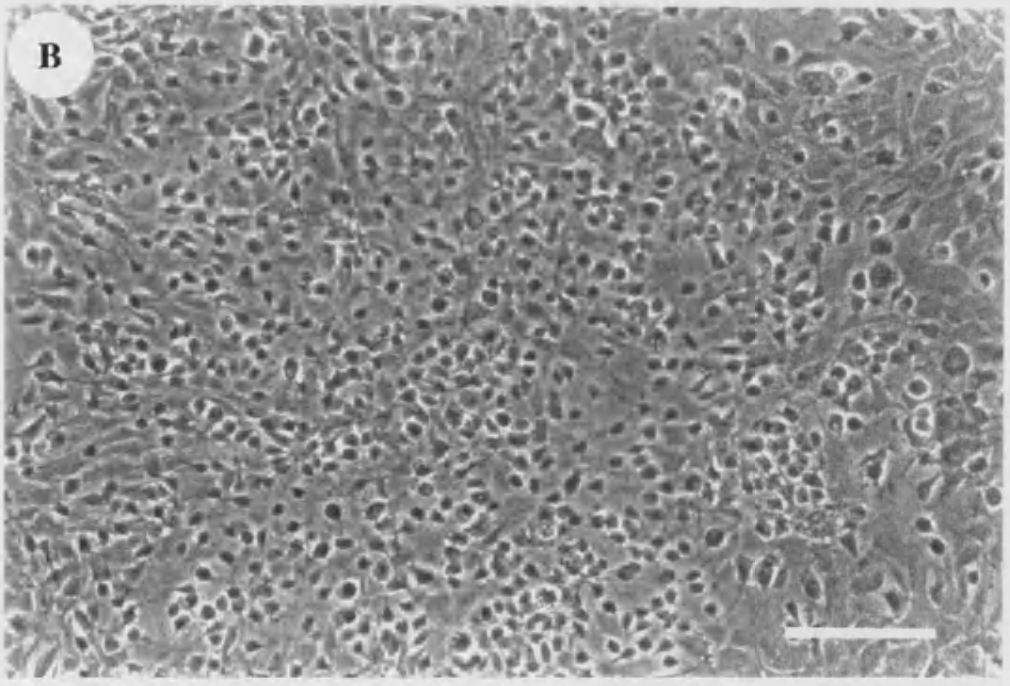
B

The effect of plating the cells on PLL or PEI followed by culturing with the two step method was also evaluated. As shown in Table 6, the former treatment produced enriched neuronal cultures but about 20% of the population of cells was non-proliferative glial cells, since PLL favours glial cell attachment. These cultures were viable for 3 to 4 weeks. Under the same two step method, plating on PEI-coated dishes proved to be the better method for producing long term (up to 7 weeks) neuronal cultures almost devoid of glial cells (5%). However, under these last conditions neuronal cultures strongly depended on the addition of all five supplements as shown in Table 7. Deletion of a single supplement resulted in immediate death or progressive loss of viability. The absence of transferrin or a concentration well below 100 μg/ml (5 μg/ml was tested) had the most marked effect, followed by insulin > selenium = progesterone > putrescine.

Deletion	Survival
transferrin	<< 1 week
Insulin	< 1 week
Selenium	1 week
Progesterone	1 week
Putrescine	1 to 2 weeks

Table 7. Growth response of hippocampal neuronal cultures to single deletions of supplements.

Plating cell suspensions in PLL-dishes and feeding the cultures with serum supplemented media were the only treatments that allowed glial proliferation.

Finally, neurons fed by replacing half the volume of old medium by fresh medium were demonstrated to remain firmly attached to the substrate and were healthier, compared with those that had been fed by a total replacement of medium.

In summary, the conditions that allowed cultures to survive for longer, that is up to 7 weeks, were as follows: *(i)* Cells had to be plated on PEI coated dishes in serum supplemented defined medium and transferred to serum-free chemically defined

medium after 2 h. ***(ii)*** Cultures had to be fed by replacing half the volume of old medium by new every 4-5 days. A culture grown under the optimised conditions is shown in Plate 4.

Morphological characterization of optimized hippocampal neuronal cultures

An indication of the degree of neuronal heterogeneity seen within a single culture maintained under the optimised conditions is provided by Plate 4. According to a previous study (Banker and Cowan, 1979), cells in hippocampal cultures could be grouped into three broad classes. (*i*) Cells which were stellate in appearance (labelled "S" in Plate 4A) with several similarly-sized dendrites that ramify from the soma in all directions: such cells were relatively uncommon in the present cultures. (*ii*) Bipolar cells (labelled "Bi") with two, comparably-sized processes that extended from opposite poles of the cell: These were more frequent than the stellate cells, but less common than the third type. (*iii*) Cells with a single dominant process that is noticeably stouter and longer than the other processes emerging from the soma, i.e. major process-dominated neurons (this cells were labelled "M" in Plate 4A).

Together these three classes of cells encompassed the great majority of the cells that developed in culture (Plate 4B). In order to estimate the relative frequency of each class of cells, photomicrographs were taken from several different cultures and the cells classified according to this scheme. About 62 ± 5% of the cells fall into the third category with one dominant process (probably a dendrite), while bipolar and stellate types account for 20 ± 3% and 8 ± 2% of the cells, respectively. Included among the third (M) class were many cells with two or more, relatively fine processes (probably dendrites) emerging from the opposite pole of the cell in addition to the major process (probably a dendrite). According to previous observations (Banker and Cowan, 1979) these cells were nominated as "pyramidal" and comprised about 42 ± 4% of all the cells present in culture. Typical pyramidal neurons that resemble their counterparts seen *in situ* in fields *CA3* and *CA1* of the embryonic hippocampus have been indicated by thick and thin arrows in Plate 4A, respectively.

Establishment and morphological characterization of cortical neuronal cultures

Growing cortical cultures under the optimized conditions for hippocampal neurons (i.e. plated on PEI dishes with serum supplemented defined medium and transferred to serum-free chemically defined medium after 2 h) was straightforward. Cultures showed to be viable for at least 4 weeks. The viability of the cultures was no further followed.

Cortical neurons were classified as pyramidal-like, bipolar, or stellate (i.e. multipolar) according to a previous report (Kriegstein and Dichter, 1983). A pyramidal-like cell had a triangular perikaryon with one prominent "apical" neurite apex and several shorter "basilar" neurites (Plate 5, arrow). If the processes emerged only from opposite poles of the perikaryon, the cell was classified as bipolar (labelled "Bi" in Plate 5). Bipolar cells often had oval somata. Cells were classified as stellate if they had multiple processes of approximately equal lengths arising from multiple sites around the perikaryon (labelled "S"). In contrast with hippocampal neuronal cultures, the proportion of pyramidal neurons in cortical cultures was smallest. They represented at most 25 ± 2% of the total neuronal population. Bipolar and stellate neurons represented 43 ± 4% and 32 ± 2%, respectively in contrast to their counterparts in hippocampal neuronal cultures (20 ± 3% and 8 ± 2%, respectively).

Glial cells, glial conditioned medium and hippocampal neurons-glia cell co-cultures

Glial cultures were only successful when hippocampal cell suspensions were plated on PLL-coated surfaces and fed with serum supplemented medium. Under these conditions, long term (more than a month) confluent astrocyte cultures were produced. The morphological appearance of glial cultures before reaching confluence was pleomorphical as seen by phase-contrast microscopy (refer to Plate 3). However,

once the cultures reached confluence, astroglia generally exhibit a rather uniform cobblestone-like appearance with individual cells lacking polarity (refer to Plate 3). In culture almost all cells presented such an appearance. The remaining astroglia usually exhibited a more irregular morphology with one or more thick processes. These glial cultures were characterized further and used for most of the studies on glia in subsequent chapters.

Plate 4. Morphological characteristics of a mature hippocampal neuronal culture.

Plate **A**. High power photomicrograph of a ten day old living culture maintained under the optimised conditions (see text). Cells which were stellate in appearance are labelled **S**; bipolar cells are labelled **Bi**; a major process-dominated neuron, i.e. with a single dominant process that is noticeably stouter and longer than the other processes emerging from the soma has been labelled **M**. Typical pyramidal cells from field *CA3* of the hippocampus are indicated by thick **arrows**. Note the pyramidal-shaped cell body, the single stout process which bifurcates about 20 μm from the soma and 3 more slender basal processes. A characteristic pyramidal neuron from *CA1* region showing an apical process which does not bifurcate but gives off a few short side branches is indicated by the thin **arrow**. **Bar: 50 μm.**

Plate **B**. Low power photomicroraph of the culture presented in Plate **1A**. **Bar: 50 μm.**

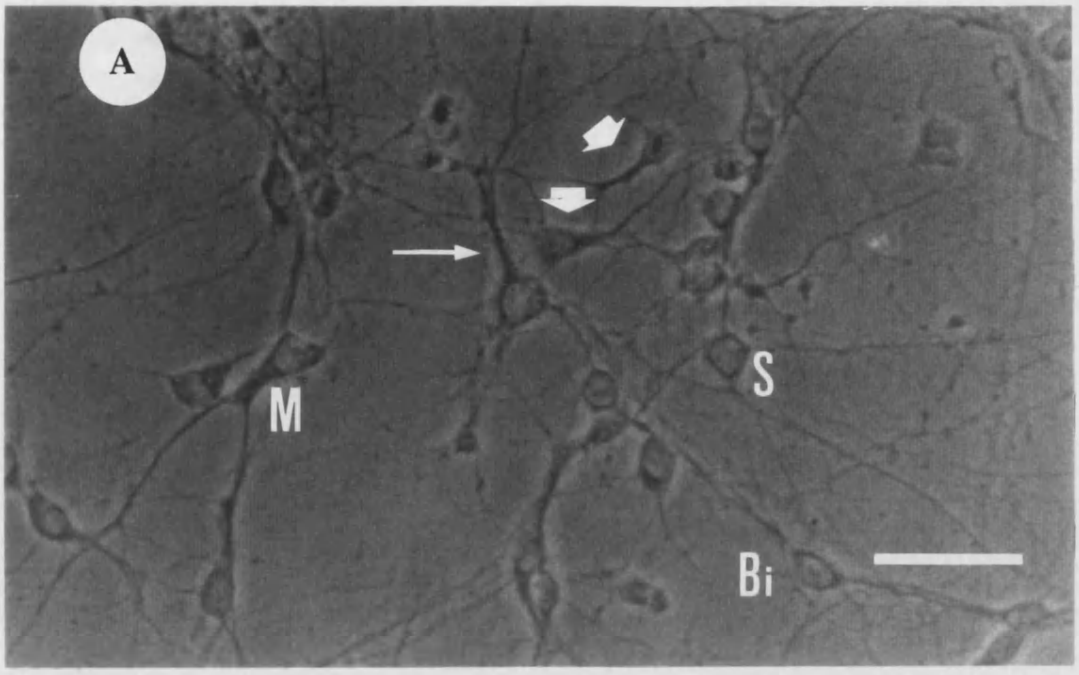
A
M
S
Bi

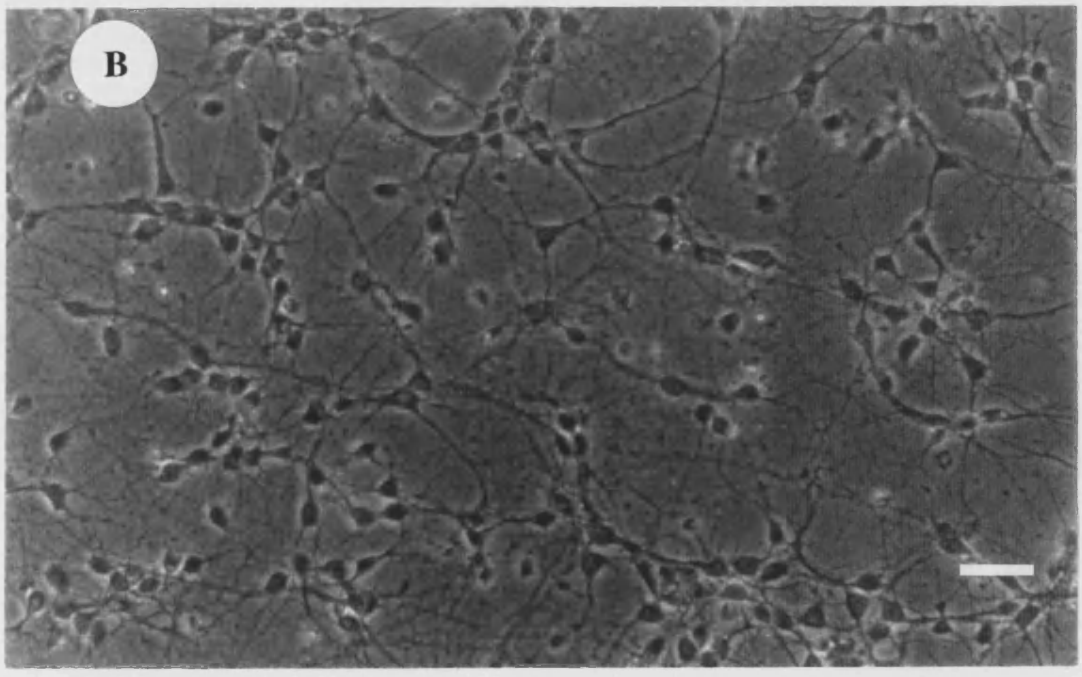
B

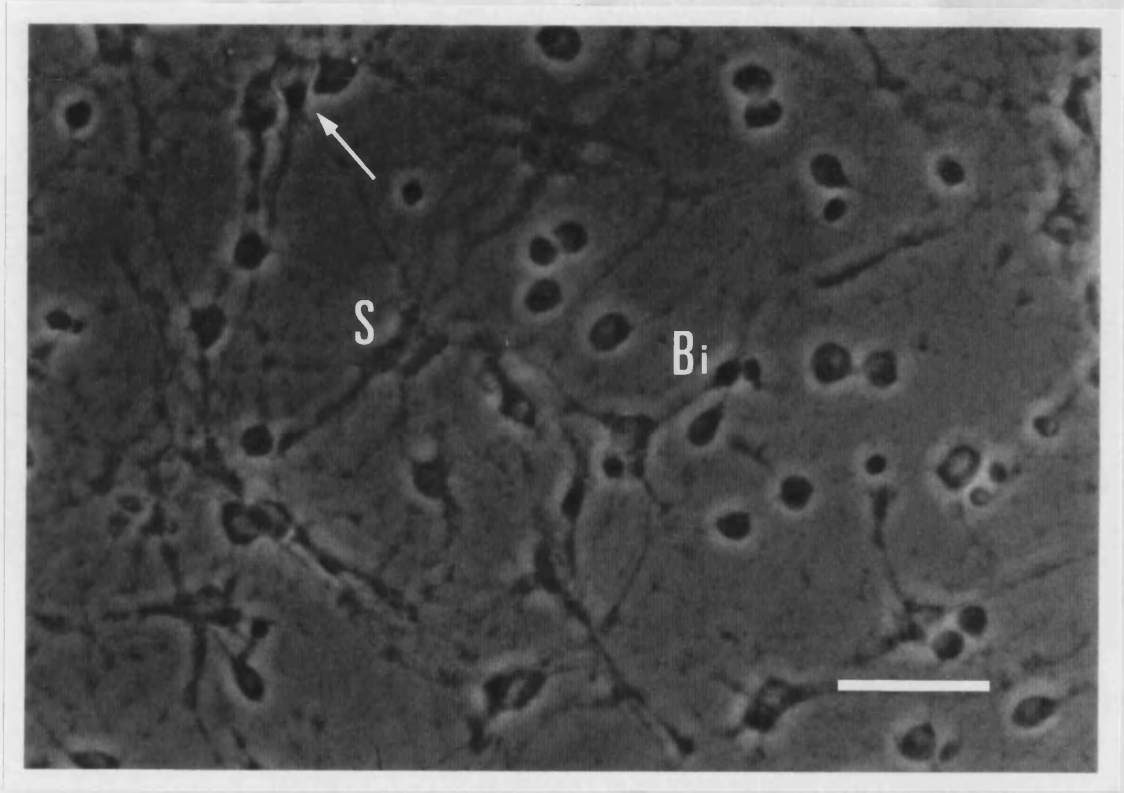

Plate 5. Morphological characteristics of a mature cortical culture.

Plate **A**. High power photomicroraph of a ten day old living culture maintained under the optimised conditions for hippocampal neuronal cultures. A stellate cell is labelled **S**; a bipolar cell is labelled **Bi**; a pyramidal cell, with a single dominant process that is noticeably stouter and longer than the other processes emerging from the soma is indicated with an arrow. **Bar: 50 μm**

To test whether the survival of hippocampal neurons in culture was increased under the effect of glial conditioned medium on neurons, glial cells feeding-medium was harvested and used to conditioning hippocampal neuronal cultures (Banker, 1980).

Glia conditioned medium in any of the proportions tested did not increase survival time, with respect to the other media used. Moreover, neat conditioned media or equivalent proportions of conditioned medium and fresh serum supplemented medium resulted in neuronal cell death after a week in culture. Only when half of the old medium was replaced each 5 days by equal proportions of glial conditioned medium and serum-free chemically defined medium were cultures viable for about 2 to 3 weeks. No morphological differences were observed when comparing neurons growing under these conditions to normal.

In addition, to test whether the survival of hippocampal neurons in culture was increased under the influence of glial cells, co-cultures were carried out (Goslin and Banker, 1991). For co-cultures with hippocampal neurons, glial cultures were grown in glass coverslips to fit into the neuronal culture well. In co-cultures, neuronal and glial cells were maintained in serum-free chemically defined medium and therefore glial cells did not proliferate.

Visual comparison between hippocampal neuronal cultures and co-cultures showed no difference in survival time for high density neuronal cultures, although the manipulations due to fitting the coverslip into the wells resulted in some detachment of neurons. On the areas underneath the paraffin dots (Fig. 3) neurons did not grow. The morphological appearance of neurons in co-culture was identical to that observed when neurons were cultured alone.

Thus, high density cultures proved to grow healthily when maintained in serum-free chemically defined medium rather than in co-culture or with conditioned medium.

2.3.2. Quantitative characterization of the cultures

In order to correlate the amount of protein with the number of neurons in culture, an estimation of the sample size was needed. Results in Fig. 5 showed that the minimum area to be measured in living cultures was 16 mm^2. This area corresponds to the first quadrant size where no further variation in the variance-mean ratio occurred. The neurons in culture were randomly distributed since the variance-mean ratio was below 1 (0.22 ± 0.01). As cell counting was performed in living cultures, there was a compromise between the number of measurements per culture and the time involved per count. Thus, 4 random measurements of an area of 25 mm^2 were adopted as standard.

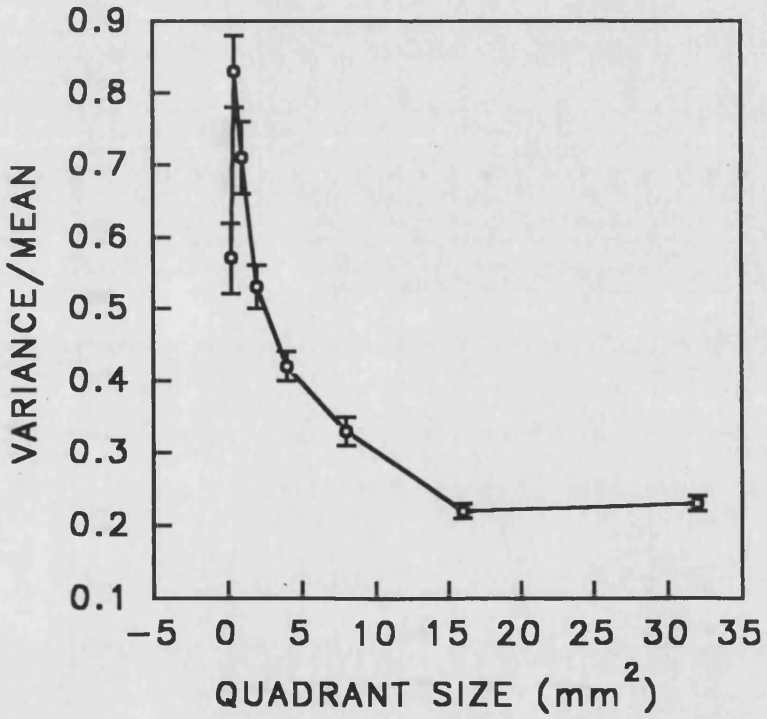

Figure 5: Determination of the minimum quadrant size for cell counts.

The minimum quadrant size to be measured per culture was estimated with the mean-squares method (Greig-Smith, 1952). The number of cells was obtained for each basic unit, being 0.25 mm^2 the smallest quadrant size used. This basic units (0.25 mm^2) was combined into oblong pairs of two units (0.5 mm^2). In turn the pairs were combined into blocks of fours (1 mm^2), the blocks of four into oblong blocks of eight (2 mm^2) and so on until an oblong block of 32 mm^2 was formed. Ten locations in three different dishes were sampled. The variance/mean ratio was then plotted against quadrant size. The minimum quadrant size to perform cell counts was considered the first where no further variation in the variance/mean ratio is observed, i.e. 16 mm^2.

Total protein values were expressed in μg per million cells (neurons were counted just prior to assay). Table 8 shows quadruplicate observations of three independent cultures followed over a period of four weeks and measurements of independent wells. As shown in Table 8, total protein in hippocampal neurons varied between 335 ± 45 μg (n=30) and 479 ± 77 μg (n=10) per 10^6 cells during the first and fourth week in culture, respectively. A significant increase of 533 ± 88 (n=14) μg protein/ 10^6 cells was reached by the third week in culture. The lack of significant increase in protein per cm^2 together with the increase of protein values were consistent with the fact that neurons developed more and thicker processes in time. The decrease in protein observed by the fourth week in culture could be attributed to neuronal death. However, such decrease was not statistically significant with respect to week 3. After the fourth week, neurons underwent a degenerative process that lead to culture death during the seventh week.

Week	μg/cm^2	μg/10^6
1 n=30	28.1 ± 3.9	335 ±45
2 n=44	32.8 ± 1.7	370 ±22
3 n=14	37.5 ± 8.3	533 ±88
4 n=10	31.8 ± 1.3	479 ±77

Table 8. Total protein in hippocampal neuronal cultures during development.

Protein estimations from hippocampal neurons were compared with those obtained for hippocampal-glial co-cultures. As shown in Table 9, total protein values

from hippocampal neurons grown in co-culture were smaller than those obtained when neurons were cultured alone (Table 8).

Week	$\mu g/cm^2$	$\mu g/10^6$
1 n=12	29.5 ±3.8	280 ±57
2 n=12	32.2 ±2.4	320 ±35
3 n=8	25.6 ±2.3	260 ±42

Table 9. Total protein in hippocampal-glial co-cultures during development.

Protein estimations from hippocampal neurons were compared with those obtained for cortical neuronal and glial cultures.

Protein values from 3 independent cortical cultures, estimated from 12 plate wells per culture were 21.5 ± 3 $\mu g/cm^2$ (n=36) and 193 ± 30 $\mu g/10^6$ neurons. These results were significantly smaller ($P < 0.05$) than those obtained for hippocampal neurons (32.8 ± 1.7 $\mu g/cm^2$ and 370 ±22 $\mu g/10^6$) at the same stage in culture.

At the stage glial cultures were assayed for protein, i.e. 14 day old, cultures were confluent making impossible any attempt to perform cell counts. Therefore, results were expressed μg per cm^2. Protein values from 3 independent cultures, estimated from 12 plate wells per culture were 29.2 ± 1 $\mu g/cm^2$ (n=36). These results were comparable with hippocampal neurons (32.8 ± 1.7 $\mu g/cm^2$) at the same stage in culture.

2.3.3. Neuronal and glial markers

The presence of neuronal cells in hippocampal and cortical cultures was demonstrated by mAb-NF indirect immunostaining.

As shown in Plate 6, almost all cells grown for two weeks under the optimised conditions (plated at high density into serum supplemented chemically defined medium and fed with serum-free chemically defined medium) showed a positive reaction to ANF-Ab. These results were independent of the age in culture.

The contribution of glial cells to the hippocampal neuronal cultures was tested with mAb-GFAP. The morphological appearance of a 2 week old hippocampal neuronal culture immunostained with mAb-GFAP is shown in Plate 7. The fact that the astrocytes shown in Plate 7 could only be recognized when immunostained, highlights the utility of glial markers to assess the actual contribution of glial cells in enriched neuronal cultures. Very few astrocytes could be seen (less than 5%) while the dominant cell type was neurons which had developed an extensive network of neurites.

Similarly as shown in Plate 8, most of the cortical cells grown for two weeks under the optimised conditions for hippocampal cultures (plated at high density into serum supplemented chemically defined medium and fed with serum-free chemically defined medium) showed a positive reaction to ANF-Ab.

However, the contribution of glial cells to the cortical cultures was greater than to hippocampal neuronal cultures (approximately 15% vs <5%). Results from a 2 week old cortical culture immunostained with mAb-GFAP are shown in Plate 9.

The morphological appearance of the non-neuronal elements stained with mAb-GFAP in hippocampal or neuronal cultures was characteristic of type 1 astrocytes.

Conversely, glial cultures (from fetal rat hippocampus and maintained in SSM) stained positively for mAb-GFAP (Plate 10A and E) (but not with mAb-NF, Plate 10F). Although the cell population in this culture system was not homogeneous, protoplasmic astrocytes (type 1) constituted the major fraction (more than 95%) of the cells.

Plate 6. mAb-NF immunostaining of hippocampal neuronal cultures.

Two week old enriched hippocampal neuronal cultures were fixed with 5% acetic acid-70% ethanol solution. Preparations were blocked with 1% normal goat serum in PBS to reduce non-specific immunostaining. Cells were incubated with mAb-NF (**A** and **B**) or control cloning medium (**C** and **D**) to determine total and non-specific immunostaining, respectively. Anti-mouse IgG-FITC conjugate was used as secondary antibody. Fields **A** and **B** correspond to the same preparation seen under u.v. filter or ordinary bright phase contrast (tungsten), respectively. Fields **C** and **D** depicts the non-specific immunostaining viewed under u.v. or tungsten light, respectively. **Bar: 50 μm**

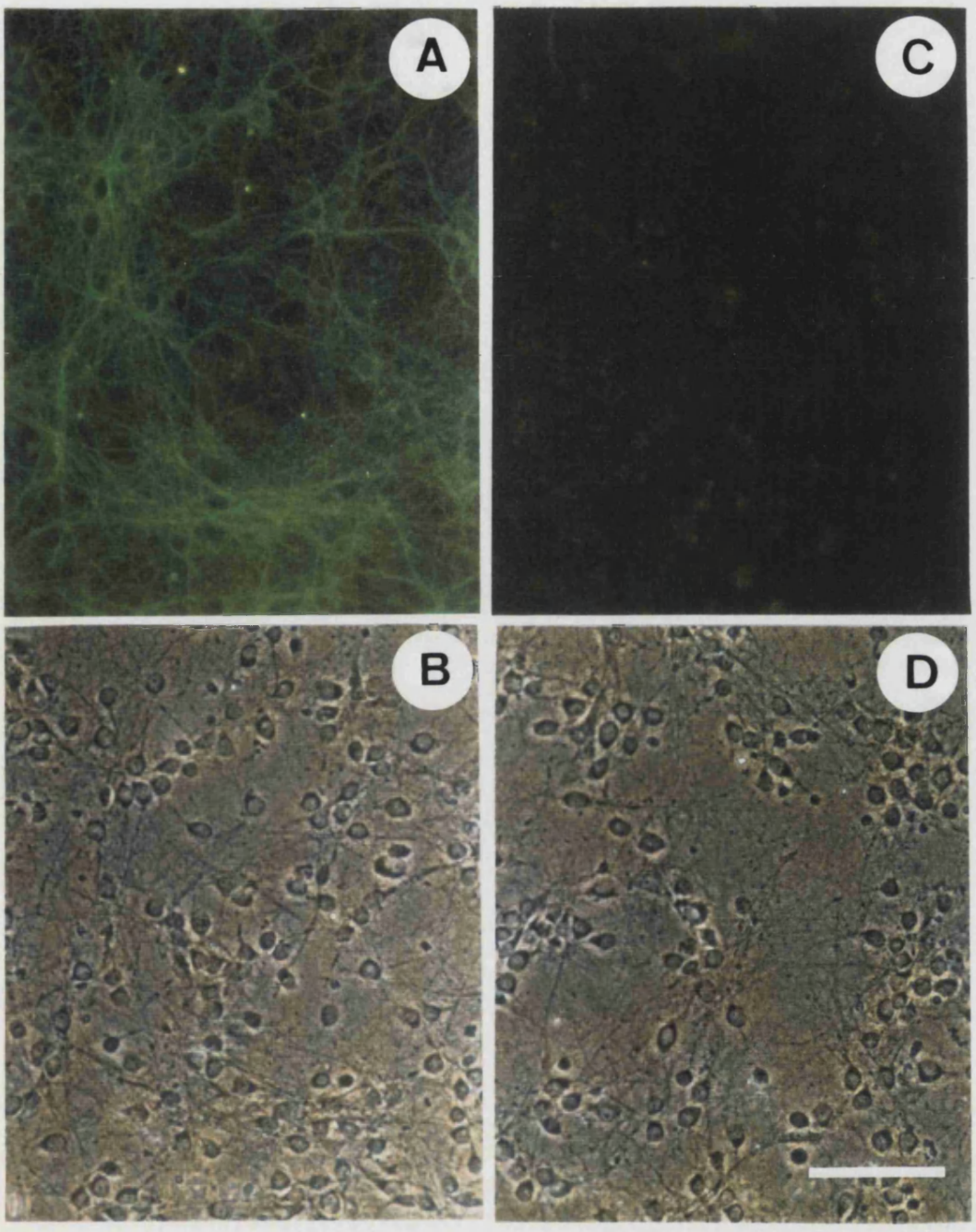
A
C
B
D

Plate 7. mAb-GFAP immunostaining of hippocampal neuronal cultures.

Two week old enriched hippocampal neuronal cultures were fixed with 5% acetic acid-70% ethanol solution. Preparations were blocked with 1% normal goat serum in PBS to reduce non-specific immunostaining. Cells were incubated with mAb-GFAP (**A** and **B**) or control cloning medium (**C** and **D**) to determine total and non-specific immunostaining, respectively. Anti-mouse IgM-FITC conjugate was used as secondary antibody. Fields **A** and **B** correspond to the same preparation seen under u.v. filter or ordinary bright phase contrast (tungsten), respectively. Fields **C** and **D** depicts the non-specific immunostaining viewed under u.v. or tungsten light, respectively. **Bar: 50** μm

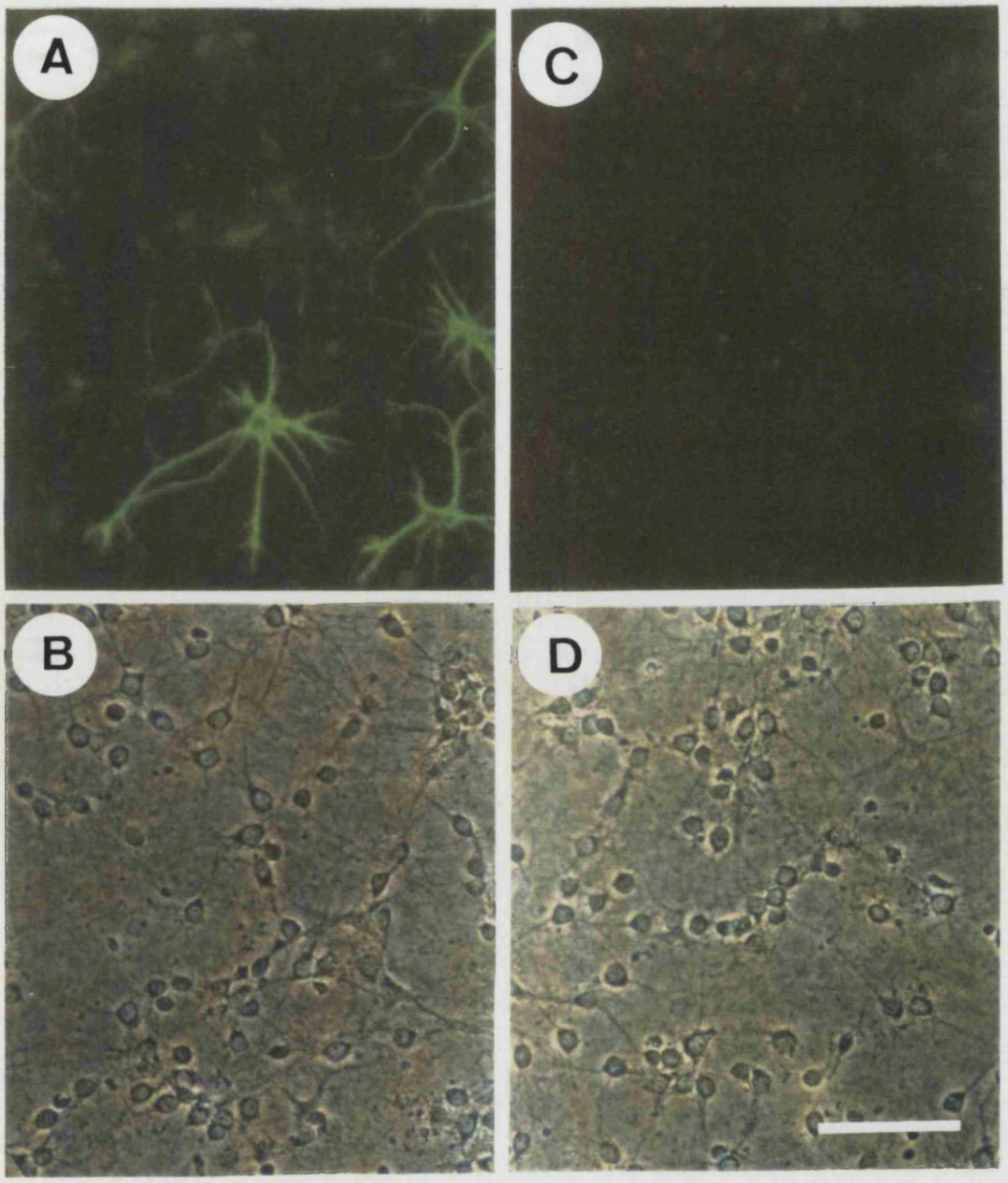
A
C
B
D

Plate 8. mAb-NF immunostaining of cortical cultures.

Two week old enriched cortical neuronal cultures were fixed with 5% acetic acid-70% ethanol solution. Preparations were blocked with 1% normal goat serum in PBS to reduce non-specific immunostaining. Cells were incubated with mAb-NF (**A** and **B**) or control cloning medium (**C** and **D**) to determine total and non-specific immunostaining, respectively. Anti-mouse IgG-FITC conjugate was used as secondary antibody. Fields **A** and **B** correspond to the same preparation seen under u.v. filter or ordinary bright phase contrast (tungsten), respectively. Fields **C** and **D** depicts the non-specific immunostaining viewed under u.v. or tungsten light, respectively. Bar: 50 μm

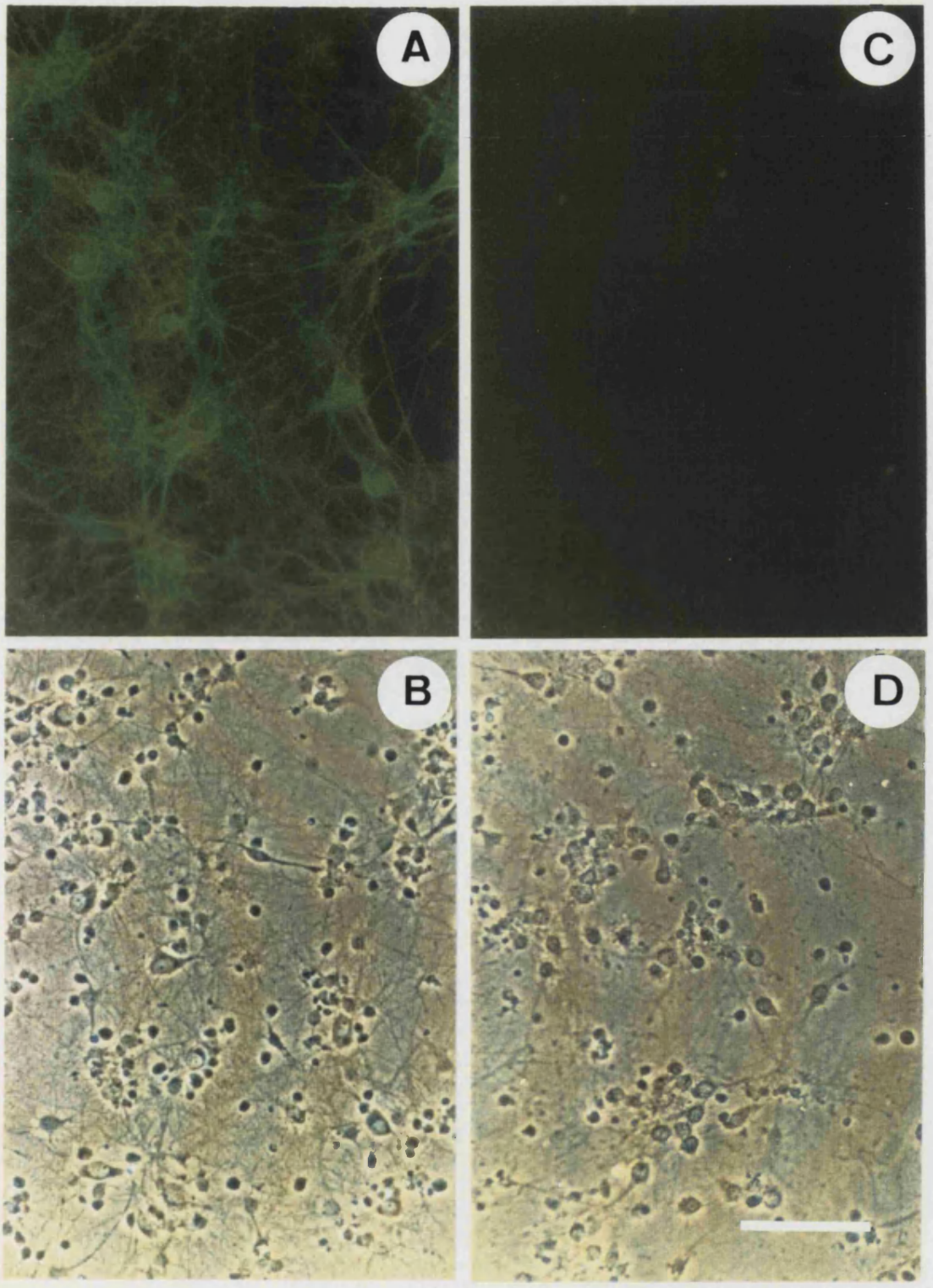
A
C
B
D

Plate 9. mAb-GFAP immunostaining of cortical cultures.

Two week old enriched cortical neuronal cultures were fixed with 5% acetic acid-70% ethanol solution. Preparations were blocked with 1% normal goat serum in PBS to reduce non-specific immunostaining. Cells were incubated with mAb-GFAP (**A** and **B**) or control cloning medium (**C** and **D**) to determine total and non-specific immunostaining, respectively. Anti-mouse IgM-FITC conjugate was used as secondary antibody. Fields **A** and **B** correspond to the same preparation seen under u.v. filter or ordinary bright phase contrast (tungsten), respectively. Fields **C** and **D** depicts the non-specific immunostaining viewed under u.v. or tungsten light, respectively. Bar: 50 μm

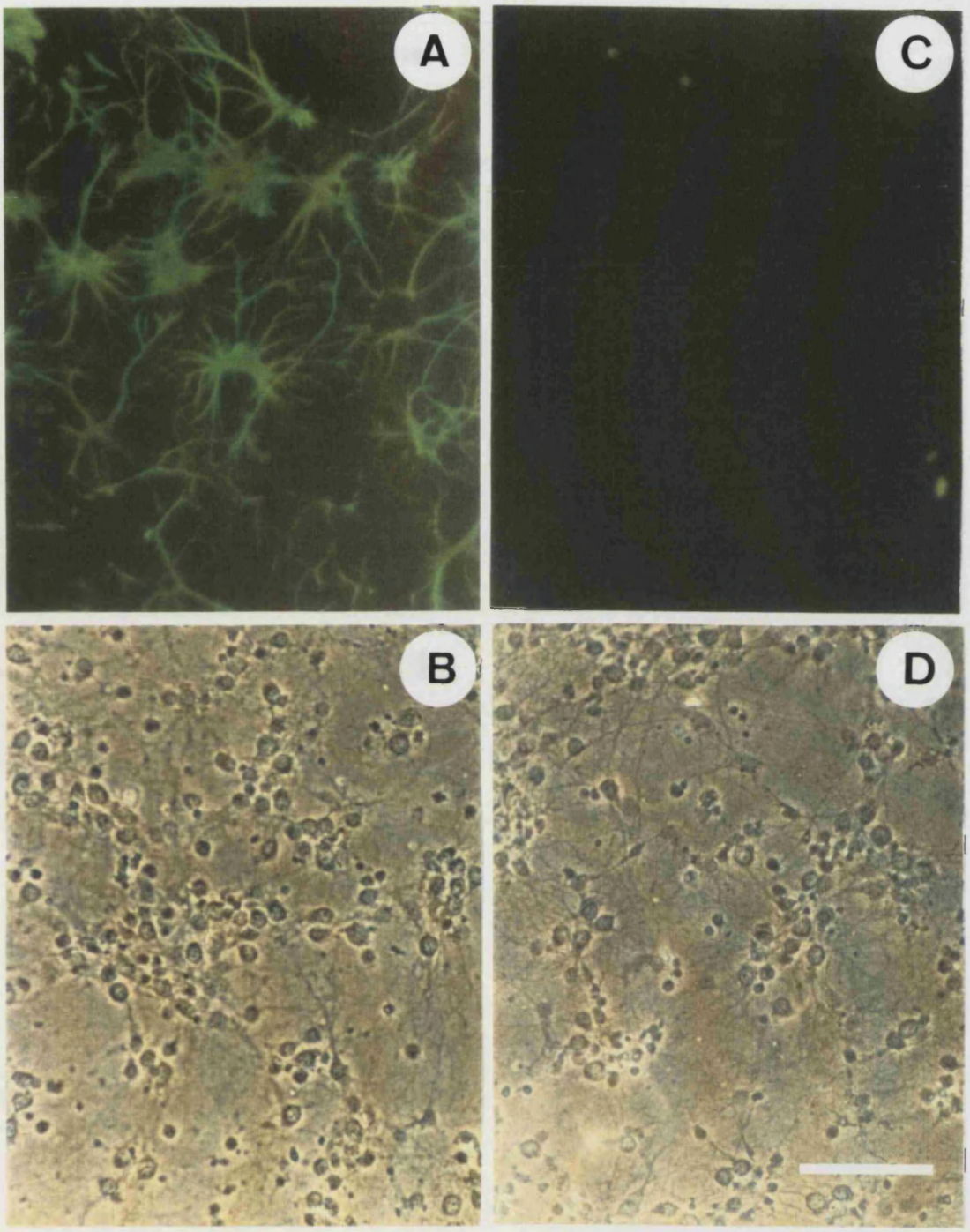
A
C
B
D

Plate 10. mAb-GFAP and mAb-NF immunostaining of glial cultures.

Two week old glial cultures were fixed with 5% acetic acid-70% ethanol solution. Preparations were blocked with 1% normal goat serum in PBS to reduce non-specific immunostaining. Cells were either incubated with mAb-GFAP (**A** and **B**), mAB-NF (**F** and **G**) or control cloning medium (**C**, **D**, **H** and **I**) to determine total and non-specific immunostaining, respectively. Anti-mouse IgM/IgG-FITC conjugate were used as secondary antibody.

Fields **A** and **B** or **F** and **G** correspond to the same preparation seen under u.v. filter or ordinary bright phase contrast (tungsten), respectively. Fields **C** and **D** or **H** and **I** depicts the non-specific immunostaining for **A** and **B** or **F** and **G**, respectively, viewed with the two different filters.

Panel **E**, a glial cell in the process of mitosis. Bar: 50 μm

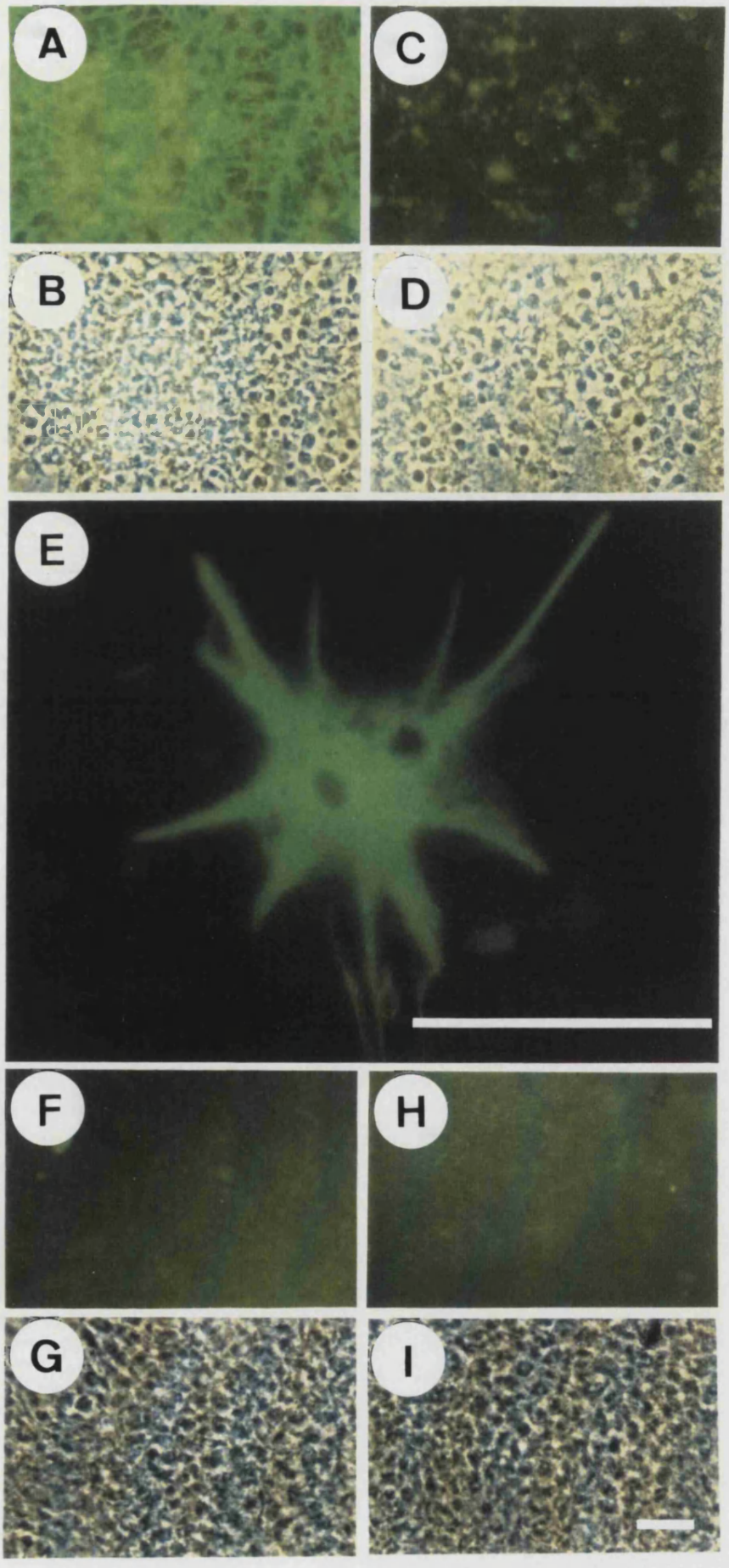
A
C
B
D
E
F
H
G
I

2.4. Discussion

The principal objective with these experiments was to define a system for culturing hippocampal neurons from rat fetuses suitable for functional and biochemical analyses of their nAChRs. This required a predominantly neuronal population of cells with a survival of several weeks to permit long term studies.

The method finally evolved differs in some aspects from that commonly employed for culturing dissociated hippocampal neurons (Goslin and Banker, 1991). Its essential features were the long-term culturing of neurons at high density on PEI-treated dishes (Seeley and Field, 1988) without the need of anti-mitotic agents.

The success in growing nerve cells depended on several interdependent variables. A substrate that allowed cells to attach before spontaneous cell aggregation occurred and also permitted growth of the desired cell type, i.e. neurons, was essential. PEI proved to be the appropriate substrate to produce high density cultures which showed little or no aggregation of neurons. One remarkable feature of the hippocampal cultures was the paucity of non-neuronal cells present. This was probably due to the fact that most gliogenesis in the rat hippocampus occurs either very late in gestation or postnatally (Goslin and Banker, 1991). However, the use of a PEI-treated substrate may also have contributed to the low percentage of glial cells in these cultures since this substrate was unsuitable for selecting non-neuronal cells.

With the appropriate substrate, i.e. PEI, culture survival was increased with a convenient medium. The rationale for testing different media was based on the generalized observation (Bottenstein, 1983) that some supplements in serum are essential for cell survival. Thus, an obvious approach was to culture cells in serum supplemented medium which is very easy to prepare. However, it has also been established that serum contains mitogens and these in turn could trigger cell division of those cells that have the potential to divide (e.g. glial cells) unless antimitotic agents are also applied (Banker and Goslin, 1991). These conditions proved not to be optimal for culturing hippocampal neuronal cultures in the present study. Thus the next step to follow was to culture hippocampal neurons in an enriched medium

supplemented with hormones. Some of these essential supplements have been characterized (Bottenstein and Sato, 1979) and since then it has been possible to produce long-term cultures in serum-free chemically defined medium (Bottenstein, 1983; Goslin and Banker, 1991). The preparation of chemically defined medium usually requires more dedication but its defined composition presents the advantage of knowing exactly under what conditions cultures are growing. In spite of this, at present there has not been a report of successful cultures grown in the complete absence of serum probably because serum-derived molecules adsorb to the culture surface and cells adhere to this layer (Bottenstein, 1983). Standard protocols usually involve a two step method which requires plating cells in serum supplemented medium and then switching to serum-free, chemically defined medium (Bottenstein, 1983; Banker and Goslin, 1991). The elimination of the requirement for serum in neuronal cultures has advantages. The variability, complexity, and largely undefined nature of serum can affect reproducibility of experiments and complicates the interpretation of the data. Furthermore, morphological differentiation and some biological parameters are enhanced in several neuronal cell cultures in defined media (Bottenstein, 1983). The most obvious advantage for the purpose of selecting neuronal cultures is the serum-dependence of glial cells.

The implementation of the two step method, i.e. plating into serum-supplemented chemically defined medium and changing to serum-free chemically defined medium was critical for neuronal development.

It has been established that similar chemically defined media to that employed in the present study for culturing neurons cannot sustain the growth of non-neuronal cell lines such as rat glioma, mouse fibroblast (Bottenstein, 1980) or rat skeletal muscle (Bottenstein, 1983). In fetal rat brain cultures, GFAP and the oligodendrocyte marker, galactocerebroside, are significantly reduced in chemically defined medium compared with serum-containing medium (Bottenstein, 1983). However, the growth requirements of primary and cell line cultures of oligodendrocytes have been

established (Bottenstein, 1986). Oligodendrocytes can be selected in a similar chemically defined medium to the one used in that present study, but the absence of fibronectin and PLL substrates is detrimental. Also, the concentration of transferrin used in the present study is suboptimal for oligodendrocyte growth (Bottenstein, 1986). Although oligodendrocytes markers were not employed in the present study, it is very unlikely that there was any contribution of oligodendrocytes to neuronal cultures due to their requirement for fibronectin, PLL and low concentrations of transferrin.

The above observations would explain the low contribution of non-proliferative glial cells (about 5%) to the enriched neuronal cultures. At present there is no method that would eliminate completely glial cells from enriched hippocampal neuronal cultures. On the other hand it has been reported that a moderate number of glial cells in neuronal cultures is beneficial (Banker and Goslin, 1991). Among the proposed astroglial functions, it is known that glial cells interact trophically with neurons (Banker, 1980; Müller and Seifert, 1982; Pentreath *et al.*, 1986). Growth factors produced by glia and released to the medium could influence neuronal development. Trophic factors produced by glia that are critical for the survival of hippocampal cultures are not known, nor is it understood how the culture environment affects their production by glia. However, at densities as low as 2000 neurons/cm^2, hippocampal neuronal cultures are viable only if they are co-cultured with glial cells ("sandwich technique", refer to fig. 4) (Bartlett and Banker, 1984a). In view of these last observations, it was decided to culture glial cells, more specifically astrocytes enriched cultures, and follow their influence on hippocampal neurons when co-cultured. As an alternative approach, the effect of glial conditioned medium on neurons was assayed. It is important to note here that in the present study, neither co-cultures nor glial conditioned media enhanced hippocampal neuronal growth and development, compared with chemically defined medium. The timecourse of hippocampal culture survival was comparable with previous studies culturing neurons

either over a monolayer of astrocytes or in co-culture ("sandwich technique") or in serum supplemented medium with mitotic inhibitors (Seeley and Field, 1988; Goslin and Banker, 1991; Banker and Goslin, 1991). This is most likely due to the higher densities employed (2.5×10^5 neurons/cm^2). In addition, these findings are consistent with studies demonstrating that immortalized hippocampal cells (Lee *et al.*, 1990) and hippocampal neurons (Whittemore *et al.*, 1988; Lauterborn *et al.*, 1993) produce their own growth factors. Therefore, this would explain why cultures fed by replacing half the volume of old medium by new developed healthier with respect to those that had been fed with a total replacement of medium. This procedure would allow neurons to be in the permanent presence of their own conditioned media and the newly replaced medium would provide those factors that had been depleted. Also the removal of half of the media would help to dilute toxic metabolites released to the medium.

A 2:1 mixture of high-glucose DMEM medium and Ham's F12 medium (see the appendix A to this thesis) was chosen as the basal medium as many neural cell lines have been cultured in one or the other of these media (Bottenstein, 1983), and together they contain a wider spectrum of components whose absence could have been potentially growth limiting, particularly the vitamins. However, neuronal cultures strongly depended on the addition of supplements. Deletion of a single supplement resulted in immediate death or progressive loss of viability. Thus, all five factors were required for the proper development of hippocampal neurons.

A number of *in vivo* and *in vitro* observations are consistent with the role of medium supplements in the growth and development of neural cells. For example, transferrin is an iron-transport protein found in high concentrations in rat plasma and cerebrospinal fluid. It is also present in developing brain despite the blood-brain barrier, suggesting local synthesis. Indeed, fetal brain and choroid plexus synthesize transferrin and several other plasma proteins (Dziegielewska *et al.*, 1984). CNS neural cells contain high levels of the peptide hormone insulin and its receptors, and they are not regulated by peripheral levels of this hormone, suggesting that it is also locally

synthesized (Havrankova *et al.*, 1981). The trace element selenium reaches adult levels in rats by 2 weeks after birth (Prohaska and Ganther, 1976). About one-fifth of it is present in glutathione peroxidase, which protects membranes by converting lipid peroxides to their corresponding monohydroxy-unsaturated fatty acids. The remainder of the selenium is mostly associated with protein. Progesterone serves as a precursor for estrogens, androgens and adrenocortical steroids. It is synthesized in the ovary, testis and adrenal from circulating cholesterol. Large amounts are also synthesized and released by the placenta during pregnancy. Its lipophilicity explains its passage of the blood-brain barrier. Progesterone receptors are present in the CNS (MacLusky and Clark, 1980). Several studies have demonstrated the modulatory effect in the CNS. In particular, when the $\alpha 4\beta 2$ nAChR subtype is expressed in *Xenopus* oocytes, the function is inhibited by progesterone concentrations comparable to those measured in rat plasma (Valera *et al.*, 1992). In the present study however, 20 nM progesterone was used whereas micromolar concentrations were needed to observe such functional inhibitions of the nAChR (Valera *et al.*, 1992). In addition, the polyamine, putrescine, has been attributed a regulatory role in neuronal cell growth. Proliferating cells have higher levels of polyamines than quiescent cells, polyamine levels are 50-fold higher in fetal than adult rat brain (Bottenstein, 1983).

Whereas neurons were shown to be dependent upon chemically defined medium, glial cells developed in serum supplemented medium. Therefore, these two contrasting media together with the differential substrate requirements, allowed the production of high density enriched neuronal cultures almost devoid of glia suitable for biochemical analysis.

It is well established that the morphological characteristics of hippocampal neurons *in vitro* resemble their counterparts *in situ* (Banker and Cowan, 1977). In the present study, cells in hippocampal cultures could be grouped into three broad classes: bipolar, stellate cells and major process-dominated neurons. Together these three classes of cells encompassed the great majority of the cells that developed in

culture in agreement with previous observations (Banker and Cowan, 1979) Major process-dominated neurons were nominated as "pyramidal" and comprised about 42 ± 4% of all the cells present in culture.

Given the highest densities at which neurons were cultured and due to technical limitations, it was impossible to distinguish between dendrites and axons. Dendrites are thick at the base but trapper rapidly to a minimum diameter of about 0.5 μm and contain polyribosomes throughout their length. Axons, are several times longer and thinner than dendrites but tapered much less and are essentially ribosome-free. Axons most commonly arise from the proximal portion of a dendrite rather than directly from the cell body as they typically do *in situ* (Bartlett and Banker, 1984a).

Cortical neuronal cultures were established in order to use them as controls for further studies. Culturing cortical neurons under the optimized conditions for hippocampal neurons was straightforward. Cortical neurons were classified as pyramidal-like, bipolar, or stellate (i.e. multipolar) according to a previous report (Kriegstein and Dichter, 1983). In contrast with hippocampal neuronal cultures, the proportion of pyramidal neurons in cortical cultures was smaller. They represented at most 25 ± 2% of the total neuronal population. Bipolar and stellate neurons represented 43 ± 4% and 32 ± 2%, respectively in contrast to its counterparts in hippocampal neuronal cultures (20 ± 3% and 8 ± 2%, respectively). The contribution of glial cells to cortical neuronal cultures was greater than to hippocampal cultures (20% vs 5% approx.).

The rationale for growing glial cultures was not only to test their ability to enhance neuronal survival but also to use them as controls for further experimentation. It was intended to rule out the possibility that any of the responses obtained in the neuronal cultures were due to the few glial cells present in culture.

The characteristics of the glial cultures in the present study were consistent with immunocytochemical studies of new born rat primary hippocampal cultures (Amruthesh *et al.*, 1993) revealing that more than 98% of the cells were GFAP

positive astrocytes. The present results were strengthened by previous observations (Levi *et al.*, 1986) reporting that glial precursor cells develop into astrocytes type 1 in serum supplemented medium 10% FCS.

2.5. Summary to chapter 2

(i) Long term (7 weeks) enriched neuronal hippocampal cultures were generated by plating hippocampal cell suspensions in PEI-treated dishes in the presence of serum-supplemented, chemically defined medium. Cultures had to be changed to serum-free, chemically defined medium 2 h after plating.

(ii) Hippocampal neuronal cultures were composed of stellate (8%), bipolar (20%) and major process-dominated neurons (62%) neurons. Included in the last category were pyramidal neurons which comprised about 42% of all the cells present in culture. Glial cells represented no more than 5% of the neuronal cultures.

(iii) Long term cortical neuronal cultures were grown following the optimized conditions for hippocampal neuronal cultures. Cortical cultures presented a different proportion of the same morphological cell types described in hippocampal cultures. Bipolar neurons represented the majority (43%), followed by stellate neurons (32%). In contrast to hippocampal cultures, pyramidal neurons represented no more than 25% of the total cortical neuronal population. The contribution of glial cells to cortical cultures (20%) was greater than to hippocampal cultures (5%).

(iv) Glial cultures were prepared by plating hippocampal cell suspensions onto PLL-treated surfaces and maintaining with serum supplemented medium. Glial cultures consisted composed of an almost homogeneous population (>95%) of astrocytes type 1.

(v) A system for culturing hippocampal and cortical neurons from rat fetuses suitable for functional and biochemical analyses of their nAChRs was established.

Chapter 3
Ligand Binding Assays

3.1. Introduction

Ligand binding assays have been widely used as a tool to characterize nAChR subtypes in CNS (refer to section 1.3.2.). [^{3}H]Nicotine and [^{125}I]-α-Bgt identify two distinct populations of nicotinic binding sites (Wonnacot, 1986). Ligand binding assays usually involve either the autoradiographic localization of high affinity [^{3}H]nicotine (α4β2 nAChR) and [^{125}I]-α-Bgt (α7) binding sites in brain slices (refer to Table 2) or preparations of brain dissected regions. However, very few such studies have been reported for primary cultures of CNS. At present, the pharmacological characterization of the nAChR that binds [^{3}H]nicotine with high affinity (i.e. α4β2) has only been reported in primary cortical neuronal cultures (Lippiello and Fernandes, 1987; Lippiello and Fernandes, 1988; Lippiello *et al.*, 1991).

Although the presence of high affinity [^{125}I]-α-Bgt in embryonic hippocampal neuronal cultures has been confirmed with autoradiography techniques (Banker and Waxman, 1988), there is no precedent for the pharmacological characterization by means of ligand binding assays of [^{125}I]-α-Bgt sites in primary cultures of embryonic rat hippocampal and cortical neurons.

The present chapter focuses on the pharmacological characterization of high affinity cholinergic radioligand biding sites in primary cultures of hippocampal neurons. Comparison is made with cortical and glial cultures. Finally, a study of the distribution of α-Bgt nAChR in hippocampal cultures is presented.

3.2. Experimental Procedures

3.2.1. Materials

Tritiated radioligands were obtained from NEN Du Pont Ltd., Wedgood Way, Stevenage, Herts, SE1 4QN, U.K.: L-(-)-[N-methyl-^{3}H]-nicotine ((-)[^{3}H]nicotine; 74.6 Ci/mmol; 1 mCi/ml), stored 10 fold concentrated with mercaptoacetic acid to minimize the oxidative degradation of nicotine which may give rise to anomalous binding data (Romm *et al.*, 1990); [3,5-^{3}H(N)]-cytisine hydrochloride ([^{3}H]cytisine; 30.5 Ci/mmol; 1 mCi/ml) and L-[Benzilate-4,4'-^{3}H]-quinuclidinyl benzilate ([^{3}H]-QNB, 45.4 Ci/mmol; 1 mCi/ml). Optiphase "Safe" scintillant (Fisons, Bishop Rd., Longhborough, Leicestershire, LE11 ORG, U.K.) and 20 ml polyethylene scintillation vials were purchased from Canberra-Packard Ltd. (14 Station Rd., Pangbourne, Berks, RG8 7DT, U.K.). Atropine, α-Bgt, fluorescein isothiocyanate conjugated α-Bgt (FITC-α-Bgt), (-)nicotine base (98-100%), Folin and Ciocalteau's phenol reagent and BSA were purchased from Sigma. $CuSO_4.7H_2O$ was bought from Fluka Chemie AG, Industriestrasse 25, 25, CH-9470, Buchsl, Switzerland). Na^{125}I was supplied from Amersham International plc., Amersham Place, Little Chalfont, Buckinghamshiere, HP7 9NA, U.K., and used to iodinate α-Bgt to a specific activity of 700 Ci/mmol as previously described (Wonnacott *et al.*, 1982). MLA (citrate salt) was synthesized by Professor M.H. Benn (Department of Chemistry, University of Calgary, Alberta, Canada). For PBS, SDS and Tris-HEPES buffer solution refer to the appendix E of this thesis.

A Minaxi TRI-CRAB 4000 series beta scintillation spectrometer, counting efficiency 45 ± 1% and a Cobra II Auto-Gamma counter [79 ± 1% efficiency] (Packard instrument company, 2200 Warrenville rd, Downers Grove, Ilinois 60515) were used.

Plots and curve fitting were carried out with the programme SigmaPlot Scientific Graphing System Version 4.10.

Cultures were photographed (400 ASA Kodak film) with a Nikon Diaphot phase contrast microscope equipped for epifluorescence.

3.2.2. Methods

3.2.2.1. Radioligand binding assays

Hippocampal neuronal (plated at 1.25 x 10^5 cells/cm^2), cortical neuronal (plated at 2 x 10^5 cells/cm^2) and hippocampal glial cultures (100% confluent) were grown in 16 mm petri dishes as described in chapter 2, section 2.2.2.1.

In situ binding assays on hippocampal neuronal cultures were performed weekly over a 3 ([^{125}I]–α-Bgt and [^{3}H]cytisine) or 4 week ([^{3}H]nicotine) period. When possible, comparisons with cortical (2 week old) and glial (2, 3 and 4 week old) cultures were performed.

On the day of the assay, cultures were washed three times with 500 µl PBS and treated as follows:

[^{125}I]-α-Bungarotoxin

Triplicate culture dishes were incubated with [^{125}I]–α-Bgt (10 nM final concentration for maximum binding, 1 nM for competition assays or 0.3 to 10 nM for saturation assays) in a total volume of 0.5 ml PBS containing 0.1% (w/v) BSA. Non-specific binding was measured in the presence of excess cold α-Bgt at 1 µM final concentration. In competition binding assays, serial dilutions of competing drugs (α-Bgt: 10^{-6}M to 10^{-12}M; MLA: 10^{-6}M to 10^{-12}M and (-)nicotine: 10^{-3}M to 10^{-8}M) were added prior to the addition of [^{125}I]–α-Bgt. After 3 h at 20°C, the cultures were rapidly washed 3 times with 500 µl PBS. The cells were solubilized overnight in 300 µl SDS solution and counted for radioactivity. Afterwards, the protein concentration

in each sample was determined (refer to section 2.2.2.2.) as previously reported (Markwell *et al.*, 1978).

Since the conditions described above did not involve any previous step of permeabilization or fixation, cells were alive throughout the binding experiment. Thus, only surface α-Bgt binding sites could be detected. However, permeabilization of cells was introduced in one experiment, performed in duplicate, to evaluate whether hippocampal neurons contain intracellular stores of α-Bgt nAChR. In this way both the membrane bound as well as intracellular α-Bgt nAChR could be studied. Hippocampal neuronal cultures were grown for ten days and divided into two groups: fixed/permeabilized and alive (standard method). Subsequently to fixation/permeabilisation as described in the appendix C to this thesis, binding assays with 10 nM α-Bgt were carried out as above.

The binding parameters, equilibrium dissociation constant (K_D), the total concentration of receptors (B_{max}) and the concentration of competitive inhibitor that blocks 50% of the binding of a radioligand to a receptor (IC_{50}) were obtained by curve fitting the equations in the appendix F to this thesis. IC_{50} values were converted to the affinity constant K_i (Cheng and Prusoff, 1973) as described in the appendix F.

(-)[^{3}H]nicotine binding

Each triplicate culture dish was incubated with 20 nM (-)[^{3}H]nicotine in 0.5 ml Tris-HEPES buffer. A final concentration of 20 nM (-)[^{3}H]nicotine was chosen since in this laboratory it was shown to give maximal levels of binding. Non-specific binding was determined in the presence of 1 mM unlabeled (-)nicotine. After 3 h at 20°C, the cultures were washed 4 times (<4 sec each) with 500 µl PBS and solubilized with SDS (300 µl). After protein quantification, samples were transferred to scintillation vials, 5 ml of scintillant added and counted in a β counter.

[^{3}H]Cytisine

Assays were carried out as described for [^{3}H]nicotine but with 5 nM [^{3}H]cytisine (final concentration).

[^{3}H]-QNB

The muscarinic ligand [^{3}H]QNB was chosen as a positive control for [^{3}H]-agonist binding assays since it presents similar kinetics and specific activities to the tritiated nicotinic agonists (Henis and Sokolovsky, 1983).

Binding assays, protein determination and radioactivity quantification were carried out as described for [^{3}H]nicotine. Culture dishes were incubated (3 h at 20^{o}C) with 2 nM [^{3}H]-QNB (final concentration) in 0.5 ml PBS containing 0.1% BSA, in the absence and presence of 10 µM atropine to determine total and non-specific binding respectively.

It was considered that binding was detectable when the difference between total and non-specific cpm (or dpm) was significantly greater than zero. The test was performed with a nested ANOVA with the cpm obtained from the total and non-specific treatments nested within each culture and altogether nested within each time.

3.2.2.2. Fluorescence binding assays: FITC-α-Bgt labelling

The distribution of α-Bgt nAChR in hippocampal cultures was determined with FITC-α-Bgt binding. In parallel, experiments were carried out on glial cultures.

Ten day old cultures grown in 16 mm 4-well dishes (Gibco BRL) were washed three times in PBS, either fixed and permeabilized (refer to the appendix C) or assayed alive. Either 10 µl (-)nicotine (1 mM final concentration) or PBS in 480 µl 1% FCS-PBS (refer to the appendix E) were added (30 min; 37^{o}C) to account for non-specific and total binding, respectively.

To determine the toxin concentration for maximum binding, three alternative dilutions were employed. To begin the reaction, 10 µl FITC-α-Bgt was added to give final concentrations of 1 µM; 100 nM; or 10 nM. To evaluate the optimal incubation time, preparations were left at 37^{o}C for 30; 60; 120 or 180 min.

Binding was terminated by aspirating the liquid and washing four times (5 min each) with PBS. Preparations were mounted with Vectashield (Vector Labs) and photomicrographed.

3.3. Results

3.3.1. Radioligand binding assays

Assessment of cholinergic binding sites

Cell cultures maintained for 14 days were assessed for membrane-bound cholinergic binding sites using saturating concentrations of radioligands. Results of ligand binding assays in cultured cells *in situ* are summarized in Table 10.

t	Radioligand	[^{125}I]-α-Bgt	[^{3}H]nicotine	[^{3}H]cytisine	[^{3}H]QNB
HIPPO	total dpm	16092 ± 2792	1214 ± 208	645 ± 53	9433 ± 101
	non-spec dpm	5419 ± 787	1091 ± 267	682 ± 29	4475 ± 211
	specific dpm	10673 ± 3578	123 ± 73	-	4958 ± 272
	fmol/mg protein	**149 ± 13**	**15 ± 7**	**-**	**729 ± 18**
	n	2	3	5	3
CORTEX	total dpm	3127 ± 225	1371 ± 300	728 ± 31	9748 ± 160
	non-spec dpm	2032 ± 97	1266 ± 355	763 ± 133	4862 ± 17
	specific dpm	1096 ± 322	106 ± 55	-	4886 ± 143
	fmol/mg protein	**29 ± 5**	**9 ± 4**	**-**	**767 ± 13**
	n	2	2	2	2
GLIA	total dpm	5147 ± 2333	1312 ± 144	741 ± 109	4398 ± 581
	non-spec dpm	5558 ± 2212	1375 ± 176	748 ± 162	4031 ± 707
	specific dpm	-			367 ± 136
	fmol/mg protein	**-**			**55 ± 25**
	n	2	4		4

Table 10. Binding of cholinergic ligands to cultures.

HIPPO: hippocampal neuronal cultures; n: number of independent experiments; t: tissue. Two week old neuronal hippocampal and cortical cultures as well as confluent monolayers of hippocampal glial cultures were assessed for membrane-bound cholinergic binding.

High affinity [^{125}I]-α-Bgt consistently gave appreciable amounts of displaceable binding in neurons. Hippocampal neurons bound about five times more [^{125}I]-α-Bgt than cortical neurons: 149 versus 29 fmol/mg protein. Glial cells displayed no specific [^{125}I]-α-Bgt binding.

The muscarinic ligand [^{3}H]QNB defined similar levels of specific binding sites in hippocampal and cortical neuronal cultures: 729 and 767 fmol/mg, respectively. The density of sites was 5 and 26 times higher than [^{125}I]-α-Bgt sites in hippocampal

and cortical neuronal cultures. In glial cultures the difference between total and non-specific values obtained with [^{3}H]QNB was greater than zero but not statistically different ($P < 0.05$).

[^{3}H]Nicotine binding was low and less reproducible, and indicated the presence of few specific binding sites relative to those for [^{125}I]-α-Bgt: 15 and 9 fmol/mg protein for hippocampal and cortical neuronal cultures, respectively. However, these values were tested for significance with the student's test. Total dpm were not significantly different from non-specific dpm ($P > 0.05$). With the student's test it was determined that the difference between total and non-specific dpm (i.e. specific dpm) should be at least 340 dpm to give statistically significant differences (at $\alpha=0.05$). This meant that in a given assay, the preparation should have had a minimum of 2 fmol of binding sites per well. Therefore 38 fmol binding sites/mg protein would be the limit of detection of the assay. However, hippocampal neuronal cultures displayed a mean specific binding of 200 dpm (0.8 fmol binding sites) per assay well that correspond to 15 fmol binding sites/mg of protein. This argument also applies to cortical cultures which displayed 106 dpm (0.6 fmol binding sites) per assay well that in turn correspond to 9 fmol binding sites/mg protein. Altogether these results demonstrated that high affinity [^{3}H]nicotine binding sites could not be detected since the concentration of sites is below the level of sensitivity of the method employed. These results were strengthened by those obtained for [^{3}H]cytisine. With this radioligand, no specific labelling of hippocampal or cortical neurons could be discerned. Glial cultures did not display high affinity binding with either of the [^{3}H]agonists. The possibility that [^{3}H]nicotine and [^{3}H]cytisine binding sites were not detected because they are expressed later during development was ruled out by performing weekly assays over a 3 ([^{3}H]cytisine) to 4 ([^{3}H]nicotine) week period. In Figure 6 total and nonspecific [^{3}H]nicotine binding in hippocampal neuronal cultures throughout a 4 week period is plotted. The differences between specific and non-specific binding were not statistically significant ($P < 0.05$). However, in week one,

dpm values for total and non-specific were significantly greater than in subsequent weeks. The data available for cortical neuronal and hippocampal glial cultures are also shown in Figure 6 where it can be seen that neither of them displayed specific binding. Figure 7 shows similar experiments carried out with [^{3}H]cytisine, clearly no specific labelling of hippocampal (neuronal or glial) or cortical neuronal cultures could be discerned.

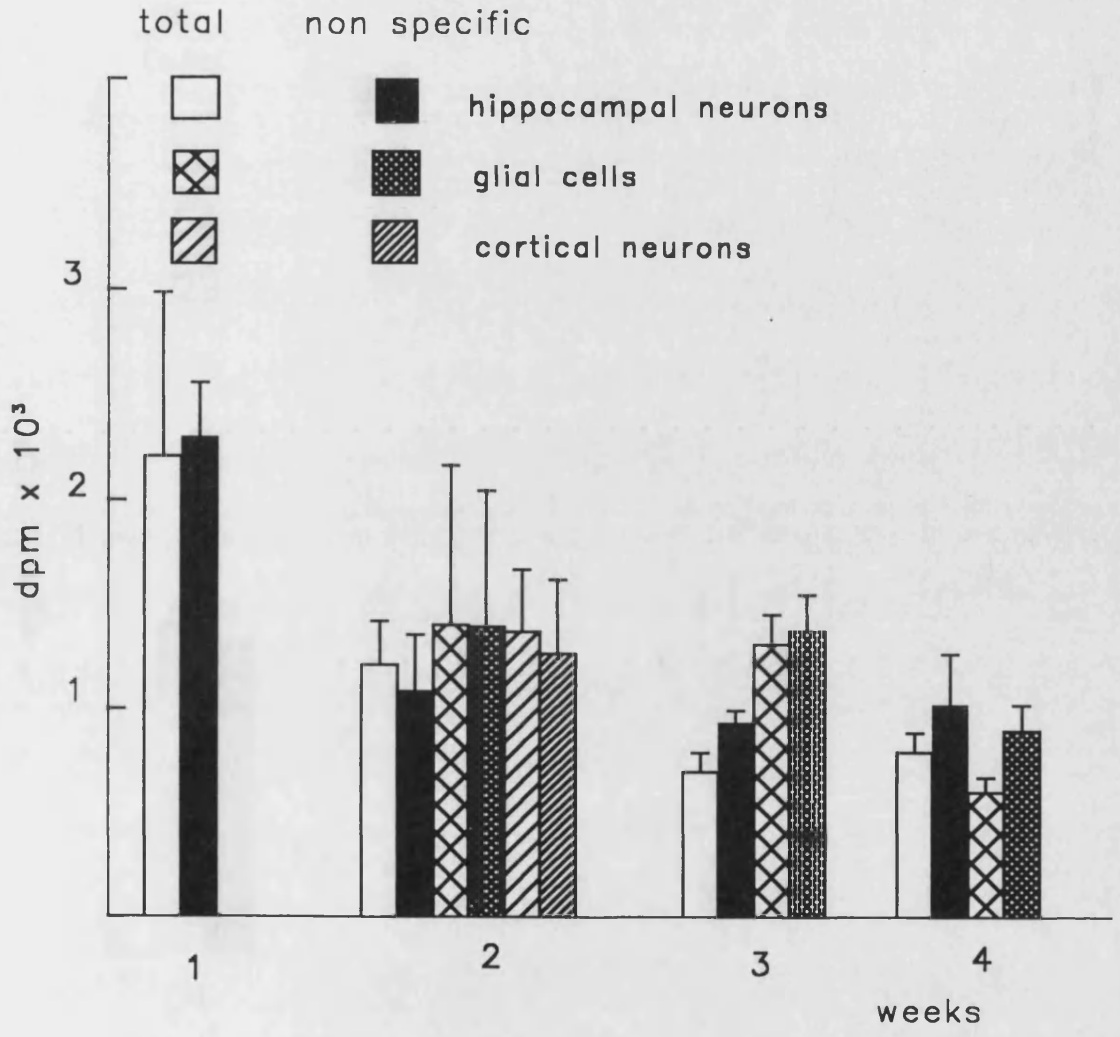

Figure 6. Weekly assessment of [^{3}H]nicotine binding to cultures.

Cultures were incubated with 20 nM [^{3}H]nicotine for 3 h at 20^{o}C. Blank incubations also contained 1 mM unlabeled nicotine. Data were obtained from at least two independent cultures followed over a period of four weeks. A nested ANOVA was employed to test whether the differences between treatments for specific and non-specific binding assays were statistically significant.

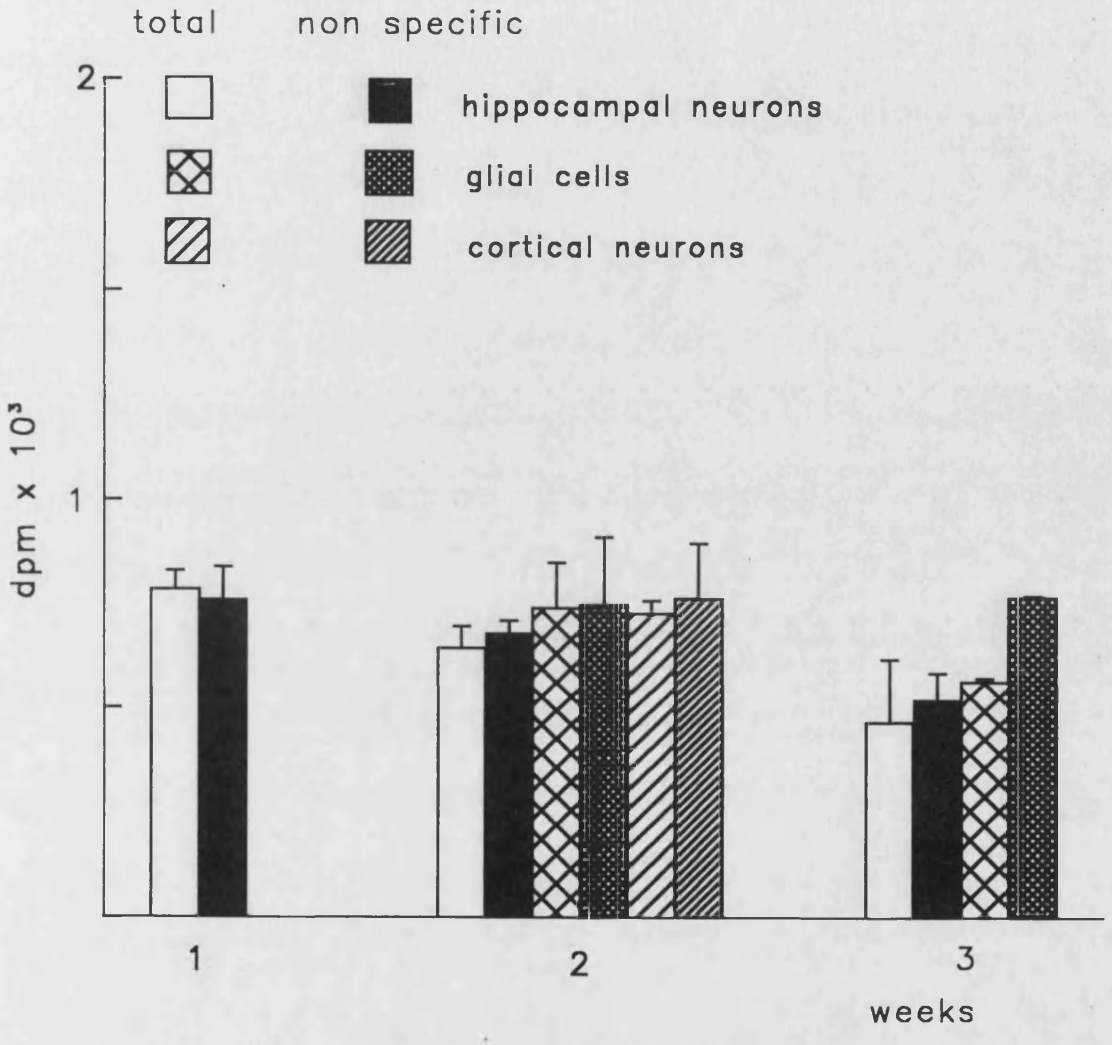

Figure 7. Weekly assessment of [^{3}H]cytisine binding to cultures.

Cultures were incubated with 5 nM [^{3}H]cytisine for 3 h at 20°C. Blank incubations also contained 1 mM unlabeled nicotine. Data were obtained from at least two independent cultures followed over a period of two weeks. A nested ANOVA was employed to test wether the differences between treatments for specific and non-specific binding assays were statistically significant.

Pharmacological profile of high affinity α-Bgt binding sites

The specific binding of [^{125}I]-α-Bgt in hippocampal cultures was explored further by constructing saturation binding curves over the range 0.3 nM to 10 nM [^{125}I]-α-Bgt. The equilibrium binding properties were studied in 7 day old hippocampal cultures. The results of a typical experiment are shown in Figure 8. Specific binding of [^{125}I]-α-Bgt was saturable over the concentration range 0.3 - 10 nM.

The equilibrium dissociation constant was $\mathbf{K_d = 0.62 \pm 0.01\ nM}$ and $\mathbf{B_{max}}$**=128 ± 7** (n=3) fmol binding sites per mg of protein. However, the B_{max} values determined in 7 day old cultures were clearly lower than values determined at saturating concentration of [^{125}I]–α-Bgt in 14 day old cultures (149 fmol, table 10). This was confirmed by following the binding of [^{125}I]–α-Bgt over a 3 week period to hippocampal neurons from the same cultures (Fig. 9). A 30% increase occurred between 7 and 14 days, and the α-Bgt binding site density had doubled between week two and three.

The nicotinic character of the hippocampal [^{125}I]–α-Bgt binding sites was confirmed in competition binding assays. Figure 10 shows the inhibition of [^{125}I]–α-Bgt binding to hippocampal cultures by unlabeled α-Bgt, MLA and (-) nicotine. The inhibition binding parameters are presented in Table 11. The K_i values derived from these studies corresponded very closely to the K_d (Table 11). That K_i values were different from IC_{50} values indicated that competitive inhibition kinetics applied. Ligands exhibit Hill coefficients (n_H) close to the unity consistent with binding to a single population of high affinity binding sites.

Inhibitor	IC_{50}	n_H	K_i
α-Bgt n=3	0.7 ± 0.6 nM	0.7 ± 0.2	0.3 ± 0.2 nM
MLA n=2	15.8 ± 6.9 nM	0.8 ± 0.1	6.1 ± 2.6 nM
(-)nicotine n=2	3.4 ± 1.6 μM	1.1 ± 0.2	1.3 ± 0.6 μM

Table 11. Inhibition binding parameters

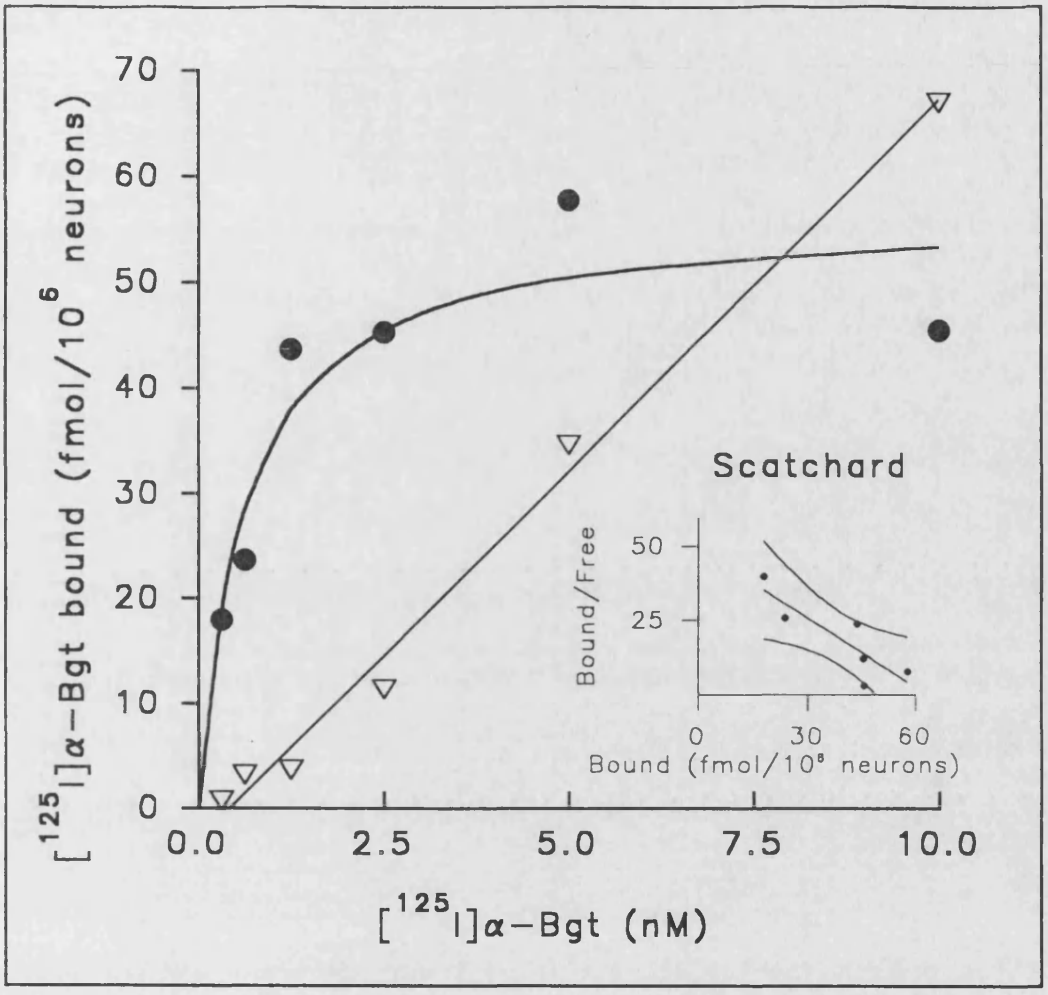

Figure 8. Saturable binding of [^{125}I]–α-Bgt in hippocampal neurons.

Neurons were incubated with varying concentration of [^{125}I]–α-Bgt (0.3 - 10 nM) for 3 h at 20^{o}C. Specific binding was estimated as the difference between total binding and blank incubations containing 1 μM unlabeled α-Bgt. The binding parameter K_d and B_{max} were estimated by non-linear curve fitting to a rectangular hyperbola. Scatchard analysis of the data is shown in the insert.

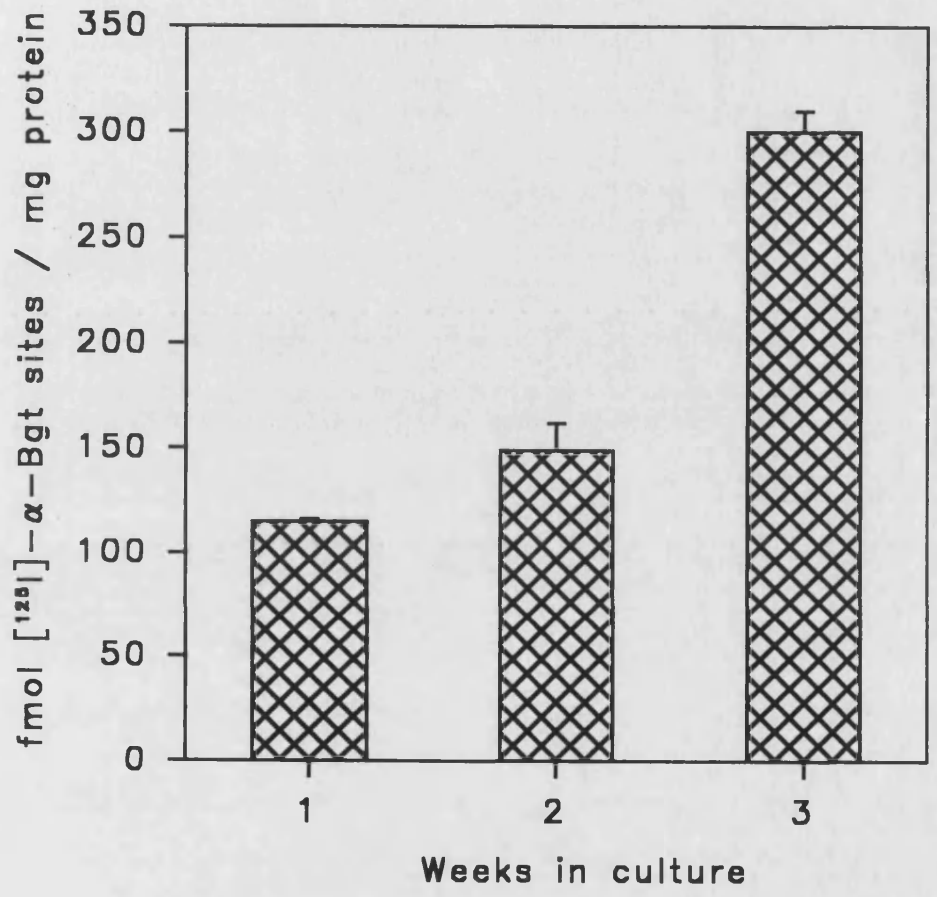

Figure 9. Developmental profile of [^{125}I]–α-Bgt in hippocampal neurons.

Neurons were incubated with 10 nM [^{125}I]–α-Bgt for 3 h at 20^{o}C. Specific binding was estimated as the difference between total binding and blank incubations containing 1 μM unlabeled α-Bgt. Protein values were obtained for each sample and values were corrected to fmol/mg of total protein. Data were obtained from two independent cultures followed over a period of three weeks.

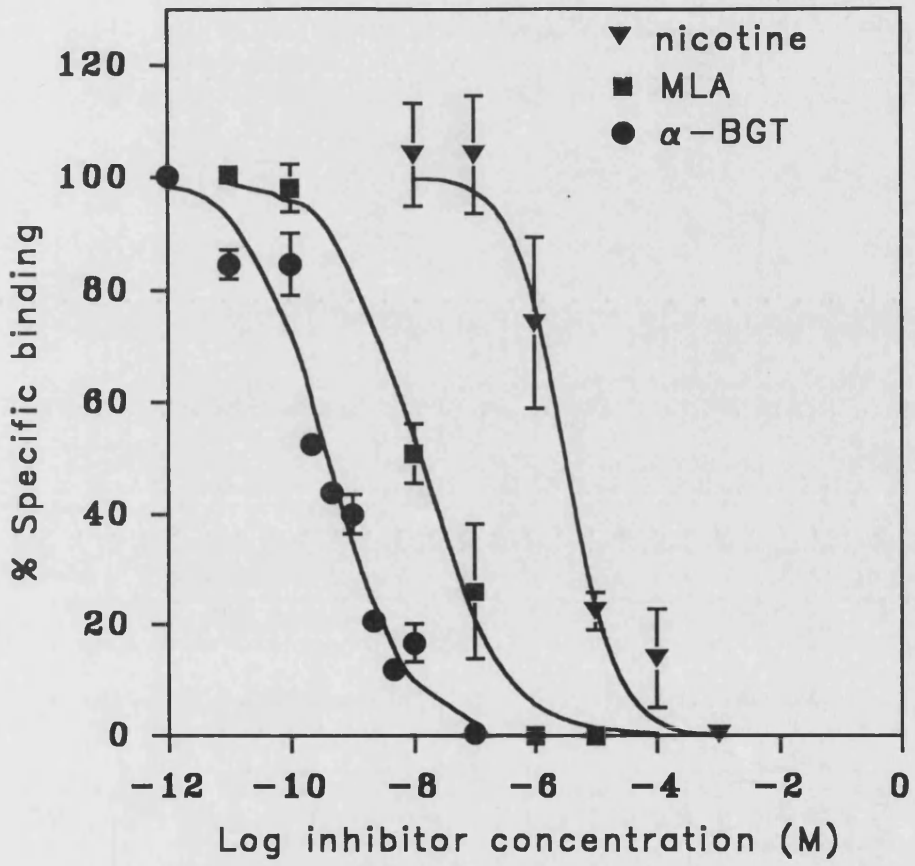

Figure 10. Competition binding assays in hippocampal neurons.

Inhibition of [^{125}I]–α-Bgt by α-Bgt, MLA and nicotine. Neurons were incubated with 1 nM [^{125}I]–α-Bgt and varying concentrations of competing compounds for 3 h at 20^{o}C. Blank incubations contained 1 μM α-Bgt. The binding parameters, IC_{50} and n_H were estimated by a non-linear curve fitting to the Hill equation.

To evaluate whether hippocampal neurons contain intracellular stores of α-Bgt nAChR, [^{125}I]–α-Bgt binding assays were carried out in either alive or fixed/permeabilized cultures and values derived from these experiments were compared. Results showed that ten day old hippocampal neurons have intracellular nAChR since binding almost doubled when cultures were permeabilized. Parallel binding assays to live cultures resulted in 111±4 fmol binding sites/mg protein or 35 ± 2 fmol binding sites/10^6 cells (n=2), compared with permeabilized cultures (198 ± 28 fmol binding sites/mg protein, 66 ± 6 fmol binding sites/10^6 cells; n=2). Thus, an intracellular store of 87 ± 22 fmol binding sites/mg protein or 31 ± 4 fmol binding sites/10^6 cells (n=2) can be calculated.

3.3.2. Fluorescence binding assays: FITC-α-Bgt labelling

The distribution of α-Bgt binding sites in hippocampal cultures was visualized using FITC-α-Bgt in live and fixed/permeabilized preparations. Under this last condition, hippocampal neuronal cultures exposed (1 h) to 10 nM FITC-α-Bgt presented at most 30% of the neurons labeled. At 100 nM and 1 μM (30 to 60 min exposure to FITC-α-Bgt), fluorescence was easily observed in more than 95% of the neurons. Photomicrographs were taken of those samples treated with 100 nM FITC-α-Bgt since fluorescence bleached very fast at lower concentrations of toxin. The total labelling obtained with 1 μM FITC-α-Bgt was very strong, however, non-specific staining was high even when the incubation with FITC-α-Bgt was lowered to 30 min. It was difficult to determine specific binding when cultures were incubated with any toxin concentration for more than one hour. Fluorescence signals obtained with alive cultures were weak and less reproducible. Therefore, exposure of the cultures to 100 nM FITC-α-Bgt for 30 min plus 4 washes (5 min each) were the conditions used to take the microphotographs.

As presented in Plate 11, specific labelling (100 nM; 30 min) of the cell bodies of more than 95% of the neurons present was evident; processes and axons were not

obviously labelled. No trend in the staining pattern was observed when the three major morphological types of neurons in culture were compared.

From this apparently even distribution of total α-Bgt sites across the neuronal population (95 % neurons labeled), and the B_{max} of 66 ± 6 fmol membrane bound [^{125}I]–α-Bgt binding sites/10^6 cells (refer to section 3.3.1.), an average site density of 4.2 ± 0.3 x 10^4 sites/cell was calculated.

Glial cultures were not stained with FITC-α-Bgt (Plate 12) thus confirming the [^{125}I]–α-Bgt binding results, therefore ruling out the presence of these sites in non-neuronal cells.

Plate 11. FITC-α-Bgt labelling to hippocampal neuronal cultures.

Cultures were incubated for 45 min at 37 ^{o}C with 100 nM FITC-α-Bgt in PBS. Non-specific binding was determined by preincubation with 1 μM α-Bgt for 30 min at 37 ^{o}C. Samples were washed thoroughly and mounted.

Plate **A**: Indicated with "**py**" (pyramidal neuron), "**bi**" (Bipolar neuron) and "**s**" (stellate neuron) are neurons that have been strongly stained. Labelled with "**PY**" (pyramidal neuron), "**BI**" (Bipolar neuron) and "**S**" (stellate neuron) are neurons that have not been strongly stained. Indicated with **short thick arrows** are cells that displayed non-specific levels of staining, probably astrocytes. Plate **B**: Phase contrast filter corresponding to field in Plate **A**. Plates **C** and **D**: non-specific immunostaining seen under u.v. or tungsten light, respectively. **Bar: 50 μm.**

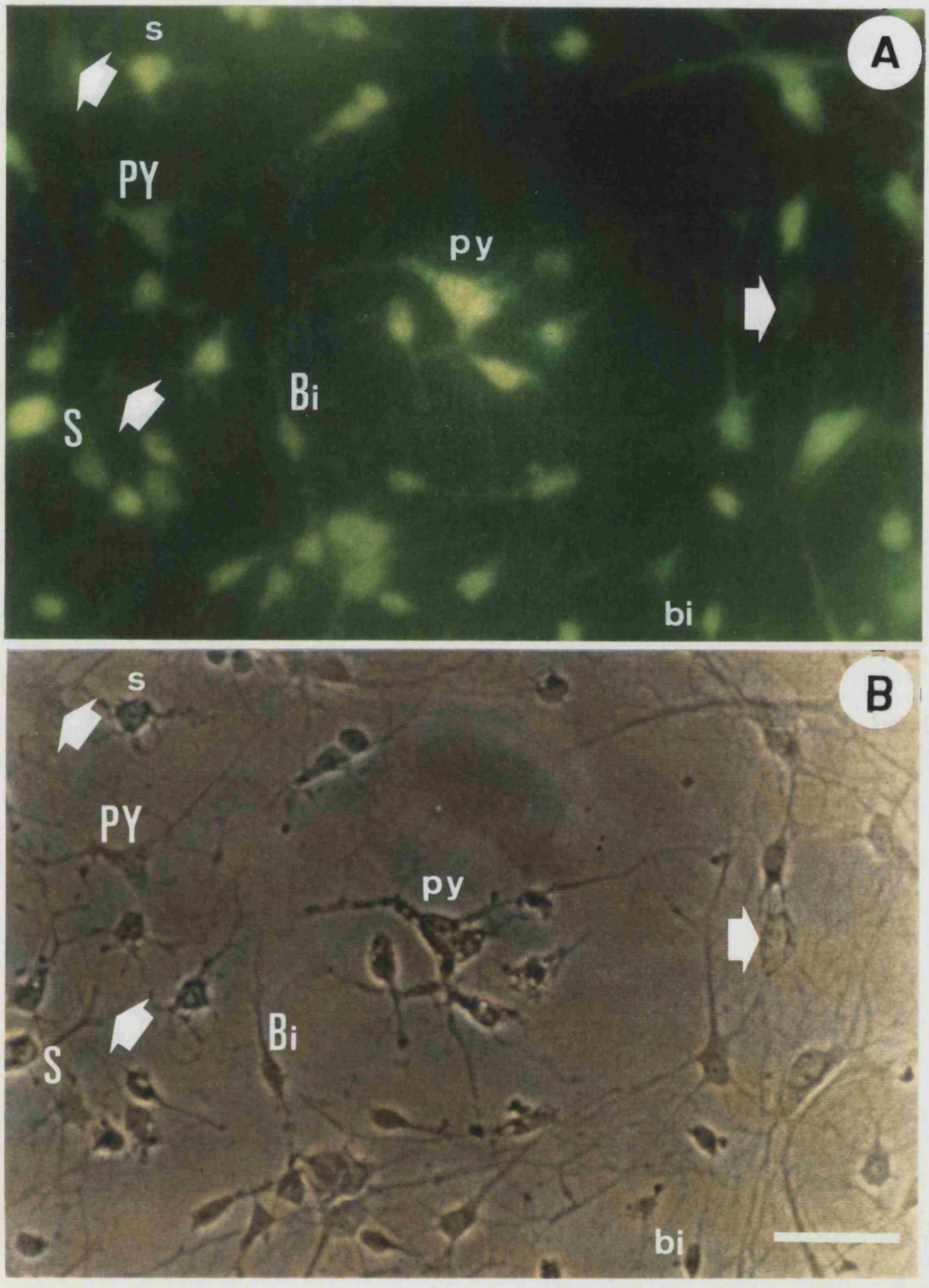
A
s
PY
py
Bi
S
bi
B
s
PY
py
Bi
S
bi

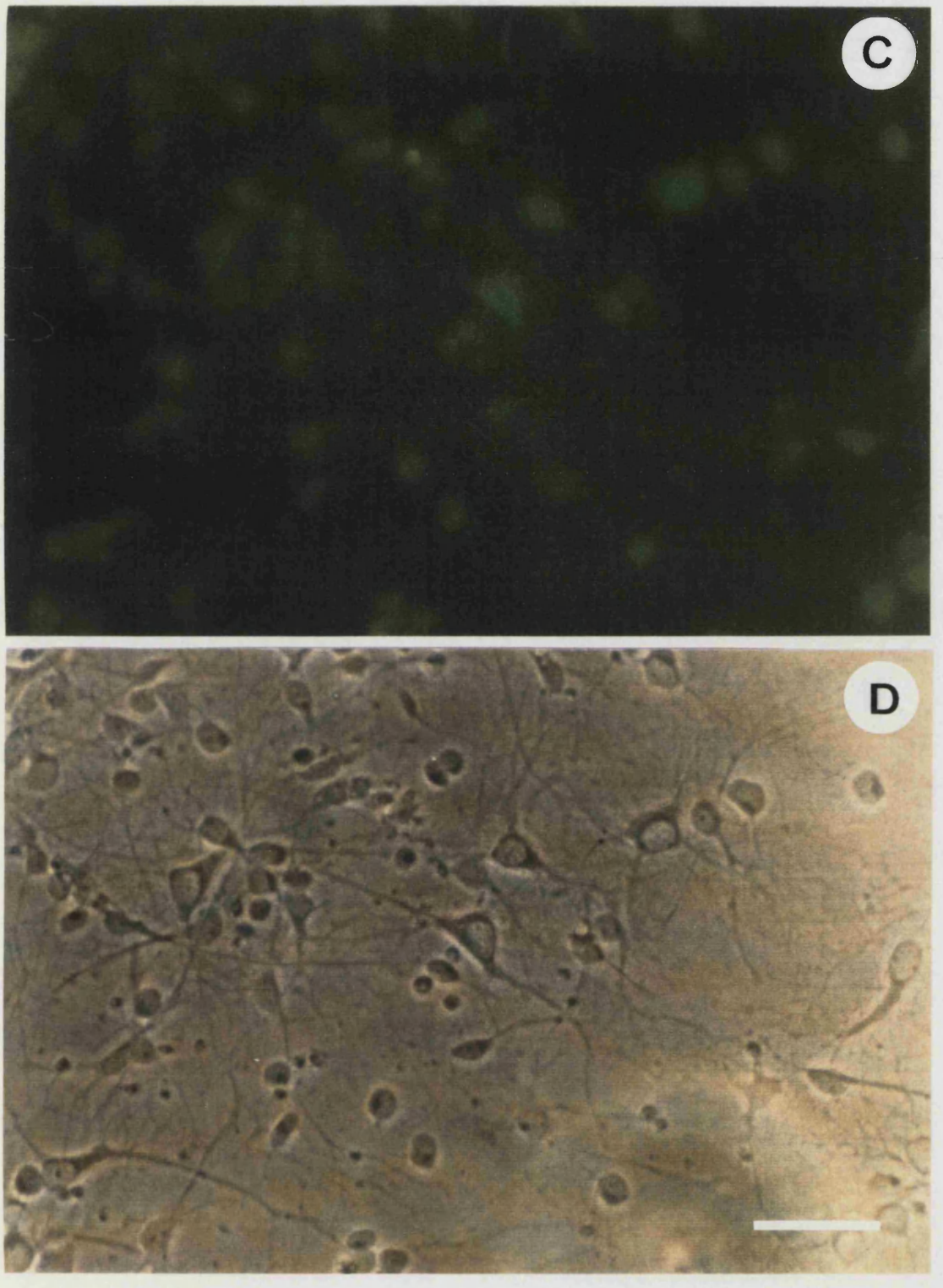
C
D

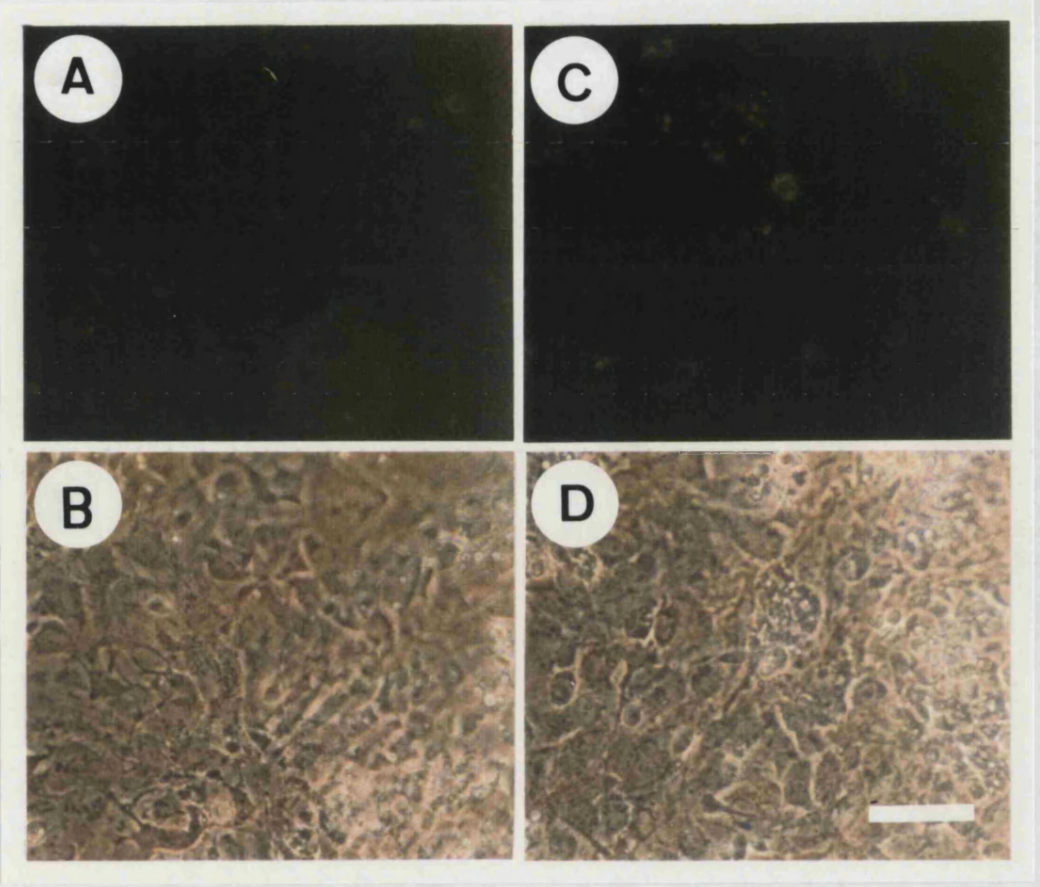

Plate 12. Assessment of FITC-α-Bgt labelling to hippocampal glial cultures.

Cultures were incubated for 45 min at 37 ^{0}C with 100 nM FITC-α-Bgt in PBS. Non-specific binding was determined by preincubation with 1 μM α-Bgt for 30 min at 37 ^{0}C. Samples were washed thoroughly and mounted.

No specific binding was observed. **Bar: 50 μm.**

3.4. Discussion

Radioligand binding assays confirmed the presence of high affinity [^{125}I]-α-Bgt nAChR in hippocampal and cortical neuronal cultures. However, the presence of high affinity [^{3}H]nicotine nAChR in these cultures was less clear cut as discussed below.

Membrane bound high affinity α-Bgt binding sites

[^{125}I]-α-Bgt consistently gave appreciable amounts of displaceable high affinity binding in hippocampal neurons. Hippocampal neurons bound about five times more [^{125}I]-α-Bgt than cortical neurons. The adult rat hippocampus is characterized by dense [^{125}I]-α-Bgt labelling (Clarke *et al.*, 1985) and the differential labelling of adult brain is reflected in the five fold difference in [^{125}I]-α-Bgt binding between hippocampal and cortical cultures. These results are complemented by the further experiments where Rd-α-Bgt labeled only 19% of cortical neurons (see chapter 4). In contrast, glial cultures showed no specific binding of [^{125}I]-α-Bgt or FITC-α-Bgt.

α-Bgt binding sites were present in more than 95% of neurons in culture as demonstrated by FITC-α-Bgt labelling. This is consistent with the observation that 93 % of hippocampal neurons in culture show α-Bgt-sensitive channels responsive to nicotinic agonists (Alkondon and Albuquerque, 1993). The FITC-α-Bgt labelling results were in agreement with autoradiographic studies (no kinetic studies have been reported so far) in embryonic hippocampal cultures where specific [^{125}I]-α-Bgt binding was detected within one week in culture, and by 2 weeks most cells exhibited toxin binding (Banker and Waxman, 1988). Labelling was present over neuronal somata and dendrites, but no labelling of the axonal network was detectable. Glial cells were also unlabelled. Similar results have been reported by Alkondon and Albuquereque (1993) who labelled embryonic hippocampal neurons with 0.01 to 1

μM Rd-α-Bgt. It is difficult to compare their labelling results with those in the present study since these authors showed only two neurons per experiment and no controls for non-specific staining were carried out. In addition these workers do not specify the age in culture which influences the number of α-Bgt sites (Fig. 9).

Saturation binding assays for [^{125}I]–α-Bgt to hippocampal cultures showed an equilibrium dissociation constant (K_d= 0.62 nM) comparable to adult hippocampal membranes [K_d= 0.54 nM, (Alkondon *et al.*, 1992)]. In addition, saturation binding assays for [^{125}I]-α-Bgt to hippocampal cultures showed a maximum number of surface [^{125}I]-α-Bgt binding sites of 128 fmol/mg of protein. In adult hippocampal membranes a lower B_{max}= 51.1 fmol/mg of protein has been reported (Alkondon *et al.*, 1992). These differences in B_{max} may reflect the nature of the preparations. In both systems, B_{max} values were expressed per mg of protein. However, total protein values from membrane preparations correspond to material of neuronal and non-neuronal origin. In culture total protein values express the amount of protein present in the whole cell, mainly composed of neurons (> 95%).

The binding of [^{125}I]–α-Bgt over a 3 week period to hippocampal cultures from the same cultures (Fig. 7) was followed. The maximum number of α-Bgt binding sites per neuron almost tripled from week one to three. In parallel, cell bodies almost tripled in size, neurites thickened and a complex network of processes became apparent. The significance of these changes in α-Bgt binding sites is not clear. Previous studies have established that α-Bgt sites in rat hippocampus appear early in development (Ben-Barak and Dudai, 1979) and reach a peak by the first days after birth, before declining to mature levels by the second week. As synaptic formation occurs between 11 and 21 days postnatally, the appearance of α-Bgt sites in rat hippocampus precedes synapse formation, and also precedes the appearance of [^{3}H]nicotine (Yamada *et al.*, 1986) and muscarinic binding sites (Ben-Barak and Dudai, 1979) (which increase gradually, attaining adult levels by the fourth and sixth

weeks postnatally, respectively). This implies that α-Bgt sites may be functionally important during development but may become silent following synapse formation and stabilization (Vijayaraghavan *et al.*, 1992). That α-Bgt sites in hippocampal cultures did not decrease by week three in culture -as might be expected from the results of Ben-Barak and Duadi (1979)- may reflect the lack of cholinergic inputs in this *in vitro* system.

The nicotinic character of the hippocampal [^{125}I]–α-Bgt binding sites was confirmed in competition binding assays. The α-Bgt binding site displayed competitive inhibition by the agonist (-)nicotine (K_i= 1.3 μM). These results are comparable with the inhibition of [^{125}I]-α-Bgt binding to rat brain preparations, where nicotine displayed a competitive inhibition with a K_i= 5.1 μM (Macallan *et al.*, 1988). In addition, K_i values matched those reported (Vijayaraghavan *et al.*, 1992) for cultured chick ciliary ganglion neurons (MLA, K_i=2.8 nM; α-Bgt, 0.7 nM) from which α7-specific mAb immunoprecipitate more than 90% of α-Bgt nAChR (Schoepfer *et al.*, 1990). However, in this system nicotine is two orders of magnitude more potent (K_i= 18 nM) than in hippocampal neurons (K_i= 1.3 μM) reflecting methodological differences as well as possible distinct posttranslational modifications or subunit combination of this α-Bgt nAChR. It is not known if α7 assembles to form homomeric nAChR in the brain. Helekar *et al.* (1994) have proposed that prolyl isomerase is required for the expression of functional homo-oligomeric α7 nAChR in *Xenopus*. In the sympathetic PC12 cell line, [^{125}I]–α-Bgt binding sites are inhibited by nicotine and α-Bgt with IC_{50} values in the micromolar and nanomolar range, respectively, (Chan and Quik, 1993). Similar results have been recently reported for native and α7 homomers expressed in *Xenopus* from chick and human (Peng *et al.*, 1994). These parameters are in agreement with those reported in the present thesis. Similar pharmacology suggest similarities in the subunit composition of α-Bgt sites.

Other studies have reported that MLA inhibits potently [^{125}I]-α-Bgt binding to adult hippocampal membranes in contrast to its weaker interaction with the high affinity [^{3}H]nicotine neuronal nAChR (Macallan *et al.*, 1988). The high affinity and selectivity of MLA for the neuronal α-Bgt nAChR (Alkondon *et al.*, 1992) may reflect the unique genes (α7 and α8) proposed to encode this receptor in the brain (Schoepfer *et al.*, 1990; Couturier *et al.*, 1990). In the present study, the ability of MLA to inhibit [^{125}I]-α-Bgt binding to cultured hippocampal neurons (K_i= 6.1 nM) was comparable to adult tissue [K_i= 4.3 nM, (Alkondon *et al.*, 1992)] and also consistent with a competitive mode of action as reflected by the Hill coefficient (Table 11). In addition, MLA was about two hundred times more potent than (-)nicotine (K_i= 6.1 nM vs 1.3 μM, respectively). However, MLA was one order of magnitude less potent than α-Bgt (K_i= 0.3 nM) in inhibiting [^{125}I]-α-Bgt binding in contrast with adult tissue where both toxins are equipotent (Alkondon *et al.*, 1992). This discrepancy could reflect differences between adult and fetal forms of nAChR since there is a precedent for that in muscle (Mishina *et al.*, 1986) and similar developmental changes may also occur in neurons.

Intracellular α-Bgt binding sites

In hippocampal neurons, intracellular high affinity α-Bgt sites represented almost the same amount as membrane-bound sites. Internal stores of assembled or partially assembled multisubunit molecules have been previously reported and may be a general pattern for plasma membrane proteins in developing cells (Jacob *et al.*, 1986; Hill *et al.*, 1993). These intracellular sites may represent endocytosis or turnover of the surface membrane nAChR. A substantial proportion of the cellular AChR content is stored intracellulary or degraded without ever reaching the surface of muscle (Merlie, 1984). Some intracellular component may represent the over-production of individual subunits that either fail to assemble or form abortive multisubunit complexes in some respect. The biological significance of intracellular

receptor that fails to be inserted into the surface membrane, however, remains obscure. Alternatively, the internal sites may represent a reserve of receptor for developmental contingencies (Jacob *et al.*, 1986).

Are membrane bound high affinity [^{3}H]nicotine binding sites detectable?

[^{3}H]Nicotine selectively labels the predominant nAChR in the brain, considered to be made up of α4 and β2 subunits (Whiting *et al.*, 1987b). [^{3}H]Nicotine binding to hippocampal and cortical neurons was low, and indicated the presence of few specific binding sites relative to those for [^{125}I]-α–Bgt. These negative results were strengthened by those obtained for [^{3}H]cytisine which labels the same α4β2 nAChR subtype (Pabreza *et al.*, 1991). With this radioligand, no specific labelling to hippocampal or cortical neurons could be discerned. [^{3}H]Cytisine was chosen as an alternative approach in an attempt to detect specific binding since its higher affinity, slower rate of dissociation from its binding site, low nonspecific binding and high stability are well established (Pabreza *et al.*, 1991).

In situ characterization of [^{3}H]nicotine sites in fixed (but not permeabilized) cortical cultures grown in a 25 cm^2 tissue culture flask at an initial density of 2 x 10^7 cells gave a B_{max}= 25 fmol / mg = **50 fmol / flask** (Lippiello *et al.*, 1991). These results are consistent with 38 fmol binding sites/mg protein estimated as the limit of detection of the assay (see section 3.3.1.). That neither cortical nor hippocampal neuronal cultures displayed high affinity [^{3}H]nicotine or [^{3}H]cytisine binding (Table 10) may be explained in terms of methodological differences, since in the present study in every experimental point 2 x 10^5 cells were employed [vs 2 x 10 ^{7}, (Lippiello *et al.*, 1991)]. A major difference is that Lippiello et al., (1988) deliberately avoided trypsinisation in the isolation of the cortical neurons by using mechanical sieving techniques instead. While it is conceivable that proteolytic attack could destroy surface binding sites, it is surprising that these are not restored after 2 weeks in culture. The weak [^{3}H]nicotine binding but no [^{3}H]cytisine binding suggests that

[^{3}H]nicotine by virtue of its lipophilicity may be entering the neurons and labelling intracellular nAChR. This interpretation is consistent with the antibody labelling pattern for cortical neurons (Lippiello *et al.*, 1991).

In hippocampal cultures, the failure to detect significant amounts of α4β2 nAChR defined by [^{3}H]cytisine or [^{3}H]nicotine binding is consistent with the paucity of α-Bgt-insensitive currents in this same *in vitro* system (Alkondon and Albuquerque, 1993). In this study only 15% of neurons gave nicotinic responses that were sensitive to n-Bgt but not to α-Bgt (10% of these cells also expressed α-Bgt-sensitive currents) while 2% of neurons had nicotinic currents blocked by mecamylamine but unaffected by either snake toxin. These currents could be attributed to nAChR channels of the types α3β4 and α4β2. In addition, the hippocampal cell line [HN33] has been shown to express low levels of [^{3}H]cytisine binding [14 fmol/mg protein] (Monteggia *et al.*, 1993). However, this last could also reflect the tumoral nature of cell lines. Finally, adult rat hippocampus has been reported to display low levels of high affinity [^{3}H]nicotine binding [less than 10 fmol/mg protein] (Marks *et al.*, 1986).

The muscarinic ligand [^{3}H]QNB which displays similar kinetics and specific activities to the tritiated cholinergic agonists, and therefore used as a positive control for the [^{3}H]cholinergic binding assays, defined high levels of specific binding sites: 729 and 767 fmol/mg in hippocampal and cortical neuronal cultures. Early studies on the rate of development of muscarinic receptors in the rat hippocampus have shown that between day ten and 14 there are about 700 fmol muscarinic sites/mg protein (Ben-Barak and Dudai, 1979).

3.5. Summary to chapter 3

(i) There are high affinity [^{125}I]-α-Bgt binding sites in hippocampal neuronal cultures, about five times more than in cortical neurons. Surface [^{125}I]-α-Bgt binding

sites represent half of the total population of α-Bgt sites in permeabilised cultures. In chapter 4 the nature of these sites is further explored.

(ii) More than 95% of neurons in culture displayed α-Bgt binding sites as shown by FITC-α-Bgt labelling. These estimations were performed on fixed/permeabilized preparation since under living conditions, signals were weaker and less reproducible. The FITC-α-Bgt probe rendered high levels of nonspecific staining therefore as presented in chapter 4, Rd-α-Bgt was employed for further experiments.

(iii) The B_{max}=50 fmol/2 x 10^7 cells (25 fmol/mg protein) reported for cortical cultures (Lippiello *et al.*, 1991) demonstrated that the sample size (2 x 10^5 cells) in the present study was below the level of sensitivity (38 fmol/mg protein) of [^{3}H]nicotine binding assays. Therefore, the α4β2 nAChR which displays high affinity for [^{3}H]nicotine and [^{3}H]cytisine must represent a relatively small proportion of the nAChR population in hippocampal neuronal and cortical cultures.

(iv) Hippocampal neurons displays high affinity [^{3}H]QNB binding comparable to that in 12 day old postnatal rat hippocampal preparations.

(v) High affinity [^{125}I]-α-Bgt binding in enriched neuronal cultures could be attributed to neurons since glial cells showed no specific [^{125}I]-α-Bgt binding.

(vi) The nicotinic nature of α-Bgt sites in neurons was confirmed by inhibition experiments with nicotine.

Chapter 4
Immunocytochemistry

4.1. Introduction

Molecular cloning methods have revealed the existence of a gene family encoding neuronal nAChR subunits (α2-α7, β2-β4, see Table 3) expressed in rat brain. Heterologous expression studies in *Xenopus* oocytes suggested that different subunit combinations assemble to form nAChR pentamers with distinct pharmacological specificities and ionic channel properties, implying that a wide variety of nAChR exist in the CNS (see section 1.3.5.). It has not been demonstrated, however, that all such combinations occur in the brain and it may be the case that additional subunits are either required or used to make functional receptors in the brain. To begin to understand the role that these different receptors may play in cholinergic neurotransmission it is necessary to establish the distribution of the distinct nAChR in the various functional systems of the brain at the cellular and subcellular level.

Several approaches have been used to localize nAChR in the brain (see sections 1.3.2. to 1.3.4.). Receptor autoradiography with radiolabelled ligands allowed the mapping of high-affinity [^{3}H]nicotine and [^{125}I]-α-Bgt binding sites in brain regions (Clarke *et al.*, 1985). These ligands are considered to label nAChR that include α4β2 and α7, respectively (see section 1.3.4.). Hybridization histochemistry has established the distribution of neurons that synthesize the mRNA coding for various nAChR subunits (Deneris *et al.*, 1989; Wada *et al.*, 1989; Boulter *et al.*, 1990; Wada *et al.*, 1990; Séguéla *et al.*, 1993). However, *in situ* hybridization procedures localize the mRNA encoding the receptor molecule and not the receptor protein, which might be localized on the soma, axon, dendrite or nerve terminal (Swanson *et al.*, 1987).

Monoclonal antibodies and cDNA have been critical and complementary probes for studying nAChR subtypes (refer to section 1.3.4.). mAbs have been made to

affinity-purified nAChR, to small synthetic peptide fragments of these proteins, and to larger peptides expressed in bacteria. These mAbs have been used in many ways for nAChR immunoaffinity purification, histological characterization, subunit identification and characterization (reviewed by Lindstrom *et al.*, 1991).

In the present work, nAChR subunit-specific antisera to fusion proteins as well as monoclonal antibodies to nAChR subunits subtypes have been employed to assess the expression and examine the distribution of nAChR subunits in hippocampal and cortical cultures.

4.2. Experimental Procedures

4.2.1. Materials

Monoclonal antibodies mAb 307 (stock 30/05/89, titer 0.1 μM) and mAb 299 (stock 07/03/90, titer 2.6 μM) were kindly provided by Dr. Jon Lindstrom. Lyophilized samples were dissolved with PBS and stored at -20°C. The monoclonal antibody mAb 307 is a mouse IgG to native and denatured chicken α-Bgt-binding nAChR. It binds to the intracellular loop between residues 380 and 400 of the chick α7 nAChR (Schoepfer *et al.*, 1990) and cross reacts with the rat α7 subunit. The monoclonal antibody mAb 299 is a rat IgG to purified rat brain nAChR which has the ability to bind to the extracellular surface of native α4 nAChR subunits (Whiting *et al.*, 1991).

Rabbit polyclonal antisera against the cytoplasmic domains of the α and β nAChR subunits were donated by Dr. Scott Rogers: α2 (4843), α3 (4860), α4 (5009), α5 (4888), β2 (4842) and β4 (4886). Antisera were produced by Rogers *et al.* (1991) using the trpE bacterial expression system to express fusion proteins with portions of putative cytoplasmic domains of α or β nAChR subunits. Following fractionation by SDS-polyacrylamide gel electrophoresis and recovery, the fusion protein was used to immunise rabbits. Four weeks later, rabbits were boosted with emulsified antigen. Two weeks later, serum was collected subsequent to ear bleeding and the antiserum was tested for immunoreactivity to bacterially expressed protein by western blot and ELISA analysis. Samples were stored at -20°C.

Anti-mouse IgG-FITC and anti-rat IgG-FITC were purchased from Sigma and stored with 50% glycerol at -20°C.

Tetramethylrhodamine α-bungarotoxin was purchased form Molecular Probes Cambridge BioScience, Swann's Rd., Cambridge, CB5 8LA, U.K..

Paraformaldehyde and cacodylate buffer were purchased from BDH Chemicals Ltd. (Poole, U.K.) and Triton x-100 from Aldrich Chemical Co. Ltd., Gillingham,

Dorset, England). Suppliers for fixative solutions are listed along with the fixative composition in the appendix C and D to this thesis.

3T3L1 mouse fibroblast cell line was donated by Dr. G. Holman and used to preadsorb the rabbit antisera as described in appendix D of this thesis.

PC12 cells were kindly donated by Dr. Yvonne Vallis, maintained as described in appendix B of this thesis and used as controls for immunocytochemistry with rabbit antisera.

M10 fibroblasts (stably transfected with α4 and β2 chicken nAChR subunits, Whiting *et al.*, 1991) were also used in control experiments. This cell line kindly donated by Dr. P. Whiting was maintained as described in appendix B of this thesis.

Cultures were analyzed in a phase contrast microscope (Nikon Diaphot) equipped for epifluorescence. Photographs were taken using Kodak 400, 1000 and 1600 ASA films.

4.2.2. Methods

Cortical cultures were employed as an approach to set up the conditions suitable to perform dual labelling with Rd-α-Bgt and mAb 307 to α7 nAChR in hippocampal neuronal cultures. As demonstrated in chapter 3, cortical cultures also have high affinity α-Bgt binding sites and have the advantage that they can be produced on a large scale.

Immunostaining with monoclonal antibody mAb 307 in neuronal cultures

To evaluate the presence of the α7 nAChR subunit, mAb 307 was employed to immunostain hippocampal (neuronal and glial) and cortical cultures.

Either neuronal or glial cultures grown for 7-10 or 14 days, respectively, were fixed/permeabilized with the acetic acid-ethanol procedure as described in the appendix C to this thesis. Subsequently, preparations were blocked with 200 µl 1% FCS-PBS for 30 min at room temperature. The solution was aspirated and mAb 307

was diluted in 200 µl 1% FCS-PBS to reach 25 nM final concentration (to ensure optimum fluorescence for photography). Cells were incubated 2 h at 37°C. A positive result was judged and graded with reference to the control incubation which was treated with 1% FCS-PBS instead of mAb 307. Cultures were washed four times with 500 µl PBS and anti-mouse IgG-FITC conjugate (1:100) was applied for 2 h at 37°C. Samples were mounted with Vectashield (Vector Labs) and photomicrographed.

Rd-a-Bgt labelling

Similar conditions as those described for FITC-α-Bgt (see section 3.2.2.2.) were employed to label α-Bgt nAChR with Rd-α-Bgt with the purpose of performing double labelling with mAb 307 and mAb 299 in enriched neuronal cultures.

Cortical cultures grown for 7 to 10 days were fixed/permeabilized with the acetic acid-ethanol procedure (appendix C). Either 10 µl (-)nicotine (6.4 mM final concentration) or 10 µl PBS in 480 µl 1% FCS-PBS were added for 30 min at 37°C to account for non-specific and total labelling, respectively.

To begin the reaction, 10 µl Rd-α-Bgt was added to give final concentrations of 1 µM; 100 nM; or 10 nM. To determine the optimal incubation time, preparations were left at 37°C for 30; 60; 120 or 180 min.

Binding was terminated by aspirating the liquid and washing four times with 500 µl PBS. Preparations were mounted with Vectashield (Vector Labs) and photomicrographed.

mAb 307-(anti-mouse IgG-FITC) / Rd-α-Bgt co-labelling in enriched neuronal cultures

The labelling pattern of Rd-α-Bgt and mAb 307 was evaluated by double-labelling hippocampal and cortical enriched neuronal cultures. The methodology employed was a combination of the immunostaining and Rd-α-Bgt binding procedures.

Neuronal cultures grown for 7 to 10 days were fixed/permeabilized with the acetic acid-ethanol procedure (appendix C) and blocked with 200 µl 1% FCS-PBS for 30 min at room temperature. The solution was aspirated and mAb 307 was diluted in 200 µl 1% FCS-PBS to reach 25 nM final concentration. Preparations were incubated 2 h at 37°C. A positive result was judge and graded with reference to the control incubation which was treated with 1% FCS-PBS instead of mAb. Cultures were washed four times with PBS and 10 µl anti-mouse IgG-FITC conjugate was applied to 470 µl 1% FCS-PBS solution for 2 h at 37°C. Thirty min after this last incubation was begun, either 10 µl (–)nicotine (6.4 mM final concentration) or 10 µl 1% FCS-PBS solution were added to account for non-specific and total binding, respectively. After a further 60 min incubation to allow (-)nicotine to block the α-Bgt sites, 10 µl Rd-α-Bgt was added to give a final concentration of 1 µM. Preparations were left at 37°C for a further 30 min. The reactions were terminated by aspirating the liquid and washing four times with 500 µl PBS. Samples were mounted with Vectashield (Vector Labs) and photomicrographed.

mAb 299-(anti-rat IgG-FITC) / Rd-α-Bgt co-labelling in enriched neuronal cultures

To evaluate the presence of α4 nAChR subunit, mAb 299 to the extracellular surface of α4 nAChR subunit (Whiting *et al.*, 1991) was employed to immunostained neuronal cortical cultures.

The method used was essentially as described in the preceding section except that the cultures were not fixed/permeabilized and mAb 299 was diluted in 200 µl 1% FCS-PBS solutions to reach 500 nM final concentration.

The proportion of neurons that were co-labelled with both fluorescence probes was obtained by direct counting of cells from high power photomicrographs and expressed as a percentage of the total number of neurons present.

Immunocytochemistry with antisera against nAChR subunits

To evaluate the presence of α2, α3, α4, α5, β2 and β4 nAChR subunits, antisera against fusion proteins containing fragments of these nAChR subunits (Rogers *et al.*, 1991) were employed in immunocytochemistry studies following the method of Rogers *et al.*, (1992).

Hippocampal neuronal (7-14 day old), glial (100% confluence) and PC12 (3 days after splitting) cultures were gently washed three times with PBS and fixed with freshly prepared 2% (w/v) paraformaldehyde in 0.1 M cacodylate buffer (pH=7.4) for 30 min. The fixative was removed and samples were washed (x3) with 500 µl PBS. Cells were permeabilized with 200 µl 0.3% Triton x-100 in blocking PBS (1% normal goat serum in PBS) for 30 min. Samples were washed (x3) with 500 µl blocking PBS and the preadsorbed antisera (refer to appendix D) added at the recommended 1:250; 1:500; 1:750; 1:1000; 1:1500 dilutions. Normal rabbit serum and growth media were used as controls. Samples were incubated for 4 h at 37^{o}C (or overnight at 4^{o}C). After washing with blocking 500 µl PBS (x3), 200 µl alkaline phosphatase conjugated goat anti-rabbit (1:1000 dilution) was applied for 1 h. The cells were first washed one time with 500 µl PBS following by two more washes with 500 µl 50 mM sodium carbonate buffer containing 2 mM $MgCl_2$ (pH=9.5). The alkaline phosphatase was visualized by adding 500 µl developing solution (refer to the appendix E) to the cells at 20^{o}C. Development was usually for 15 to 30 min with fresh developing solution added every 15 min. The reaction was stopped with 500 µl 2 mM EDTA in PBS. Cultures were mounted in glycerol-PBS (3:1) and photomicrographed.

4.3. Results

4.3.1. Immunocytochemistry with monoclonal antibodies to nAChR subunits

4.3.1.1. Cortical neuronal cultures

mAb 307 immunoreactivity

The presence of the α7 nAChR subunit in cortical cultures was demonstrated by the positive immunoreactivity of mAb 307. This monoclonal antibody to α-Bgt-binding nAChR was raised against the intracellular loop of chicken α7 nAChR but cross reacts with the rat α7 subunit (Schoepfer *et al.*, 1990). Although the recommended mAb concentration was 10 nM, experimentation showed 25 nM to give optimal fluorescence signal for photomicrography.

As shown in Plate 13, mAb 307 labelled those neurons with either pyramidal, bipolar or stellate appearance. However, the small, round cells also present in cortical cultures were either labelled less or not at all. In Plate 13A, a typical labelled pyramidal neuron has been indicated with a short thick arrow, whereas a group of non-labelled small, round cells have been indicated with a long arrow. The contribution of FITC fluorescence to the rhodamine filter was almost nil as indicated in Plate 13B. This was a useful control for further dual-labelling experiments. As shown in Plate 13D, non-specific immunostaining of anti-mouse IgG-FITC was very low.

Rd-α-Bgt labelling

Cortical neurons were labelled with Rd-α-Bgt, the optimum conditions were determined empirically. Rd-α-Bgt was added to give final concentrations of 1 μM; 100 nM; or 10 nM and preparations were left at 37^{o}C for 15; 30; 60; 120; 180 or 240 min. At 10 nM Rd-α-Bgt there was no labelling even when incubations were as long as 240 min. At 100 nM most of the neurons were stained when incubation times were

greater than 30 min, however there was not enough fluorescence to take photomicrographs. The signal obtained with 1 μM Rd-α-Bgt (30 min at 37°C) allowed photomicrographs to be taken. However this last condition rendered the highest non-specific labelling; this was significantly reduced with four washes (5 min each). Thus, 30-40 min incubations with 1 μM Rd-α-Bgt plus four washes (5 min each) with PBS were implemented to perform dual labelling experiments.

As shown in Plate 14A, Rd-α-Bgt labelled those neurons with either pyramidal, bipolar or stellate appearance. However, the small, round cells were clearly not labelled. The contribution of the fluorescence to the fluorescein filter by the rhodamine probe was almost nil as indicated in Plate 14B. As shown in Plate 14D, non-specific staining of Rd-α-Bgt was very low.

mAb 307-(anti-mouse IgG-FITC) / Rd-α-Bgt co-labelling

Double-labelling studies were carried out to test whether α-Bgt binding sites and α7 nAChR subunit collocated in the same neurons. As shown in Plate 15, α-Bgt binding sites and α7 nAChR subunit proved to be collocalized within bipolar, pyramidal and stellate neurons. The same labelling pattern obtained with the single labelling experiments was observed (see legend to Plates 15 and 16).

The proportion of cortical neurons that were co-labelled with α-Bgt and mAb 307/anti-mouse IgG-FITC was obtained by direct counting of cells from high power photomicrographs and expressed as a percentage of the total number of neurons present. On average, 36 ± 4% (n=12, i.e. 4 fields from 3 independent cultures) of cortical neurons were co-labelled.

mAb 299-(anti-rat IgG-FITC) / Rd-α-Bgt co-labelling

Cortical cultures were treated with mAb 299 to native α4 nAChR. Therefore as a preliminary approach, fixation procedures were avoided to prevent the possibility of altering the antigenic region.

The various manipulations involved in this procedure were detrimental to the integrity of the cultures. However, these preliminary experiments clearly showed (Plate 17) that mAb 299 to α4 nAChR subunit immunostained all the cortical neurons. Rd-α-Bgt stained 19 ± 2% of the cells in culture most of which were pyramidal (indicated with an arrow in Plate 17), bipolar or stellate in appearance.

Plate 13. Staining pattern of mAb 307 against α7 nAChR subunit in cortical neurons.

Cultures grown for 10 days were fixed and permeabilized with 5% acetic acid-70% ethanol solution and mAb 307 (25 nM final concentration) was added (Plate A, B and C). A positive result was judged and graded with reference to the control incubation for non-specific staining which was treated with 1% FCS-PBS instead of mAb 307 (Plate D, E and F). After 2 h at 37°C neurons were washed four times with PBS and anti-mouse IgG-FITC conjugate was added for 2 h at 37°C. The reactions were terminated by aspirating the liquid and washing four times with PBS. Samples were mounted and photomicrographed.

A and **D**: total and non-specific immunostaining for mAb 307 viewed with the fluorescein filter, respectively.

B and **E**: total and non-specific immunostaining for mAb 307 viewed with the rhodamine filter, respectively.

C and **F**: Fields viewed with phase contrast corresponding to photomicrographs **A-B** and **D-E**, respectively.

A labelled pyramidal neuron has been indicated with a **short thick arrow** whereas a group of non-labelled small, round cells have been indicated with a **long arrow**.

Bar: 50 μm.

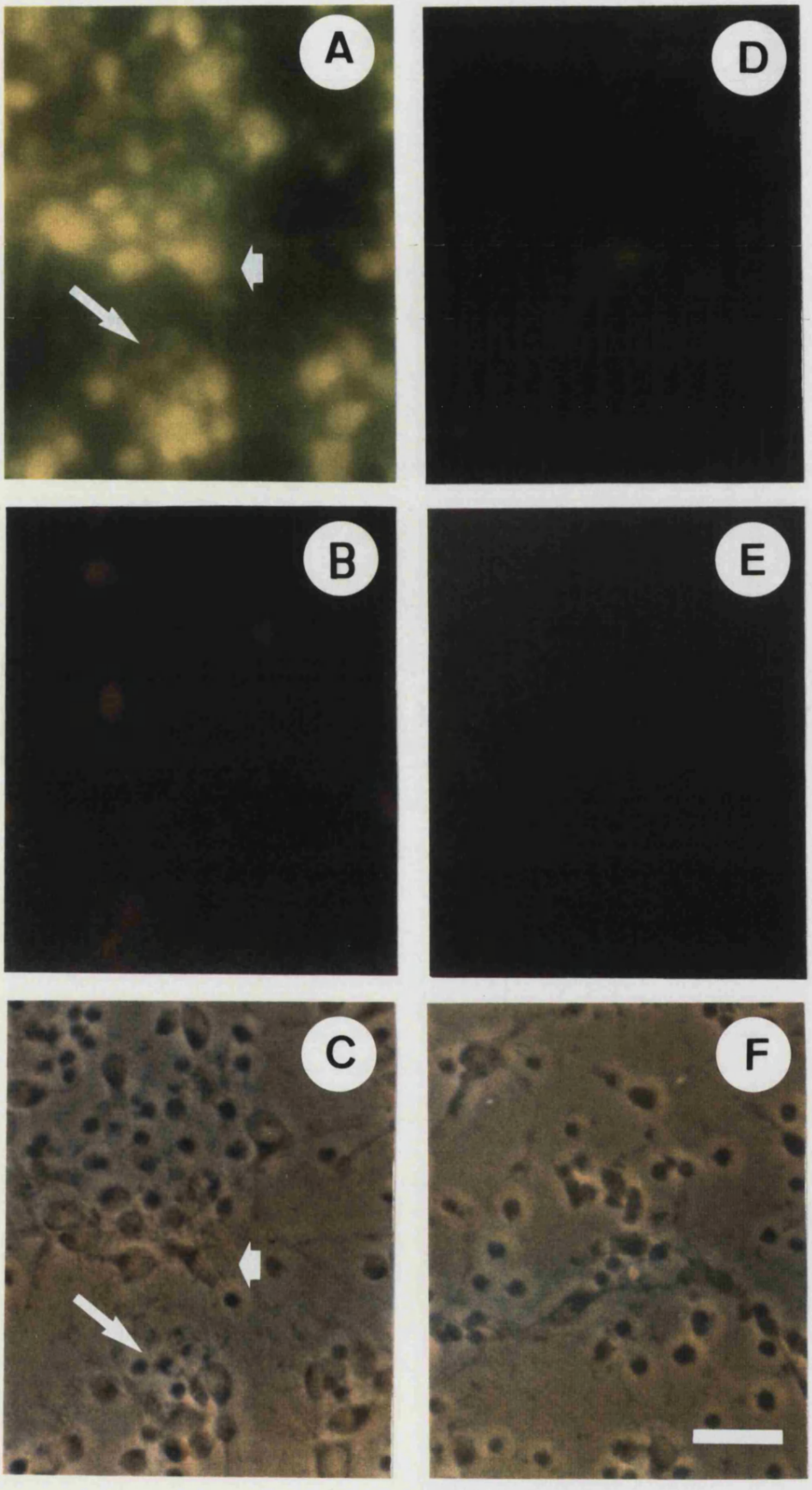
A
D
B
E
C
F

Plate 14. Staining pattern of total Rd-α-Bgt binding sites in cortical neurons.

Cultures grown for 10 days were fixed and permeabilized with 5% acetic acid-70% ethanol solution and either 1% FCS-PBS or (-)nicotine (6.4 mM final concentration) were added to account for total Rd-α-Bgt (**A, B and C**) and non-specific (**D, E and F**) binding, respectively. After 30 min at 37°C, Rd-α-Bgt (1 μM final concentration) was added and preparations left at 37°C for a further 40 min. The reactions were terminated by aspirating the liquid and washing four times with PBS. Samples were mounted and photomicrographed.

A and **D**: total and non-specific Rd-α-Bgt binding viewed with the rhodamine filter, respectively.

B and **E**: total and non-specific binding for Rd-α-Bgt viewed with the fluorescein filter, respectively.

C and **F**: Fields viewed with phase contrast corresponding to photomicrographs **A-B** and **D-E**, respectively.

A bipolar neuron has been indicated with a **short thick arrow** whereas a group of non-labelled small, round cells have been indicated with a **long arrow**.

Bar: 50 μm.

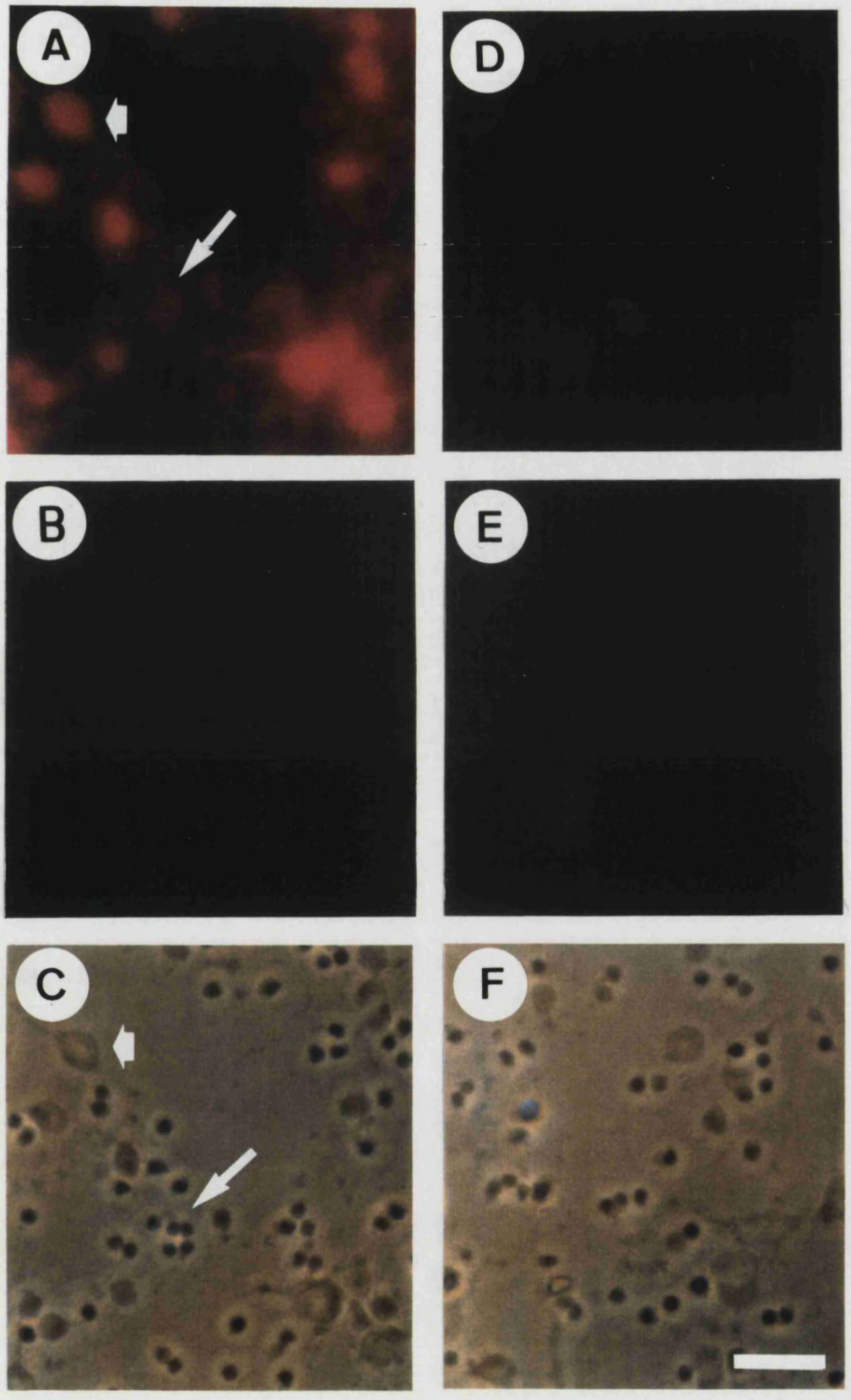
A
D
B
E
C
F

Plate 15. Double labelling of cortical cultures with Rd-α-Bgt and mAb 307 against α7 nAChR subunit.

Cultures grown for 10 days were fixed and permeabilized with 5% acetic acid-70% ethanol solution and mAb 307 (25 nM final concentration) was added (Plate **A, B** and **C**). A positive result was judged and graded with reference to the control incubation for non-specific staining which was treated with 1% FCS-PBS as vehicle instead of mAb 307 (Plate **D, E** and **F**). After 2 h at 37°C neurons were washed four times with PBS and anti-mouse FITC-IgG conjugate was added for 2 h at 37°C. Thirty min after the start of this last incubation, (-)nicotine (6.4 mM final concentration) or 1% FCS-PBS were added to account for non-specific (Plate **D, E** and **F**) and total Rd-α-Bgt binding (Plate **A, B** and **C**), respectively. After a further 60 min incubation Rd-α-Bgt (1 mM final concentration) and preparations left at 37°C for a further 30 min. The reactions were terminated by aspirating the liquid and washing four times with PBS. Samples were mounted and photomicrographed.

Arrows indicate small, round cells that were stained weakly or not at all with the IgG-FITC probe. With Rd-α-Bgt the same cells were not stained.

Bar: 50 μm.

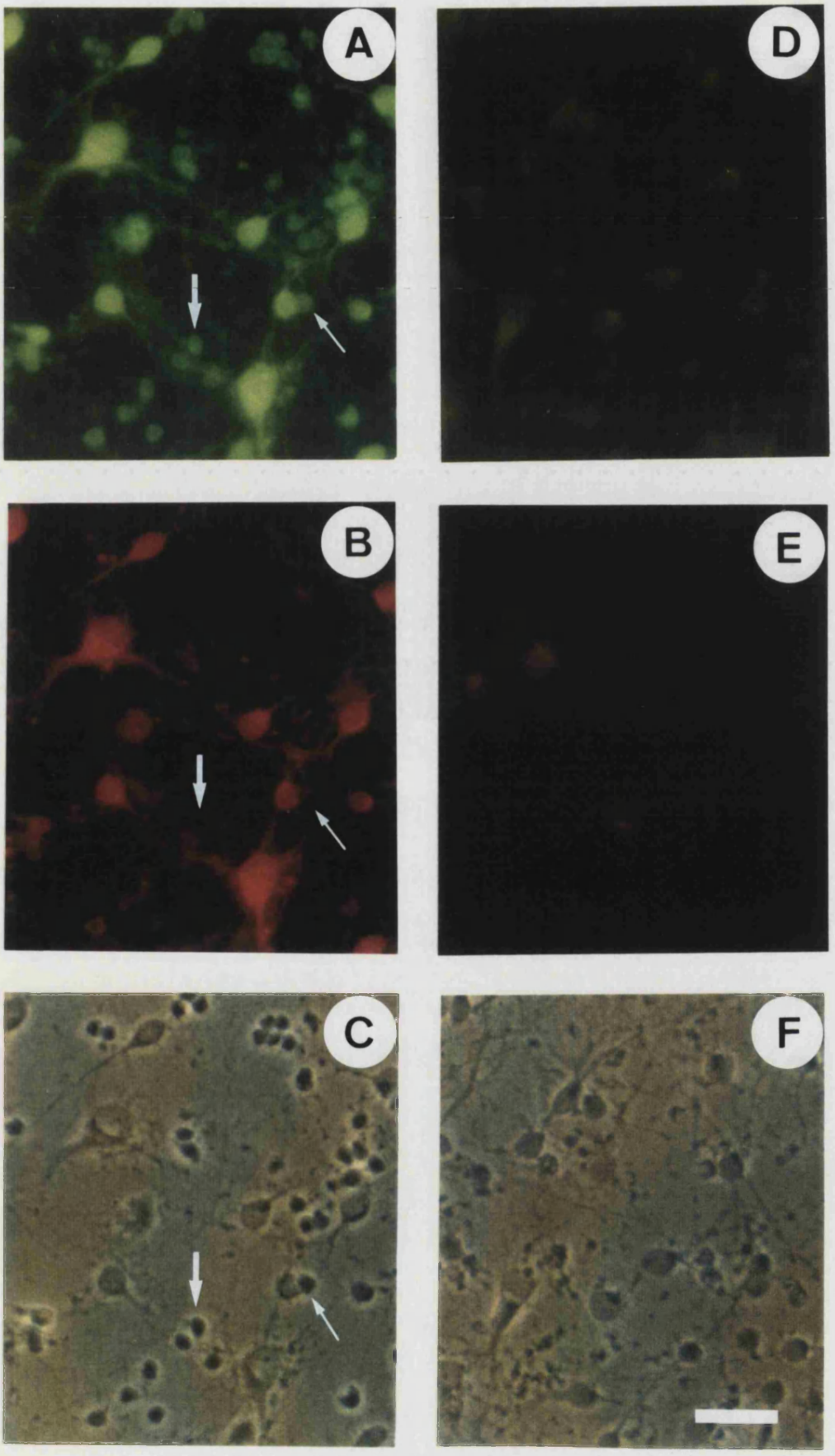
A
D
B
E
C
F

Plate 16. Low power photomicrographs of the staining pattern of total Rd-α-Bgt sites and mAb 307 against α7 nAChR subunit in cortical neurons.

Cultures grown for ten days were fixed and permeabilized, mAb 307 against α7 nAChR and Rd-α-Bgt were added as described in methods and in the legend to **Plate 15**.

A and **D**: total and non-specific immunostaining for mAb 307 viewed with the fluorescein filter, respectively.

B and **E**: total and non-specific binding for Rd-α-Bgt viewed with the rhodamine filter, respectively.

C and **F**: Fields viewed with phase contrast corresponding to photomicrographs **A-B** and **D-E**, respectively.

Arrows indicate small, round cells that were stained weakly or not at all with the IgG-FITC probe. With Rd-α-Bgt the same cells were not stained.

Bar: 100 μm.

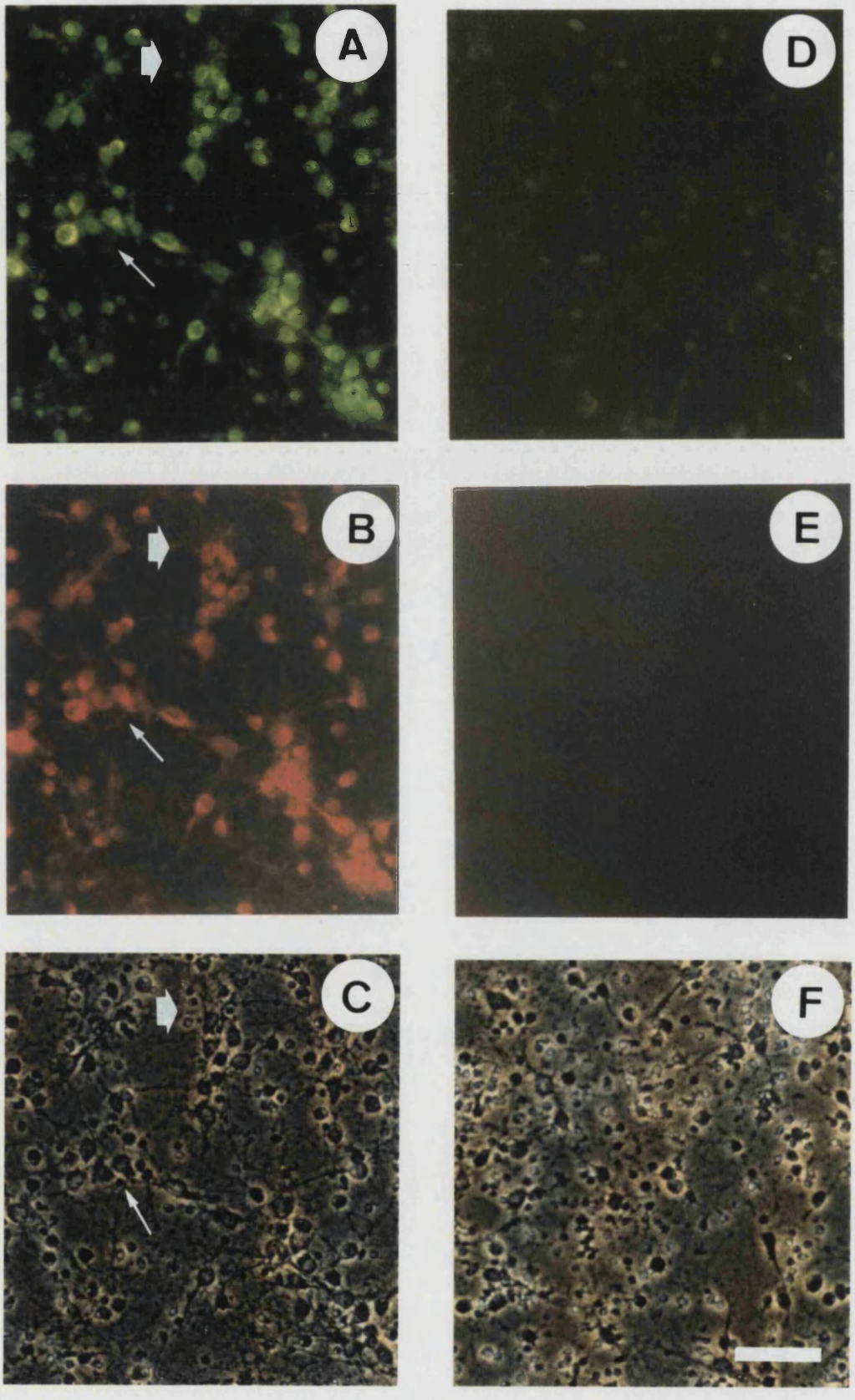
A
D
B
E
C
F

Plate 17. Staining pattern of Rd-α-Bgt and mAb 299 against α4 nAChR subunit in unfixed cortical neurons.

Unfixed cultures grown for 9 days were treated as described in methods and in legend to **Plate 15** except that 500 nM mAb 299 was added.

A and **D**: total and non-specific immunostaining for mAb 299 viewed with the fluorescein filter, respectively.

B and **E**: total and non-specific binding for Rd-α-Bgt viewed with the rhodamine filter, respectively.

C and **F**: Fields viewed with phase contrast corresponding to photomicrographs **A-B** and **D-E**, respectively.

The **arrow** indicates a pyramidal neuron that has been double labelled with mAb 299 and Rd-α-Bgt.

Bar: 50 μm.

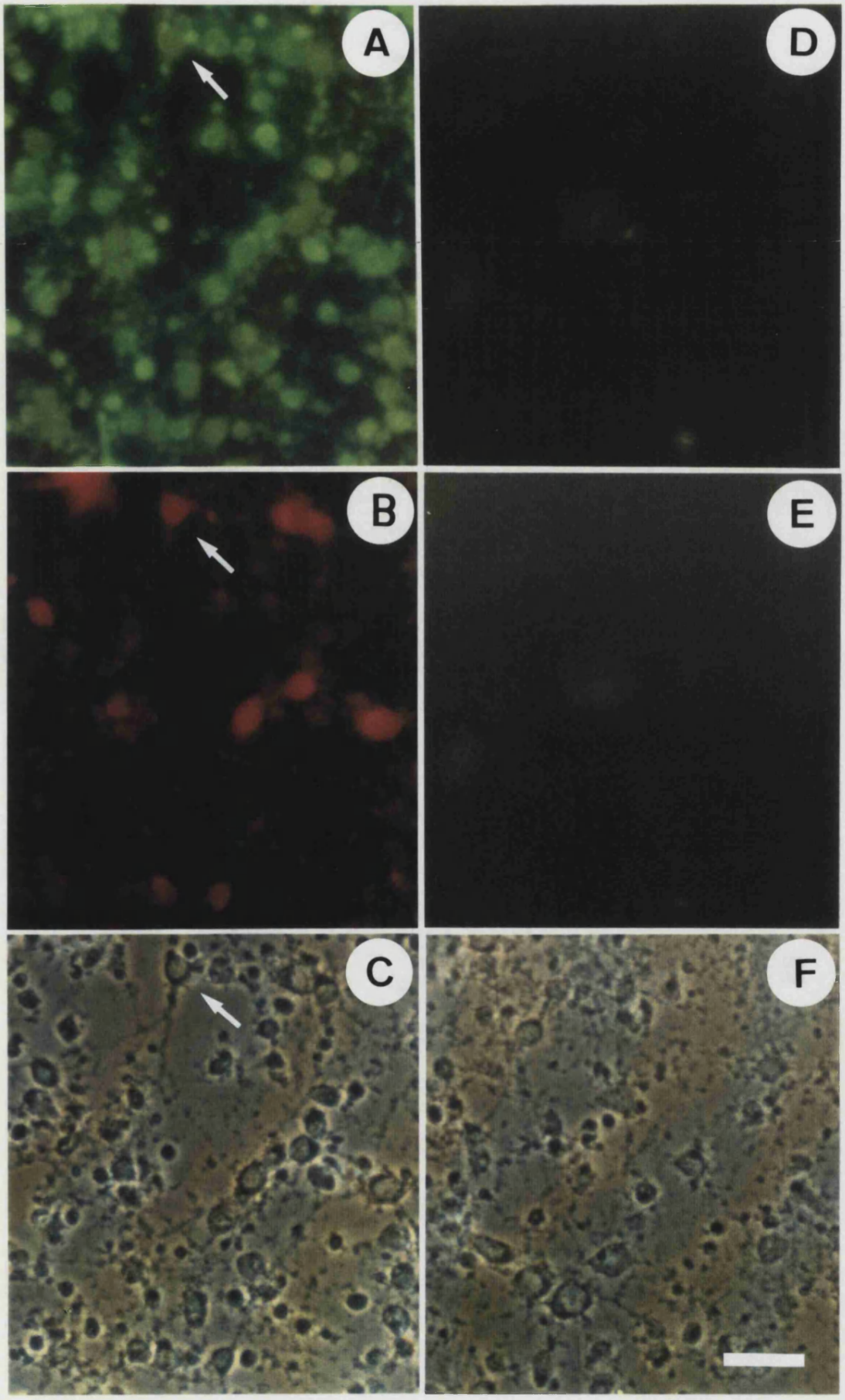
A
D
B
E
C
F

4.3.1.2. Hippocampal neuronal cultures

mAb 307-(anti-mouse IgG-FITC) / Rd-α-Bgt co-labelling

Double-labelling studies were carried out to test whether α-Bgt binding sites and α7 nAChR subunits collocated in the same neurons. As shown in Plates 18 and 19, α-Bgt binding sites and α7 nAChR subunits were clearly colocalised.

Thus, hippocampal neurons stained with Rd-α-Bgt were also positive for anti α7 mAb/IgG-FITC. On average, 95 ± 3% (n=12, i.e. 4 fields from 3 independent cultures) of cells in culture were double-labelled.

mAb 299-(anti-rat IgG-FITC) / Rd-α-Bgt co-labelling

Preliminary experiments in live hippocampal neuronal cultures clearly showed (Plate 20) that mAb 299 to native α4 nAChR subunit immunostained those hippocampal neurons that were not labelled by Rd-α-Bgt.

On average, 60 ± 3% (n=5, i.e. different fields of the same culture) were labelled with Rd-α-Bgt whereas 40 ± 2% (n=5, same as above) displayed specific immunoreactivity to mAb 299 to α4 nAChR subunit.

4.3.1.3. Glial cultures

To test for non-specific immunostaining of mAb 307 directed against the α7 nAChR subunit, hippocampal glial cultures were treated with this mAb. As shown in Plate 21, there was no specific binding of mAb 307 and the non-specific immunostaining was low.

Plate 18. Double labelling of hippocampal cultures with Rd-α-Bgt and mAb 307.

Cultures grown for ten days were fixed and permeabilized, mAb 307 against α7 nAChR and Rd-α-Bgt were added as described in methods and in the legend to **Plate 15**.

A and **D**: total and non-specific immunostaining with mAb 307 viewed with the fluorescein filter, respectively.

B and **E**: total and non-specific binding for Rd-α-Bgt viewed with the rhodamine filter, respectively.

C and **F**: Fields viewed with phase contrast corresponding to photomicrographs **A-B** and **D-E**, respectively.

Indicated with a **long arrow** is a round cell which has been less stained with both fluorescent probes. A **thick arrow** indicates a doublet of cells: a neuron with a stout apical bituffed neurite that has been strongly stained with both probes and a round cell which has been poorly stained by either probe.

Non-specific immunostaining for the fluorescent probes (fields **D** and **E**) was low.

Bar: 50 μm.

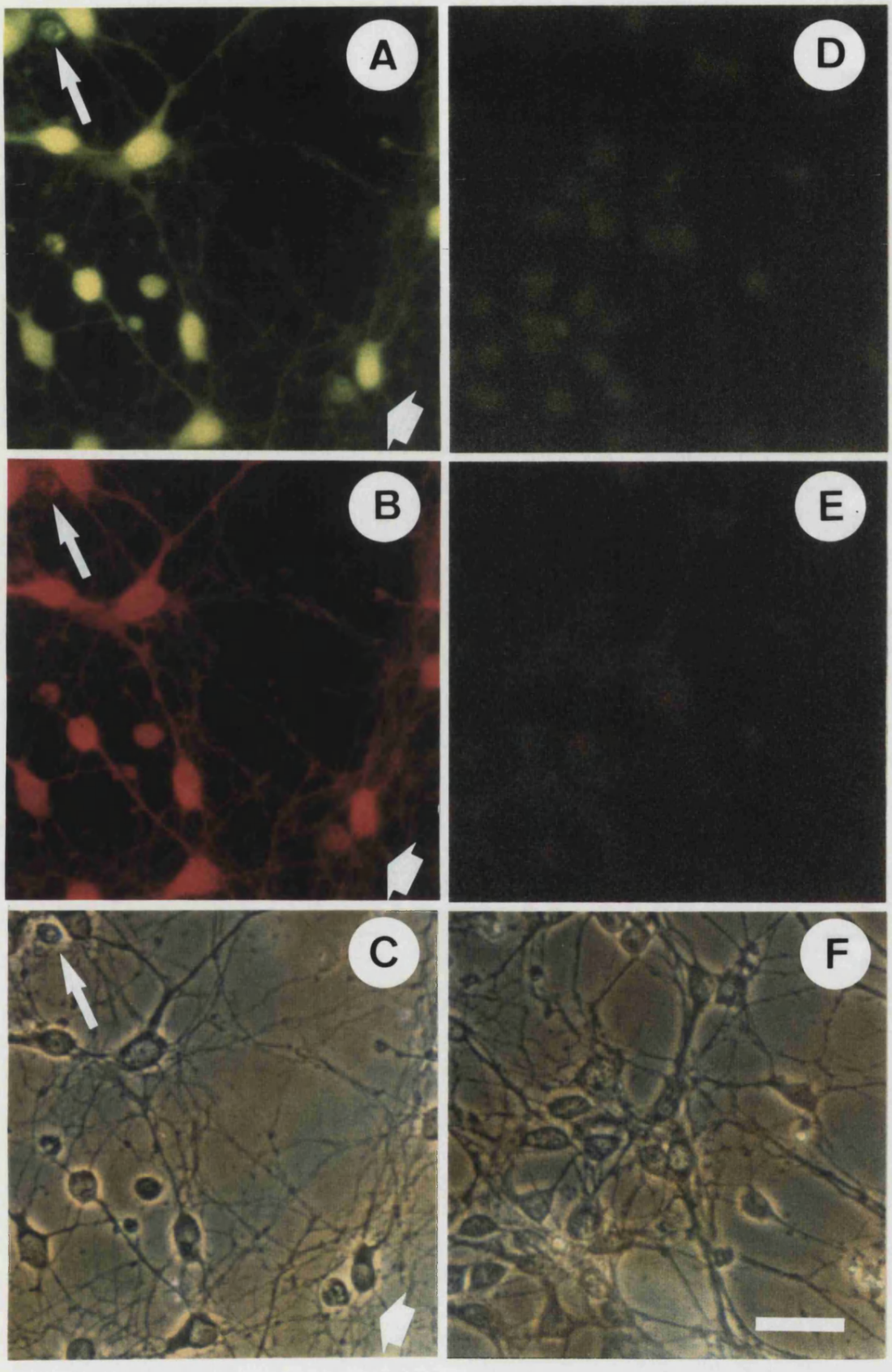
A
D
B
E
C
F

Plate 19. Low power photomicrographs of the staining pattern of total Rd-α-Bgt sites and mAb 307 in hippocampal neurons.

Cultures grown for ten days were fixed and permeabilized, mAb 307 against α7 nAChR and Rd-α-Bgt were added as described in methods and in the legend to **Plate 15.**

A and **D**: total and non-specific immunostaining with for mAb 307 viewed with the fluorescein filter, respectively.

B and **E**: total and non-specific binding for Rd-α-Bgt viewed with the rhodamine filter, respectively.

C and **F**: Fields viewed with phase contrast corresponding to photomicrographs A-B and D-E, respectively.

Indicated with **arrows** are small, round cells that were either labelled less or not at all.

Bar: 100 μm.

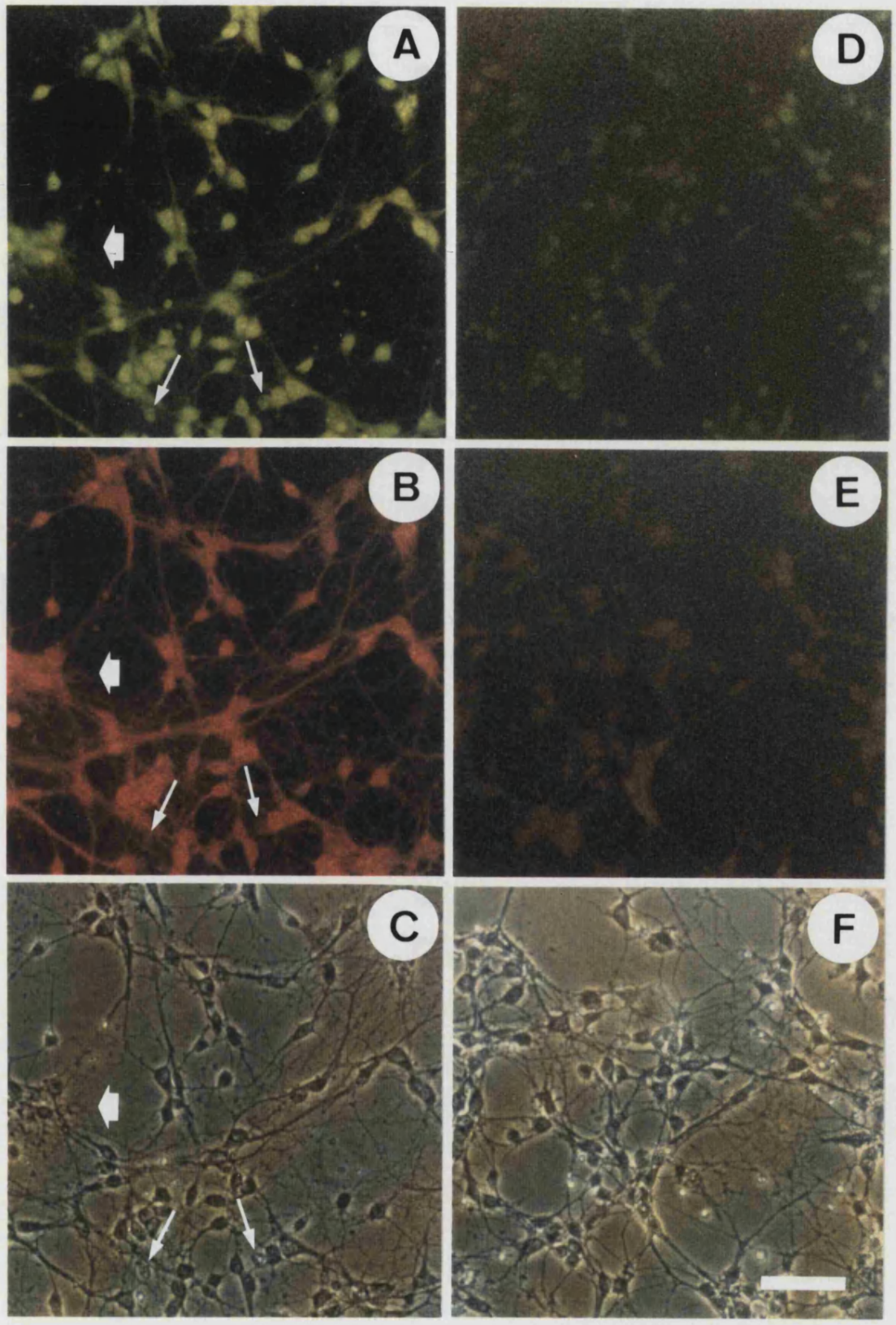
A
D
B
E
C
F

Plate 20. Staining pattern of Rd-α-Bgt and mAb 299 against α4 nAChR subunit in hippocampal neurons.

Unfixed cultures grown for 9 days were treated as described in methods and in the legend to **Plate 15** except that mAb 299 was used.

A and **D**: total and non-specific immunostaining for mAb 299 viewed with the fluorescein filter, respectively.

B and **E**: total and non-specific binding for Rd-α-Bgt viewed with the rhodamine filter, respectively.

C and **F**: Fields viewed with phase contrast corresponding to photomicrographs **A-B** and **D-E**, respectively.

An **arrow** indicates a group of four cells which have been differentially stained, one cell has been only immunostained with mAb 299 whereas three adjacent cells have only been stained with Rd-α-Bgt.

Bar: 100 μm.

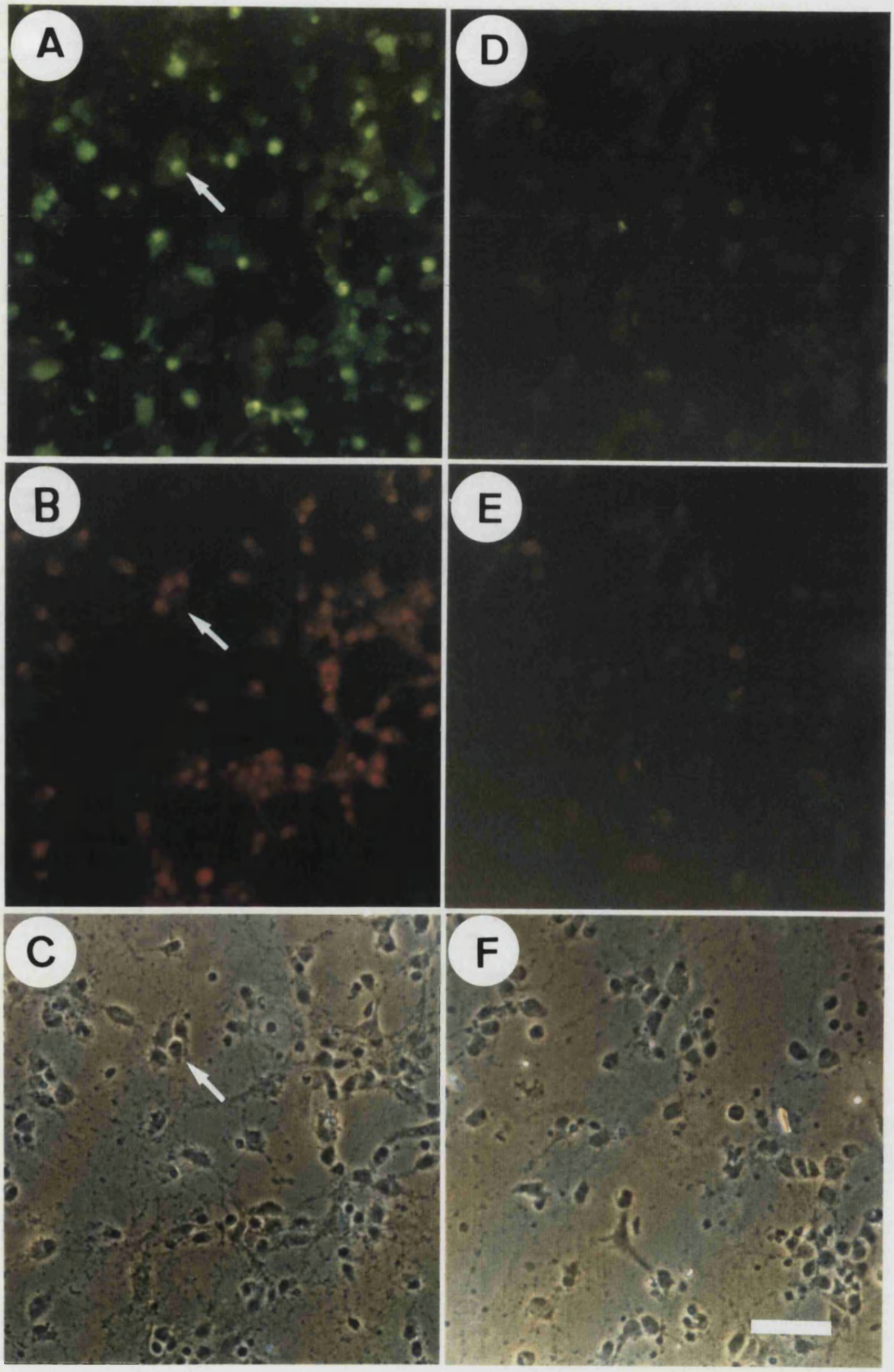
A
D
B
E
C
F

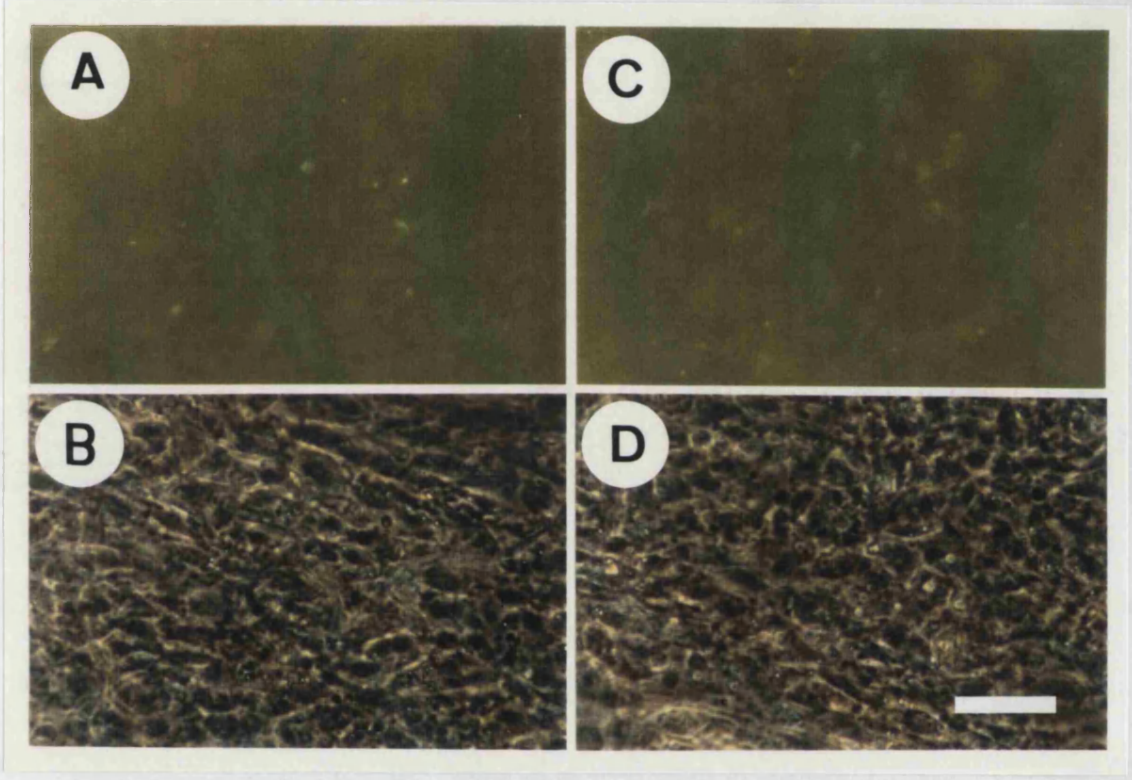

Plate 21. Assessment of mAb 307 in hippocampal glial cultures.

Confluent glial cultures grown for 14 days were fixed and permeabilized (30 min), mAb 307 was added as described in methods and in the legend to **Plate 13**.

A and **C**: total and non-specific immunostaining for mAb 307 viewed with the fluorescein filter, respectively. There was no specific immunostaining to glial cultures.

B and **D**: Fields viewed with phase contrast corresponding to photomicrographs **A** and **B**, respectively.

Bar: 50 μm.

4.3.2. Immunocytochemistry with antisera against nAChR subunits

Putative nAChR subunit subtypes in hippocampal neurons were evaluated using subunit-specific antisera. Immunocytochemistry was following the method of Rogers *et al.*, (1992). Results showing the pattern of immunoreactivity to the antisera tested in hippocampal neurons, PC12 and glial cells are summarized in table 12 and presented in Plate 20. Immunoreactivity to antisera was graded from strong to non-detectable. Hippocampal neurons showed strong immunoreactivity to *α5* and none to the other antisera with the dilutions tested (1:500 to 1:1500). The pattern of immunoreactivity shown by the control, i.e. PC12 cells, was α3, α5, β2 and β4 moderate, α2 and α4, non-detectable (Table 12), in accordance with previous studies (Rogers *et al.*, 1992). The negative control available for α5 was the mouse M10 cell line transfected with α4 and β2 subunits (Whiting *et al.*, 1991). However, when M10 cells were incubated with either α4, α5 and β2 at 1:500 dilutions, no immunoreactivity was observed. There was no immunoreactivity to any of the antisera in hippocampal glial cultures.

Antisera	Dilution	hippocampal Neurons	PC12 Cells	Glial Cells
α2	1:1500	-	-	-
	1:1000	-	-	-
	1:500	-	-	-
α3	1:1500	-	+	-
	1:1000	-	+	-
	1:500	-	++	-
α4	1:1500	-	-	-
	1:1000	-	-	-
	1:500	-	-	-
α5	1:1500	+++	+	-
	1:1000	+++	+	-
	1:500	+++	++	-
β2	1:1500	-	+	-
	1:1000	-	++	-
	1:500	-	++	-
β4	1:1500	-	+	-
	1:1000	-	+	-
	1:500	-	++	-
NRS	1:1500	-	-	-
	1:1000	-	-	-
	1:500	-	-	-

Table 12. nAChR subunits subtypes immunoreactivity.

+++: strong reactivity, ++: moderate reactivity, +: low reactivity, -: non-detectable reactivity.

Plate 22. nAChR subunit-specific antisera immunoreactivity in hippocampal neuronal and glial cultures and PC12 cells.

Hippocampal neuronal and glial cultures grown for two weeks and PC12 cells were fixed with paraformaldehyde in 0.1% cacodylate buffer and permeabilized with 0.3% Triton. Cells were incubated at room temperature for 4 hours with nAChR subunit-specific antisera (α2-α5, β2 and β4) or normal rabbit serum (NRS) at 1:500 dilutions. Alkaline phosphatase conjugate goat anti-rabbit was used as secondary antibody.

A, H and **O**: immunoreactivity to antisera against **α2** nAChR fusion protein in hippocampal neurons, PC12 and glial cells, respectively.

B, I and **P**: immunoreactivity to antisera against **α3** AChR fusion protein in hippocampal neurons, PC12 and glial cells, respectively.

C, J and **Q**: immunoreactivity to antisera against **α4** nAChR fusion protein in hippocampal neurons, PC12 and glial cells, respectively.

D, K and **R**: immunoreactivity to antisera against **α5** nAChR fusion protein in hippocampal neurons, PC12 and glial cells, respectively.

E, L and **S**: immunoreactivity to antisera against **β2** nAChR fusion protein in hippocampal neurons, PC12 and glial cells, respectively.

F, M and **T**: immunoreactivity to antisera against **β4** nAChR fusion protein in hippocampal neurons, PC12 and glial cells, respectively.

G, N and **U**: immunoreactivity to **normal rabbit serum** (negative control) in hippocampal neurons, PC12 and glial cells, respectively.

Bar: 50 μm.

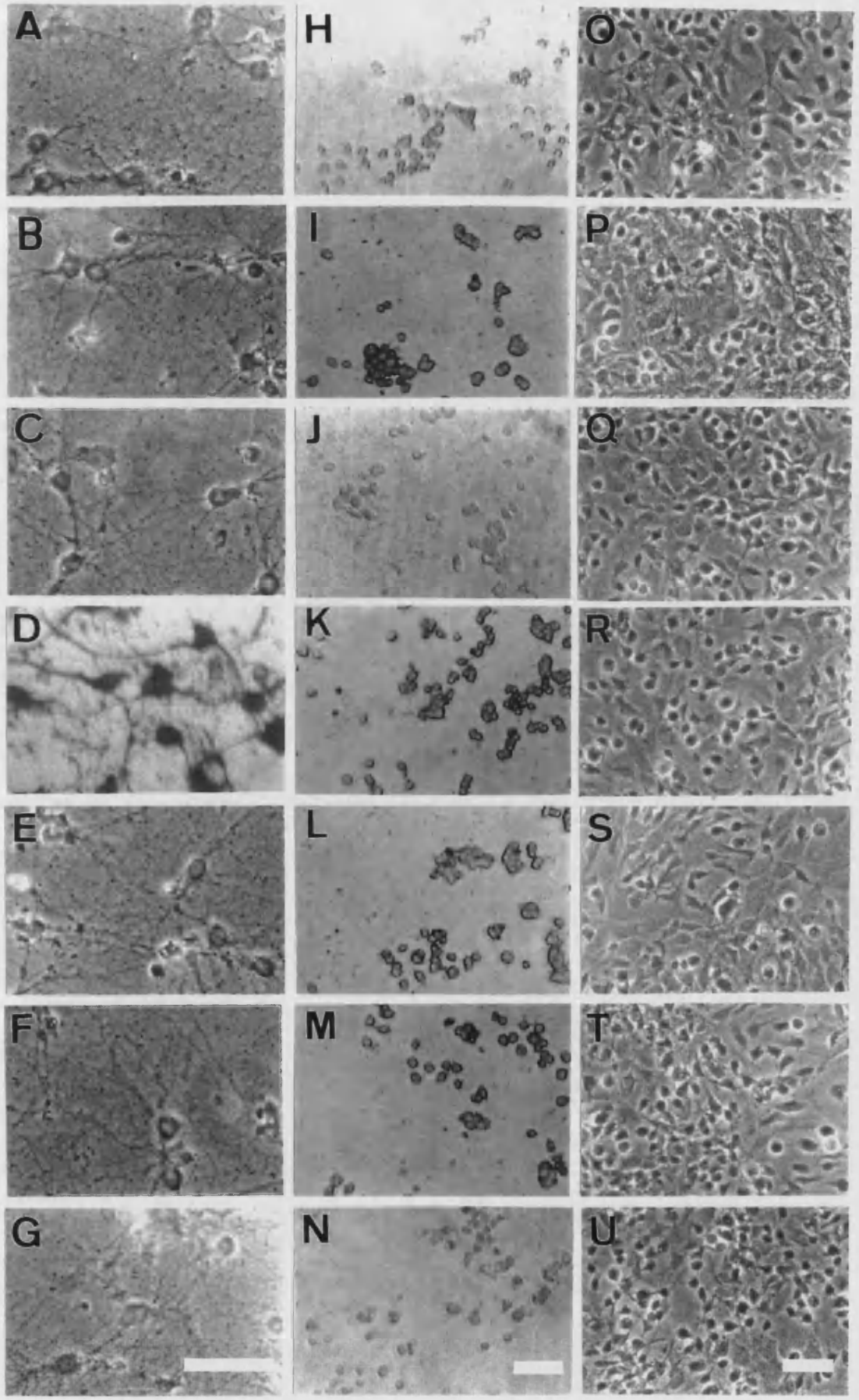
A
H
O
B
I
P
C
J
Q
D
K
R
E
L
S
F
M
T
G
N
U

4.4. Discussion

The experimental approaches presented in this chapter aimed to localize nAChR subunits at the cellular level. To this end, monoclonal antibodies directed against unique regions of α7 (cytoplasmic) and α4 (extracellular) subunits, as well as polyclonal antisera raised against fusion protein constructs containing the putative cytoplasmic domains of α2, α3, α4, α5, β2 and β4 nAChR subunits were employed. This approach is possible by virtue of the dispersed nature of the neuronal cultures not found in, for example, slice preparations.

4.4.1. α7 nAChR subunit expression in hippocampal and cortical neurons

The presence of the nAChR α7-subunit protein in rat hippocampus and cortex was confirmed by the positive immunoreactivity with mAb 307. Specificity of the immunostaining was demonstrated by performing parallel experiments in hippocampal glial cultures which do not display specific binding for either [^{125}I]-α-Bgt or FITC-α-Bgt (refer to Table 10 and Plate 12) and were not stained by mAb 307.

In hippocampal neuronal cultures, immunoreactivity of mAb 307 to α7 nAChR was observed in the cell body of almost all the neurons (95 ± 3%) and its localization parallelled that of Rd-α-Bgt sites. However, the subcellular distribution of the receptor protein (which might also be localized in the axon or dendrites) was not assessed since more sophisticated microscopy was needed. The present findings are in good agreement with other approaches intending to solve the issue of nAChR subunit heterogeneity. *In situ* hybridization methods have allowed the identification of brain regions expressing the gene coding for the α7 subunit (Séguéla *et al.*, 1993). Strong α7 mRNA expression has been reported in the adult rat hippocampus, where most of the staining corresponds to the granule cell layer in the *dentate gyrus* and pyramidal cells in the *stratum pyramidale*. In addition, interneurons in the *stratum oriens* and *stratum moleculare* of fields *CA1-CA4* present high transcription levels (Séguéla *et al.*, 1993) [the cytoarchitecture of the rat hippocampus is illustrated in Fig. 1]. This

cellular distribution relates to the staining pattern observed in the present study since a relatively high proportion of neurons in culture are pyramidal neurons. In addition, interneurons are also present in embryonic hippocampal cultures. However, it was not possible to assess immunostaining to mAb 307 in granule cells since at E18 (stage at which cultures were prepared) the generation of cells from the *dentate gyrus* has scarcely begun (Goslin and Banker, 1991). The *in situ* hybridization pattern matches the autoradiographic localization of [^{125}I]-α-Bgt sites in adult rat hippocampus (Clarke *et al.*, 1985).

As shown in chapter 3 (section 3.3.1.), surface [^{125}I]-α-Bgt binding sites represent half of the total population of a-Bgt sites in permeabilised cultures. With Rd-α-Bgt labelling it was possible to determine that surface α-Bgt sites were on 60% of neurons and almost all neurons (95 %) labelled Rd-α-Bgt after permeabilization. Therefore, most of hippocampal neurons in culture (10 day old) have the potential to express α-Bgt nAChR although only 60% of neurons do so.

In cortical neuronal cultures however, although Rd-α-Bgt sites colocalised with mAb 307 staining (36 ± 4% of neurons), some of the cells that did not bind Rd-α-Bgt still showed a weak positive immunostaining to mAb 307. The significance of this is not clear since the possibility of non-specific immunostaining of the mAb was ruled out by treating glial cultures with mAb 307. One possibility is that those cells were dead neurons at the moment of fixation. In that case, the toxin binding sites could have been changed (e.g. denatured). Therefore mAb 307, that binds to native and denatured α7 receptor, was still able to bind the epitope whereas Rd-α-Bgt was not. However, moderate to high α7 mRNA hybridization signals in superficial and deep layers of the cortex have been reported (Séguéla *et al.*, 1993). The *in situ* hybridization pattern in cortex matches with the autoradiographic localization of [^{125}I]-α-Bgt sites in adult rat cortex (Clarke *et al.*, 1985).

In cortical cultures 19 % of neurons displayed surface Rd-α-Bgt sites (in contrast to hippocampal neurons, 60%). These results are complemented by [^{125}I]-α-

Bgt binding (refer to Table 10). The labelled neurons doubled in number towards permeabilization indicating that some neurons have the potential to express α-Bgt sites. Therefore, hippocampal and cortical neurons have intracellular α-Bgt stores. As discussed in section 3.4., internal stores of assembled or partially assembled multisubunit molecules have been previously reported and may represent turnover of the surface membrane nAChR or subunits that fail to assemble or a reserve of receptor for developmental contingencies (Jacob *et al.*, 1986).

4.4.2. α4 nAChR subunit expression in hippocampal and cortical neurons

The presence of α4 nAChR subunits was demonstrated in hippocampal and cortical neuronal cultures by immunostaining these preparations with mAb 299 to the extracellular epitope of α4 nAChR subunit.

Immunocytochemical localization revealed immunoreactivity in the cell body of about 40% of the hippocampal neurons in culture. *In situ* hybridization studies in adult rat have shown that mRNA encoding α4 and β2 nAChR subunits are moderately expressed only in the *stratum pyramidale* (Wada *et al.*, 1989). The autoradiographic localization of [^{3}H]nicotine binding sites has only been reported in the *stratum moleculare* of the *dentate gyrus* of adult rat hippocampus (Clarke *et al.*, 1985). In the present thesis, whereas [^{3}H]nicotine/[^{3}H]cytisine binding sites have not been detected, immunostaining of mAb 299 to α4 nAChR subunit was apparent. Therefore, immunocytochemistry proved to be a more sensitive approach to detect this nAChR subunit subtype whose expression in hippocampus is low. Alternatively, the α4 subunit could be associated with a nAChR subunit different from β2 and therefore neither [^{3}H]nicotine nor [^{3}H]cytisine would bind to this receptor. It is interesting to note here that embryonic hippocampal cultures present a very low proportion of neurons whose nAChR display a pharmacology which matches that of the α4β2 nAChR heterologously expressed in *Xenopus* oocytes (Alkondon and Albuquerque, 1993). In hippocampal neuronal cultures, those neurons which

displayed surface Rd-α-Bgt labelling (60 ± 3%) did not show positive immunoreaction to mAb 299. Therefore, there was no overlap of α-Bgt with α4 nAChR expressing cells. This implies that in the embryonic hippocampus different cells express different nAChR subtypes.

All of the cortical neurons were immunostained with mAb 299 and the immunostaining pattern indicates that α4 nAChR subunit is expressed in the cell bodies. Rd-α-Bgt and mAb 299 labelling colocalised in 19 ± 2% of the cells, most of which were pyramidal. These results match radioligand binding assays presented in the present thesis (refer to Table 10): [^{125}I]-α-Bgt binding sites in hippocampal neuronal cultures were about five times more than in cortical neurons. *In situ* hybridization studies have revealed that α4 (and β2) mRNA is expressed in all cortical layers from adult rat (Wada *et al.*, 1989). However whereas, high affinity [^{3}H]nicotine binding sites are present in cortical layers I, III, and IV, high affinity [^{125}I]-α-Bgt sites are only localized in layer VI in the adult rat (Clarke *et al.*, 1985).

4.4.3. Immunocytochemistry with antisera against nAChR subunits

In order to investigate further which nAChR subtypes are expressed in primary cultures of hippocampal neurons, rabbit polyclonal antisera against the cytoplasmic domains of the rat subunits α2, α3, α4, α5, β2 and β4 nAChR subunits were used.

Hippocampal neurons showed strong immunoreactivity to α5, and weak or no staining to the other antisera (refer to Table 12 and Plate 22). These results are in good agreement with western blots carried out in parallel by A. Rogers (personal communication). PC12 cells that were employed as positive controls for α3, α5, β2 and β4 antisera displayed a moderate immunoreactivity in accordance with a previous report (Rogers *et al.*, 1992). The rat pheochromocytoma cell line PC12 has nAChR that does not display high affinity for [^{3}H]nicotine (Whiting *et al.*, 1987c). However, this sympathetic-like nerve line has high affinity binding to [^{125}I]-α-Bgt (Patrick and Stallcup, 1977). PC12 cells have been reported to express multiple RNA coding for

nAChR subunits including α3, α5, β2 and β4 (Boulter *et al.*, 1990; Rogers *et al.*, 1992). The positive control for α4 and β2 was the M10 cell line. This mouse fibroblast cell line transfected with chicken α4 and β2 nAChR subunits (Whiting *et al.*, 1991) did not display immunoreactivity. Since antisera were directed to rat constructs and M10 cells express chicken α4β2 nAChR this could explain the lack of immunoreactivity. Whereas immunoreactivity to the α4 nAChR subunit was observed with mAb 299, antiserum to fusion protein expressing α4 nAChR subunit gave negative immunoreactivity. Since mAb 299 was supplied in very low quantity it was not possible to test its specificity in the M10 cell line. That α4 was only detected with mAb 299 may reflect the sensitivity of the different methodologies employed to develop the immunoreactivity to the monoclonal antibodies (fluorescence) and to the antisera (alkaline phosphatase). In addition, different epitopes were involved: whereas mAb 299 was raised against an extracellular epitope, antisera to α4 subunit was produced to an intracellular epitope.

The significance of α5 immunoreactivity is not clear. *In situ* hybridization studies have reported strong α5 mRNA expression in *stratum pyramidale* of the *subiculum* but weak expression in the *stratum pyramidale* of *CA1* and *CA3* of adult rat hippocampus (Wada *et al.*, 1990). In the present study, however, most of the neurons were strongly immunoreactive to α5 antiserum. The specificity of this antiserum has also been tested by A. Rogers in the TE671 cell line which expresses muscle α1βγδ nAChR subunits (Schoepfer *et al.*, 1988; Luther *et al.*, 1989) and does not hybridize with human α5 cDNA (Chini *et al.*, 1992). Surprisingly there was a strong immunoreaction of antisera to α5 (personal communication). Since in the present study glial cells did not immunoreact to α5 antisera, the strong immunoreactivity to this antisera might be due to cross reactivity (i.e. non-specific reactivity) to a protein of unknown origin absent in glial cells.

4.5. Summary to chapter 4

(i) The presence of the nAChR α7-subunit protein in rat hippocampus and cortex was confirmed by the positive immunoreactivity with mAb 307. Specificity of the immunostaining was demonstrated by performing parallel experiments in hippocampal glial cultures which do not display specific binding for either [^{125}I]-α-Bgt or FITC-α-Bgt and were not stained by mAb 307.

(ii) In fixed hippocampal neuronal cultures almost all the neurons (95 ± 3%) showed positive immunoreaction to mAb 307 against the α7 nAChR subunit and also displayed Rd-α-Bgt labelling suggesting that most of the neurons in culture have the potential to express α-Bgt nAChR. However, about half of the neuronal population presented membrane-bound α-Bgt sites.

(iii) Preliminary results suggests that α4 nAChR subunits are expressed by those neurons which do not present membrane-bound α-Bgt sites.

(iv) Hippocampal neurons displayed strong immunoreactivity to antisera against α5 nAChR subtype, probably due to cross reactivity.

(v) In cortex, despite the fact that Rd-α-Bgt sites colocalised with mAb 307, some of the cells that did not bind Rd-α-Bgt still showed a weak positive immunostaining to mAb 307.

(vi) Preliminary results showed that the majority of cortical neurons, in contrast to hippocampal neurons, were immunostained with mAb 299 against α4 nAChR subunit. Few of them express membrane-bound α-Bgt sites.

Chapter 5
Functional assays: Intracellular free Ca^{2+} measurements

5.1. Introduction

The use of fluorescent Ca^{2+} indicators and electrophysiological studies have revealed variations in intracellular free Ca^{2+} $[Ca^{2+}]_i$ in response to nicotinic agonists (refer to section 1.4.).

More intracellular studies have been done with indicators for Ca^{2+} than with any other ion (Lauder, 1993). This emphasis reflects the pivotal importance of Ca^{2+} in cellular signal transduction. Ca^{2+} fluctuations play a particularly major role in neurobiology as the key link between membrane depolarization and intracellular biochemical activation.

In the present chapter functional assays with the calcium indicator Fura-2 have been carried out in hippocampal neuronal cultures The purpose of the present study was to evaluate the functional status of α-Bgt binding sites in hippocampal neurons by measuring agonist-induced fluorescence changes.

5.1.1. The use of fluorescent indicators for measurements of $[Ca^{2+}]_i$ in cell populations

The development of optical indicator dyes sensitive to changes in $[Ca^{2+}]_i$ (Grynkiewicz *et al.*, 1985; Cobbold and Rink, 1987; Tsien, 1989) has enabled the direct measurement of $[Ca^{2+}]_i$ variations in cells.

Fluorescent indicators have been modelled on EGTA (Grynkiewicz *et al.*, 1985), which has a selectivity for Ca^{2+} over Mg^{2+} of about 6 orders of magnitude, and is well suited to buffering Ca^{2+} in the physiological range of 10^{-8}-10^{-6}M in the presence of physiological Mg^{2+} concentrations of 10^{-4}-10^{-3}M. Binding of Ca^{2+} to the indicator alters its fluorescence properties. These fluorescence changes are used to

calculate the proportions of dye in the Ca^{2+}-bound and Ca^{2+}-free forms, and hence the concentration of free Ca^{2+} with which the indicator is in equilibrium.

5.1.2. Loading of Ca^{2+} indicators into the cells

The newer indicators lend themselves to loading as membrane permeant esters, without the requirement for disruption of the cell membrane (reviewed by Tsien, 1989). This is usually achieved by incubating intact cells with an esterified form (acetoxymethyl esters) of the indicator. Since the esterified form of the dyes are uncharged and hydrophobic, they readily cross cell membranes. Once in the cytosol, endogenous esterases release the free acid form of the indicator which does not permeate the cell membrane. This results in the accumulation of trapped indicator in the cytosol. Once extracellular dye has been removed, the cells (either in suspension or attached to a non-fluorescent surface) are placed into the sample compartment of the fluorimeter. Subsequently, fluorescence signals from the cytosolic dye can be recorded and used to calculate $[Ca^{2+}]_i$.

5.1.3. Calibration for $[Ca^{2+}]_i$ measurements

Ca^{2+} measurements rely on the change in fluorescent properties following Ca^{2+} binding to report the degree of Ca^{2+} saturation of the indicator. At equilibrium, this is related to the free Ca^{2+} concentration according to the mass action equation:

$$Ca^{2+} = K_D \times ([CaX] / [X]),$$

where **X** is the fluorescent indicator which binds Ca^{2+} with dissociation constant K_D

With dyes such as fura-2, which give a shift in fluorescence spectrum, measurements can be carried out at two wavelengths to obtain signals which are proportional to Ca^{2+}-bound and Ca^{2+}-free indicator. The ratio of fluorescence at the

two wavelengths is directly related to the ratio of the two forms of the dye and therefore can be used to calculate $[Ca^{2+}]_i$. The advantage of the ratio approach is that indicator concentration terms and instrument sensitivity parameters do not need to remain constant throughout the experiment, as is the case in the single-wavelength mode. The equation which relates the measured Ca^{2+}-bound/Ca^{2+}-free fluorescence ratio (**R**) to $[Ca^{2+}]_i$ (Grynkiewicz *et al.*, 1985) is:

$$[Ca^{2+}]_i = K_D \times [(R-R_{min})/(R_{max}-R)] \times (S_{f2}/S_{b2})$$

where $\mathbf{R_{max}}$ and $\mathbf{R_{min}}$ are the fluorescence ratio values under saturating and Ca^{2+}-free conditions, respectively, and $\mathbf{S_{f2}/S_{b2}}$ is the ratio of fluorescence values for Ca^{2+}-bound/Ca^{2+}-free indicator measured at the wavelength used to monitor the Ca^{2+}-free indicator. These are unitless values which depend on the chemical properties of the indicator. Calibration measurements at zero and saturating levels of Ca^{2+} are required to determine the constants R_{min}, R_{max} and S_{f2}/S_{b2}.

Overall, the objective of calibration is to determine the fluorescence levels under conditions of maximum and minimum Ca^{2+} binding. This can be achieved with ionophores which allow extracellular Ca^{2+} to go inside the cell and in turn saturate the indicator. Subsequently Mn^{2+} is added to quench intracellular dye fluorescence since it binds to the indicator with higher affinity than Ca^{2+}, allowing to estimate the minimum fluorescence (Fig. 11A). $[Ca^{2+}]_i$ values derived from the above equation (Grynkiewicz *et al.*, 1985) can be plotted throughout the experiment (Fig. 11B)

5.1.4. Characteristics of fluorescent Ca^{2+} indicators

Fura-2 (Grynkyewicz et al, 1985)

Fura-2 is currently the most widely used fluorescent Ca^{2+} indicator dye and is the indicator of choice for imaging studies. It is about 30 times more fluorescent than

quin-2 (Tsien *et al.*, 1982) has a higher K_D (224 nM) for Ca^{2+}, less Mg^{2+} sensitivity, is less susceptible to photobleaching and can be used in the ratio mode (see section 5.1.3). Fura-2 is used at intracellular concentrations in the tens of micromolar as opposed to the millimolar range used for quin-2, and as a result has much less of a Ca^{2+} buffering effect. It is suitable for measuring $[Ca^{2+}]_i$ up to several micromolar. The main problems which have been encountered with fura-2 relate to the incomplete hydrolysis of the acetoxymethyl ester (AM) form and the propensity of this dye to become compartmentalized in subcellular organelles during loading.

The fluorescence excitation maximum of fura-2 shifts to a lower wavelength on Ca^{2+} binding with negligible shift in the emission maximum. This allows fura-2 to be utilized as a dual excitation indicator, Ca^{2+}-free fura-2 is usually monitored at 380 nm and Ca^{2+}-bound dye at 340 nm (Fig. 11A).

Fura-2 has been widely used in neurobiology (Tsien, 1989). Fura-2 imaging is a powerful tool to study how $[Ca^{2+}]_i$ varies from one part of a neuron to another in response to agonists or antagonists. Neurotransmitter actions are also studied at the population level. These studies are carried out either with cell suspensions, cell monolayers or thin tissues and do not require the use of imaging techniques.

Indo-1 (Grynkyewicz et al., 1985)

Indo-1 is the only currently available Ca^{2+} indicator other than fura-2 that can be used for ratio measurements of $[Ca^{2+}]_i$. In contrast to fura-2, it shows a shift in its emission maximum on Ca^{2+} binding. In experiments using aclar plastics (i.e., samples remain in the same position throughout the experiment), indo-1 is less suitable than fura-2 since the former is more susceptible to photobleaching than fura-2. However indo-1 gives less problems in terms of incomplete hydrolysis and compartmentation.

Fluo-3 (Minta et al., 1989) and Quin2 (Tsien et al., 1982)

Fluo-3 is excited in the visible range of light and does not undergo a wavelength shift on Ca^{2+} binding, therefore it must be used in a single-wavelength mode similar to quin-2, the first Ca^{2+} indicator to be used widely. Thus, they are less useful than fura-2 for single-cell and cell population measurements of $[Ca^{2+}]_i$.

5.1.5. Problems encountered using fluorescent Ca^{2+} indicators

It should be noted that the absolute values of $[Ca^{2+}]_i$ determined in this manner can be influenced by a variety of factors that are difficult to measure and control (Thomas and Delaville, 1991). Among these are the incomplete dye hydrolysis, intracellular pH, viscosity, ionic strength, binding to proteins and cell constitutents, impurities in commercial preparations of Ca^{2+} indicators, effects of other ions, changes in cellular dye-independent fluorescence, photobleaching, buffering of cytosolic Ca^{2+} changes, temporal resolution and toxicity of indicators. Hence, one should view the values of $[Ca^{2+}]_i$ only as estimates and should concentrate on the relative changes produced by various treatments.

5.2. Experimental Procedures

5.2.1. Materials

A PTI dual-excitation spectrophotofluorimeter, excitation, emission, 4 nm slit width, equipped with a PTI software version 2.060 and manufactured by Photon Technology International Inc. (Deerpark Drive, South Brunswick, NJ 08852 USA) was generously facilitated by Professor J. Westwick.

Non-fluorescent Aclar plastic (Pro Plastics, Inc, USA) was cut into 15 mm diameter discs (to fit into 16 mm well dishes) and autoclaved before use.

Fura-2 acetoxymethyl ester {1-[2-(5-carboxyoxazol-2-yl)-6-aminobenzofuran-5-oxy]-2-(2'-amino-5'-methylphenoxy) ethane N,N,N',N'- tetraacetic acid} was purchased from Molecular Probes. Cytisine, glutamate, (-)nicotine tartrate salt, $NiCl_2$ (>99.5 %) and tetrodotoxin were purchased from Sigma. Ionomycin was purchased from Calbiochem Novabiochem Ltd. (Nottingham, UK). MLA (citrate salt) was prepared by Professor M.H. Benn (Department of Chemistry, University of Calgary, Alberta, Canada). $CaCl_2$ (dehydrate, >99.5 %), KCl (dehydrate, >99.5 %) were purchased form FSA Laboratory (Bishop, Meadow Rd, Loughborough, LE11 ORG, UK). $CdCl_2$ (>99.5 %) and $MnCl_2.4H_2O$ (>98 %) were acquired from BDH.

HEPES calcium-free buffer solution (HBS) was prepared as described in the appendix E to this thesis.

5.2.2. Methods

Ten day old hippocampal neurons, cultured as described in chapter 2 were grown on Aclar plastics, discs (3.5×10^5 cells/disc) to fit into 16 mm wells (Monck *et al.*, 1988). After washing three times in 500 µl HBS, cells were loaded with 5 µM Fura-2 acetoxymethyl ester in HBS containing 0.25% w/v BSA to improve solubilization of the dye (Thomas and Delaville, 1991). After 30 min incubation at 20^oC excess dye was eliminated with three washes with 500 µl HBS. Cultures were

further incubated at 37°C for 20 min to facilitate completion of the de-esterification reactions (Thomas and Delaville, 1991).

Subsequently, a magnetic flea was dispensed into a standard cuvette and the plastic discs with cells attached were fitted diagonally into the cuvette. HBS (2ml) with 1 μM tetrodotoxin (TTX) was added. Since it is known that cultured hippocampal neurons form synaptic interconnections and fire bursts of excitatory postsynaptic potentials spontaneously and repetitively, TTX was added to exclude any increase in $[Ca^{2+}]_i$ due to this spontaneous activity (Kudo *et al.*, 1988). The cuvette was placed into the spectrophotofluorimeter such that the cells were at 45° to the emission detector. The cuvette compartment was equipped with a magnetic stirrer. Temperature was maintained at 37°C throughout the measurements. For optimal separation of fluorescence due to the two forms of the indicator, Ca^{2+}-free fura-2 was monitored at 380 nm and Ca^{2+}-bound dye at 340 nm. To begin the experiment, first a pulse of 20 μl 100 mM $CaCl_2$ was added, followed by agonists and subsequently 50 mM KCl was given as a positive control. Finally calibration drugs were added. Ca^{2+}-fura-2-fluorescence calibration was achieved by adding 10 μl 2 mM ionomycin (to give fluorescence at saturating Ca^{2+}) and 2 mM $MnCl_2$ (to give fluorescence at "zero" Ca^{2+}). $[Ca^{2+}]_i$ was calculated using the standard equation of Grynkiewicz *et al.*, (1985) (refer to section 5.1.3.).

Agonists: hippocampal neurons were challenged with a range (per assay) of nicotine or cytisine concentrations.

The dose-response curve for cytisine was performed by correcting cytisine-induced $[Ca^{2+}]_i$ increase with respect to its resting $[Ca^{2+}]_i$. It was considered that 10^{-4} M cytisine was the concentration of agonist which produced the maximum response since at higher concentrations there was a non-specific Ca^{2+}-independent fluorescence increase.

Blockers: MLA (1 μM MLA final concentration) was applied to the cuvette prior to assay. Ca^{2+} channel blockers were applied 3 min before testing: Ni^{2+} 100 μM, Cd^{2+} 200 μM (Vijayaraghavan *et al.*, 1992).

A flow diagram is given in order to summarise the order of drug additions described above:

1	2	3	4	5	6
MLA or Ni^{2+} or Cd^{2+} in antagonism assays	Ca^{2+} (omitted in Ca^{2+} free assays)	Agonist Nicotine or cytisine	K^+ control for depolarization	Ionomycin for Ca^{2+} maximum	Mn^{2+} for Ca^{2+} minimum

$[Ca^{2+}]_i$ measurements were also carried out on glial cells grown on plastics discs for 14 days. Samples in the presence of 1 mM Ca^{2+} were challenged with 50 μM nicotine, followed by glutamate 50 μM as a positive control. Calibration was carried out as for neurons.

5.3. Results

5.3.1. The establishment of the system

Several control measurements were performed before nicotinic agonists experiments were carried out:

Cell loading

Loading the cells with 5 μM Fura-2 acetoxymethyl ester (Thomas and Delaville, 1991) was straightforward. However, the plating density used routinely for binding assays and immunocytochemistry had to be doubled (3.5×10^5 cells/discs), otherwise there were no fluorescence signals. To determine whether the cells had been successfully loaded, preparations were observed under the fluorescent microscope. Usually all of the neurons presented a uniform distribution of the dye throughout the soma. A spotty distribution was indicative of compartmentalization of the dye (Franklin and Johnson, 1992). The resolution of the microscope, however, did not allow the determination of whether the dye had been distributed throughout neuronal processes. Attention was given to loading the cells with 5 μM fura-2 acetoxymethyl ester at 20°C followed by 20 min incubation at 37°C to guarantee complete de-esterification and diffuse distribution of the dye (Franklin and Johnson, 1992).

Unloaded cultures grown on plastic discs did not display autofluorescence as determined by visual inspection of the cultures under the fluorescent microscope.

Calibration

A typical calibration curve is shown in Fig. 11A. The effect of 1 mM $CaCl_2$ in hippocampal neurons was followed for 40 sec and any Ca^{2+}-induced fluorescence increase was ruled out. Subsequently, 50 mM KCl was used as a positive control. The calibration was achieved in the presence of 2 mM ionomycin followed by 2 mM $MnCl_2$. Figure 11B indicates that in this experiment $[Ca^{2+}]_i$ at rest was 210 nM and KCl elevated $[Ca^{2+}]_i$ to 500 nM.

Figure 11. Ratio calibrations with Ca^{2+} ionophore

A: The effect of 1 mM of Ca^{2+} in loaded cells was followed for 40 sec. Subsequently, 50 mM KCl was used as a positive control. The calibration was achieved in the presence of 2 mM ionomycin (for maximum fluorescence) followed by 2 mM $MnCl_2$ (for minimum fluorescence).

B: $[Ca^{2+}]_i$ has been plotted throughout the experiment. $[Ca^{2+}]_i$ values were derived from the Grynkiewicz *et al.*, (1985) equation (refer to section 5.1.3.).

C: fluorescence has been monitored upon addition of several pulses of HBS in replace of agonist.

D: Unloaded cells were placed into the cuvette with 2 ml HBS and challenged with a pulse of 20 µl 10 mM nicotine.

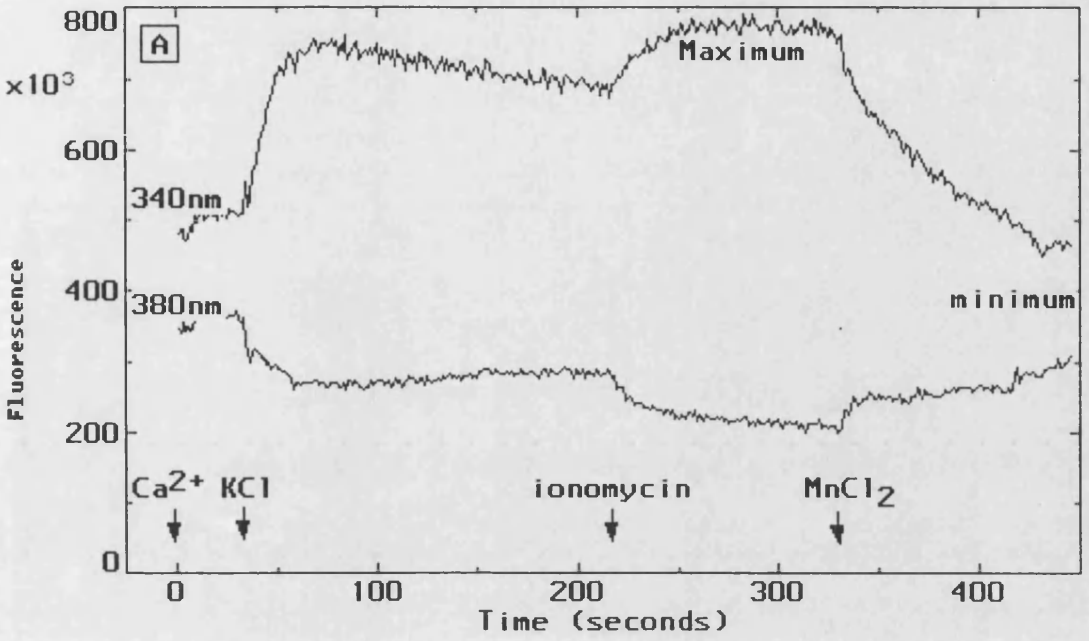
A
800
x10³
600
400
200
0
Fluorescence
340nm
380nm
Maximum
minimum
Ca2+
KCl
ionomycin
MnCl2
0
100
200
300
400
Time (seconds)

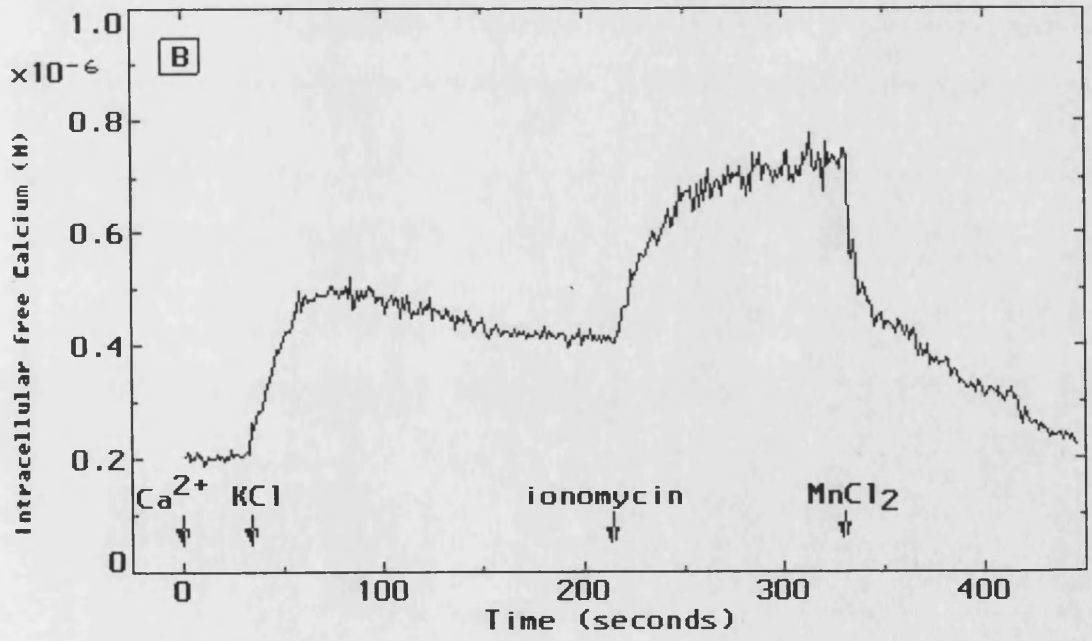
B
1.0
x10⁻⁶
0.8
0.6
0.4
0.2
0
Intracellular free Calcium (M)
Ca2+
KCl
ionomycin
MnCl2
0
100
200
300
400
Time (seconds)

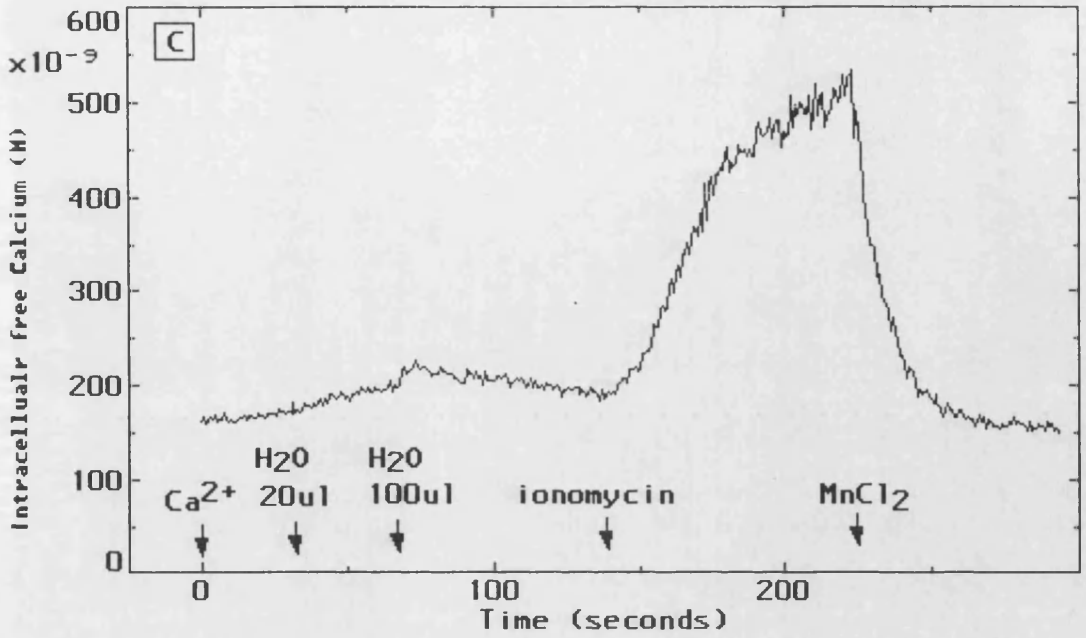
C
600
x10⁻⁹
500
400
300
200
100
0
Intracellualr free Calcium (M)
Ca2+
H20
20ul
H20
100ul
ionomycin
MnCl2
0
100
200
Time (seconds)

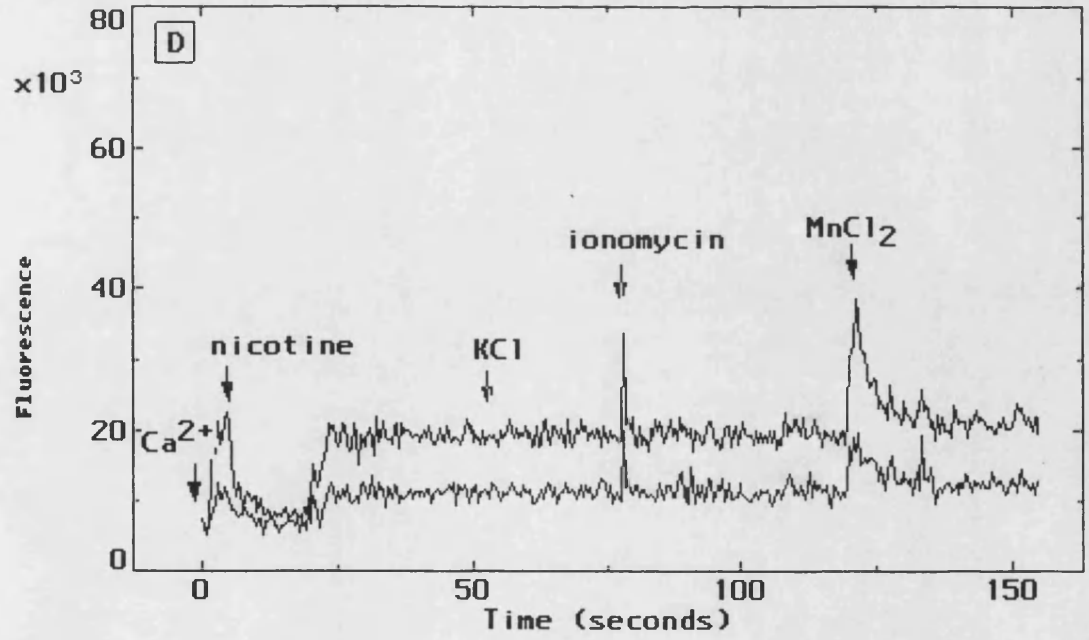
D
80
x10³
60
40
20
0
Fluorescence
nicotine
KCl
ionomycin
MnCl2
Ca2+
0
50
100
150
Time (seconds)

In the calibration curve shown in Fig. 11C the basal fluorescence has been monitored upon addition of several pulses of HBS instead of agonist. The baseline remained unchanged indicating that changes in volume did not contribute to any apparent agonist-induced fluorescence increase.

Assay drugs were screened for autofluorescence. Unloaded cells were placed into the cuvette with 2 ml HBS and drugs were subsequently added either individually or in combination. There were no apparent changes in fluorescence. In Fig. 11 D the fluorescence before and after treatment with 20 µl 10 mM nicotine (final concentration 0.1 mM) is shown.

Reproducibility of the data

This system proved to be reproducible. However, successful results strongly depended on variables such as: good quality and loading of the dye, viability of the cultures, the time between loading and performing the experiment and the spectrophotofluorimenter which needed period maintenance.

The sharpness of the increases in fluorescence in response to stimuli was variable but comparisons showed that taking the plateau values compensates for differences in the initial slope.

5.3.2. Nicotine-induced Ca^{2+} flux

Preliminary experiments: several trials had to be carried out in order to obtain reproducible nicotine-evoked $[Ca^{2+}]_i$ increases. A range of 1:5 serial dilutions of nicotine (10^{-3}-10^{-9} M) were tried. From a total of 30 preliminary experiments, 10 samples did not respond to nicotine or KCl despite the cells being properly loaded as indicated by the calibrations. Another 9 samples did not respond to nicotine in contrast to KCl which induced small fluorescence increases of at most 20% over the basal fluorescence. In addition, variable responses to nicotine and KCl were observed in 11 out of 30 samples only at agonist concentrations above 1 µM. Nicotine 50 µM

was the concentration used in further assays since this rendered the most consistent responses. Therefore, the $[Ca^{2+}]_i$ values presented below represent measurements from further experiments that gave consistent responses for nicotine and KCl.

Further nicotine experiments: Cultured neurons in the presence of 1 mM Ca^{2+} were challenged with a pulse of nicotine (Fig. 12A). At 50 μM, the agonist produced a detectable response. The plot in Fig. 12D shows that an average net increase of 100% over the resting levels was observed [244 ± 16 nM (n=3) to 478 ± 33 nM (n=3), respectively]. Depolarization of the cells by application of 50 mM KCl caused a further increase in fluorescence over the resting levels (533 ± 56 nM (n=3)]. MLA at 1 μM blocked the nicotine induced-increase (Fig. 12B), as expected for α-Bgt sites, while having no effect on the KCl-induced increase (504 ± 21 nM, refer to Fig. 12D). Tetrodotoxin at 1 μM had no effect, indicating that tetrodotoxin-sensitive voltage-gated Na^+ channels did not contribute significantly to any of the responses. Replacing the extracellular Ca^{2+} with buffer, abolished both the nicotine-induced and the KCl-induced increases, and these were restored upon application of 1 mM $CaCl_2$, demonstrating that extracellular Ca^{2+} was required (Fig.12C). The results are consistent with activation of nAChR triggering a Ca^{2+}-dependent increase in fluorescence.

To establish whether the response to 50 μM of nicotine was specific, glial cells were similarly treated (as described above). Glial cells did not respond to 50 μM nicotine in contrast to the glutamate-induced fluorescence observed. Glial cells $[Ca^{2+}]_i$ at rest was 150 ± 35 nM (n=3). Glutamate (50 μM) elevated $[Ca^{2+}]_i$ to 540 ± 70 nM (n=3) (Fig. 13).

Figure 12. Nicotine-induced Ca^{2+} flux in hippocampal neurons

A: $[Ca^{2+}]_i$ recordings after a 50 μM nicotine (NIC) pulse. Subsequently a 50 mM KCl pulse was routinely employed. Calibration was carried out with ionomycin (Im) and Mn^{2+} to account for maximal and minimal fluorescence, respectively.

B: MLA at 1 μM blocked nicotine induced-increase in $[Ca^{2+}]_i$ observed in **A** whereas the response to 50 mM KCl was unaltered. Subsequently calibration was carried out.

C: nicotine-induced $[Ca^{2+}]_i$ increased was dependent on extracellular Ca^{2+}

D: $[Ca^{2+}]_i$ for the alternative treatments carried out in triplicate.

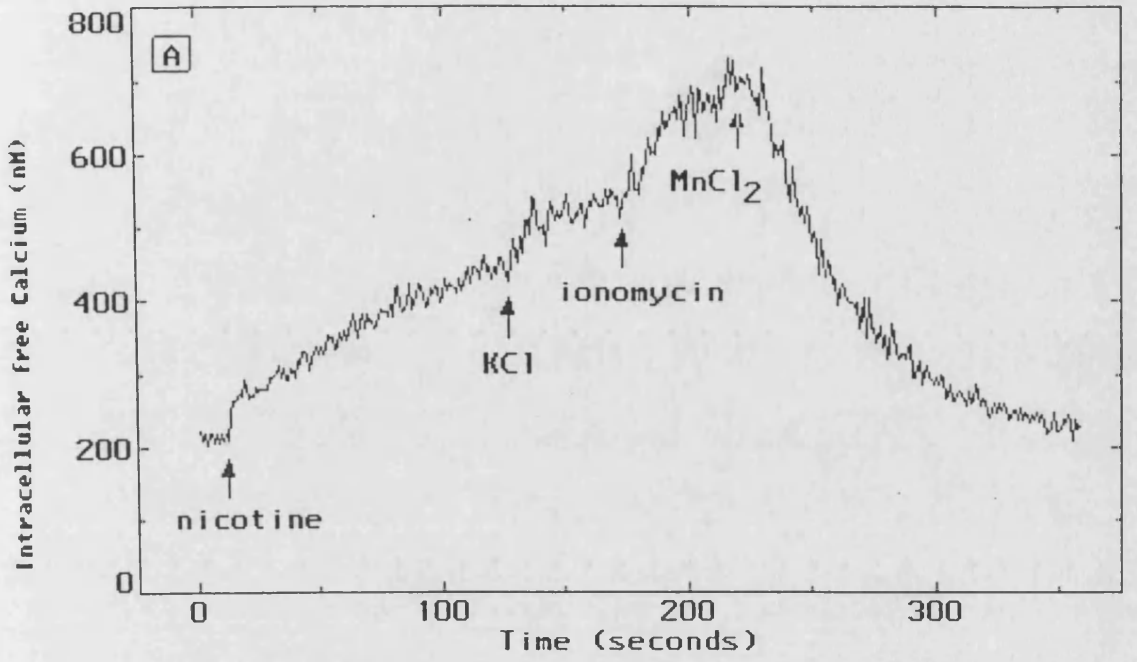
A
800
600
400
200
0
Intracellular free Calcium (nM)
nicotine
KCl
ionomycin
MnCl2
0
100
200
300
Time (seconds)

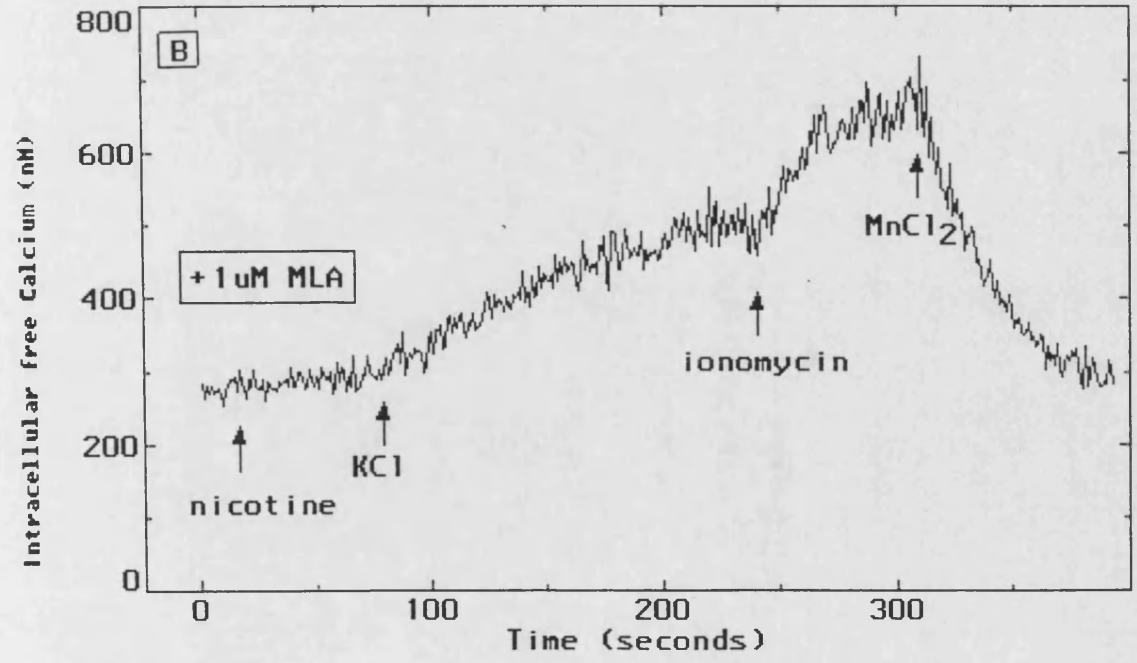
B
800
600
400
200
0
Intracellular free Calcium (nM)
+1uM MLA
nicotine
KCl
ionomycin
MnCl2
0
100
200
300
Time (seconds)

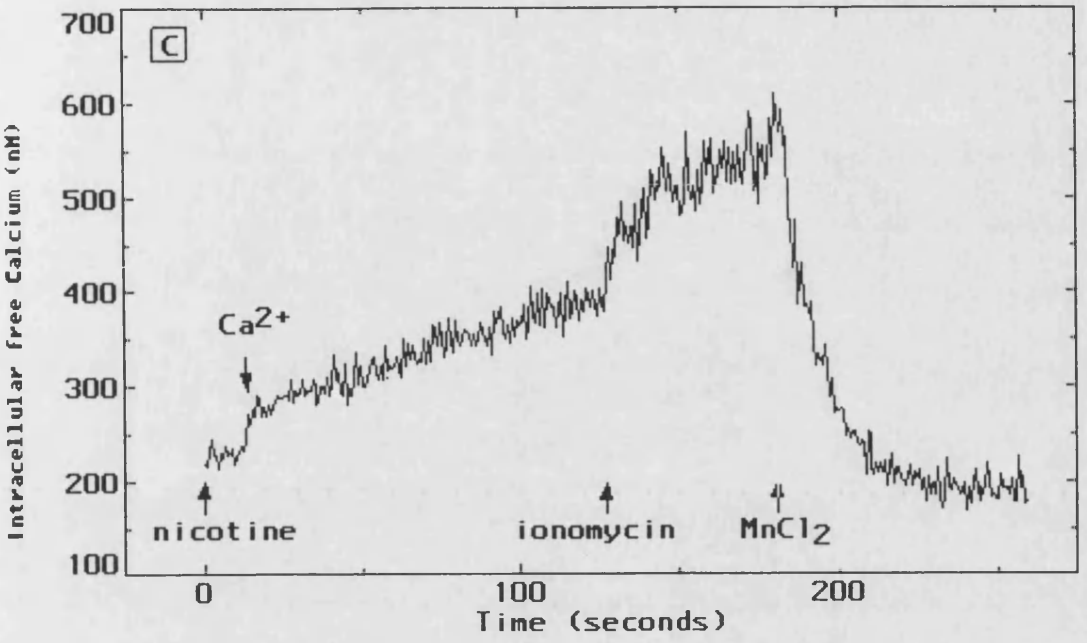
C
Intracellular free Calcium (nM)
700
600
500
400
300
200
100
Ca2+
nicotine
ionomycin
MnCl2
0
100
200
Time (seconds)

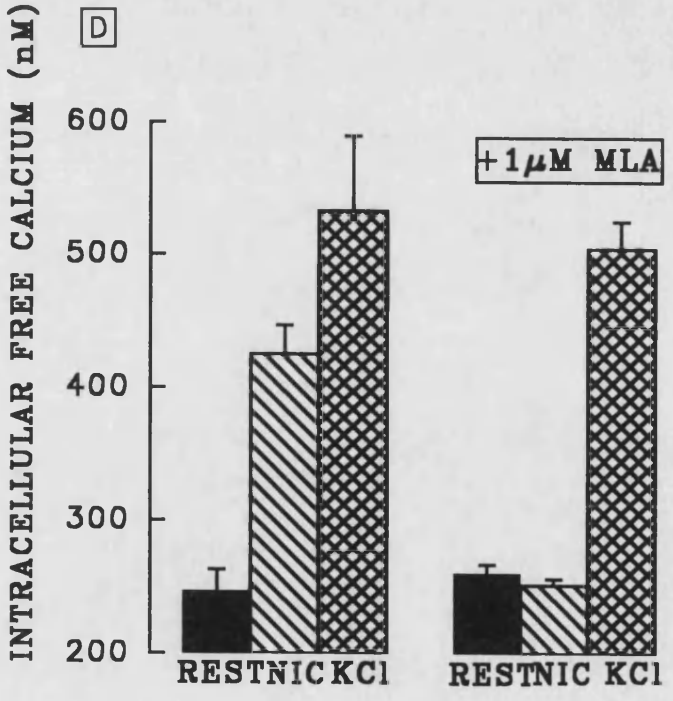
D
INTRACELLULAR FREE CALCIUM (nM)
600
500
400
300
200
+1μM MLA
REST
NIC
KCl
REST
NIC
KCl

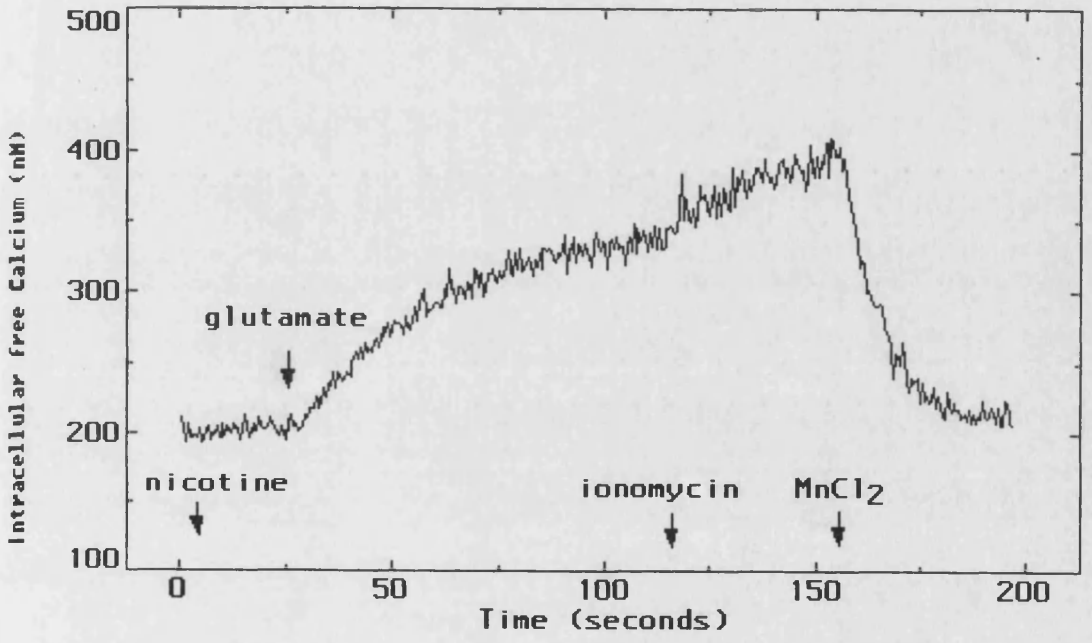

Figure 13. Glutamate induced Ca^{2+} flux in glial cells

A: $[Ca^{2+}]_i$ recordings after a 50 μM nicotine (NIC) pulse. Subsequently a 50 mM glutamate (GLU) pulse was routinely employed. Calibration was carried out with ionomycin (Im) and Mn^{2+} to account for maximal and minimal fluorescence, respectively.

5.3.3. Cytisine induced Ca^{2+} flux

To begin to explore the agonist specificity of the response a second agonist, i.e. cytisine, was investigated. Ca^{2+} measurements were carried as described for nicotine. Cultured neurons in the presence of 1 mM Ca^{2+} were challenged with cytisine (Fig. 14A). At 50 μM, the agonist produced a significant response. The plot in Fig. 14D shows that an average net increase of 100% over the resting levels was observed [317 ± 3 nM (n=3) to 618 ± 26 nM (n=3), respectively]. Depolarization of the cells by application of 50 mM KCl caused a further increase in fluorescence over the resting levels [653 ± 40 nM (n=3)].

MLA at 1 μM blocked the cytisine induced-increase (Fig. 14B) while having no effect on the KCl-induced increase (557 ± 76 nM, refer to Fig. 14D). These experiments were performed in the presence of 1 μM TTX indicating that tetrodotoxin-sensitive voltage-gated Na^{+} channels did not contribute to the responses. Replacing the extracellular Ca^{2+} with buffer, prevented the cytisine-induced increases that were restored upon application of 1 mM Ca^{2+} (Fig. 14C).

To further quantify the effect of cytisine, a dose response curve was constructed (Fig. 15), concentrations from 5 x 10^{-9} to 10^{-4}M were examined by adding one agonist concentration per cuvette. Concentrations above 5 10^{-8}M elicited an increase in $[Ca^{2+}]_i$; the curve could be fitted to a sigmoidal Hill equation, which gave an EC_{50} for cytisine of 1.2 ± 0.3 (n=2) μM. It is important to note here that it was not possible to construct a dose response curve for nicotine since at concentrations below 1 μM responses were not consistently observed.

Figure 14. Cytisine-induced Ca^{2+} flux in hippocampal neurons

A: $[Ca^{2+}]_i$ recordings after a 50 μM cytisine (CYT) pulse. Subsequently a 50 mM KCl pulse was routinely employed. Calibration was carried out with ionomycin (Im) and Mn^{2+} to account for maximal and minimal fluorescence, respectively.

B: MLA at 1 μM blocked cytisine induced-increase in $[Ca^{2+}]_i$ observed in **A** whereas the response to 50 mM KCl was unaltered. Subsequently calibration was carried out.

C: cytisine-induced $[Ca^{2+}]_i$ increase was dependent on extracellular Ca^{2+}

D: $[Ca^{2+}]_i$ measurements for the alternative treatments carried out in triplicate.

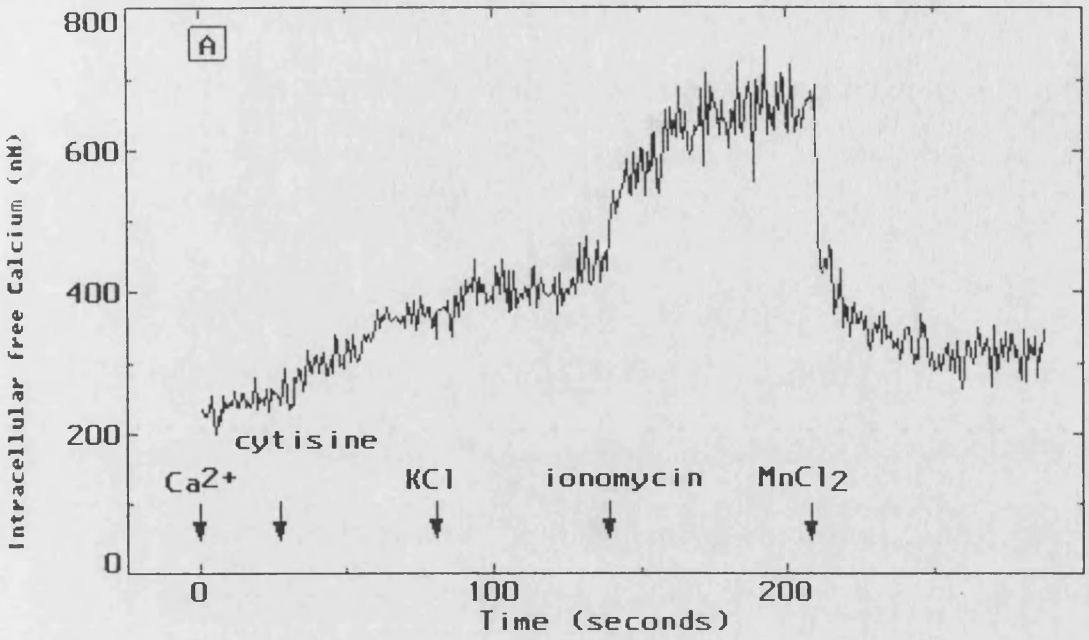
A
800
600
400
200
0
Intracellular free Calcium (nM)
cytisine
Ca2+
KCl
ionomycin
MnCl2
0
100
200
Time (seconds)

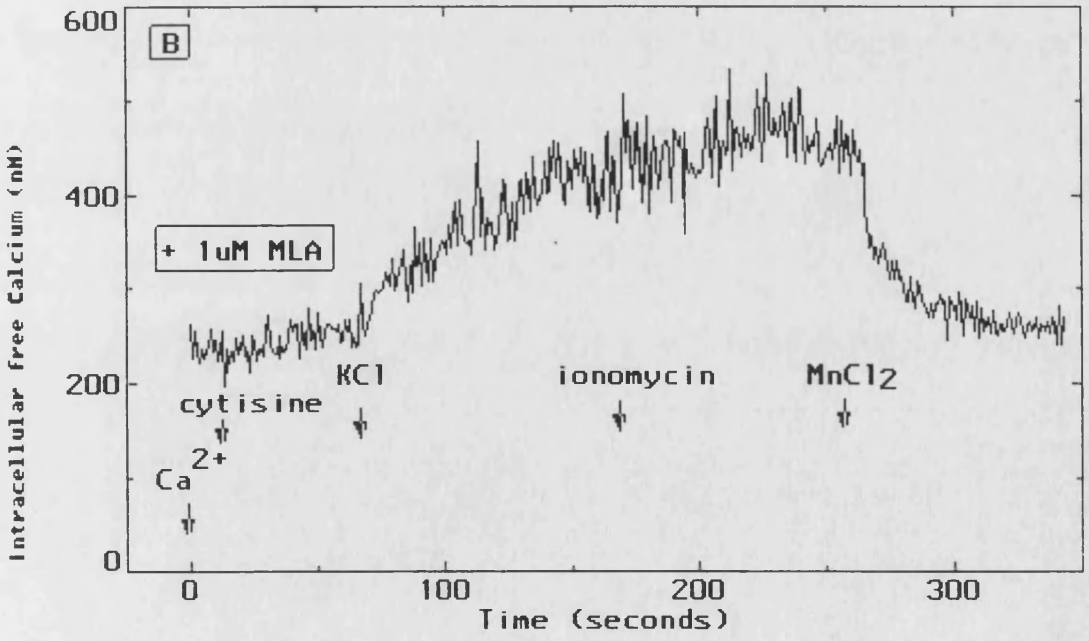
B
600
400
200
0
Intracellular free Calcium (nM)
+ 1uM MLA
cytisine
KCl
ionomycin
MnCl2
Ca2+
0
100
200
300
Time (seconds)

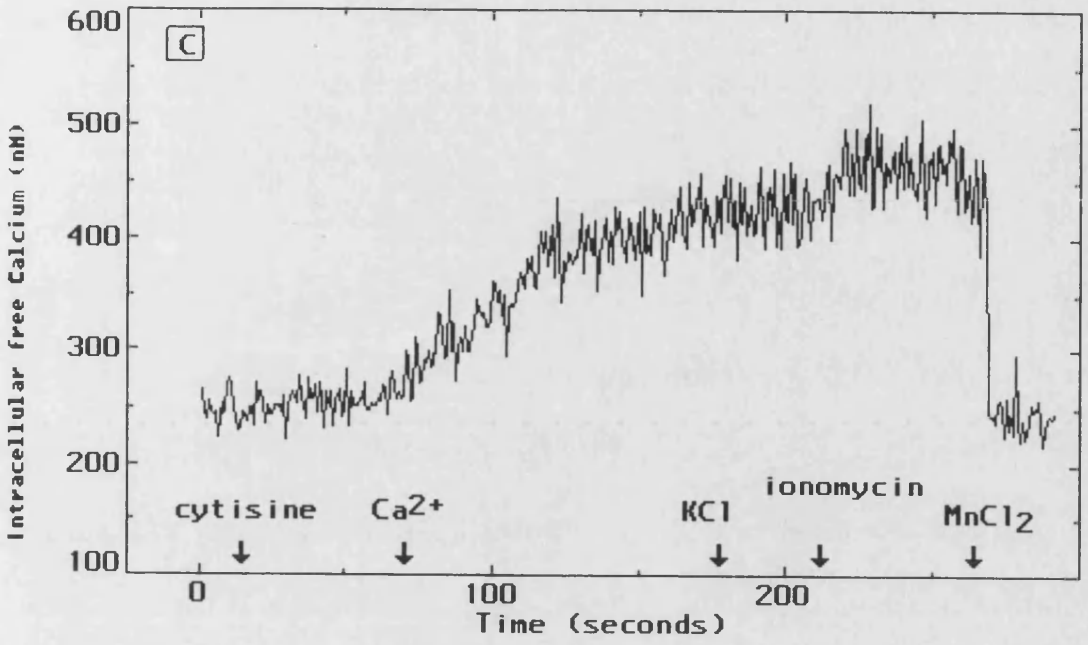
C
Intracellular free Calcium (nM)
600
500
400
300
200
100
cytisine
Ca2+
KCl
ionomycin
MnCl2
0
100
200
Time (seconds)

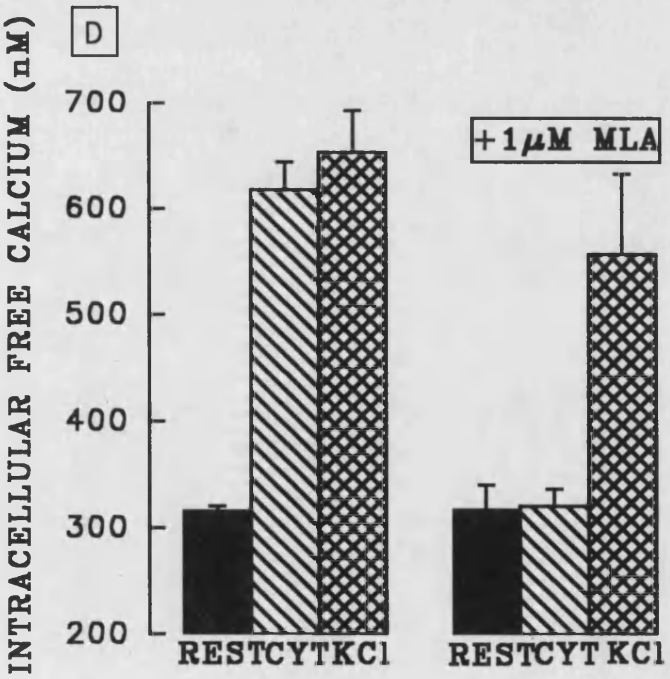
D
INTRACELLULAR FREE CALCIUM (nM)
700
600
500
400
300
200
+1μM MLA
REST
CYT
KCl
REST
CYT
KCl

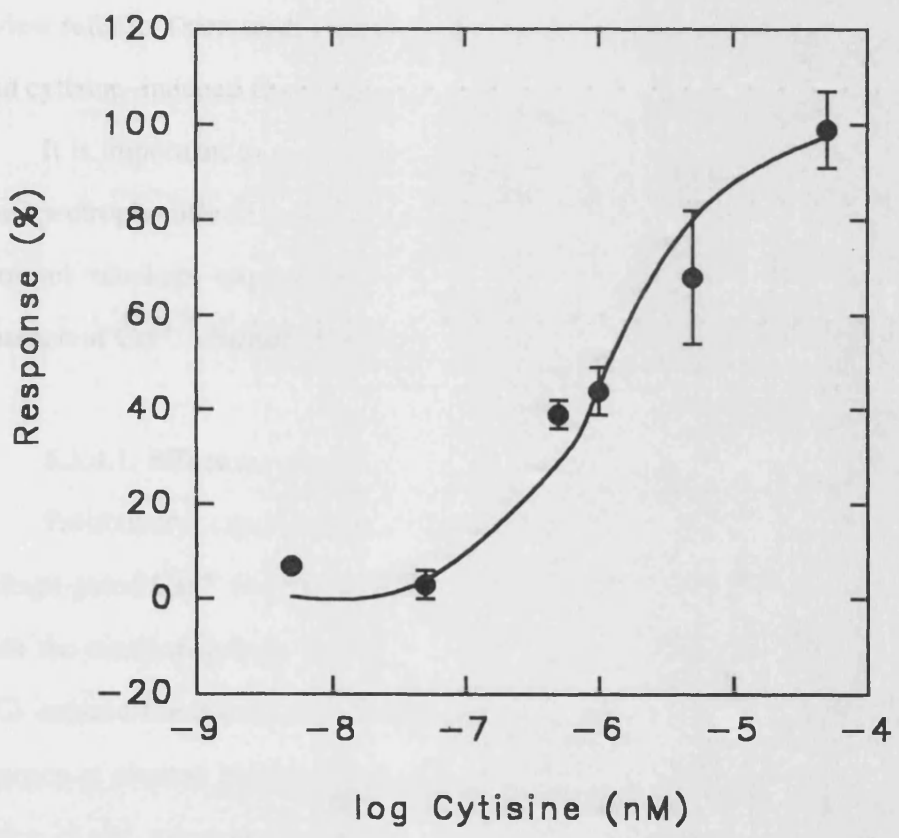

Figure 15. Dose response curve for cytisine in hippocampal neurons

EC_{50} =1.2 ± 0.3 (n=2) μM.

5.3.4. Ca^{2+} channels

The above experiments demonstrate that agonist-evoked increases in $[Ca^{2+}]_i$ are dependent on extracellular Ca^{2+} and therefore reflect an influx of the cation.

If α-Bgt binding sites in hippocampal neurons function as ligand-gated ion channels as expected (Zhang *et al.*, 1994), they could in principle elevate Ca^{2+} levels either directly by being permeable to the cation themselves or indirectly by producing sufficient current to depolarize the membrane and activate voltage–gated Ca^{2+} channels (see section 1.4.). To test the latter possibility, Ca^{2+} channel blockers (for review refer to Tsien and Tsien, 1990) were examined for their effects on the nicotine and cytisine–induced fluorescence signal.

It is important to note a limitation of the method employed in the present study. The spectrophotofluorimeter was not adapted to perfuse the samples. Therefore, Ca^{2+} channel blockers experiments were compared with parallel experiments in the absence of Ca^{2+} channel blockers.

5.3.4.1. Effect on nicotine-induced $[Ca^{2+}]_i$ increase

Preliminary experiments with Cd^{2+}, an ion that blocks several classes of voltage-gated Ca^{2+} channels (Tsien and Tsien, 1990) showed that it largely blocked both the nicotine-induced [from 245 ± 5 nM (n=2) to 270 ± 30 nM (n=2)] and the KCl-induced fluorescence responses [280 ± 20 nM (n=2)]. Control experiments in the absence of channel blockers (carried out in duplicate) showed that at rest $[Ca^{2+}]_i$ was 280 ± 70 nM, whereas 50 μM nicotine and 50 mM KCl elevated $[Ca^{2+}]_i$ to 475 ± 105 nM and 515 ± 103 nM, respectively. Ni^{2+}, an ion thought to block low threshold Ca^{2+} channels (T-Type channels, Tsien and Tsien, 1990) preferentially blocked the nicotine-induced fluorescence [from 178 ± 28 (n=2) nM to 225 ± 25 nM (n=2)] and most of the KCl-induced fluorescence [275 ± 25 (n=2) nM]. These results have been normalized by expressing all experimental data as a percentage of $[Ca^{2+}]_i$ at rest (Fig. 16).

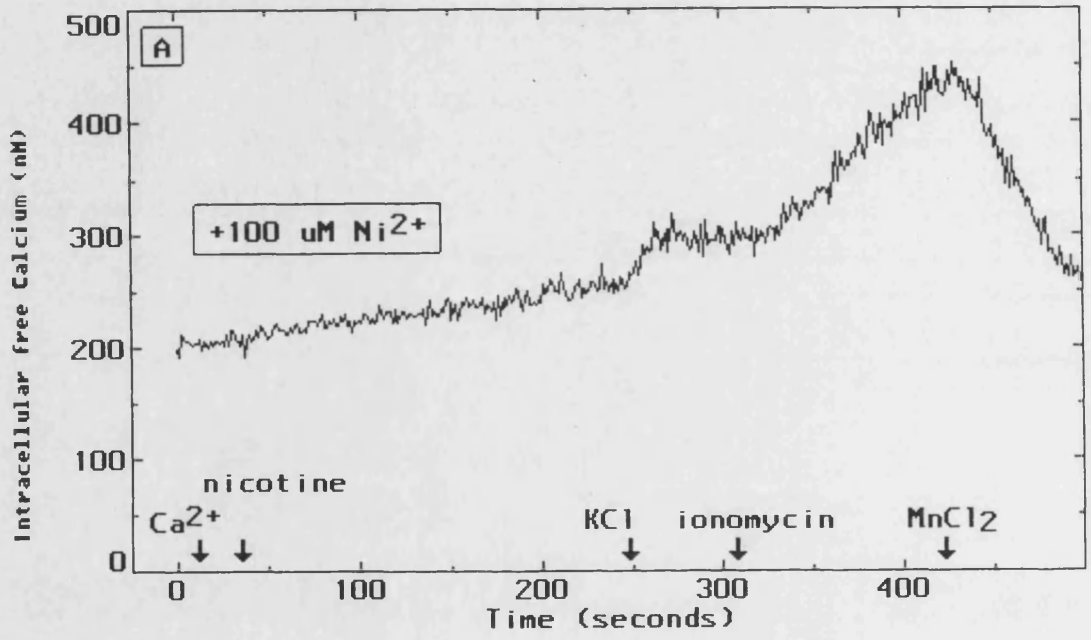

Figure 16. Assessment of nicotine-induced $[Ca^{2+}]_i$ increase in the presence of Ca^{2+} channel blockers.

A: Typical trace in response to Ni^{2+}

B: Typical trace in response to Cd^{2+}

C: $[Ca^{2+}]_i$ measurements for the alternative treatments carried out in duplicate. Values have been corrected for $[Ca^{2+}]_i$ at rest.

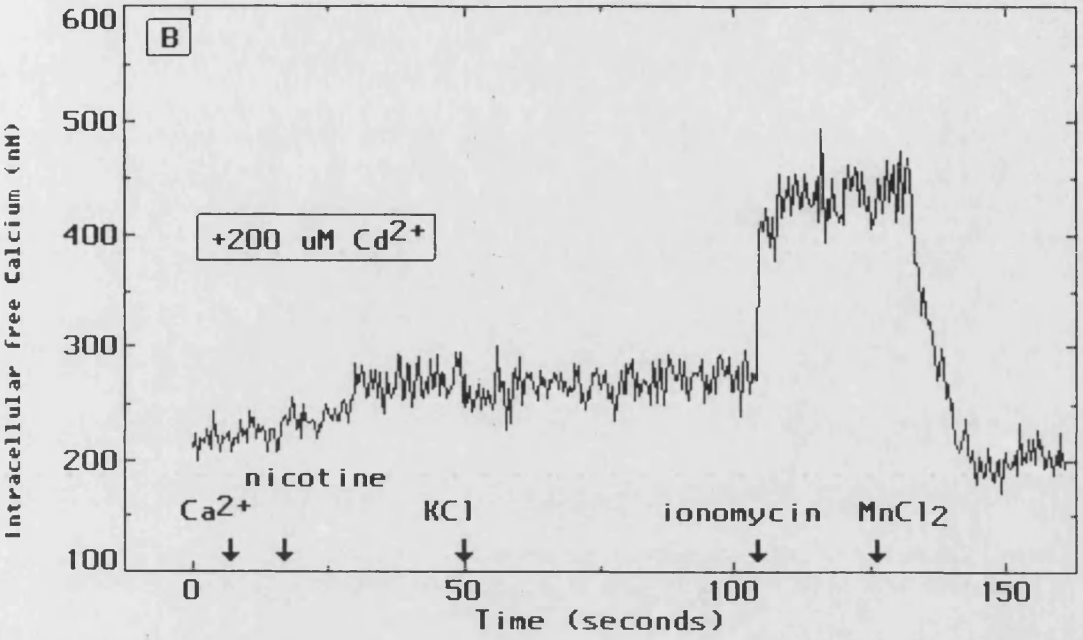
B
600
500
400
300
200
100
Intracellular free Calcium (nM)
+200 uM Cd2+
nicotine
Ca2+
KCl
ionomycin
MnCl2
0
50
100
150
Time (seconds)

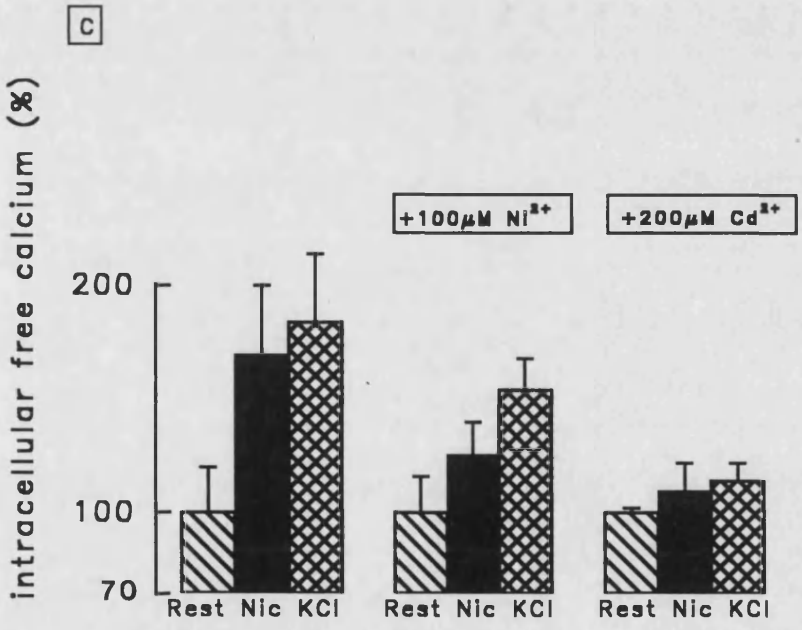
C
intracellular free calcium (%)
+100μM Ni2+
+200μM Cd2+
200
100
70
Rest Nic KCl
Rest Nic KCl
Rest Nic KCl

5.3.4.2. Effect on cytisine-induced $[Ca^{2+}]_i$ increase

Similar results were obtained when Ni^{2+} was applied to cytisine treated samples. Control experiments in the absence of Ni^{2+} (carried out in duplicate) showed that at rest $[Ca^{2+}]_i$ was 295 ± 45 nM, whereas 50 μM cytisine and 50 mM KCl elevated $[Ca^{2+}]_i$ to 595 ± 145 nM and 725 ± 75 nM, respectively. Ni^{2+} preferentially blocked the nicotine-induced fluorescence [from 200 ± 10 nM (n=2) to 235 ± 35 nM (n=2)] and most of the KCl-induced fluorescence [280 ± 30 nM (n=2)]. These results have been normalized by expressing all experimental data as a percentage of $[Ca^{2+}]_i$ at rest (Fig. 17).

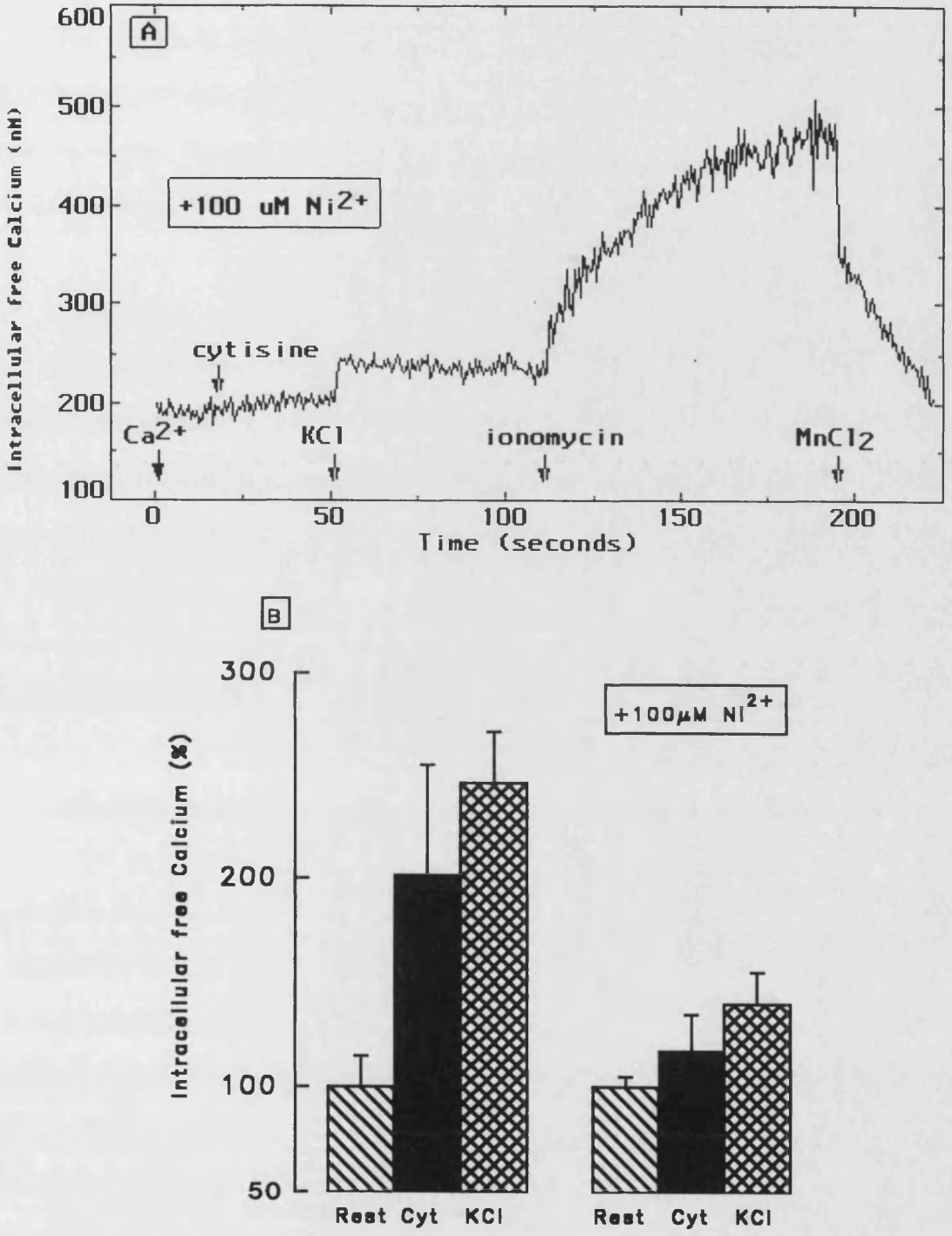

Figure 17. Assessment of cytisine-induced $[Ca^{2+}]_i$ increase in the presence of Ni^{2+}.

A: Typical trace in response to Ni^{2+}; B: $[Ca^{2+}]_i$ measurements for the alternative treatments carried out in duplicate. Values have been corrected for $[Ca^{2+}]_i$ at rest.

5.4. Discussion

The purpose of the present study was to evaluate the functional status of α-Bgt binding sites in hippocampal neurons using fura-2 measurements. The results reported here show that agonists elevated $[Ca^{2+}]_i$ in hippocampal neurons. The $[Ca^{2+}]_i$ increase was 100% over the resting levels and was dependent on extracellular Ca^{2+}.

Comparison of basal $[Ca^{2+}]_i$ in hippocampal neurons with previous studies

Single cell Fura-2 fluorescent measurements in hippocampal neurons have shown 100 nM $[Ca^{2+}]_i$ at rest (Kudo *et al.*, 1988; Iijima *et al.*, 1990). In this thesis, however, $[Ca^{2+}]_i$ at rest doubled probably reflecting methodological differences, in particular, calibration strategies. In such studies, stimulation with muscarinic agonists or KCl induces an increase of $[Ca^{2+}]_i$ to 400 nM and 700 nM, respectively. KCl-evoked $[Ca^{2+}]_i$ increases to 700 nM (Kudo *et al.*, 1988) are similar to those presented in this thesis (590 ± 84 nM; n=17).

MLA blocks agonist-induced $[Ca^{2+}]_i$ elevation

That nicotine or cytisine-induced fluorescence signals were mainly due to activation of α-Bgt binding sites was indicated by 1 μM MLA sensitive blockade. As discussed in chapter 3, MLA competes with high affinity [^{125}I]-α-Bgt binding sites in hippocampal neurons. In rat striatal synaptosomes which bind [^{3}H]nicotine with high affinity (α4β2 nAChR) and in superior cervical ganglion (a likely representative of a nAChR subtype including the α3 subunit) MLA (10 μM) has been shown to block nicotine-mediated dopamine release, lower MLA concentrations were almost ineffective in rat striatum (Drasdo *et al.*, 1992). However, MLA (10 μM) blocks the responses of chick α3β2 and α4β2 nAChR expressed in *Xenopus* (Drasdo *et al.*, 1992). To demonstrate unequivocally that α7 mediates these responses in the hippocampal neurons described here, the experiments could have been repeated with 10 nM MLA. In hippocampal neurons, electrophysiological recordings have shown

that nicotine-induced currents are blocked by 1 nM MLA (type 1A) in 85% of the neurons, whereas 5% are blocked by 100 nM and only 2 % are insensitive to 100 nM MLA (Alkondon and Albuquerque, 1993). The similarities between the characteristics of type 1A (MLA-sensitive) currents and those reported from α7 nAChR reconstituted from α7 subunits (Couturier *et al.*, 1990; Séguéla *et al.*, 1993; Amar *et al.*, 1993; Peng *et al.*, 1994) suggest that type 1A currents could arise from activation of nAChR assembled from α7 subunits. Therefore, in the present study it seems plausible that agonist-induced responses sensitive to MLA involve the major nAChR present in hippocampal neurons, i.e. the putative α7 nAChR. However, the possibility that other unknown nAChR could also be involved remains open.

Cytisine-induced $[Ca^{2+}]_i$ elevation: Comparison of EC_{50} with other systems

The EC_{50} value for cytisine reported in this thesis (1.2 ± 0.3 μM) is one order of magnitude lower than the EC_{50} for cytisine-evoked currents in hippocampal neurons (49 ± 18 μM, Alkondon and Albuquerque, 1993) and similar to those in α7 nAChR expressed *Xenopus* oocytes (5.6 ± 1.3 μM, Amar *et al.*, 1993).

Despite that equilibrium binding assays are likely to reflect binding to the desensitised state of the receptor, and this is associated with higher affinity (Lena and Changeux, 1993), the cytisine concentration required to bind half the [^{125}I]-α-Bgt sites in rat membrane preparations (1.1 μM, Amar *et al.*, 1993) is the same as the cytisine concentration needed to activate half the sites reported in the present study (1.2 ± 0.3 μM).

Channel Blockers

Nicotine and cytisine-evoked increases in $[Ca^{2+}]_i$ were dependent on extracellular Ca^{2+} and were abolished by Ca^{2+} channel blockers, suggesting that α7 type nAChR causes the opening of voltage-gated Ca^{2+} channels. The possibility that the blockade of nicotine or cytisine-induced fluorescence signals arose from a direct

effect of the Ca^{2+} channel blockers on the nicotinic channel cannot be addressed with this technique. For testing this, parallel electrophysiological recordings of agonist-induced currents in the presence of channel blockers would have helped to address this issue. In chick ciliary ganglion neurons, activation of native α-Bgt binding sites induced $[Ca^{2+}]_i$ increases sensitive to 10 nM MLA and channel blockers; this has been demonstrated using fluo-3 imaging and electrophysiological recordings (Vijayaraghavan *et al.*, 1992). The present results are entirely in agreement with those of Vijayaraghavan *et al.* (1992).

Glial cells as a control for nicotine specificity

Glial cells did not display a nicotinic response suggesting that $[Ca^{2+}]_i$ increases in response to agonist in hippocampal neurons was specific. These results complement with those presented throughout the present thesis. Glial cells did not display high affinity binding sites nor did they present immunoreactivity to any of the antibodies against nAChR subunits. However, glutamate induced an increase in $[Ca^{2+}]_i$ in glial cells in agreement with previous reports (McCarthy and Salm, 1991). It is evident that the receptor mediated changes in Ca^{2+} by cultured astroglia is not dependent on continued interactions with neurons.

5.5 Summary to Chapter 5

(i) Nicotine or cytisine elevated $[Ca^{2+}]_i$ about 100% over the resting levels in hippocampal neurons.

(ii) Nicotine or cytisine-induced fluorescence signals were MLA-sensitive, in contrast to K^+-evoked increases in $[Ca^{2+}]_i$.

(iii) The nicotinic increase in $[Ca^{2+}]_i$ was dependent on extracellular Ca^{2+} and blocked by Ni^{2+} and Cd^{2+}.

(iv) Nicotine and cytisine-induced fluorescence signals were insensitive to TTX, indicating that tetrodotoxin-sensitive voltage-gated Na^+ channels did not contribute to the responses.

(v) Glial cells did not display a nicotinic response, in contrast to glutamate-evoked increases in $[Ca^{2+}]_i$.

(vi) All together these results suggest that activation of $\alpha 7$ type nAChR causes the opening of voltage-gated Ca^{2+} channels.

Chapter 6
Conclusions

Primary cultures of hippocampal neurons were established and used as a model system to characterize neuronal α-Bgt nAChR, whose physiological role is unknown. This *in vitro* system proved to be suitable for the characterization of nAChR in embryonic rat hippocampus.

The culture conditions were selected to enrich for neurons and indeed very few glial cells were present, therefore glial cultures from hippocampus were established and the presence of nAChR in these cultures was assessed. Glial cells do not have nAChR as demonstrated with radioligand binding, immunocytochemical and functional assays. Nevertheless glial cells proved to be a suitable system to use as a negative control, specially for immunocytochemistry experiments.

The nicotinic character of α-Bgt sites was demonstrated with competition experiments in which nicotine inhibited [^{125}I]-α-Bgt binding with a K_i=1.3 μM. That [^{125}I]-α-Bgt sites represent a distinct population of nAChR than that of [^{3}H]nicotine (Wonnacott, 1986) can be deduced from the inhibition parameters. Whereas nanomolar concentrations of α-Bgt were enough to displace [^{125}I]-α-Bgt binding, nicotine was needed in micromolar concentrations, while nanomolar concentrations of nicotine are sufficient to displace [^{3}H]nicotine (Wonnacott, 1986). The inhibition displayed by nicotine and MLA in hippocampal cultures is, in general terms, comparable with that reported for several other systems (discussed in section 3.4.) where the α7-type nAChR is involved. However, some disparities in agonist potency were observed and this may reflect differences in subunit combination or posttranslational modifications of this α-Bgt nAChR.

That a-Bgt sites in hippocampal cultures did not decrease by week three in culture -as might be expected from the results of Ben-Barak and Duadi (1979)- may reflect the lack of cholinergic inputs in this *in vitro* system. In the CNS the function of

α-Bgt sites and their role in development is not known. In ganglia extrasynaptically α-Bgt binding sites have recently been shown to elevate intracellular Ca^{2+} levels in response to agonists (Vijayaraghavan *et al.*, 1992) and to function as ligand-gated ion channels (Zhang *et al.*, 1994). Thus α-Bgt may influence a variety of cellular events using Ca^{2+} as second messenger, as for example neurite extension and synaptic remodelling. Recent studies have demonstrated that nicotine inhibits neurite outgrowth of PC12 cells in culture by interacting with α-Bgt nAChR since this effect is prevented in the presence of α-Bgt (Chan and Quik, 1993).

In hippocampal neurons, α-Bgt sites colocalise with α7 nAChR subunits as demonstrated with double labelling experiments. In agreement with radioligand binding assays, Rd-α-Bgt labelling to hippocampal neurons demonstrated the existence of intracellular α-Bgt nAChR stores. As discussed in sections 3.4 and 4.4., intracellular stores of nAChR have been reported in other systems. These intracellular sites may represent turnover of the membrane surface nAChR, individual subunits that either fail to assemble or a reserve of receptor for developmental contingencies (Jacob *et al.*, 1986). In addition, preliminary results suggest that α4 nAChR subunits are expressed by those hippocampal neurons which do not present membrane-bound α-Bgt sites suggesting that different neurons express distinct receptors. The majority of cortical neurons, in contrast to hippocampal neurons, were immunostained with mAb 299 against α4 nAChR subunit. Few of them also express membrane-bound α-Bgt sites in agreement with [^{125}I]-α-Bgt binding studies (Chapter 3). Altogether, dual-labelling experiments showed that hippocampal and cortical neurons present a distinct pattern of nAChR expression.

[^{3}H]Nicotine or [^{3}H]cytisine bind with high affinity to rat brain α4β2 nAChR (see section 1.3.4.); in the present study these sites were not detected with radioligand binding assays. However, both hippocampal and cortical neurons were labelled with mAb against α4 nAChR subunit. This disparity may reflect the association of the α4

subunit with nAChR subunits different from β2 to form a receptor that does not bind either [^{3}H]nicotine or [^{3}H]cytisine.

The purpose of the Fura-2 fluorescence measurements was to evaluate the functional status of α-Bgt sites in hippocampal neurons. Functional assays showed that two nicotinic agonists (nicotine and cytisine) increased the intracellular free Ca^{2+} ($[Ca^{2+}]_i$). This effect was prevented by MLA, in contrast to K^+-evoked increases in $[Ca^{2+}]_i$. Agonist-induced fluorescence signals were insensitive to TTX, indicating that tetrodotoxin-sensitive voltage-gated Na^+ channels did not contribute to the responses. However, the nicotinic increase in $[Ca^{2+}]_i$ was dependent on extracellular Ca^{2+} and blocked by Ni^{2+} and Cd^{2+}, suggesting that activation of α7 nAChR causes the opening of voltage-gated Ca^{2+} channels. Ca^{2+} permeability through coupled voltage-gated Ca^{2+} channels on neurons suggests involvement in longer term regulatory processes using Ca^{2+} as a second messenger.

There is evidence that neurotransmitters can regulate neurite outgrowth by modulating levels of intracellular free Ca^{2+} (reviewed by Lauder, 1993; see also section 1.4.). The fact that neurotransmitter receptors develop before synaptogenesis (Ben-Barak and Dudai, 1979), lends additional evidence to support the premise that modulation via these receptors may influence synaptogenesis.

Further Perspectives

An interesting question to αddress would be whether α-Bgt sites are present in the neuronal processes, particularly in the nerve terminal.

Co-culturing dissociated basal forebrain neurons and hippocampal neurons provides a model for studying the influence of cholinergic inputs on α-Bgt sites in the target cells.

Appendix A

Culture Media

Glia conditioned medium:

To select for glia, hippocampal cell suspensions were plated in PLL coated flasks at a density of 10^4 cells/cm^2. Cultures were fed every three days with serum supplemented medium. On reaching confluence (9 days approximately) medium was harvested for up to two weeks towards medium changes, and either used straightforward or stored at 4^oC.

Serum-free chemically defined medium:

(Bottenstein and Sato, 1979)

Glucose 4.5 g/l DMEM (Gibco) / Nutrient Mixture F-12 (Ham) with L-glutamine (Gibco) were mixed in 3 to 1 proportions; 1 mM sodium pyruvate (Sigma), 2 mM L-glutamine (Sigma) and penicillin / streptomycin (Flow ICN) 50 IU/ml and 50 µg/ml, respectively (Flow ICN) were added to the basal medium. A 5 ml aliquot of this preparation was used to dissolved the following supplements purchased from Sigma: 100 µg/ml human transferrin, 100 µM putrescine, 5 µg/ml insulin, 20 nM progesterone and 30 nM sodium selenite. This supplement containing solution was filter sterilize and added to the basal medium. The preparation was stored at 4^oC and used within 4 weeks.

Serum supplemented chemically defined medium:

FCS 10% (v/v) (ICN Flow) was added to the chemically defined medium which was stored at 4^oC and displayed within 4 weeks.

Serum supplemented medium:

L-glutamine 2 mM, penicillin/streptomycin (50 IU/ml, 50 µg/ml, respectively), 10% FCS and 10% foetal horse serum (Flow ICN) heat inactivated (40 min at 56^{0}C) were added to the basal medium (DMEM 4.5 g/l). The preparation was stored at 4^{0}C and used within 4 weeks.

Appendix B

Cell Lines

M10 fibroblasts:

Fibroblasts were maintained in 4.5 g/l DMEM supplemented with 2 mM L-glutamine, penicillin/streptomycin (50 IU/ml, 50 µg/ml, respectively) 0.5 mg/ml G418 geneticin (Sigma) and 10% FCS.

One day before the experiments, cells were plated out in maintenance medium without geneticin. Fibroblasts were differentiated with 1 µM dexamethasone (Sigma) and used for experiments within the next three days.

PC12 Cells:

Cultures were maintained in low glucose DMEM (1 g/l) with 2 mM L-glutamine, penicillin/streptomycin (50 IU/ml, 50 µg/ml, respectively) and 10% FCS.

Passages were done by shaking and splitting the suspension in a 1:3 ratio. Medium was changed each three days.

Appendix C

Fixation and Permeabilization

Fixation and permeabilization of cells with acetic acid-ethanol:

Fixative and permeabilizing solution: for 100 ml solution, 5 ml acetic acid (May & Baker LTD., Dagenham, England), 70 ml absolute ethanol (May & Baker LTD) and 25 ml H_2O were mixed and stored at -20°C until the moment of the experiment.

Method: cultures grown in 16 mm 4-well dishes (Gibco BRL) were washed two times in PBS and fixed/permeabilized by dropwise addition of 200 µl cold 5% acetic acid-70% ethanol solution. The fixation-permeabilization time was determined empirically. Neurons were fixed-permeabilized for 15 min whereas glial cells for 30 min. Subsequently, cultures were washed three times with 500 µl PBS and ready to use for cytochemistry experiments. This procedure allowed preparations to be stored at 4°C for several weeks.

Appendix D

Immunocytochemistry

Preadsorption of antisera against nAChR subunits:

The antisera were preadsorbed against 3T3L1 mouse fibroblast confluent cell line to minimize background (no rat cell line was available). Cultures were gently washed three times with PBS and fixed with freshly prepared 2% (w/v) paraformaldehyde in 0.1 M cacodylate buffer (pH=7.4) for 30 min. The fixative was removed and samples were washed three times with PBS. Cells were permeabilized with 0.3% Triton x-100 in blocking PBS (1% normal goat serum in PBS) for 30 min. Cultures were washed three times in blocking PBS. The antisera was diluted at the working concentration in blocking PBS and subsequently rocked across the monolayer of fibroblasts for 2 hours at room temperature. Antisera were harvested and used for assayed into hippocampal neuronal, glial and PC12 cells.

Appendix E

Solutions

Solutions were prepared with double distilled water, otherwise stated.

Developing solution:

$MgCl_2$ (2 mM) [>99.5 %, BDH], 0.5 mg/ml 5-bromo-4-chloro-3-indolyl phosphate (Sigma) and 1 mg/ml nitro blue tetrazolium (Sigma) were added to 50 mM sodium carbonate buffer (pH=9.5).

1% FCS-PBS:

For 100 ml dispersion, 1 ml FCS was added to 99 ml PBS prior to assay.

HBS:

Millipore water was used to dissolve 10 mM Hepes (Sigma), 145 mM NaCl (>99.5%, Fisons Analytical Reagent, Bishop, Meadow Rd, Loughborough, England), 5 mM KCl, 1 mM $MgCl_2$, 0.5 mM Na_2HPO_4 (Fisons) and 5.5 mM glucose (Fisons); pH=7.4.

10 mM PBS:

The solution was prepared by dissolving 10 mM KH_2PO_4/K_2HPO_4 (>99 %, FSA) and 0.15 M NaCl; pH 7.4 which was stored at 4^oC.

SDS solution:

The solution was prepared by dissolving 2% (w/v) Na_2CO_3 (>99%, FSA); 0.4% (w/v) NaOH (>99 %, Fisons); 0.16% (w/v) $C_4H_4KNaO_6.4H_2O$ (Sigma) and 1% (w/v) SDS (Sigma) which was stored at room temperature.

Tris-HEPES buffer:

The solution was prepared by dissolving 118 mM NaCl, 4.8 mM KCl, 2.5 mM $CaCl_2$, 20 mM HEPES, 200 mM Tris (BDH), 0.1% (v/v) NaN_3 (Sigma), 1 mM EDTA (Sigma) and 0.1 mM phenylmethylsulphonyl fluoride (Sigma). Aliquots were stored at -20^{o}C.

Appendix F

Statistics

[^{125}I]-α-BGT saturation binding assays

The parameters dissociation constant (K_D) and maximum concentration of receptors (B_{max}) were obtained by curve fitting using the equation that describes a rectangular hyperbole as follows:

$B = B_{max} \times L / (K_D + L)$

where,

B = concentration of receptor-radioligand complex referred to as amount bound

L = concentration of radioligand

[^{125}I]-α-BGT inhibition binding assays

The parameters IC_{50} and n_H were obtained from a curve fitting using the sigmoidal equation:

$B = B_0 - (B_0 \times (1 / (1 + (IC_{50} / I)^{nH})))$

where,

IC_{50} = concentration of competitive inhibitor that blocks 50 percent of the binding of a radioligand to a receptor

n_H = Hill number, coefficient that indicates the way the receptor interacts with the ligand

I = concentration of inhibitor

B = percentage of the specific binding of a radioligand to a receptor, defining B_0 = 100% as the value of B in the absence of inhibitor

Using Cheng-Prusoff equation, IC_{50} values were converted to an affinity constant (K_i) (Cheng and Prusoff, 1973)

$K_i = IC_{50} / (1 + (S / K_D))$

where S is the concentration of radioligand.

References

Alkondon, M. and Albuquerque, E.X. (1991) Initial characterization of the nicotinic acetylcholine receptors in rat hippocampal neurons. *Journal of receptor research* **11**, 1001-1021.

Alkondon, M. and Albuquerque, E.X. (1993) Diversity of nicotinic acetylcholine receptors in rat hippocampal neurons. I. Pharmacological and functional evidence for distinct structural subtypes. *J. Pharmacol. Exp. Ther.* **265**, 1455-1473.

Alkondon, M., Pereira, E.F.R., Wonnacott, S., and Albuquerque, E.X. (1992) Blockade of nicotinic currents in hippocampal neurons defines Methyllycaconitine as a potent and specific receptor antagonist. *Mol. Pharmacol.* **41**, 802-808.

Amar, M., Thomas, P., Johnson, C., Lunt, G.G., and Wonnacott, S. (1993) Agonist pharmacology of the neuronal α7 nicotinic receptor expressed in *Xenopus* oocytes. *FEBS* **327**, 284-288.

Amaral, D.G. and Kurz, J. (1985) An analysis of the origins of the cholinergic and noncholinergic projections to the hippocampal formation of the rat. *J. Comp. Neur.* **240**, 37-59.

Amruthesh, S.C., Boerschel, M.F., McKinney, J.S., Willoughby, K.A., and Ellis, E.F. (1993) Metabolism of Arachidonic acid to epoxyeicosatrienoic acids, hydroxyeicosatetraenoic acids, and prostaglandins in cultured rat hippocampal astrocytes. *J. Neurochem.* **61**, 150-159.

Anand, R. and Lindstrom, J. (1990) Nucleotide sequence of the human nicotinic acetylcholine receptor β2 subunit gene. *Nucl. Acids Res.* **18**, 4272.

Anand, R., Peng, X., Ballesta, J.J., and Lindstrom, J. (1993) Pharmacological characterization of α-Bungarotoxin-sensitive acetylcholine receptors immunostained from chick retina: Contrasting properties of α7 and α8 subunit-containing subtypes. *Mol. Pharmacol.* **44**, 1046-1050.

Arantius, J.S. (1587) *De humano foetu...ejusdem anatomicorum observationum liber, Venetiis, pp 44-45. (As translated by Meaker, S.R., Department of Anatomy, Harvard Medical School, USA),*

Argos, P., Garavito, R.M., Eventoff, W., and Rossmann, M.G. (1978) Similarities in active center geometries of zinc-containg enzymes, proteases and dehydrogenases. *J. Mol. Biol.* **126**, 141-158.

Ashizawa, T., Stanton, B.E., and Appel, S.H. (1982) Interaction of myasthenic immunoglobulins and cholinergic agonists on acetylcholine receptors of rat myotubes. *Ann. Neurol* **11**, 22-27.

Banker, G. and Goslin, K. (1991) *Culturing nerve cells*, Cambridge, Massachusetts, MIT Press.

Banker, G.A. (1980) Trophic interactions between astroglial cells and hippocampal neurons in culture. *Science* **209**, 809-810.

Banker, G.A. and Cowan, W.M. (1977) Rat hippocampal neurons in dispersed cell culture. *Brain Res.* **126**, 397-425.

Banker, G.A. and Cowan, W.M. (1979) Further observations on hippocampal neurons in dispersed cell culture. *J. Comp. Neur.* **187**, 469-494.

Banker, G.A. and Waxman, A.B. (1988) Hippocampal neurons generate natural shapes in cell culture. In: *Intrinsic determinants of neuronal form and function*, 61-82. Edited by Lasek, R.J. and Black, M.M., New York, Alan R. Liss, Inc.

Bartlett, W.P. and Banker, G.A. (1984a) An electron microscopic study of the development of axons and dendrites by hippocampal neurons in culture. I. Cells which develop without intercellular contacts. *The Journal of Neuroscience* **4**, 1944-1953.

Bartlett, W.P. and Banker, G.A. (1984b) An electron microscopic study of the development of axons and dendrites by hippocampal neurons in culture. II. Synaptic relationships. *J. Neurosci.* **4**, 1954-1965.

Bayer, S.A. (1980) Development of the hippocampal region of the rat. I. Neurogenesis examined with ^{3}H-thymidine autoradiography. *J. Comp. Neurol.* **190**, 87-114.

Bayer, S.A. (1985) Hippocampal region. In: *The rat nervous system*, 335-352. Edited by Paxinos, G., Sydney, Academic Press, Inc.

Ben-Barak, J. and Dudai, Y. (1979) Cholinergic binding sites in rat hippocampal formation: Properties and ontogenesis. *Brain Res.* **166**, 245-257.

Bertrand, D., Galzi, J.-L., Devillers-Thiéry, A., Bertrand, S., and Changeux, J.-P. (1993) Stratification of the channel domain in neurotransmitter receptors. *Curr. Opin. Cell. Biol.* **5**, 688-693.

Bliss, T.V.P. and Collingridge, G.L. (1993) A synaptic model of memory: long-term potentiation in the hippocampus. *Nature* **361**, 31-39.

Boksa, P. and Quirion, R. (1987) ^{3}H-Methyl-carbachol, a new radioligand for nicotinic cholinergic receptors in brain. *Eur. J. Pharmacol.* **139**, 323-333.

Bottenstein, J. (1980) Serum-free culture of neuroblastoma cells. In: *Advances in neuroblastoma research*, 161-170. Edited by Evans, A., New York, Raven Press.

Bottenstein, J.E. (1983) Defined media for dissociated neural cultures. In: *Current methods in cellular neurobiology*, 107-132.

Bottenstein, J.E. (1986) Growth requirements *in vitro* of oligodendrocyte cell lines and neonatal rat brain oligodendrocytes. *Proc. Natl. Acad. Sci. USA* **88**, 1955-1959.

Bottenstein, J.E. and Sato, G.H. (1979) Growth of a rat neuroblastoma cell line in serum-free supplemented medium. *Proc. Natl. Acad. Sci. USA* **76**, 514-517.

Boulter, J., Connolly, J., Deneris, E., Goldman, D., Heinemann, S., and Patrick, J. (1987) Functional expression of two neuronal nicotinic acetylcholine receptors from cDNA clones identifies a gene family. *Proc. Natl. Acad. Sci. USA* **84**, 7763-7767.

Boulter, J., Evans, K., Goldman, D., Martin, G., Treco, D., Heinemann, S., and Patrick, J. (1986) Isolation of a cDNA clone coding for a possible neuronal nicotinic acetylcholine receptor α subunit. *Nature* **319**, 368-374.

Boulter, J., O'Shea-Greenfield, A., Duvoisin, R.M., Connolly, J.G., Wada, E., Jensen, A., Gardner, P.D., Ballivet, M., Deneris, E.S., McKinnon, D., Heinemann, S., and Patrick, J. (1990) α3, α5 and β4: Three members of the rat neuronal nicotinic acetylcholine receptor-related gene family form a gene cluster. *J. Biol. Chem.* **265**, 4472-4482.

Bradley, P.B. (1989) *Introduction to neuropharmacology*, 1-351, London, Butterworth & Co. Ltd.,.

Briggs, C.A., Hughes, M.L., Monteggia, L.M., Arneric, S.P., Downen, M., Wainer, B.H., and Giordano, T. (1993) Electrophysiologic evaluation of nicotinic responsiveness in immortalized hippocampal and septal fusion cell lines. *Soc. Neurosci. Abs.* **19**, 290.

Caceres, A., Banker, G., Steward, O., Binder, L., and Payne, M. (1984) MAP2 is localized to the dendrites of hippocampal neurons which develop in culture. *Developmental Brain Research* **13**, 314-318.

Caceres, A., Banker, G.A., and Binder, L. (1986) Immunocytochemical localization of tubulin and microtubule-associated protein 2 during development of hippocampal neurons in culture. *The Journal of Neuroscience* **6**, 714-722.

Chan, J. and Quik, M. (1993) A role for the nicotinic α-Bungarotoxin receptor on neurite outgrowth in PC12 cells. *Neuroscience* **56**, 441-451.

Changeux, J.-P. (1993) Chemical signaling in the brain. *Scientific American* **November**, 30-37.

Cheng, Y.-C. and Prusoff, W.H. (1973) Relationship between the inhibition constant (Ki) and the concentration of inhibitor which causes 50 per cent inhibition (I50) of an enzymatic reaction. *Biochemical Pharmacology* **22**, 3099-3108.

Chini, B., Clementi, F., Hukovic, N., and Sher, E. (1992) Neuronal-type α-bungarotoxin receptors and the α5-nicotinic receptor subunit gene are expressed in neuronal and nonneuronal human cell lines. *Proc. Natl. Acad. Sci. USA* **89**, 1572-1576.

Clarke, P.B.S. (1990) The central pharmacology of nicotine: electrophysiological approaches. In: *Nicotine Psychopharmacology*, 158-193. Edited by Wonnacott, S., Russell, M.A.H., and Stolerman, I.P., Oxford, Oxford University Press.

Clarke, P.B.S. (1992) The fall and rise of neuronal α-bungarotoxin binding proteins. *Trends in P. Sciences* **13**, 407-413.

Clarke, P.B.S., Schwartz, R.D., Paul, S.M., Pert, C.B., and Pert, A. (1985) Nicotinic binding in rat brain: Autoradiographic comparison of [^{3}H]nicotine, and [^{125}I]-α-Bungarotoxin. *J. Neurosci.* **5**, 1307-1315.

Cobbold, P.H. and Rink, T.J. (1987) Fluorescence and bioluminescence measurements of cytoplasmic free calcium. *Biochem. J.* **248**, 313-328.

Conti-Tronconi, B.M., Dunn, S.M.J., Barnard, E.A., Dolly, J.O., Lai, F.A., Ray, N., and Raftery, M.A. (1985) Brain and muscle nicotinic acetylcholine receptors are different but homologous proteins. *Proc. Natl. Acad. Sci. USA* **82**, 5208-5212.

Couturier, S., Bertrand, D., Matter, J-M., Hernandez, M-C., Bertrand, S., Millar, N., Valera, S., Barkas, T., and Ballivet, M. (1990) A neuronal nicotinic acetylcholine receptor subunit (α7) is developmentally regulated and forms a homo-oligomeric channel blocked by α-BTX. *Neuron* **5**, 847-856.

Couturier, S., Erkman, L., Valera, S., Rungger, D., Bertrand, S., Boulter, J., Ballivet, M., and Bertrand, D. (1990) α5, α3, and non-α3: three clustered avian genes encoding neuronal nicotinic acetylcholine receptor-related subunits. *J. Biol. Chem.* **265**, 4472-4482.

Dale, H.H. (1914) The action of certain esters and ethers of choline and their relation to muscarine. *J. Physiol.* **6**, 147-190.

Davis, L., Banker, G.A., and Steward, O. (1987) Selective dendritic transport of RNA in hippocampal neurons in culture. *Nature* **330**, 477-479.

Davis, L., Burger, B., Banker, G.A., and Steward, O. (1990) Dendritic transport: Quantitative analysis of the time course of somatodendritic transport of recently synthesized RNA. *The Journal of Neuroscience* **10**, 3056-3068.

Deadwyler, S.M., Hampson, R.E., Bennett, B.A., Wang, S., Mu, J., Fluhler, E.N., and Lippiello, P.M. (1992) Effects of nicotine on cultured central nervous system neurons. In: *The biology of nicotine: Current research issues*, 39-54. Edited by Lippiello, P.M., Collins, A.C., Gray, J.A., and Robinson, J.H., New York, Raven Press, Ltd.

Deneris, E.S., Boulter, J., Swanson, L.W., Patrick, J., and Heinemann, S. (1989) β3: a new member of nicotinic acetylcholine receptor gene family is expressed in brain. *J. Biol. Chem.* **264**, 6268-6272.

Deneris, E.S., Connolly, J., Boulter, J., Wada, E., Wada, K., Swanson, L.W., Patrick, J., and Heinemann, S. (1988) Primary structure and expression of β2: A novel subunit of neuronal nicotinic acetylcholine receptors. *Neuron* **1**, 45-54.

Deneris, E.S., Connolly, J., Rogers, S.W., and Duvoisin, R. (1991) Pharmacological and functional diversity of neuronal nicotinic acetylcholine receptors. *Trends in P. Sciences* **12**, 34-40.

Dotti, C.G. and Banker, G.A. (1987) Experimentally induced alteration in the polarity of developing neurons. *Nature* **330**, 254-256.

Dotti, C.G., Sullivan, C.A., and Banker, G.A. (1988) The establishment of polarity by hippocampal neurons in culture. *The Journal of Neuroscience* **8**, 1454-1468.

Doucette-Stamm, L., Monteggia, L.M., Donnelly-Roberts, D., Tai Wang, M., Lee, J., Tian, J., and Giordano, T. (1993) Cloning and sequence of the human α7 nicotinic acetylcholine receptor. *Drug Development Research* **30**, 252-256.

Drasdo, A., Caulfield, M., Bertrand, D., Bertrand, S., and Wonnacott, S. (1992) Methyllycaconitine: A novel nicotinic antagonist. *Molecular and cellular neurosciences* **3**, 237-243.

Duvoisin, R.M., Deneris, E.S., Patrick, J., and Heinemann, S. (1989) The functional diversity of the neuronal nicotinic acetylcholine receptors is increased by a novel subunit: β4. *Neuron* **3**, 487-496.

Dziegielewska, K., Evans, C., New, H., Reynolds, M., and Saunders, N. (1984) Synthesis of plasma-protein by rat fetal brain and choroid-plexus. *Int. J. Dev. Neurosci.* **2**, 215-222.

Fiszman, M.L., Barker, J.L., and Jones, S.V.P. (1991) Electrophysiological responses to muscarinic receptor stimulation in cultured hippocampal neurons. *Brain Res.* 1-4.

Flores, C.M., Rogers, S.W., Pabreza, L.A., Wolfe, B.B., and Kellar, K.J. (1992) A subtype of nicotinic cholinergic receptor in rat brain is composed of α4 and β2 subunits and is up-regulated by chronic nicotine treatment. *Mol. Pharmacol.* **41**, 31-37.

Fluhler, E.N., Lippiello, P.M., and Fernandes, K.G. (1992) Localization and function of high-affinity nicotine receptors on cultured cortical neurons from rat brain. In: *The biology of nicotine: Current research issues*, 23-37. Edited by Lippiello, P.M., Collins, A.C., Gray, J.A., and Robinson, J.H., New York, Raven Press, Ltd.

Forloni, G., Angeretti, N., Chiesa, R., Monzani, E., Salmona, M., Bugiani, O., and Tagliavini, F. (1993) Neurotoxicity of a prion protein fragment. *Nature* **362**, 543-546.

Fornasari, D., Chini, B., Tarroni, P., and Clementi, F. (1990) Molecular cloning of human neuronal nicotinic receptor α3-subunit. *Neuroscience Letters* **111**, 351-356.

Franklin, J.L. and Johnson, E.M.,Jr. (1992) Supression of programmed neuronal death by sustained elevation of cytoplasmic calcium. *Trends Neurosci* **15(12)**, 501-507.

Frotscher, M., Schlander, M., and Léránth, C. (1986) Cholinergic neurons in the hippocampus. A combined light' and electron-microscopic immunocytochemical study in the rat. *Cell and Tissue Research* **246**, 293-301.

Fuchs, J.L (1989) [^{125}I]α-*Bungarotoxin binding marks primary sensory areas of developing rat neocortex. *Brain Res.* **501**, 223-234.

Geller, A.I. and Freese, A. (1990) Infection of cultured central nervous system neurons with a defective herpes simplex virus 1 vector results in stable expression of *Escherichia coli* beta-galactosidase. *Proc. Natl. Acad. Sci. USA* **87**, 1149-1153.

Geller, H.M., Quiñones-Jenab, V., Poltorak, M., and Freed, W.J. (1991) Applications of immortalized cells in basic and clinical neurobiology. *J. Cell. Biochem* **45**, 279-283.

Giulian, D. (1987) Ameboid microglia as effectors of inflamation in the central nervous system. *Journal of Neuroscience Research* **18**, 155-171.

Giulian, D. and Baker, T.J. (1986) Characterization of ameboid microglia isolated from developing mammalian brain. *J. Neurosci.* **6**, 2163-2178.

Goldman, D., Deneris, E., Luyten, W., Kochlar, A., Patrick, J., and Heinemann, S. (1987) Members of a nicotinc acetylcholine receptor gene family are expressed in different regions of the mammalian central nervous system. *Cell* **48**, 965-973.

Goslin, K. and Banker, G. (1991) Rat hippocampal neurons in low-density culture. In: *Culturing nerve cells*, 251-281. Edited by Banker, G. and Goslin, K., Cambridge, Massachusetts, MIT Press.

Goslin, K., Schreyer, D.J., Pate Skene, J.H., and Banker, G. (1988) Development of neuronal polarity: GAP-43 distinguishes axonal dendritic growth cones. *Nature* **336**, 672-674.

Goslin, K., Schreyer, D.J., Pate Skene, J.H., and Banker, G. (1990) Changes in the distribution of GAP-43 during the development of neuronal polarity. *The Journal of Neuroscience* **10**, 588-602.

Görne-Tschelnokow, U., Strecker, A., Kaduk, C., Naumann, D., and Hucho, F. (1994) The transmembrane domains of the nicotinic acetylcholine receptor contain α-helical and β structures. *EMBO J.* **13**, 338-341.

Greig-Smith, P. (1952) The use of random and contiguous quadrats in the study of the structure of plant communities. *Ann. Bot. Lond,N. S.* **16**, 293-316.

Grynkiewicz, G., Poenie, M., and Tsien, R.Y. (1985) A new generation of Ca^{2+} indicators with greatly improved fluorescence properties. *The Journal of Biological Chemistry* **260**, 3440-3450.

Haas, H.L. (1983) Amine neurotransmitter actions in the hippocampus. In: *Neurobiology of the hippocampus*, 139-155. Edited by Seifert, W., London, Academic Press .

Hamassaki-Britto, D., Brzozowska-Prechtl, A., Karten, H., and Lindstrom, J. (1993) Bipolar cells of the chick retina containing α-bungarotoxin-sensitive nicotinic acetylcholine receptors. *Visual Neuroscience* **11**, 63-70.

Harel, R. and Futerman, A.H. (1993) Inhibition of sphingolipid synthesis affects axonal outgrowth in cultured hippocampal neurons. *The Journal of Biological Chemistry* **268**, 14476-14481.

Harrison, R.G. (1907) Observations on the living developing nerve fiber. *Anat. Rec.* **1**, 116-118.

Haruhiko, B., Nakamura, M., Honda, Z., Izumi, T., Iwatsubo, T., Seyama, Y., Ogura, A., Kudo, Y., and Shimizu, T. (1992) Platelet-Activating factor (PAF) receptor in rat brain: PAF mobilizes intracellular Ca^{2+} in hippocampal neurons. *Neuron* **9**, 285-294.

Havrankova, J., Brownstein, M., and Roth, J. (1981) Insulin and insulin receptors in rodent brain. *Diabetologia* **20**, 268-273.

Helekar, S.A., Char, D., Neff, S., and Patrick, J. (1994) Propyl isomerase requirement for the expression of functional homo-oligomeric ligand-gated ion channels. *Neuron* **12**, 179-189.

Henis, Y.I and Sokolovsky, M. (1983) Muscarinic antagonists induce different receptor conformations in rat adenohypophysis. *Mol. Pharmacol.* **24**, 357-365.

Hill, J.A., Zoli, M., Bourgeois, J.-P., and Changeux, J.-P. (1993) Immunocytochemical localization of a neuronal nicotinic receptor: The β2-subunit. *The Journal of Neuroscience* **13**, 1551-1568.

Iijima, T., Kudo, Y., Ogura, A., Akita, K., and Matsumoto, G. (1990) Variation in the pattern of $[Ca^{2+}]_i$ change induced by acetylcholine in cultured hipoocampal neurons. *Brain Res.* **521**, 273-280.

Imoto, K., Busch, C., Sakmann, B., Mishina, M., Konno, T., Nakai, J., Bujo, H., Mori, Y., Fukuda, K., and Numa, S. (1988) Rings of negatively charged amino acids determine the acetylcholine receptor channel conductance. *Nature* **335**, 645-648.

Imoto, K., Konno, T., Nakai, J., Wang, F., Mishina, M., and Numa, S. (1991) A ring of uncharged polar amino acids as a component of channel constriction in the nicotinic acetylcholine receptor. *FEBS* **289**, 193-200.

Ip, N.Y., Li, Y., van de Stadt, I., Panayotatos, N., Alderson, R.F., and Lindsay, R.M. (1991) Ciliary neurotrophic factor enhances neuronal survival in embryonic rat hippocampal cultures. *The Journal of Neuroscience* **11**, 3124-3134.

Isaacson, R.L. (1974) *The limbic system*, 1-292, New York, Plenum Press.

Isenberg, K.E. and Meyer, G.E. (1989) Clonning of a putative neuronal nicotinic acetylcholine receptor subunit. *J. Neurochem.* **52**, 988-991.

Jacob, M.H., Lindstrom, J.M., and Berg, D.K. (1986) Surface and intracellular distribution of a putative neuronal nicotinic acetylcholine receptor. *The Journal of Cell Biology* **103**, 205-214.

Jaffe, D.B., Johnston, D., Lasser-Ross, N., Lisman, J.E., Miyakawa, H., and Ross, W.N. (1992) The spread of Na^+ spikes determines the pattern of dendritic Ca^{2+} entry into hippocmapal neurons. *Nature* **357**, 244-246.

Karlin, A. (1993) Structure of nicotinic acetylcholine receptors. *Curr. Opin. Neur.* **3**, 299-309.

Kemp, G., Bentley, L., McNamee, M.G., and Morley, B.J. (1985) Purification and characterization of the α-bungarotoxin binding protein from rat brain. *Brain Res.* **347**, 274-283.

Keyser, K.T., Britto, L.R.G., Schoepfer, R., Whiting, P., Cooper, J., Conroy, W., Brozozowska-Prechtl, A., Karten, H.J., and Lindstrom, J. (1993) Three subtypes of α-bungarotoxin-sensitive nicotinic acetylcholine receptors are expressed in chick retina. *The Journal of Neuroscience* **13**, 442-454.

Kleiman, R., Banker, G.A., and Steward, O. (1990) Differential subcellular localization of particular mRNAs in hippocampal neurons in culture. *Neuron* **5**, 821-830.

Konno, T., Busch, C., Von Kitzing, E., Imoto, K., Wang, F., Nakai, J., Mishina, M., Numa, S., and Sakmann, B. (1991) Rings of anionic amino acids as structural determinants of ion selectivity in the acetylcholine receptor channel. *Proc. R. Soc. Lond. Ser. B* **244**, 69-79.

Kostyuk, P.G. (1989) Diversity of calcium ion channels in cellular membranes. *Neuroscience* **28**, 253-261.

Kriegstein, A.R. and Dichter, M.A. (1983) Morphological classification of rat cortical neurons in cell culture. *J. Neurosci.* **3**, 1634-1647.

Kudo, Y., Ogura, A., and Iijima, T. (1988) Stimulation of muscarinic receptor in hippocampal neuron induces characteristic increase in cytosolic free Ca^{2+} concentration. *Neuroscience Letters* **85**, 345-350.

Lamar, E., Miller, K., and Patrick, J. (1990) Amplification of genomic sequences identifies a new gene, α6, in the nicotinic acetylcholine receptor gene family. *Soc. Neurosci. Abstr.* **16**, 681.

Lauder, J.M. (1993) Neurotransmitters as growth regulatory signals: role of receptors and second messengers. *Trends Neurosci* **16**, 133-240.

Lauterborn, J.C., Trans, T.M.D., Isackson, P.J., and Gall, C.M. (1993) NGF mRNA and GAD_{67} mRNA are colocalized in select neurons of hippocampus. *Soc. Neurosci. Abs.* **19**, 249.

Lee, H.J., Hammond, D.N., Large, T.H., Roback, J.D., Sim, J.A., Brown, D.A., Otten, U.H., and Wainer, B.H. (1990) Neuronal properties and trophic activities of immortalized hippocampal cells from embryonic and young adult mice. *The Journal of Neuroscience* **10**, 1779-1787.

Lees, G., Ortells, M.O., and Lunt, G. (1994) Molecular biology and fine structure of ion channels: Potential targets for general anaesthetics in the central nervous system. *Anaest. Phar. Rev.* **2**, 11-28.

Lena, C. and Changeux, J.-P. (1993). Allosteric modulations of the nicotinic acetylcholine receptor. *Trends Neurosci* **16**, 181-186.

Lendahl, U. and McKay, R.D.G. (1990) The use of cell lines in neurobiology. *Trends Neurosci* **13**, 132-137.

Lester, R.A.J., Quarum, M.L., Parker, J.D., Weber, E., and Jahr, C.E. (1989) Interaction of 6-Cyano-7-nitroquinoxaline-2,3-dione with the N-Methyl-D-aspartate receptor-associated Glycine binding site. *Mol. Pharmacol.* **35**, 565-570.

Levi, G., Gallo, V., and Ciotti, M.T. (1986) Biopotential precursors of putative fibrous astrocytes and oligodendrocytes in rat cerebellar cultures express distinct surface features and "neuron-like" γ-aminobutyric acid transport. *Proc. Natl. Acad. Sci. USA* **83**, 1504-1508.

Lewis, P.R., Shute, C.C.D., and Silver, A. (1967) Confirmation from choline acetylase analyses of a massive cholinergic innervation to the rat hippocampus. *J. Physiol.* **191**, 215-224.

Lindstrom, J., Schoepfer, R., Whiting, P., Anand, R., Conroy, W.G., Saedis, M.S., and Das, M. (1991) Monoclonal antibody probes for nicotinic receptors of muscles and nerves. *Biochem. Soc. Trans.* **19**, 115-120.

Lingle, C.J., Maconochie, D., and Steinbach, J.H. (1992) Activation of skeletal muscle nicotinic acetylcholine receptor. *J. Membrane Biol.* **126**, 195-217.

Lippiello, P.M. and Fernandes, K.G. (1987) Identification of putative high affinity nicotinic receptors on cultured cortical neurons. *J. Pharmacol. Exp. Ther.* **246**, 409-416.

Lippiello, P.M. and Fernandes, K.G. (1988) Identification of putative high affinity nicotinic receptors on cultured cortical neurons. *J. Pharmacol. Exp. Ther.* **246**, 409-415.

Lippiello, P.M., Fernandes, K.G., Langone, J.J., and Bjercke, R.J. (1991) Characterization of nicotinic receptors on cultured cortical neurons using anti idiotipic antibodies and ligand binding. *J. Pharmacol. Exp. Ther.* **257**, 1216-1224.

Lipton, S.A. and Kater, s.b. (1989) Neurotransmitter regulation of neuronal outgrowth, plasticity and survival. *Trends Neurosci* **12**, 265-270.

Lorente de Nó, R. (1934) Studies on the structure of the cerebral cortex. II. Continuation of the study of the ammonic system. *Journal of Psychology and Neurology* **46**, 113-177.

Lowry, O.H., Rosebrough, J.N., Farr, A.L., and Randall, R.J. (1951) Protein measurement with the folin phenol reagent. *J. Biol. Chem.* **193**, 265-275.

Luebke, J.I., Dunlap, K., and Turner, T.J. (1993) Multiple Calcium channel types control glutamatergic synaptic transmission in the hippocampus. *Neuron* **11**, 895-902.

Lukas, R.J. (1991) Effects of chronic nicotinic ligand exposure on functional activity of nicotinic acetylcholine receptors expressed by cells of the PC12 rat pheochromocytoma or the TE671/RD human clonal cell line. *J. Neurochem.* **56**, 1134-1145.

Luther, M.A., Schoepfer, R., Whiting, P., Casey, B., Blatt, Y., Montal, M.S., Montal, M., and Lindstrom, J. (1989) A muscle acetylcholine receptor is expressed in the human cerebellar medulloblastoma cell line TE671. *The Journal of Neuroscience* **9**, 1082-1096.

Macallan, D.R.E., Lunt, G.G., Wonnacott, S., Swanson, K.L., Rapoport, H., and Albuquerque, E.X. (1988) Methyllycaconitine and (+)-anatoxin-a differentiate between nicotinic receptors in vertebrate and invertebrate nervous systems. *FEB* **226**, 357-363.

MacLusky, N. and Clark, C.R. (1980) Hormone receptors in the central nervous system. In: *Proteins of the nervous system*, 2nd Ed., 331-383. Edited by Bradshaw, R. and Schneider, D., New York, Raven Press.

Malgaroli, A. and Tsien, R.W. (1992) Glutamate-induced long-term potentiation of the frequency of miniature synaptic currents in cultured hippocampal neurons. *Nature* **357**, 134-139.

Marks, M.J., Stitzel, J.A., Romm, E., Wehner, J.M., and Collins, A.C. (1986) Nicotinic binding sites in rat and mouse brain: Comparison of acetylcholine, nicotine and α-bungarotoxin. *Mol. Pharmacol.* **30**, 427-436.

Markwell, M.A.K., Haas, S.M., Bieber, L.L., and Tolbert, N.E. (1978) A modification of the Lowry procedure to simplify protein determination in membrane and lipoprotein samples. *Anal. Biochem.* **87**, 206-210.

Mattson, M.P (1988) Neurotransmitters in the regulation of neuronal cytoarchitecture. *Brain Research Reviews* **13**, 179-212.

Mattson, M.P., Cheng, B., Culwell, A.R., Esch, F.S., Lieberburg, I., and Rydel, R.E. (1993) Evidence for excitoprotective and intraneuronal calcium-regulating roles for secreted forms of the β-amyloid precursor protein. *Neuron* **10**, 243-254.

Mattson, M.P., Murrain, M., Guthrie, P.B., and Kater, s.b. (1989) Fibroblast growth factor and glutamate: Opposing roles in the generation and degeneration of hippocampal neuroarchitecture. *J. Neurosci.* **9**, 3728-3740.

McCarthy, K.D. and Salm, A.K. (1991) Pharmacologically-distinct subsets of astroglia can be identified by their calcium response to neuroligands. *Neuroscience* **41**, 325-333.

McLachlan, A.D. (1979) Gene duplication in the structural evolution of chymotrypsin. *J. Mol. Biol.* **128**, 49-79.

McLane, K.E., Wu, X., and Conti-Tronconi, B.M. (1990) Identification of a brain acetylcholine receptor α subunit able to bind α-bungarotoxin. *J. Biol. Chem.* **265**, 9816-9824.

Merlie, J.P (1984) Biogenesis of the acetylcholine receoptor, a multisubunit integral membrane protein. *Cell* **36**, 573-575.

Miller, R.J. (1987) Multiple calcium channels and neuronal function. *Science* **235**, 46-52.

Milner, T. and Bacon, C. (1989) GABAergic neurons in the rat hippocampal formation: Ultrastructure and synaptic relationships with catecholaminergic terminals. *J. Neurosci.* **10**, 3410-3427.

Minta, A., Kao, R., and Tsien, R.Y. (1989) Fluorescent indicators for cytosolic calcium based on rhodamine and fluorescein chromophores. *J. Biol. Chem.* **264**, 8171-8178.

Mishina, M., Takai, T., Imoto, K., Noda, M., Takahashi, T., Numa, S., Methfessel, C., and Sakmann, B. (1986) Molecular distinction between fetal and adult forms of muscle acetylcholine receptor. *Nature* **321**, 406-411.

Monck, J.R., Reynolds, E.E., Thomas, A.P., and Williamson, J.R. (1988) Novel kinetics of single cell Ca^{2+} transients in stimulated hepatocytes and A10 cells measured using fura-2 and fluorescent videomicroscopy. *J. Biol. Chem.* **263**, 4569-4575.

Monteggia, L.M., Sullivan, J.P., Briggs, C.A., Hughes, M.L., Arneric, S.P., Downen, M., Wainer, B.H., and Giordano, T. (1993) Analysis of nicotinic receptor subtypes in immortalized hippocampal and septal fusion cell lines. *Soc. Neurosci. Abs.* **19**, 290.

Mulle, C., Choquet, D., Korn, H., and Changeux, J.-P. (1992) Calcium influx through nicotinic receptor in rat central neurons: Its relevance to cellular regulation. *Neuron* **8**, 135-143.

Müller, H.W. and Seifert, W. (1982) A neurotrophic factor (NTF) released from primary glial cultures supports survival and fiber outgrowth of cultured hippocampal neurons. *Journal of Neuroscience Research* **8**, 195-204.

Nef, P., Oneyser, C., Allioid, C., Couturier, S., and Ballivet, M. (1988) Genes expressed in the brain define three distinct neuronal nicotinic acetylcholine receptors. *EMBO J.* **7**, 595-601.

Pabreza, L.A., Dhawan, S., and Kellar, K.J. (1991) [^{3}H]Cytisine binding to nicotinic cholinergic receptors in brain. *Mol. Pharmacol.* **39**, 9-12.

Paton, W.D.M. and Zaimis, E.J. (1949) The pharmacological actions of polymethylene bistrimethylammonium salts. *British Journal of Pharmacology* **4**, 381-400.

Patrick, J. and Stallcup, B. (1977) α-Bungarotoxin binding and cholinergic receptor function on rat sympathetic nerve line. *The Journal of Biological Chemistry* **252**, 8629-8633.

Paxinos, G. and Watson, C. (1986) *The rat brain in stereotaxic coordinates*, 2nd Ed., Sydney, Academic Press.

Peng, X., Katz, M., Gerzanich, V., Amand, R., and Lindstrom, J. (1994) Human α7 acetylcholine receptor: Cloning of the α7 subunit from the SH-SY5Y cell line and determination of pharmacological properties of native receptors and functional α7 homomers expressed in *Xenopus* oocytes. *Mol. Pharmacol.* **45**, 546-554.

Pentreath, V.W., Morrison, J.H., and Magistretti, P.J. (1986) Transmitter mediated regulation of energy metabolism in nervous tissue at the cellular level. *Neurochem. Int.* **9**, 1-10.

Pfrieger, F.W., Gottmann, K., and Lux, H.D. (1994) Kinetics of $GABA_B$ receptor-mediated inhibition of calcium currents and excitatory synaptic transmission in hippocampal neurons in vitro. *Neuron* **12**, 97-107.

Poulter, L., Earnest, J.P., Stroud, R.M., and Burlingame, A.L. (1989) Structure, oligosaccharide structures, and posttranslationally modified sites of the nicotinic acetylcholine receptor. *Proc. Natl. Acad. Sci. USA* **86**, 6645-6649.

Prohaska, J. and Ganther, H. (1976) Selenium and glutathione peroxidase in developing rat brain. *J. Neurochem.* **27**, 1379-1387.

Regehr, W. and Tank, D.W. (1992) Calcium concentration dynamics produced by synaptic activation of CA1 hippocmapal pyramidal cells. *J. Neurosci.* **12**, 4202-4223.

Robinson, D. and McGee, R. (1985) Agonist-induced regulation of the neural nicotinic acetylcholine receptor of PC12 cells. *Mol. Pharmacol.* **27**, 409-417.

Rogers, A.T. (1988) *Spinal cord cell culture, a model for neuronal development & disease*, University of Bath,

Rogers, S.W., Gahring, L.C., Papke, R.L., and Heinemann, S. (1991) Identification of cultured cells expressing ligand-gated ion channels. *Protein Expression Purification* **2**, 108-116.

Rogers, S.W., Mandelzys, A., Deneris, E.S., Cooper, E., and Heinemann, S. (1992) The expression of nicotinic acetylcholine receptors by PC12 cells trated with NGF. *J. Neurosci.* **12**, 4611-4623.

Romm, E., Lippiello, P.M., Marks, M.J., and Collins, A.C. (1990) Purification of L-(^{3}H)nicotine eliminates low affinity binding. *Life Sci.* **46**, 935-945.

Rossmann, M.G. and Argos, P. (1976) Exploring structural homology of proteins. *J. Mol. Biol.* **105**, 75-95.

Rossmann, M.G. and Argos, P. (1977) The taxonomy of protein structure. *J. Mol. Biol.* **109**, 99-129.

Sargent, P. (1993) The diversity of neuronal nicotinic acetylcholine receptors. *Ann. Rev. Neurosci.* **16**, 403-443.

Schlessinger, A.R., Cowan, W.M., and Swanson, L.W. (1978) The time of origin of neurons in Ammon's horn and the associated retrohippocampal fields. *Anat. Embryol.* **154**, 153-173.

Schoepfer, R., Conroy, W.G., Whiting, P., Gore, M., and Lindstrom, J. (1990) Brian α-Bungarotoxin binding protein cDNAs and MAbs reveal subtypes of this branch of the Ligand-Gated ion channel gene superfamily. *Neuron* **5**, 35-48.

Schoepfer, R., Halvorsen, S.W., Conroy, W.G., Whiting, P., and Lindstrom, J. (1989) Antisera against an acetylcholine receptor α3 fusion protein bind to ganglionic but not to brain nicotinic acetylcholine receptors. *FEB* **257**, 393-399.

Schoepfer, R., Luther, M., and Lindstrom, J. (1988) The human meduloblastoma cell line TE671 expresses a muscle'like acetylcholine receptor: Cloning of the α subunit cDNA. *FEBS Lett.* **226**, 235-240.

Schoepfer, R., Whiting, P., Esch, F., Blacher, R., Shimasaki, S., and Lindstrom, J. (1988) cDNA clones coding for the structural subunit of a chicken brain nicotinic acetylcholine receptor. *Neuron* **1**, 241-248.

Seeley, P.J. and Field, P.M. (1988) Use of colloidal gold complexes of wheat germ agglutinin as a label for neural cells. *Brain Res.* **449**, 177-191.

Segal, M. (1992) Acetylcholine enhances NMDA-evoked calcium rise in hippocampal neurons. *Brain Res.* **587**, 83-87.

Séguéla, P., Wadiche, J., Dineley-Miller, K., Dani, J.A., and Patrick, J.W. (1993) Molecular cloning, functional properties, and distribution of rat brain $\alpha 7$: A nicotinic cation channel highly permeable to calcium. *J. Neurosci.* **13**, 596-604.

Shepherd, G.M. (1988) *Neurobiology*, 2nd Ed., 1-689, Oxford, Oxford University Press.

Swanson, L.W., Simmons, D.M., Whiting, P.J., and Lindstrom, J. (1987) Immunohistochemical localization of neuronal nicotinic receptors in the rodent central nervous system. *J. Neurosci.* **7**, 3334-3342.

Thomas, A.P and Delaville, F. (1991) The use of fluorescent indicators for measurements of cytosolic-free calcium concentrations in cell populations and single cells. In: *Cellular calcium*, 1-54. Edited by McCormack, J.G. and Cobbold, P.H., Oxford, Oxford University Press.

Tsien, R.W. and Tsien, R.Y. (1990) Calcium channels, stores, and oscillations. *Ann. Rev. Cell Biol.* **6**, 715-760.

Tsien, R.Y. (1989) Fluorescent probes of cell signaling. *Annual Review of Neuroscience* **12**, 227-253.

Tsien, R.Y., Pozzan, T., and Rink, T.J. (1982) Calcium homeostasis in intact lymphocytes: Cytoplasmic free Ca^{2+} monitored with a new, intracellularly trapped fluorescent indicator. *J. Cell Biol.* **94**, 325-334.

Unwin, N. (1993a) Neurotransmitter Action: Opening of ligand-gated ion channels. *Cell* **72**, 31-41.

Unwin, N. (1993b) Nicotinic acetylcholine receptor at 9 Å resolution. *J. Mol. Biol.* **229**, 1101-1124.

Valera, S., Ballivet, M., and Bertrand, D. (1992) Progesterone modulates a neuronal nicotinic acetylcholine receptor. *Proc. Natl. Acad. Sci. USA* **89**, 9949-9953.

Vijayaraghavan, S., Pugh, P.C., Zhang, Z-w., Rathouz, M.M., and Berg, D.K. (1992) Nicotinic receptors that bind α-Bungarotoxin on neurons raise intracellular free Ca^{2+}. *Neuron* **8**, 353-362.

Villarroel, A., Herlitze, S., Koenen, M., and Sakmann, B. (1991) Location of a threonine residue in the α-subunit M2 transmembrane segment that determines the ion flow through the acetylcholine receptor channel. *Proc. R. Soc. Lond. Ser. B* **243**, 69-74.

Villarroel, A. and Sakmann, B. (1992) Threonine in the selectivity filter of the acetylcholine receptor channel. *Biophys. J.* **62**, 196-208.

Wada, E., McKinnon, D., Heinemann, S., Patrick, J., and Swanson, L.W. (1990) The distribution of mRNA encoded by a new member of the neuronal nicotinic acetylcholine receptor gene family (α_5) in the rat central nervous system. *Brain Res.* **526**, 45-53.

Wada, E., Wada, K., Boulter, J., Deneris, E., Heinemann, S., Patrick, J., and Swanson, L.W. (1989) Dstribution of alpha2, alpha3, alpha4, and beta2 neuronal nicotinic receptor subunit mRNAs in the central nervous system: A hybridization histochemical study in the rat. *J. Comp. Neurol.* **284**, 314-335.

Wada, K., Ballivet, M., Boulter, J., Connolly, J., Wada, E., Deneris, E.S., Swanson, L.W., Heinemann, S., and Patrick, J. (1988) Functional expression of a new pharmacologycal subtype of brain nicotinic acetylcholine receptor. *Science* **240**, 330-334.

Walicke, P., Cowan, W.M., Ueno, N., Baird, A., and Guillemin, R. (1986) Fibroblast growth factor promotes survival of dissociated hippocampal neurons and enhances neurite extension. *Proc. Natl. Acad. Sci. USA* **83**, 3012-3016.

Ward, J.M., Cockcroft, V.B., Lunt, G.G., Smillie, F.S., and Wonnacott, S. (1990) Methyllycaconitine: a selective probe for neuronal α-bungarotoxin binding sites. *FEBS* **270**, 45-48.

Werner, P., Voigt, M., Keinänen, K., Wisden, W., and Seeburg, P.H. (1991) Cloning of a putative high affinity kainate receptor expressed predominantly in hippocampal CA3 cells. *Nature* **351**, 742-744.

Whiting, P., Esch, F., Shimasaki, S., and Lindstrom, J. (1987a) Neuronal nicotinic acetylcholine receptor β-subunit is coded for by the cDNA clone α4. *FEBS Lett.* **219**, 459-463.

Whiting, P. and Lindstrom, J. (1987b) Affinity labelling of neuronal acetylcholine receptors localizes the neurotransmitter binding site to their β subunit. *FEBS Lett.* **213**, 55-60.

Whiting, P. and Lindstrom, J.M. (1987a) Purification and characterization of a nicotinic acetylcholine receptor from rat brain. *Proc. Natl. Acad. Sci. USA* **84**, 595-599.

Whiting, P., Schoepfer, R., Lindstrom, J., and Priestley, T. (1991) Structural and pharmacologycal characterization of the major brain nicotinic acetylcholine receptor subtype stably expressed in mouse fibroblasts. *Mol. Pharmacol.* **40**, 463-472.

Whiting, P.J. and Lindstrom, J.M. (1986) Purification and characterization of a nicotinic acetylcholine receptor from chick brain. *Biochemistry* **25**, 2082-2093.

Whiting, P.J., Liu, R., Morley, B.J., and Lindstrom, J.M. (1987b) Structurally different neuronal nicotinic acetylcholine receptor subtypes purified and characterized using monoclonal antibodies. *J. Neurosci.* **7**, 4005-4016.

Whiting, P.J., Schoepfer, R., Swanson, L.W., Simmons, D.M., and Lindstrom, J.M. (1987c) Functional acetylcholine receptor in PC12 cells reacts with a monoclonal antibody to brain nicotinic receptor. *Nature* **327**, 515-517.

Whiting, P.J., Schoepfer, R., Shimasaki, S., Esch, F., Keyser, K., Conroy, W.G., Gore, M., and Lindstrom, J. (1991) Expression of nicotinic AChR subtypes in brain and retina. *Molecular Brain Research* **10**, 61-70.

Whittaker, V.P. (1990) The contribution of drugs and toxins to understanding of cholinergic function. *Trends in P. Sciences* **11**, 8-13.

Whittemore, S.R., Friedman, P.L., Larhammar, D., Persson, H., Gonzalez-Carvajal, M., and Holets, V.R. (1988) Rat β nerve growth factor sequence and site of synthesis in the adult hippocampus. *J. Neurosci. Res.* **20**, 403-410.

Wonnacott, S. (1986) α-Bungarotoxin binds to low-affinity nicotine binding sites in rat brain. *J. Neurochem.* **47**, 1706-1712.

Wonnacott, S. (1990a) Characterization of nicotine receptor sites in brain. In: *Nicotine Psychopharmacology. Molecular, cellular and behavioural aspects*, 226-277. Edited by Wonnacott, S., Russell, M.A.H., and Stolerman, I.P., Oxford, Oxford University Press.

Wonnacott, S. (1990b) *Nicotine Psychopharmacology. Molecular, cellular and behavioural aspects*, 1-427, Oxford, Oxford University Press.

Wonnacott, S., Harrison, R., and Lunt, G.G. (1982) Immunological cross-reactivity between the α-bungarotoxin binding component from rat brain and nicotinic acetylcholine receptor. *Journal of Neuroimmunology* **3**, 1-13.

Yamada, S., Kagawa, Y., Isogai, M., Takayanagi, N., and Hayashi, ,E. (1986) Ontogenesis of nicotinic acetylcholine receptors and presynaptic cholinergic neurons in mammalian brain. *Life Sci.* **38**, 637-644.

Zhang, Z-W., Vijayaraghavan, S., and Berg, D.K. (1994) Neuronal acetylcholine receptors that bind α-Bungarotoxin with high affinity function as ligand-gated ion channels. *Neuron* **12**, 167-177.

Zhou, Z. and Neher, E. (1993) Calcium permeability of nicotinic acetylcholine receptor channels in bovine adrenal chromaffin cells. *European Journal of Physiology* **425**, 511-517.

Zilberter, Y.I., Uteshev, V.V., Sokolova, S.N., Motin, L.G., and Eremjan, H.H. (1990) Potentiation of glutamate-activated currents in isolated hippocampal neurons. *Neuron* **5**, 597-602.

Zorumski, C.F., Thio, L.L., Isenberg, K.E., and Clifford, D.B. (1992) Nicotinic acetylcholine currents in cultured postnatal rat hippocampal neurons. *Mol. Pharmacol.* **41**, 931-936.